UNIVERSITY OF
PLYMOUTH

THE DIETARY BIOACCUMULATION AND DETECTION OF ENGINEERED NANOSILVER IN FISH

by

Nathaniel James Clark

A thesis submitted to the University of Plymouth
in partial fulfilment for the degree of

DOCTOR OF PHILOSOPHY

School of Biological and Marine Sciences

February 2019

Copyright Statement

Acknowledgements:

This work would not have been possible without the supervisory team of Professors Richard Handy and Tom Hutchinson, and Dr Ben Shaw. Specifically, I'd like to express my gratitude to Richard, as my DOS, whose continued support, advice and comments during these three years have helped push me to achieve more than I thought possible.

I would also like to thank Dr David Boyle in helping to shape both the way I approach problems at the bench, and to be critical of my own data to get the best from it. I'd also like to say thank you for always being present to bounce (mostly useless) ideas off of – I have no doubt our chats helped save me many disappointing hours in the lab. I would also like to thank Dr Robert Clough who taught me more about ICP-MS and chemistry than I thought I would need as a mere biologist. To both, I am greatly thankful for all of your teachings and I am working on the papers, I promise.

No piece of work would be complete without the input of excellence from technical staff, and this thesis was no different. I would like to thank Dr Andrew Fisher (ICP-MS/ICP-OES), Andy Atfield (4th floor assistance and fish sampling), Ben Eynon and Dr Gareth Readman (fish husbandry), Waldemar Woznica (rodent husbandry), Glenn Harper (TEM), Dr Jo Triner (histology) and Dr Will Vevers (Nanoparticle tracking analysis). I would also like to thank Charlotte Crowther, Dr Audrey Barranger and Dr Richard Maunder for their help on sampling days, and Dr Lee Hutt for our chats about the *viva voce*.

The utmost thanks goes to my mother, Lynda Clark, who would happily listen to me moan about anything related to my thesis, despite not having the faintest idea – and neither did I most of the time. A special thanks to my step dad, Stephen Foot, for his support over the years. Also a thank you to my girlfriend, Kathy Redfern, who never lost faith in me, even when I had.

Author's Declaration

At no time during the registration for the degree of *Doctor of Philosophy* has the author been registered for any other University award without prior agreement of the Doctoral College Quality Sub-Committee.

Work submitted for this research degree at the University of Plymouth has not formed part of any other degree either at the University of Plymouth or at another establishment.

This study was financed with the aid of a studentship from the European Commission (NanoFASE, grant number 646002).

Publications:

Clark, N. J., Shaw, B. J. and Handy, R. D. (2018). Low hazard of silver nanoparticles and silver nitrate to the haematopoietic system of rainbow trout. *Ecotoxicology and Environmental Safety*. 152, 121-131. DOI: https://doi.org/10.1016/j.ecoenv.2018.01.030

Clark, N. J., Boyle, D. and Handy, R. D. (2019). An assessment of the dietary bioavailability of silver nanomaterials in rainbow trout using an *ex vivo* gut sac technique. *Environmental Science: Nano*. 6, 646-660. DOI: https://doi.org/10.1039/C8EN00981C

Clark, N. J., Boyle, D., Eynon, B. P. and Handy, R. D. (2019). Dietary exposure to silver nitrate compared to two forms of silver nanoparticles in rainbow trout: bioaccumulation potential with minimal physiological effects. *Environmental Science: Nano*. 6, 1393-1405. https://doi.org/10.1039/C9EN00261H

Poster presentation contributions at conferences:

Clark, N. J., Boyle, D. and Handy, R. D. (2017). Investigation of the Dietary Bioavailability of Silver Nanoparticles in Rainbow Trout Using an Ex Vivo Technique. Nanomaterial Safety Assessment Conference, February 7-9th, Malaga, Spain. Abstract number 1518.

Shaw, B. J., Letsinger, S. G. R., Correia, M., Ehrlich, N., Clark, N. J., Sharma, V. and Handy, R. D (2017). The Effects of Surface Coating on the Toxicity of CuO Engineered Nanomaterials to Early Life-stage Zebrafish (*Danio rerio*). Nanomaterial Safety Assessment Conferences February 7-9th, Malaga, Spain. Abstract number 1628.

Clark, N. J., Clough, R., Boyle, D. and Handy, R. D. (2017). Development of Single Particle ICP-MS to Measure Engineered Nanomaterials in Biological Matrices. Current Trends in Nanotoxicology Symposium, 2nd June, Plymouth, U.K. Abstract number P.07.

Clark, N. J., Boyle, D. and Handy, R. D. (2017). An Assessment of the Dietary Bioavailability of Pristine and Aged Silver Nanomaterials in Rainbow Trout Using an Ex Vivo Gut Sac Technique. International Conferences on the Environmental Effects of Nanoparticles and Nanomaterials, September 3-6th, Birmingham, U.K. Abstract number 24.

Boyle, D., Clark, N. J. and **Handy, R. D.** (2017). Development of a tiered approach for the assessment of the dietary bioavailability of engineered copper oxide nanomaterials in rainbow trout. International Conferences on the Environmental Effects of Nanoparticles and Nanomaterials, September 3-6th, Birmingham, U.K. Abstract number 26.

Platform presentation contributions at conferences:

Boyle, D., Clark, N. J. and Handy, R. D. (February 7-9th, 2017). Assessment of Dietary Uptake of Copper Oxide Nanomaterials in Rainbow Trout Using an In Vitro Gut Sac Technique. Nanomaterial Safety Assessment Conference. Malaga, Spain.

Clark, N. J., Boyle, D. and Handy, R. D. (13-18th May, 2018). Development of a Rapid Screen to Assess Bioaccumulation Potential: from *Ex Vivo* to *In Vivo* Using Pristine and Aged Nanomaterials in Fish. Society of Environmental Toxicology and Chemistry. Rome, Italy.

Clark, N. J., Clough, R., Boyle, D., Sharma, V. and Handy, R. D. (26-30th May, 2019). Detection of nano-sized particles in fish tissues following an in vivo dietary exposure: a case study using silver nitrate, silver nanoparticles and silver sulphide nanoparticles. Society of Environmental Toxicology and Chemistry. Finland, Helsinki.

Word count of main body of thesis: 66,609

Signed:

Date:

In loving memory of my father, Nigel Thomas Clark.

Abstract

The dietary bioaccumulation and detection of engineered nanomaterials in fish

Nathaniel Clark

Emerging contaminants, including engineered nanomaterials (ENMs), need to undergo environmental risk assessment, whereby they are tested for properties of persistence in the environment, toxicity or bioaccumulation. To date, little data exists for the bioaccumulation of ENMs in animals, particularly fish, with a focus on alternative methods to *in vivo* testing. Also, interpretation of data for hazard assessment is hampered by the lack of routine methods to detect the form of materials in the tissues following exposure. Therefore, there were three main aims to the thesis; the first was to determine the dietary accumulation of ENMs into fish, using a tiered testing approach. The first step was using a short term (4 h) gut sac technique to demonstrate the bioavailability of Ag materials, using pristine (Ag NPs) and aged (Ag_2S NPs) materials. The order of total Ag accumulation was $AgNO_3$ > Ag NPs = Ag_2S NPs; in the mid intestine muscularis, there was 457 ± 111, 38 ± 8 and 39 ± 20 ng/g, respectively. The next step in the testing strategy was an *in vivo* exposure, whereby fish were fed diet containing 100 mg Ag/kg for 4 weeks. Following this, the liver was the main organ of accumulation for all materials, with 4 weeks of exposure leading to concentrations of 122 ± 10, 129 ± 17 and 11 ± 1 µg/g in the $AgNO_3$, Ag NPs and Ag_2S NPs, respectively. The order of bioaccumulation was $AgNO_3$ = Ag NPs > Ag_2S NPs. Various gut transformations (e.g. dissolution) may have been responsible for the similarity of the $AgNO_3$ and Ag NP treatments, and differences between order in the short term gut sac experiment. The second aim was to develop a method of determining the form of the material in the tissues (particulate versus dissolved). A method was developed using the pristine Ag NPs, whereby a series of potential extractants were used. The only suitable extraction method was tetramethylammonium hydroxide + 5 mM $CaCl_2$, and was verified by extracting Ag as $AgNO_3$ and Ag NPs from gut sac tissues without any change to the form of Ag. When this method was applied to *in vivo* samples (as above), it showed 83 ± 20, 73 ± 17 and 5 ± 2 $x10^9$ particles/g dw in the liver of $AgNO_3$, Ag NPs and Ag_2S NP, respectively. Particles were also found in the hind intestine and kidney. The presence of particles in the $AgNO_3$ treatment support the idea that nano-sized particles can be synthesised in the gut lumen or gut tissue, and subsequently transported around the body to the liver. The third aim of this work was to compare rodent gut accumulation with fish, in an exploratory attempt to determine whether rodent bioaccumulation testing can be replaced by fish. This utilised the gut sac technique (as above for fish) in Wistar rats. The total Ag tissue concentrations were higher in the rat (2514 ± 267, 907 ± 284, 1482 ± 668 ng/g in the $AgNO_3$, Ag NPs and Ag_2S NPs, respectively), but showed the same accumulation profile of $AgNO_3$ > Ag NPs > Ag_2S NPs as in fish. One species difference was transepithelial accumulation was shown in the rat, but not in fish. In conclusion, the *ex vivo* gut sac technique with adequate characterisation information, could predict the pattern of *in vivo* bioaccumulation of the Ag materials used here. Particles were present in the hind intestine, liver and kidney of all Ag treatments following dietary exposure, and to a lesser extent in the Ag_2S NP treatment, indicating ENM chemistry has an important role in

bioavailability. Finally, the rat gut sac experiment did not produce the same data as the fish gut sac experiment, but shows the current risk assessment of dissolved Ag will cover Ag ENMs.

Contents

List of Figures

List of Tables

List of abbreviations and symbols

Abbreviation	Description
µg	Microgram
µL	Microlitre
µmol	Micromolar
3R’s	Reduction, refinement, replacement
ADME	Adsorption, distribution, metabolism and excretion
Ag	Silver
Ag NPs	Silver nanoparticles
Ag_2O	Silver oxide
Ag_2S NPs	Silver sulphide nanoparticles
AgCl	Silver chloride
$AgNO_3$	Silver nitrate
Al	Aluminium
Au	Gold
Au NPs	Gold nanoparticles
BB	Body burden
BCF	Bioconcentration factor
BLM	Biotic ligand model
Ca^{2+}	Calcium ion
$CaCl_2$	Calcium chloride
$CaNO_3$	Calcium nitrate
Cd	Cadmium
cm	Centimetres
CO_2	Carbon dioxide

CPS	Counts per second
Cu	Copper
Cu NPs	Copper nanomaterials
CuO	Copper oxide nanomaterials
DLVO theory	Theory of colloidal behaviour
DOC	Dissolved organic carbon
dw	Dry weight
EDTA	Ethylenediaminetetraacetic acid
ENM	Engineered nanomaterial
Fe	Iron
g	Gram
GSH	Total glutathione
h	Hour
H^+	Hydrogen ion
Hg	Mercury
ICP-MS	Inductively coupled plasma mass spectrometry
ICP-OES	Inductively coupled plasma optical emission spectrometry
In	Indium
Ir	Iridium
K^+	Potassium ion
K_1	Uptake rate
K_2	Excretion rate
KCl	Potassium chloride
kg	Kilogram
KNO_3	Potassium nitrate

L	Litre
LOD	Limit of detection
m/z	Mass-to-charge ratio
mg	Milligram
Mg^{2+}	Magnesium ion
$MgSO_4$	Magnesium sulphate
mins	Minutes
mL	Millilitre
mmol	Millimolar
Mn	Manganese
n	Number of replicates
NA	Not applicable
Na^+	Sodium ion
NaCl	Sodium chloride
$NaH_2PO_4.H_2O$	Sodium phosphate monobasic monohydrate
$NaHCO_3$	Sodium bicarbonate
$NaNO_3$	Sodium nitrate
ND	Not determined
ng	Nanogram
Ni	Nickel
nm	Nanometres
NTA	Nanoparticle Tracking Analysis
O_2	Oxygen
OECD	Organisation for economic co-operation and development
-OH	Hydroxyl group

Pb	Lead
PBT	Persistence, bioaccumulation and toxicity
PEC	Predicted environmental concentration
PNEC	Predicted no effect concentration
r^2	Coefficient of determination
REACH	Registration, evaluations, authorisation and restriction of chemicals
S.D.	Standard deviation
S.E.M.	Standard error
-SH	Sulfhydryl groups
spICP-MS	Single particle ICP-MS
SWCNTs	Single walled carbon nanotubes
TBARS	Thiobarbituric acid reactive substances
TEM	Transmission electron microscopy
TiO_2	Titanium dioxide
TMAH	Tetramethylammonium hydroxide
ww	Wet weight
Zn	Zinc
ZnO	Zinc oxide nanomaterials

Chapter 1 - Literature review

1.1 Introduction

New and emerging contaminants, such as engineered nanomaterials (ENMs), are assessed for environmental safety under the registration, evaluations, authorisation and restriction of chemicals (REACH) guidelines in the European Union. Much of the regulatory testing involves experimental designs which were developed for dissolved chemicals and at relatively high concentration in order to demonstrate dose-response which may not capture the environmentally relevant predicted exposure concentrations. While the REACH guidelines can be applied to ENMs, there are some practical problems with implementation. For example, in order to calculate risk of ENMs, exposure and hazard needs to be known, but there is a shortage of validated data on the measured environmental concentrations of ENMs (Lead et al. 2018). Instead, there is reliance on modelling for predicted exposure concentrations with computer models that seldom account for specific particle behaviour and colloid chemistry. However, while there are now many scientific reports of the ecotoxicity of ENMS (e.g. reviews Menard et al. 2011; Bondarenko et al. 2013; Ma et al. 2013), these studies have mostly been on fundamental research rather than with the data requirements of REACH in mind. Consequently, there is a significant lack of no observed effect concentrations (NOECs), which are needed for the risk assessment. Without a predicted environmental concentration (PEC) and predicted no effect concentrations (PNEC), the risk assessment has an unacceptable level of uncertainty and cannot be satisfactorily completed.

Under the REACH legislation, the industrial production of any new substances over 1 metric tonnes per year requires the substance to be tested for its environmental safety. The testing strategy includes determination of the physico-chemical properties of the substance in environmental media (e.g. freshwater) and chemical characteristics that are a

matter for public safety (e.g. flammability of chemicals); also data from ecotoxicity tests and information on mammalian toxicology are required (see Crane et al. 2008 for the testing strategy). In general, risk assessors are looking for three main factors of concern for any chemical: (i) persistence in the environment (ii) toxicity to wildlife and humans, (iii) bioaccumulation potential (i.e., PBT). REACH legislation on substances applies to both naturally occurring chemicals (e.g., metals extracted by mining) and to man-made organic chemicals.

There have been many studies on the fate and chemical behaviour of substances in the environment (e.g., Ag, Luoma et al. 1995, Cu, Flemming and Trevors 1989; organics, Karickhoff 1984) and also on toxicity of environmental contaminants to aquatic and terrestrial organisms (e.g., Ag, Luoma et al. 1995 [and references therein], Cu, Fjällborg and Dave 2004; organics, Pereira et al. 2009). However, over recent years, effort has focused on the bioaccumulation potential and trophic transfer of new substances, especially those with only partial documentation under REACH (e.g. Hou et al. 2013; Tangaa et al. 2016). This is partly driven by the REACH legislation which now requires environmental agencies to take direct responsibility for environmental aspects of human health (e.g. the integrity of the food chain) and the notion that bioaccumulation presents a persistent internal exposure of potentially toxic chemicals to wildlife. Thus bioaccumulation is associated with the long term health of wildlife and the life-time environmental exposure risks in humans.

For REACH and for fundamental research, a clear definition of bioaccumulation is needed in order to distinguish it from other related processes including bioconcentration and biomagnification. Bioconcentration is defined as an increase in the organism's tissue burden of an organic chemical(s) or toxic metal(s) above that measured in the external water (OECD 2012). Bioaccumulation is a similar idea to bioconcentration but refers to the

point at which the net uptake of the substance exceeds net excretion, such that a tissue burden occurs in the animal from the respiratory media or diet (OECD 2012, Handy et al. 2018). Bioaccumulation is usually measured over several weeks so that the internal tissue concentrations are in steady-state with that in the surrounding medium (Veith et al. 1979). Bioaccumulation testing was originally designed to compare the concentration of a soluble chemical in the water with that of fish tissues after 32 days exposure (Veith et al. 1979). One practical problem with the test is maintaining the exposure, especially for poorly soluble chemicals. Consequently, a dietary bioaccumulation test was devised (e.g. OECD 305) and "dietary bioaccumulation factor" is a specific term relating to exposure through food. The OECD 305 states this test leads to a calculated biomagnification factor. This is not technically true; biomagnifiction is increased tissue burden with trophic level but this terminology allows the two tests (e.g. waterborne or dietary exposure) to be distinguished. In the present review, bioaccumulation is used to describe accumulation from dietary exposure only as less is understood about this exposure route.

The bioaccumulation of organic chemicals or metals is regarded as a "snap shot" in time of various biological processes; notably adsorption into an organism, distribution around the body, metabolism within tissues, and excretion from the body (termed ADME). Bioaccumulation is the sum of these events. From a practical perspective, for the bioaccumulation potential of a substance to be assessed, sampling must be frequent enough to demonstrate an increase in the body burden over time such that internalisation reaches steady state (i.e., long experiments with multiple time points). However, in regulation it is recognised that a lengthy bioaccumulation test can be expensive and so it is also permissible to calculate a kinetic bioaccumulation factor based on the initial rates of uptake (k_1) and elimination (k_2) in the revised OECD test method (OECD 2012). The suggestion is now that the dietary exposure method used for "difficult to handle substances" in OECD TG305

can be applied to other emerging pollutants, including engineered nanomaterials (Handy et al. 2018).

Nanotechnology is the application of ENMs in products and processes, with its emergence being of economic and societal importance. An ENM is manufactured to have novel properties arising from the nanoscale, yet an internationally agreed definition of an ENM for regulatory purposes is still a subject of debate. For example, the Joint Research Council use a definition with two components; where a nanomaterial is a substance with a primary particle size is below 100 nm, and a size distribution where at least 50% of the particles are below 100 nm (Bleeker et al. 2013 and references therein). The latter caveat was added to the definition to distinguish an intended nanomaterial from a bulk material that was not intended to be produced as nano but may contain an incidental fraction at the nanoscale. Some authors argue the different properties that exist at the nanoscale compared to the dissolved metal or bulk form are more important (surface reactivity, crystallinity and thermodynamic stability) and should be included in the definition, or at least be key parameters in any hazard assessment (Stone et al. 2010). The logic for the latter is that the reactive surface area and therefore the potential for toxicity may increase exponentially at very small size, e.g., < 30 nm (Auffan et al. 2009; Klaine et al. 2012). These differences could complicate traditional size based classification and thus it may be beneficial to separate ENMs into two further categories (1-30nm and > 30nm), although toxicological data supporting this idea is yet to be found. A more traditional classification system based on the chemical composition of ENMs is available. ENMs fall into four broad categories; carbon based (single- and multi-walled nanotubes, and fullerenes), mineral based (metals and metal oxides), organic (polymers dendrimers and surfactant coatings) and composites (more than one component e.g. quantum dots, and doped metals and metal oxides; Stone et al. 2010). The novel properties at the nanoscale may lead to chemical behaviours and

toxicities not expected from the traditional form of the same chemical substance. Given the breadth and variety of new ENMs being produced (e.g. composites, surface functional groups, etc.), there are too many variants to test each substance as a new chemical. Thus screening methods and/or a tiered approach to testing is required, where only materials of most concern are put forward for *in vivo* bioaccumulation testing. This approach to testing also has an ethical implication for animal welfare (3 R's) and is intended to reduce use of vertebrate animals in the testing strategy.

The aim of this review is to address two emerging aspects of bioaccumulation testing for ENMs: (i) can a tiered approach to environmental assessment of bioaccumulation in fish be applied to ENMs, and (ii) will the bioaccumulation test work and be validated for use with ENMs. For the latter, specifically whether a bioaccumulation test for difficult to handle substances can be used with colloids (e.g., ENMs). Additionally, this review aims to outline the cellular pathway of uptake an ENM may take from the external environment (e.g. fish gut) to the internal compartments and the biological processes involved in the adsorption, distribution, metabolism and excretion (ADME) of nanomaterials.

1.2 Hazard assessment strategy and bioaccumulation testing

The initial steps in REACH include the examination of data on closely related chemicals and where "read across" is possible then less new testing may be required of the new substance. In order to avoid a full suite of testing, a new chemical needs to demonstrate similarity to the existing chemical. In the context of ENMs, this would aim to show, for example, that carbon and carbon nanotubes have similar ecotoxicity and physico-chemical (Gajewicz et al. 2015). However, this may be problematic for ENMs, due to their complex

behaviour in environmental media such as agglomeration, aggregation, dissolution, as well as transformation of the surface properties and formation of coronas on the particles (e.g., reviews Lowry et al. 2012; Walkey and Chan 2012). Clearly ENM specific properties should be incorporated into the risk assessment such as size, shape and surface reactivity. Under the current testing paradigm by REACH for solutes, there is a logistical concern of producing a specific environmental risk assessment for each ENM as a new substance (e.g., Voelker et al. 2015), which will be impractical given the diversity (e.g. surface coatings and functionalisation) and the rate of ENM production.

To produce an environmental risk assessment for ENMs, four components are required: problem and hazard identification, exposure assessment, effect assessment and risk characterization (Koelmans et al. 2015). This is a toxicologically orientated approach looking to document the effects of ENMs on biota. Both effect assessment and risk characterization involve using the predicted exposure concentration (PEC) and predicted no effect concentration (PNEC) values. The PEC/PNEC ratio is a trigger for additional testing. If the PEC/PNEC ratio is >1, then there is a problem that requires in depth risk analysis. Currently, there is heavy reliance on the PEC, relative to the PNEC with respect to toxicity to the organisms. This approach is simple and pragmatic, and has found utility in hazard assessment of dissolved chemicals (Comber et al. 2003).

The PEC/PNEC approach is problematic for some substances, especially ENMs. The routine detection of ENMs in the natural environment is currently not available, although methods are being developed (Von Der Kammer et al. 2012). Exposure information for the risk assessment currently relies on surface water models to give predicted environmental concentrations. For ENMs these predictions are in the low µg/L range (Gottschalk et al. 2013; Dumont et al. 2015). Some actual measurements of ENMs in the environment are now being reported, but these are often only for metal particles that

are less difficult to measure. For example, Kiser et al. (2009) found 17 µg/L titanium in the tertiary effluent of a wastewater treatment plant (although this represents a 91% reduction compared to the influent). Such titanium particles were identified by SEM and were composed entirely of TiO_x primary particles less than 100 nm; the authors concluded that these were the same shape and size as those used in industrial and food products (Kiser et al. 2009). The above gives probable cause for environmental exposure, and consequentially PBT should be assessed for ENMs. The strategic issue for testing is whether or not bioaccumulation tests for ENMs should be performed sooner in the testing strategy, or given more importance in the overall hazard assessment. So far the focus for ENMs has been on ecotoxicity (Menard et al. 2011; Shaw and Handy 2011; Ma et al. 2013; Rana and Kalalchelvan 2013; Khan et al. 2015) and PEC values (Mueller and Nowack 2008; Gottschalk et al. 2013), with little attention being paid to bioaccumulation potential. Bioaccumulation potential is often not the first trigger for a substance of concern in the environment. Bioaccumulation tests would usually come later in the testing strategy, often after a base set of acute aquatic toxicity tests on algae, *Daphnia* and fish.

The assessment of the bioaccumulation of ENMs in organisms, especially fish has not been addressed. Bioaccumulation tests are an important aspect of the testing strategy; it is a chronic test, at sub-lethal concentrations with no mortality (beyond incidental background deaths), resulting in a chronic NOEC value. Bioaccumulation tests are set around the principle of uptake of solutes and achieving a steady state in tissues relative to the exposure media concentration – for this reason experiments tend to be long.

The OECD bioaccumulation test gives a choice of either an aqueous or dietary exposure method. In aqueous tests, the behaviour of ENMs causes several problems; notably the tendency for agglomeration and settling from the water column (Praetorius et al. 2014a; Labille et al. 2015). For example, Ward and Kach (2009) demonstrate that

aggregates of ENMs were preferentially taken up by mussels over dispersed ENMs. In terms of fish species, this could mean that benthic demersal species should be investigated over pelagic species. Ultimately, this does not mean that pelagic species will not be exposed as a plethora of studies have demonstrated waterborne exposures result in metal internalisation (e.g., Shaw et al. 2012), but may mean the risk of uptake is predominantly through food chain transport. Pragmatically, this would suggest a dietary bioaccumulation test as the most ecologically relevant method.

Bioaccumulation tests are long (e.g. 28 days), expensive, and animal intensive; therefore it is appropriate to use a tiered approach to screen materials to ensure suitable testing. In the context of a dietary bioaccumulation test, such a tiered testing approach has been proposed to include (Handy et al. 2018): physico-chemical analysis and chemical triggers for ENMs of concern, the use of *in silico* models and read-across from invertebrate studies, a fish gut digestibility assay to identify bioavailable fractions of ENMs, *ex vivo* experiments to demonstrate uptake by the gut (e.g. gut sacs and perfused intestines) and finally *in vivo* testing (e.g. dietary bioaccumulation). In addition, for ENMs intended as agrochemicals such as pesticides, trophic transfer (e.g. comparison of BCF factors across trophic levels), and mesocosm experiments may be needed. This tiered approach would be useful for screening materials. For example, early chemistry-based steps would identify ENMs that dissolve in simulated fish gastrointestinal fluid, whereby current paradigms of tissue uptake kinetics would explain bioaccumulation. In the case of ZnO ENM, the first step is to consider the physico-chemical properties; these may benefit from being conducted in the media used for actual testing (e.g. saline and at differing pH values for gut sac experiments; Al-Jubory et al. 2013) as well as being physiologically relevant. One common approach to ENM characterization for assessing the fraction of dissolved to particulate material is the use of a dialysis experiment. Such physico-chemical assessments should be

conducted in biologically appropriate exposure media; for example, digestibility and gut sac experiments utilise saline at pH 7.8, which is physiologically relevant to the intestinal area of the fish gastrointestinal tract. Such experiments should also be conducted in pH 2-5 to represent other areas of the digestive tract (Bucking and Wood 2009), notably the stomach in carnivorous fishes that use acid digestion. Under such acidic conditions, ZnO is likely to dissolve; the implications of this on the testing strategy are straight forward; fully dissolved ZnO will have the same bioconcentration factor (see below) for dissolved Zn. Consequently, no addition testing in the ZnO form is required.

1.3 Applying the Difficult to Handle Substances Approach to ENMs

One of the original drivers for determining bioconcentration factors (BCF; i.e. tissue concentration divided by the external aqueous concentration) was the difficulty and expense of determining concentrations of organic chemicals in the water and in the tissue of wildlife. Thus, pragmatically, if a bioconcentration factor could be derived, one might be able to estimate the internal concentration inside an organism, armed only with data on the exposure concentration and time. These ideas have been applied to bioconcentration measurements for organic chemicals of varying lipophobicity and works for lipophilic organic chemicals because they are easily taken up across biological membranes by diffusion, and do not necessarily require a specific transporter pathway like other solutes or more polar compounds. It has long been postulated that the lipid solubility of an organic chemical may therefore inform on its bioaccumulation potential. The lipid solubility of chemicals is measured using the n-octanol-water partition coefficient determination. This test compares the fraction of substance dissolved in octanol and water. This is now a standard OECD test (OECD 1995) which identifies how much a substance will dissolve in

a lipid compared to a water phase. There have been several attempts to correlate the octanol-water partition coefficients with actual measurements of bioaccumulation in fishes and other animals (e.g. Veith et al. 1979; McKim et al. 1985; Wu et al. 2008; Wu et al. 2011). In general, the correlations are reasonable predictors of bioaccumulation of organic chemicals, but there are exceptions and problems.

The traditional bioaccumulation tests (Veith et al. 1979) used water as the exposure media over a period of 32 days. These were successful at achieving steady-state between the compartments (water and fish tissue) for partially soluble organic chemicals (e.g. phenolic compounds, organic acids etc.), but very hydrophobic materials were problematic (benzene, toluene etc.). The use of solvents, such as soaps and detergents, can help maintain stability in water, but these can also be toxic to fishes. Within the last 20 years, researchers conceded that aqueous exposure may not be the most practical way of achieving a long-term exposure for hydrophobic chemicals.

1.3.1 Dietary bioaccumulation tests for dissolved chemicals

While there was agreement on the necessity for a dietary bioaccumulation test for substances that were difficult to handle in aqueous media, how the oral dose of organic chemical should be administered to the fish has been the subject of debate to encompass differences in the experimental aims, but also to consider (or not) the environmental realism of the dosing method. Two approaches have been used: oral gavage and dietary feeding studies. Oral gavage is the process whereby a fish is anaesthetised and a dose of a liquid sample is injected through the mouth near the pylorus and posterior intestine. The former method has merit for assessing parent compound bioaccumulation due to the behaviour of organics in the stomach; under high pH conditions, the parent compound is likely to be

altered (e.g. hydrolysed), thereby increasing its polarity and making it less bioavailable by simple diffusion. In addition, the gavage method can allow for careful quantification of the dose administered to each fish. This technique has limitations from a physiological relevance perspective. Fish would not normally ingest a bolus of saline. Furthermore, the technique is dependent on recovery of the fish from the treatment and anaesthetic, where high wastage of fish is possible. In response to this, a dietary feeding method using food containing the chemical of interest is used as the vehicle for exposure. This overcomes the issues of physiological relevance, allows for calculation of an average amount of feed (with a known concentration) administered to a tank and treatment of fish and can be maintained for long periods of time without the need for anaesthesia. Consequently, a dietary bioaccumulation method was developed by the OECD (OECD 2012).

While the n-octanol-water partition coefficient is successful in predicting bioaccumulation potential of hydrophobic substances, a different approach was required for hydrophilic substances. Dissolved metals are water soluble, so the octanol-water coefficient is not a useful tool for predicting bioaccumulation potential. The idea here was to assess bioaccumulation potential through measuring uptake (K_1) and excretion (K_2) rates. Some metals are known to be bioaccumulative; notably the trace metals with no known biological function, where the organisms have not evolved metal-specific excretion mechanisms (e.g., Ag, Cd, Hg, Pb). The nutritionally required metals (e.g., Zn, Cu), are controlled by well-known homeostatic mechanisms and tend not to be bioaccumulative. However, this does not mean that the latter are harmless to organisms in excess.

The kinetic bioaccumulation potential can be mathematically modelled. Kinetic models are diverse and range from simple (2-box model) to complex (multiple-box model). For simple models, the two compartments can simply represent the internal and external environment of an organism. In complex models, each organ and the circulatory system

can be represented by separate compartments that are kinetically indistinguishable and that once entered into a compartment, it is uniformly distributed (Barron et al. 1990).

1.3.2 Applying a dietary bioaccumulation test to ENMs

The methods used for assessing bioaccumulation potential may not be appropriate for ENMs based on the fundamental fact they are not at equilibrium (e.g., non-steady-state). While it may be functional for carbon based materials (e.g. Jafvert and Kulkarni 2008), the n-octanol-water partition coefficient does not work for most ENMs; the founding assumption that diffusion into the two phases on the base of lipophilicity is not valid in ENMs (Xiao and Wiesner 2012; Praetorius et al. 2014b). Thus, one of the key triggers for bioaccumulation testing is not valid for ENMs. The difficulty of maintaining hydrophobic chemicals in waterborne tests are even more challenging for ENMs. For example, the use of dispersants can aid in maintaining adequate exposure by preventing particle settling, but (i) the dispersing agents that work best for ENMs are often highly toxic (Handy et al. 2012), and (ii) their use only slows the rate at which the ENMs aggregate and settle; it does not prevent it. Stirring and shaking of test vessels containing ENMs could be used, but there are concerns of mechanical injury to the test organisms. For a waterborne test method involving very small fish or early life stages, these problems are partly resolved with modified test equipment (e.g. Shaw et al. 2016). However, this may not be suitable for the larger fish needed for a bioaccumulation test.

This difficulty of maintaining adequate suspensions of ENMs indicates that dietary exposure is more appropriate. By using fish feed that contains a known ENM concentration; an ingested BCF can be calculated. Indeed, the issues of bioavailability remain in the gut lumen (i.e., the external media) as the food is broken down in the gut, presumably releasing

particles that aggregate and settle. However, there may be a propensity to overestimate the bioaccumulation potential across the gut compared to the gills given that the latter is an exceptionally tight epithelium, whereas the gut is comparatively leaky. Similar to an aqueous test, if the k_1 and k_2 rate constants could be calculated for the gut, the bioaccumulation potential of ENMs could be calculated.

The guidelines of the fish bioaccumulation test 305 for using difficult to handle substances (OECD 2012) state a list of prior physico-chemical properties and information criteria that should be known about the chemical. This is not an exhaustive list, but is guidance to aid data interpretation. This list includes: 1) analytical sensitivity in the matrix of interest (e.g. food and tissue), 2) water solubility, 3) n-octanol-water partition coefficient, 4) stability in water, 5) stability in food, 6) relevant phototransformations under test conditions, 7) vapour pressure, 8) biota and abiotic degradation in water (e.g. biodegradability), 9) information on metabolites, and 10) the acid dissociation constant. For metal or metal oxides ENMs, knowledge can be gained of numbers 1 (analytical standards, reference materials, spike recovery tests), 2 (dialysis experiments), 4 (light scattering methods to determine settling), 5 and 10 (*in chemico* digestibility assays). Criteria 6 are largely unknown for ENMs, yet under gut conditions, the presence of the microbiome could result in biotransformation, and the effects of gut microbiome on the bioaccumulation test is not included in the OECD list of criteria.

Applying models to ENM bioaccumulation is not currently possible due to the fundamental issue of the lack of data currently available in fish species. For example, it is unknown whether the liver is a central compartment for ENM exposure, as it is for dissolved metals (see later). In addition, the behaviour in the blood and body distribution of ENMs is unknown. Models (Barron et al. 1990) assume solute chemistry and the extracellular space associated with tissues. However, there is no certainty on how an ENM

spreads around these fluids. With this in mind, the fundamental understanding of ENM behaviour in organisms urges the use of simple two-compartment models (Handy et al. 2012).

To ensure the most accurate and reliable data for a given ENM concentration, it is clear that a dietary bioaccumulation test approach is required. Currently there is very little data produced on their bioavailability across the gut. The rest of this review is devoted to suggesting the potential path of an ENM from the external environment (e.g., gut lumen) into the body and potential fate within the fish through the processes of adsorption, distribution, metabolism and excretion (ADME).

1.4 Vertebrate gastrointestinal physiology

The gastrointestinal tract is a predominantly tubular, semi-permeable barrier which extends from anterior (head/buccal cavity) to posterior (anus) of the fish and separates the external (gut lumen) from the internal (cellular and tissue) environments. The aim here is not to give a detailed account of the physiology and morphology of the gastrointestinal tract found throughout individual fish and between species, which are described elsewhere (e.g., Bakke et al. 2011), but to describe its function within the context of ENM exposure. However, appropriate physiological differences between fish species will be highlighted.

Various physiological factors will underpin the ingested dose and the exposure time. The amount of contaminated food ingested will be a product of ration size and feeding frequency, both of which alter the gut transit time (i.e., exposure time of the epithelium). The uptake efficiency also changes with exposure concentration in the food and with ration size (Kamunde and Wood 2003). In general, uptake efficiency declines exponentially with concentration, and can be considered as a protective mechanism to limit the absorption of

toxic chemicals at high concentrations in the gut lumen. In order to produce a standardised test, the ration and feeding regime needs to be fixed. In addition, the gut conditions under which the dietary bioaccumulation study is occurring should be near optimal for the species of fish (e.g. water temperature and a ration size). Practical considerations need to be given to diet preparation as the digestibility of the food influences exposure. Three methods are commonly used for diet preparation; (i) top dressing where chemicals are added to the food by coating pre-made pellets and fixing in place with gelatine, (ii) pellet formulation whereby chemicals are sprayed onto the raw materials and the pellet formed with a homogenous distribution of the test substance throughout the pellet, and (iii) biologically incorporated food where exposed invertebrates are subsequently prepared into a feed (e.g. dried, ground and pelleted) or fed fresh. Regardless of the chemical addition to the food, it would be relatively easy to over- or under-regulate the risks from ENMs if the food is easily digested or indigestible, respectively.

While it is clear that various physiological factors will affect the exposure of the gastrointestinal tract to ENMs, how the ENMs affect the gut is less clear. The gastrointestinal tract has four main physiological functions: motility, secretion, digestion and absorption. These processes result in the gastrointestinal tract lumen being a dynamic environment that changes with physiology. Each of these functions will be considered for potential consequences under ENM exposure.

The gut has two associated neural networks; one under the mucosa and one between the muscularis. These neural networks communicate with the central nervous system and influence the gut motility to assist passage of chyme and digestion. While there have been no assessments on the effects of ENMs on neurological control of gut motility, ENMs have been demonstrated to cause pathology in the brain during waterborne exposure to Cu NPs (Al-Bairuty et al. 2013). So it may be plausible for dietary exposure to affect gut neural

networks, but the resultant effect on motility and digestive processes remains unknown. Stretch receptors are also present within the gastrointestinal tract to register stomach fullness and prevent over eating, but it is not certain if ENMs interfere with their functioning. Consequently, ENM exposure may cause gut motility to function to fast (resulting in diarrhoea), or too slow. When motility is slow, the time for adsorption goes up, so the efficiency improves for a while. However, the nerves also coordinate secretory functions and the precise timings of the release components of the digesta – failure of this could lead to very inefficient digestion.

Accessory organs, such as the liver and pancreas, play a role in secretion of enzymes and hormones into the gut lumen. Given that some enzymes are secreted from the pancreas into the gut lumen in an inactivated mode (with subsequent enzymatic activation; Bakke et al. 2011), this could be a problem given that some ENMs prevent enzymes from working (see below). The liver releases acidic steroids that have detergent like properties (Bakke et al. 2011). Whether these would interact with the ENMs in a similar manner to dispersants added to stock solutions in waterborne exposures is unknown, but it is a natural source of dispersants that could enhance ENM stability and bioavailability. More so, if these detergents interacted with the ENMs, the resultant effect on their biological use (i.e. breaking down complex lipids) remains unknown. Currently, hepatopancreatic and hepatobiliary recycling of enzymes and detergents is hypothesised (Bakke et al. 2011), but it is also unknown if these processes are likely to function with ENM interaction (binding or chemical alteration).

Digestion is a process mainly affiliated with enzyme action and exactly how the ENM presence will affect this process is currently unknown. Some ENMs demonstrate inhibition of enzymes (e.g. MacCormack et al. 2012), but the enzymes of interest tend to be intracellular. Of those found within the gut lumen of fish, α-amylase has demonstrated

increased catalytic properties when immobilized with ENMs in conjunction with altered pH and temperature optimum (e.g. Khan et al. 2013; Sohrabi et al. 2014). A wealth of data has been provided demonstrating the catalytic properties of ENMs, analogous to those of enzymes (review Wei and Wang 2013). The most frequent reaction is those of oxidase enzymes, indicating that simple reactions could occur and assist in digestion. It must be noted that the majority of literature reviewed by Wei and Wang (2013) is concerned with chemical reactions in highly controlled environments, and not complex matrices such as those in the gut lumen. Indeed, particulate exposure to the gastrointestinal tract is not a new phenomenon. Tropical species of fish have been known to ingest calcareous food (e.g. Parrotfish on sponges; Wulff 1997), which is indigestible and passes through the gut. ENMs may behave in a similar manner, but could enhance the digestion of food items through mechanical breakdown. Some fish species have enhanced breakdown of food items, particularly carbohydrates, through microbial fermentation. Given that Ag ENMs show antibacterial properties to fish gut microbes *in vitro* (Soltani et al. 2009), *in vivo* evidence of this effect is lacking (Merrifield et al. 2013). However, Cu ENMs caused a significant alteration (as determined by denaturing gradient gel electrophoresis) to the gut microbiome of zebrafish exposed to 500 mg Cu/kg for 14 days (Merrifield et al. 2013). Such changes to the gut microbiome will be of particular concern in herbivorous fish.

Adsorption is the active or passive processes that transport nutrients from the gut lumen across the mucosal layer and pass through the apical membrane into the cell. Whilst the mucus layer has multiple functions (Handy and Maunder 2009), in the context here, the most important is its tissue protective properties for separating the gut surface muscle from the potentially corrosive chemical environment in the lumen. While irritants such as chemicals can cause a sloughing of the mucus; this sloughing capability is finite and can eventually result in tissue being exposed directly to the gut lumen chemistry. While

sloughing is not an ENM specific response, should exposure to ENMs come under other sufficiently stressful circumstances, the gut as a biological barrier could be damaged. Under these circumstances, the principle of a bioaccumulation test becomes superfluous and obsolete. In addition, it has recently been suggested that problems with gut mucosal health can lead to a multitude of infective and hormonal pathologies in humans (Bron et al. 2017), with data for this in fish species yet to be obtained.

Currently there is no data on the effects of ENMs on the absorption efficiency of nutrients. Ultimately, it will depend on nutrient-ENM interactions. Given that most absorptive processes are enzymatically mediated, it is possible that the potential issues highlighted for digestion will occur here. As nutrients are either taken into the cell through passive diffusion (fats) or by active uptake (simple carbohydrates and amino acids from proteins), interactions with ENMs within the lumen, such as binding, may slow this process. It would seem logical that any interference with adsorption of essential nutrients would manifest itself in poor growth, yet the opposite was observed by Zhou et al. (2009) when 0.5 mg/kg selenium nanoparticles was added to the diet. The same effect was also found in the dissolved metal equivalent (Zhou et al. 2009). In this study, selenium was the only nutrient altered, with the effect of form assessed (e.g. ENM versus dissolved).

1.5 Differences between solute and colloid chemistry

The theory behind electrolyte behaviour in solutions is well established. A substance that is truly dissolved has a hydration shell of water and can move through the solvent (e.g. freshwater) by diffusion. This diffusion is limited by hydrogen bonding with water molecules in the case of organic chemicals (effectively increasing the apparent mass, so slowing the molecule down). For metals, their mobility in water depends on their hydrated

ionic radius and charge, with the charge density determining its mobility. Small ions of low charge move faster, thus H^+ is the fastest ion in solution and mobility is measured relative to that of H^+. Metals such as lead and cadmium move slower due to large mass and charge density (see Handy and Eddy 2004).

The behaviour of ENMs in solvents is much different to those of solutes. ENMs are much larger, which results in much slower diffusion rates through liquids than ions and small molecules. The diffusion of colloids is influenced by their surface charge (electrostatic repulsion) and van der Waals forces; collectively termed the DLVO theory. The DLVO is useful for predicting settling rates based on size and mass of the ENM, and the composition of the water (pH, ionic strength, Ca^{2+} concentration, dissolved organic matter; see Handy et al. 2008b).

1.5.1 Bioavailability and fate of dissolved chemicals in the gastrointestinal tract

The first step in the accumulation of any substance, whether it is dissolved or dispersed in the environmental media, is for it to move from the bulk volume of the liquid (e.g., gastrointestinal chyme) to the epithelial or other surfaces of the organism (Handy et al. 2008a). The propensity of a substance to associate with biological surfaces and be subsequently absorbed is termed bioavailability (Meyer 2002). The internally absorbed fraction is sometimes called the 'bioaccessible fraction', while the fraction that initiates biological responses or effects might be regarded as a 'bioreactive' component.

For organic chemicals the bioavailability is a function of water pH (influencing the charge and/or polarity of the substance, and thus its ability to diffuse), the temperature (speed of diffusion), as well as the presence of organic matter or other ligands that may hinder diffusion of the chemical molecules. Finally, according to the principles of diffusion

(Fick equation), the concentration of the substance and the inward concentration gradient is also important (see Visscher and Johnson 1953), along with the surface area of the organism and the innate permeability of the gut epithelium or other relevant external surface.

When metals are dissolved in water, they are not always as an ion, but can form various complexes. Common inorganic complexes are with anions, such as hydroxides and chloride; thus metal speciation in water is often a function of either water pH or anion difference. In the presence of organic matter in the gut lumen, metals will also bind according to their charge and mobility, with –SH groups in the organic matter being particularly good at binding metals. In addition, electroneutral complexes (no charge) can be formed and so diffuse like some organic chemicals directly through cell membranes (review Escher and Sigg 2004). Redox chemistry, and hence speciation of dissolved metals, is influenced by pH of the media. For example, aluminium is sparingly soluble between pH 6 and 8, and so is of less concern to biota in relatively neutral conditions (Spry and Weiner 1991). The pH of the media has a second influence on the bioavailability of metals; it competes with other ions for uptake via protein channels. This occurs for essential metals, even when the metal is in excess over the hydrogen ion (e.g. Na^+; Handy and Eddy 1991). Therefore, pH can either decrease (by competing for uptake) or increase (alter metal speciation to highly bioaccessible form) the bioavailability of dissolved metals (Spry and Wiener 1991). These processes controlling dissolved metal bioavailability in water are applicable to the bioavailability of the gut, but the dissolved organic carbon is likely to be higher and so the dominant factor affecting bioavailability.

The mucous layer in the gut is that which is situated between the chyme and the cells. It is primarily composed of water (~95%), with the remainder being comprised of salts, small soluble molecules, protein and mucins (Handy and Maunder 2009). The

chemical composition of the mucous, which will change with regards to the external environment (e.g. freshwater and marine water), gives rise to its physical properties. Mucous is important in forming the unstirred layer (Fig. 1-1). For the gill surface, dissolved metals have certain binding affinities which have led to models such as the biotic ligand model (BLM) and the free ion model. These models predictive binding affinity alter with the surrounding chemistry. Such detailed information is yet to be obtained for the gut.

1.5.2 Bioavailability and fate of ENMs in the gastrointestinal tract

The DLVO theory is attributed to describe the behaviour and fate of colloids (Verwey and Overbeek 1948) such as ENMs. Properties of ENMs, such as surface charge, will affect the fate of the material (Christian et al. 2008) through interactions with the gut lumen chemistry. Consider a negatively charged particle in water, the presence of H^+ will neutralize its charge, but not all of the H^+ will be used in this process. The result is excess H^+ ions that remain in the vicinity of the particle through electrostatic attraction. This process creates two layers: one formed by the charged surface of the particle and the second of oppositely charged ions. However, in nanoecotoxicology we are dealing with more complicated systems with more than one particle and so there will be an interaction between double layers of particles. The diffuse double layer creates stability for the colloid suspension to prevent agglomeration (called peptization) and depends on the presence of ions, but the excess addition of these ions can disrupt the system through flocculation and agglomeration (full description in Verwey and Obverbeek 1948). The degree of aggregation will be a function of temperature and particle movement, predominantly through Brownian motion (Handy et al. 2008a). The double layer forces are hence a factor causing aggregation, but this is in an additive manner with Van Der Waals interactions; the

former force acts as a negative interaction while the latter force acts in a positive fashion. The sum influence of these interactions will be a function of size of the particle and how the double layer thickness changes in comparison to particle size (Verwey and Overbeek 1948). This theory has been accepted to explain the behaviour of colloid materials.

The gut lumen environment of fishes is dynamic in nature and changes in relation to the region of the gut (e.g., pH, ionic strength; Bucking and Wood 2006; 2007; 2009) as well as environment (e.g., freshwater and marine waters; Hickman 1968; Shehadeh and Gordon 1969). This will have a profound effect on the DLVO theory for predicting ENM aggregation and behaviour (Deniz et al. 2009; Zhang et al. 2010b). While freshwater fish do not drink their external water in sufficient quantities, the ionic strength of the gut lumen is still sufficient enough to cause aggregation. The only compartment of the gastrointestinal tract where this may be shielded is in the low pH stomach where H^+ can screen charges to prevent aggregation of ENMs. The form of DOC along the gastrointestinal tract will also vary throughout the digestive process and depends on absorption and turnover rates. As surface chemistry is important for uptake, it is important to note that transit through the entire gastrointestinal tract will result in ENM exposure to different environments which may alter surface chemistry and hence behaviour. Ultimately, given the shape of the gut lumen, ENMs are likely to aggregate and settle to become associated with the mucosal layer of the gut.

As for dissolved solutes, data regarding the binding affinity of ENMs to the gut mucosa is currently unavailable. It is reasonable to assume that charged ENMs will behave in a similar manner to the equivalent dissolved metals in terms of becoming tangled in the mucous, and hence it is theoretically possible to model with a BLM-like system. Currently there is no data on the diffusion rate or the dissolution rate of ENMs within a mucous environment given that it has slightly different properties compared to the gut lumen. Given

the properties of the mucus, ENMs are likely to aggregate at the boundary between the gut lumen content and the mucus (Praetorius et al. 2014b). Altered rheological properties of the mucus will result in environment dependent binding of ENMs. What is not clear is whether the rheological property difference between fish in these environments will differ in terms of binding affinity of ENMs.

1.6 Uptake of dissolved solutes compared to ENMs

Absorption is often defined as the uptake of a substance across a membrane from the external environment to the circulatory system of the animal. In fish there are several potential routes for taking substances up from the water including the gills, the skin, entry through the olfacatory bulb into the CNS, and uptake via the gut through drinking. Dermal uptake and absorption via the olfacatory bulb or other sense organs has not been well investigated (Sovová et al. 2014). Although it is theoretically possible for dermal uptake of neutral ENMs in fish, this is yet to be assessed and may suffer from the same issues of uptake via the olfactory bulb. For dietary exposures, uptake via the gut is assumed, but depending on the feeding method of the animal food particle may be broken up to also release a suspended or aqueous fraction. In the context of ENM, exposures via the water to aquatic organisms have been conducted (e.g., Shaw et al 2012) and a few studies via the food of fishes (e.g., Ramsden et al. 2009). The epithelial morphology and anatomy is generally conserved between vertebrate animals (Handy et al. 2008a). Given that the processes underpinning branchial uptake are better understood, it is reasonable to speculate they will be similar in the gut.

1.6.1 Uptake of dissolved solutes across the gastrointestinal tract

In the case of the gill and the gut they are both wet mucous epithelia, and therefore share some similarities with regard to the overall steps of uptake. There are several anatomical differences of the gut compared to the gills which may alter the rate of uptake; notably a thick muscularis layer increasing the diffusional distance and a viscous complicated external media called chyme that will affect the bioavailability (Fig. 1-1). Uptake will occur once a chemical has diffused through the bulk water (i.e. external environment) into the steady-state diffusion layer (or unstirred layer; Köster and van Leeuwen 2004) which consists of water, ions and mucus secretions (mucoproteins) from the neighbouring epithelial cells (Handy et al. 2008a). Underneath the unstirred layer is the epithelial cell layer through which uptake must occur. Uptake of external soluble chemicals across a membrane involves various steps. The intracellular and extracellular contents of cells are different for several reasons: anion differences (Donnan equilibria), the relative permeability of ions and the sources of molecules (i.e. products of metabolism). This results in energy expenditure during uptake across a biological membrane (Handy and Eddy 2004). For solutes to enter the circulatory system of vertebrates, several steps need to occur; adsorption to the surface of the membrane, subsequent transport across the membrane, intracellular trafficking and distribution, export across the basolateral membrane into the blood (Williams 1981; Handy and Eddy 2004). In the context of solutes, the first step is to diffuse into the unstirred layer, then binding to ligands on the surface of the epithelium. Once bound, transport across the apical membrane is through facilitated diffusion on protein carriers (electrolytes, metals, polar organic chemicals) and sometimes by non-specific diffusion (hydrophobic substances). In most cases, moving the substance from gill or gut epithelium is against the electrochemical gradient and the final step involves active

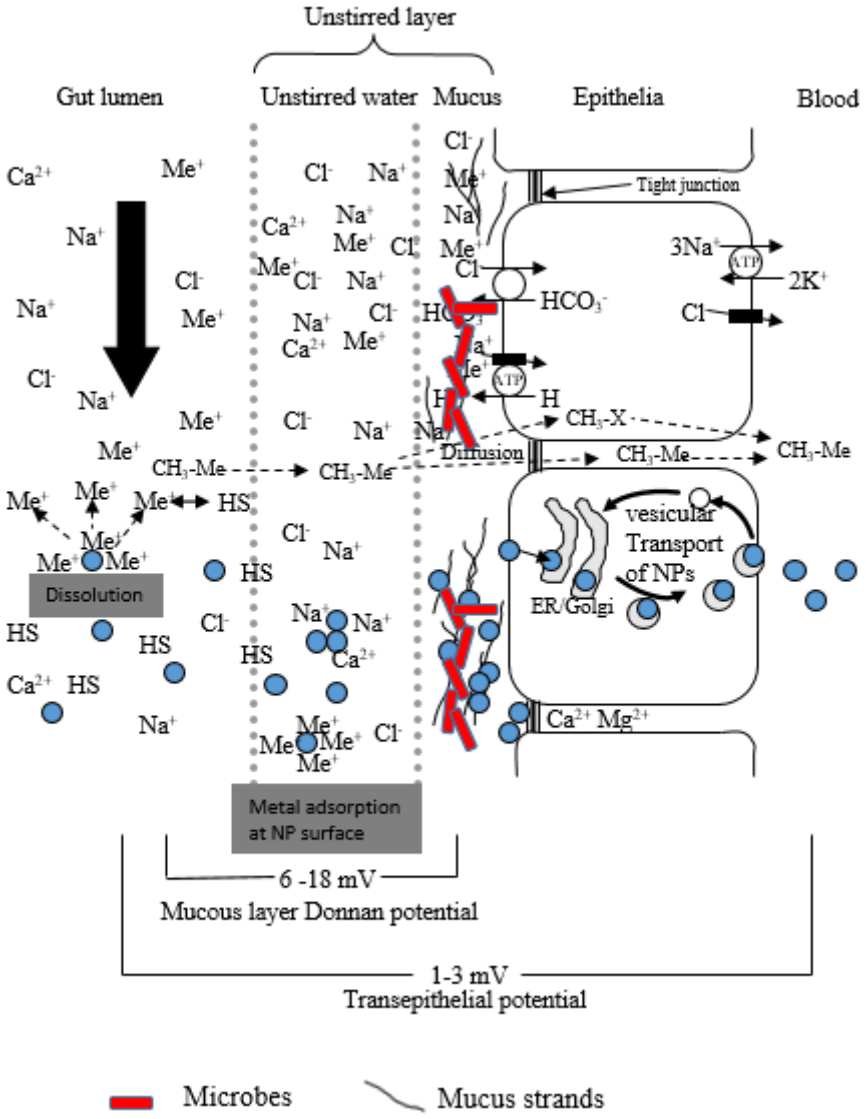

Figure 1-1. An idealised view of organic (CH_3-X), metals (Me^+) and nanoparticles (filled circles) uptake across the gut epithelium of freshwater fish. The substances, including essential ions, must diffuse from the gut lumen into the unstirred layer of water. Given the difference in physical properties of each layer (gut lumen, unstirred water, mucus), ENMs are likely to rest at the boundary layers. The top half of the diagram encompasses organic and dissolved metal uptake, whereas the bottom focusses on the uptake of ENMs. Organic chemicals are free to diffuse across the membrane (either paracellularry or transcellularly). This is also true for organometallics such as methylmurcury. Dissolved metals (with charge) are mediated through active protein carriers. For essential metals, transporters exist (e.g. copper; Crtl and DMT, zinc; Zip proteins), and non-essential metals potentially highjack these systems (e.g. silver using copper transporters). Various uptake processes occur for ENMs: passive, phagocytosis, micropinocytosis, and caveolin mediated, clathrin and caveolin independent mechanisms. It is unknown if the gut microbes have an effect on uptake/transformative processes. Adapted from Handy et al. (2008a).

basolateral transport involving coupling reactions (e.g., on ATP-ases; Fig. 1-1).

For dissolved organic chemicals, the diffusional uptake results from passage of the substance through the apical membrane, diffusion across the cell and entry into the blood through diffusion across the basolateral membrane. For metals, more certainty exists for specific uptake pathways with well-described transporters. A lot of research has occurred using copper (Cu) to locate the region of gut accumulation. Using radiolabelled Cu, Clearwater et al. (2000) demonstrated the anterior and hind intestinal regions had the highest newly acquired Cu in the tissue. Nadella et al. (2006) measured Cu from a single feed and measured Cu in the liquid and solid phase of the chyme and related this to an absorbable marker as a reference point for uptake. The authors concluded that a significant reduction in chyme copper in relation to the marker was indicative of Cu uptake in the stomach, mid and hind intestine, and the anterior intestine contributed to Cu load in the chyme (Nadella et al. 2006). Regardless, some physiological information relating to uptake has been gathered. For example, apical copper uptake is protein carrier mediated through Ctrl and divalent metal transporters on the gill, and so it is reasonable to assume similar structures are present in the gut (Grosell 2012). Evidence of this comes from *in vitro* data where it was determined that Cu accumulation is Na-insensitive, but may use pH- and K-sensitive pathways (Burke and Handy 2005). Regardless, once in the cell as Cu^{+}, it is chaperoned by proteins and/or interacts with the golgi apparatus. Of the Cu^{+} not utilised in the cell, there is evidence of mid and hind intestine Cu:Cl symporter that removes copper from the cell (Handy et al. 2000). Both essential and non-essential metals are carrier mediated, with these kind of pathways similar for other dissolved metals of similar size and charge, including silver.

Ultimately, the uptake of organics and dissolved metals is dependent on the concentration gradient across the epithelia, the diffusion distance, the surface area of the

epithelia and the innate permeability of the epithelia. The uptake of chemicals may be bigger over the gut epithelia given that it is leakier than the gill and so allows easier paracellular transport. The factors affecting the uptake of dissolved solutes are all captured in the Fick equation and the facilitated diffusion through transports derived from it. Using nominal concentrations in Fick's equation could be erroneous as either the bioavailable fraction (Lillicrap et al. 2016) or free ionic concentrations should be used (e.g. Campbell et al. 1999).

1.6.2 Uptake of ENMs across the gastrointestinal tract

One question that arises is whether the Fick equation can be applied to ENMs. Given the behaviour of ENMs, they are in a dynamic and not at steady state equilibrium; therefore ENM diffusion is a function of factors influencing particle attraction (e.g. size, shape and number of particles in dispersions). The resultant hyperbola produced by the Fick equation is unlikely to escribe the true features of ENM uptake. In addition, the uptake mechanisms (i.e., endocytosis) of ENMs are different which may affect the rate of uptake.

Uptake across the gills has received more attention and been reviewed (Handy et al. 2008a), with some comments also relevant to the gut epithelia. Ultimately, uptake of ENMs across the membrane barrier can occur in one of two fundamental ways: transcellular transport (through the cell) and paracellular (between junctions of cells) transport. Handy et al. (2008a) highlight the theoretical possibility for ENM uptake between cells at junctions, but given the high presence of Mg^{2+} and Ca^{2+}, it is likely to cause aggregation and slow entry into the body. The cells of the gills are tightly bound together in an attempt to reduce leaking of ions to a hyposmotic environment but the cells of the gut are not so tightly bound and hence more leaky, and may represent a higher uptake potential for

paracellular uptake. Interestingly, there is evidence supporting the idea that ENMs increase the permeability of endothelial cells (Setyawati et al. 2013), indicating this being a potential uptake route, although how much this contributes to overall uptake is likely to be low.

Given their size, ENMs are unlikely to use solute transporters for uptake. The gut epithelium of fish can take up large particles such as macromolecules like oral vaccines, and so ENM uptake should not be difficult (Handy et al. 2008a). The gut of fish is also known to absorb colloidal iron and so the propensity to absorb other colloids is present. Yet, one issue that may arise is the difference in particulate uptake of in the GI tracts between fish and mammalian species. Rodent gastrointestinal studies may have additional routes in which uptake can occur across the gut barrier, such as M cell layers of Peyer's patches. These anatomical regions have been studied for years in relation to iron absorption and we now understand that metal particles can be detected in these patches (review; Powell et al. 2010). Treuel et al. (2013) reviewed uptake mechanisms in mammalian systems and highlighted literature indicating passive uptake of zero valent ENMs in a similar manner for hydrophobic organic chemicals. Such evidence was focused on the use of red blood cells which are used primarily as they do not have a nucleus and so cannot regulate organelle uptake (Treuel et al. 2013). In fish this may not be true given they have red blood cells with a nucleus as part of their normal biology (circulating nucleated cells in a mammal is indicative of pathology). Regardless, such experiments demonstrating this process using an epithelia or fish tissue are required for this to be a process that contributes to significant uptake from the external environment. Given that this passive process is slow due to ENM size, it is thought to be a fraction of active processes; therefore alternative explanations are required, with a focus on endocytosis-related mechanisms (Handy et al. 2008a; Al-Jubory and Handy 2013; Gitrowski et al. 2014).

The uptake mechanisms for endocytosis have been reviewed for mammalian systems (Treuel et al. 2013), with a conclusion that ENM may be taken up by pinocytosis, clathrin-mediated endocytosis, caveolae-mediated endocytosis and clathrin- and calveolae independent mechanisms (Conner and Schmid 2003; Taylor and Simkiss 2004; Treuel et al. 2013). Two mechanisms for endocytotic uptake occur: phagocytosis and pinocytosis (Fig.1-1). The former is concerned with the uptake of larger particles (i.e. those of bacterial size), while the latter can ingest smaller particles, predominantly in a fluid phase (Taylor and Simkiss 2004). Phagocytosis occurs when the extension of plasma membrane surrounds external material from more than one side, fusion of the membrane and subsequent ingestion. Pinocytosis can be broken down into four pathways. Macropinocytosis is where part of the plasma membrane protrudes out (in a similar fashion to that of phagocytosis, but one side only), surrounds particulate matter and binds to the plasma membrane, in a wave-like fashion (Conner and Schmid 2003). Caveolae-mediated, clathrin-mediated and, clathrin- and caveolin-independent endocytosis pathways all involves invaginations of the plasma membrane and appear to only differ in the proteins used and the signal to trigger vesicle separation from the membrane (Conner and Schmid 2003; Taylor and Smith 2004; Treuel et al. 2013). All involve the interaction of a receptor in the plasma membrane and there uptake they internalise cholesterol, low density lipoproteins and proteins (Conner and Schmid 2003). The above mechanisms are well described for mammalian systems and invertebrates, yet there is evidence of similar phagocytic and non-pathway descriptive pinocytotic systems in fish (e.g. Rombout et al. 1985; Gargiulo et al. 1998; Ringø, et al. 2010). Given the ingestion size of particulates, it is reasonable to assume potential ENM uptake via these pathways.

From one view point, given their size, it does not seem likely that they will interact with surface receptors. However, if the receptor is a metal binding ligand (e.g., -SH group

on a cysteine), then a number of metal based ENMs could bind. Furthermore, it is unclear whether the ground state of the metal will be attracted to the receptor. Literature supporting particle uptake in gut cells (e.g. Gitrowski et al. 2014) is sparse, but has been demonstrated. However, such studies of *in vitro* systems (e.g. cell cultures; Gitrowski et al. 2014) have experimental designs where the ENMs can settle on top of the tissue where an increase in cell concentration would be expected over time. In this type of test system, there is no quantification of the amount of ENM at the surface of the cells, which would be logistically difficult. Therefore it may be more prudent to engage in *ex vivo* systems for uptake as rapid surface binding experiments can be conducted (e.g. Al-Jubory and Handy 2013).

Once in the cell, it is likely that the ENM will be encompassed in a vesicle of some sort. The above endocytotic uptake mechanisms have cellular pathways for which they transport traditional material. If ENMs interact with the membrane in a similar fashion to this material, it is likely that they will have the same fate. For example, clathrin-coated vesicles within the cell can fuse to form early endosomes. Such endosomes either form lysosomes or are recycled to the surface of the endothelium. Endosomes can also cross the cell and exocytose (Taylor and Simkiss 2004) the ENM across the basolateral membrane into either the blood or the muscle. If ENMs are taken across the gut epithelia and exported basolaterally, there should be evidence of ENMs in the blood (or the serosal side of *ex vivo* experiments). While haematological assessments are frequent (Perera and Pathiratne 2012; Karthikeyeni et al. 2013; Suganthi et al. 2015; Clark et al. 2018), attempts to assess the concentration in blood or plasma are yet to be made.

Al-Jubory and Handy (2013) found evidence of both solute transporter and endocytosis uptake of TiO_2, or Ti from TiO_2, in rainbow trout. However, this evidence should be treated with caution for several reasons; firstly, the concentrations found associated (taken up) within the gut tissue was approaching the inductively coupled plasma

optical emission spectrometry (ICP-OES) detection limit. Secondly, a physiological saline at pH 7.2 was used throughout the entire gastrointestinal tract whereas the gut pH will change with compartments in live fish. Although a dialysis experiment was conducted to quantify the dissolution of Ti from TiO_2, it was again at pH 7.2 and so does not represent GI transit of TiO_2. The main limitation in understanding the molecular uptake mechanisms of ENMs is the inability to distinguish between dissolved and particulate forms of the ENM metals at the surface of an epithelium, and inside the cells.

1.7 Distribution

After adsorption into the cardiovascular system or other intracellular fluid, substances may be distributed around the body to target organs, where they may be stored, metabolised or excreted. Soluble substances can also be excreted directly from the blood (e.g. via the kidney). Substances have an affinity for different tissues, and hence target organs. These organs can act as an intermediary for storage, become metabolised and/or excreted. Excretory pathways in fish include the gills, bile form the liver and the kidney. It must be noted that seawater fish do not produce sufficient amounts of urine which may cause the relative excretion pathway (i.e. gills and bile) of the same soluble or colloid chemical to change (i.e. increase) with fish habitat.

Dissolved chemicals have a distribution around the body based on chemical affinity. Organic chemicals are transported in the cardiovascular system attached to fat molecules, with the target organs also being lipophilic tissue. For example, persistent organic pollutants and organometals have known to be a hazard in the fat and milk glands of Polar Regions (Borgå et al. 2004; Sørmo et al. 2006). For dissolved metals, their reactivity and affinity for molecules causes them to become complexed when internalised by cells by

chloride, sulphide, glutathione, proteins and amino acid side chains. When entering the cardiovascular system, an extracellular mechanism of distribution is required, with some evidence indicating metal adsorption to red blood cells. For essential metals, carrier proteins exist for some metal ions in the blood, for example Cu^{2+} and ceruloplasmin and Zn^{2+} and albumin (review; Hogstrand 2012).

For metal toxicology, through dietary exposure, certain target organs for accumulation are evident (Table 1-1). Accumulation within the gut and liver are common, with some notation of accumulation in the gills occurring. While the gut is the first barrier of uptake, high concentrations here are logical. However, the main organ of accumulation is the liver which is the main detoxifying organ. Dissolved copper is taken across the gut epithelia and along the hepatic portal vein to the liver where it can be stored as inert granules (Lanno et al. 1987). The data in Table 1-1 are from highly controlled studies that allow detailed information at centration exposure concentrations. Recently, there have been several studies assessing environmental bioaccumulation in anthropogenically polluted waters. In general, laboratory studies are congruent with field observations. Both demonstrate accumulation within the liver for Cd, Zn and Cu. These studies also demonstrate species differences in accumulation and areas of study (Dhanakumar et al. 2015; Hermenean et al. 2015; Leung et al. 2014; Mendoza-Carranza et al. 2016; Schenone et al. 2014).

Distribution of ENMs around the body system will be a result of ENM entry into the cardiovascular system, similar for metals. There is now *in vitro* evidence that ENMs can bind to plasma proteins, like metals, in human cells (single walled carbon nanotubes, SWCNTs; Ge et al. 2011) but needs to be verified in fish species. Conclusive evidence of ENM distribution around the body is currently unavailable, partly due to inadequate routine

Table 1-1. Bioaccumulation data of select internal tissues after exposure to various dissolved metals in fish.

Species	Metal	Diet	Exposure time	Tissue accumulation	Authors
Rainbow trout	Cu (as $CuSO_4$)	10 g Cu/kg nominal concentration dry weight and fed to satiation.	4 weeks	Significant increase in Cu concentration of the gills at all-time points. Increase in liver and muscle Cu concentration compared to controls at days 21 and 28.	Handy et al. 1993
Rainbow trout	Cu (as $CuSO_4.5H_2O$)	Control and exposure diets contained 16.3 and 489 mg Cu/kg dry weight. Amount of	3 months	Cu concentration significantly increases in liver at months 2 and 3. No significant changes in the gut or kidney at any time points.	Handy et al. 1999
Atlantic salmon	Cu	Up to 1750 mg Cu/kg (dry or wet weight not specified) from an automated feeder for 5 s every 7, 24 h a day	4 weeks	35 and 700 mg/kg treatments significantly increase intestinal Cu by day 28. Only 700 mg/kg treatment caused a significant increase in liver Cu at day 28. No difference in the gill concentrations.	Lundebye et al. 1999
Rainbow trout	Cu (as ^{64}Cu)	Exposure diet of 3 µg Cu/g dry weight and 3-4% ration.	3 days	Significant increase in the liver and gall bladder after 1, 2 and 3 days exposure. Plasma had significantly more Cu than the carcass at day 3.	Clearwater et al. 2000
Rainbow trout	Cu (as $CuSO_4$ and ^{64}Cu)	Low (0.8 µg/g), medium (3.2 µg/g) or high (282 µg/g) Cu diets dry weight and 4% ration.	7 weeks	High diet increases whole body Cu concentration. 40% of Cu body burden in the gut after 2 weeks, but this is not different by the end of the study. Liver Cu burden is at ~70% by week 7. Gill Cu body burden significantly reduces in the high diet compared to low diet Cu.	Kamunde et al. 2002
Nile Tilapia (*Oreochromis*)	Cu	Control diet of 3.22 mg Cu/kg or exposure diet of 1968 mg Cu/kg dry weight.	7 weeks (+3 depuration)	After 7 weeks there was an increase in the intestine, liver and gills compared to controls. Depuration period reduced gills and intestine Cu load. but increased liver Cu concentration.	Shaw and Handy 2006

African walking catfish (*Clarias gariepinus*)	Cu	15.6 and 1495 mg Cu/kg dry weight control and exposure diet, respectively and fed to satiation twice daily.	30 days	Significantly elevated intestine and liver Cu concentrations from day 10 onwards. Gill Cu concentration increased from day 20 onwards.	Hoyle et al. 2007
Rainbow trout	Zn	Low (228 mg/kg), medium (1441 mg/kg) and high (4820 mg/kg) diets at 1.5% ration.	40 days	Significantly more Zn in high Zn diet carcass compared to low Zn diets at day 40. No effect on blood cells or plasma concentration.	Sappal et al. 2009
Rainbow trout	Cd (as $CdSO_4$)	10 g Cd nominal concentration.	28 days	Significant increase in the intestinal mucus at day 28. Significant increase at days 7 to 28 in the kidney, liver, gill and muscle.	Handy 1993
Atlantic salmon	Cd	Up to 250 mg Cd/kg from an automated feeder for 5 s every 7 mins, 24 h a day.	4 weeks	All groups except 0.5 mg/kg increase intestinal Cd concentration. 300 fold increase in the liver from 250 mg/kg exposure. Elevated gill concentrations in all treatments.	Lundebye et al. 1999
Rainbow trout	Pb	Nominal diet concentrations up to 1 mg Pb/kg with rations ranging from 1 to 3% body weight.	32 weeks	No effect on accumulation. Majority of Pb in the faeces.	Hodson et al. 1978
Rainbow trout	Ag_2S	Ag_2S added to grounded commercial feed from 3 to 3000 mg/kg Ag (nominal) and fed to fish until satiated.	58 days	No significant difference between treatment intestine total Ag concentrations. After 43 days, the liver of the highest treatment was significantly elevated compared to all other treatments and persisted until the end of the experiment. Gill showed significant increase in Ag of the top two treatments at day 24, but returned to no difference at day 43.	Galvez and Wood 1999

Rainbow trout	Ag	Waterborne exposure to silver thiosulfate incorporated into diet (3.12 µg/g) and fed to trout until satiation.	126 days	The intestine contained more Ag in the silver treatment at day 36 and 88, but returned to normal by day 126. At day 16, 36, 88 and 126, the liver of silver fed fish was significantly elevated compared to the controls. Kidney Ag elevated from controls at day 126 only.	Galvez et al. 2001

detection of particulates within tissues and a scarcity in studies performed. Of the ENMs that have been tested, there seems to be evidence of bioavailability into the body, but this is often variable between studies (Table 1-2). Equally, all appropriate controls are not necessarily used, depending on the hypothesis being tested. It seems that ENMs compromised of non-essential elements are easier to detect in tissues and can have lower exposure concentrations, such as gold NPs (Table 1-2). There is currently limited data on the use of silver-based ENMs. However, increases in accumulation from ENMs of essential elements appear possible; both CuO and ZnO ENMs are bioavailable, despite being unknown in form, to goldfish and accumulate in the liver and gills (Ates et al. 2015). No imaging was conducted to assess the pathology or how the ENMs were deposited. Currently, there is no reason to suggest why CuO would not also manifest as granules similar to dissolved copper (Lanno et al. 1987). Al-Bairuty et al. (2013) found a histological increase in liver foci of hepatitis-like injury after 4 days waterborne exposure to 100 µg/L Cu ENMs. These injuries look morphologically similar to hepatic granules (Lanno et al. 1987), and could represent deposition of particulate metal. However, there was no appreciable liver Cu accumulation at this time point (Shaw et al. 2012) which would be expected.

Insights of target organs may be obtained from waterborne exposures and intravenous injection studies. Waterborne studies show that ENMs accumulate in the gills (Shaw et al. 2012), intestine and liver (Johari et al. 2014), muscle (Ates et al. 2015) and brain (Zhao et al. 2011). Intravenous injections of ENM in fish has been used minimally, partly due to its lack of environmental relevance, but can be used to understand the importance of the external barriers, or to give a defined internal dose (e.g. Boyle et al. 2013), thus avoiding the problems of achieving stable dispersions in aqueous exposure

Table 1-2. Bioaccumulation data of select internal tissues after exposure to various engineered nanomaterials in fish.

Species	ENM	Diet	Exposure time	Tissue accumulation	Authors
Rainbow trout	TiO_2	10 and 100 mg/kg (measured as 5.4 and 53.6 mg/kg, respectively) fed to satiation.	8 weeks	Significantly elevated Ti in both TiO_2 exposed fish intestine, gill and liver compared to the controls following 6 weeks. Transient changes in all tissues. No bulk material used.	Ramsden et al. 2009
Rainbow trout	TiO_2	1 and 10 g Ti/kg at a 1% body weight ration.	21 days	No Ti was found in the control gill, but was present in the low and high concentration. Trace amounts of Ti were found in the control intestine (0.11), which was significantly less compared to the low (0.36) and high (1.49) concentrations. No Ti was found in the liver, brain, skin or blood.	Johnston et al. 2010
Zebrafish	TiO_2	Daphnia exposed to 0.1 and 1.0 mg/L (equates to 4.5 and 61.1 mg/g dw, respectively) for 24 h before being fed to fish (=8% ration).	2 weeks	Whole body accumulation increased over the experiment, with the highest at the end of the exposure (120 and 500 mg/kg in the low and high exposure conditions, respectively). No bulk material control.	Zhu et al. 2010
Sea bream	CuO	2, 4, 6 or 8 mg/kg added to a commercial diet (background unknown), fed twice a day until satiation.	60 days	All concentrations (except the lowest) had significantly higher Cu concentration in the whole body and liver compared to the controls. No significant difference compared to the dissolved metal control.	El Basuini et al. 2016
Goldfish	CuO and ZnO	1 or 10 µg/ml exposed Artemia, and fed (0.2-0.25g) to fish tanks once daily.	3 weeks	Low and high concentrations were both significantly elevated in the intestine, liver, gill and muscle. No significant difference in the heart, and brain. No dissolved metal controls.	Ates et al. 2015

Rainbow trout	ZnO	300 or 1000 mg/kg at a 2% body weight ration.	10 days	The gill, intestine and liver at the highest concentration was significantly elevated compared to the control following the exposure.	Connolly et al. 2016
Fathead minnow	SWCNTs	10 µL of 318 µg/ml administered as oral gavage.	1 week	No appreciable organ accumulation as detected by near infrared fluorescence. Signal remained in the gut. No carbon black control used.	Bisesi et al. 2014
Zebrafish	CdSe/ZnS quantum dots	Fed 10 daphnia contaminated with quantum dots, equating to 4% body weight ration.	14 day uptake, 7 day elimination	Whole body accumulated Cd over the 14 day uptake phase to around 8 mg/kg. At day 15 (1 day on clean diet), the body burden reduced to less than 1 mg/kg. No metal salt used.	Lewinski et al. 2011
Zebrafish	CdS	4 µg CdSNPs/g of feed at a 2 or 0.8% body weight ration. Equates to 40 and 100 ng/day/g body weight for 60 and 36 day exposures.	36 or 60 days	No difference in liver Cd concentration following 36 days to higher exposure. However, significant elevation of Cd found in the liver of CdSNP exposed fish after 60 days exposure to lower concentration.	Ladhar et al. 2014
Mummichog (*Fundulus heteroclitus*)	CdSe/ZnS	2 lab made food disks containing either 0.07 or 0.74 µg Cd. $CdCl_2$ contained 1.42 µg Cd.	85 days	Only the high concentration was the liver and intestine (42 and 103 ng/g) significantly elevated compared to the control treatment (no added Cd). Dissolved salt also showed the same profile for liver and intestine (5627 and 18734).	Blickley et al. 2014
Zebrafish	Au	8 mg/fish/day of either 4.5 or 5.3 mg Au/kg.	60 days	No difference between the two gold treatments, with concentrations at ~1, 3-6 and ~5 µg/g dw in the skeletal muscle, liver and brain, respectively. No Au was detected in the fish on the control diet.	Geoffrey et al. 2012

media to achieve a steady exposure rate via the gills. Interestingly, this changes with intravenous injection where the effects on the liver are minimal or non-existent, and the kidney becomes a target organ (Scown et al. 2009; Boyle et al. 2013; Boyle et al. 2018) potentially through bypassing the liver in the cardiovascular system. Therefore, under likely environmental uptake routes, it indicates that ENMs are more likely to be processed by the liver rather than the kidney. Microinjection of carbon ENMs into the yolk sac of zebrafish larvae demonstrated body distribution through circulation of the blood (Zhao et al. 2014). ENMs could interact with cell surfaces and their body distribution would be a function of tissue affinity. Some of these haematological assessments are made after 96 h but are not supported with dissolution experiments of the ENMs. For ENMs with low levels of dissolution, it is reasonable to assume that the damage to the cardiovascular system is through the ENM form. However, many dissolution experiments are done to reflect the exposure conditions, which will not account for the behaviour of the ENM once it has been taken within the body (i.e. formation of a corona; Lundqvist et al. 2008; Lesniak et al. 2012). Despite these limitations, the beginnings of target organ toxicity can be observed.

1.8 Metabolism

Organic chemicals are metabolised through phase I and II reactions, which predominantly occur in the liver, but the enzymatic machinery is also found in the intestine (cytochrome P450). Phase I enzymes perform reactions (e.g., oxidation, hydrolysis) to increase the solubility of organic chemicals. Following this, phase II enzymes conjugate natural organic molecules (e.g. glutathione) which can then be used for excretion. Metals, however, are not metabolised per se, but have preferential binding affinities for tissues, as described above.

Although the question of ENM metabolism is still unanswered, there has been evidence of biomodification within the gut lumen of Daphnids. A dose-dependent response was demonstrated for an LPS coated SWCNT, where growth significantly increased until 0.5 mg/L SWCNT exposure. In addition, ENMs with –OH surface functionalisation could be oxidised in the low pH stomach region.

Despite showing an interaction with metabolic systems in bacteria (El-Sayed et al. 2016), evidence is lacking to demonstrate that ENMs are metabolised by Phase 1 and Phase 2 enzymes in vertebrates. While it is theoretically possible for charged surface group interactions with metabolic enzymes, it seems unlikely given ENM size and is likely to inhibit interactions due to steric hindrance. With the increasing use of high throughput techniques such as proteomics, the expression of global organ proteomes may give an insight to this process.

1.9 Excretion

While uptake assessments are numerous, excretion studies are less so. Metals can be excreted through the gills, gut, kidney or bile. Some demonstrate a long time to depurate (e.g. Ag; Wood 2012), whilst others tend to remain accumulated (Cd in the kidney; McGeer et al. 2012). Dissolved metals can be excreted from the body via hepatic and renal pathways. The former pathway seems to be more important due to higher excretion rates and the proportion of renal excretion is partially dependent on time of acquisition (Grosell et al. 1998). The latter may be an issue for essential metals and may not be for non-essential metals. More evidence of reliance on hepatic excretion comes from Shaw and Handy (2006). Being fed 2,000 mg Cu/kg feed for 6 weeks, there was an increase in intestine, gills and heptic Cu concentration. Following the exposure, when fed a normal Cu concentration

diet (3 mg/kg), the gill and intestine concentrations reduced, but the hepatic Cu concentration increased (Shaw and Handy 2006). After a single feeding event of contaminated food, the majority of (up to 96%) can be removed from fish tissue (Xu and Wang 2002). It should be noted that highly bioavailable material does not necessarily mean high toxicity as some species of metals (e.g. $Ag[S_2O_3]^{n-}_{n}$) can be easily removed from the body due to their solubility (Hogstrand and Wood 1998). Such complexes are easily eliminated from the blood through the copious amounts of urine produced by freshwater fish.

Similarly to metabolism, the exact pathways of excretion have not been assessed but have been hypothesised by Handy et al. (2008a) who propose that small ENMs (<60 kDa) can exit the kidney through glomerular filtration, excretion through bile via the liver, or complete dissolution of the ENM (metals and metal oxides) and excretion in the urine. Scown et al. (2009) found accumulation of titanium from TiO_2 exposure with no apparent impairment of renal function. Accumulation in the kidney may eventually lead to impaired functioning, possibly resulting in passive loss of ENMs through glomerular filtration. Manabe et al. (2011) looked at the excretion of nano-sized latex particles after three days exposure to *Oryzias latipes* embryos. There was a size dependent decrease in fluorescence from the embryos over time up until 168 h (Manabe et al. 2011), indicating some regulated excretion. After three days exposure to waterborne 20 nmol/L Au ENMs, *Oryzias latipes* were given a period of five days over which clearance from the organs were assessed. Au ENMs with a half-life of 12 h were more readily excreted from the intestine than those of 24 h; the concentrations of 12 h half-life Au ENMs reached around zero after 24 h, while the Au ENMs with a half-life of 24 h approached zero after 120 h (Zhu et al. 2010). The exact mechanisms of excretion are yet to be determined in fish.

Souris et al. (2010) injected mice with ENMs into the tail-vein, where blood flow is known to transport to the liver. A time course shows initial deposition within the liver, but after 4 hours only a modest signal came from the liver and a predominant proportion was in the duodenum and jejunum. Zhao et al. (2014) attribute the low levels of ENMs presence in the liver of mice (Souris et al. 2010) as evidence of a lack of hepatobiliary excretion. Although the liver concentrations vary between studies, it demonstrates that this organ may represent a potential excretion route. In order for better interpretation as the liver as a major source of ENM excretion, the presence of the ENMs in the bile duct should be assessed. If the liver excretes ENMs through biliary secretion, it raises the question over exposure; do the same particles get exposed to the gastrointestinal tract again.

The intestine also represents a potential route for ENM excretion. Zhao et al. (2014) used microinjection of activated carbon NPs into the yolk sac of zebrafish larvae. After 4 days of development, imaging techniques demonstrated the NP presence within the intestinal tract. By day 7, the NPs had moved down the gastrointestinal tract through peristalsis and were then excreted. On day 8, NPs were liberated from other tissues and translocated to the gastrointestinal tissue (Zhao et al. 2014). Given that the gastrointestinal tract of embryos is not fully formed, histological analysis provides evidence that ENM movement was not due to a more permeable membrane. Other vertebrate models can serve for comparisons for renal excretion. For example, male rats and mice exposed to quantum dots could excrete aggregates below 5.5 nm (Choi et al. 2007). However, there was no structural examination of the kidney which would elucidate if the excreted quantum dots were the result of organ damage. Furthermore, there was no dialysis experiment in a media to represent the blood to indicate the dissolution rates. Therefore, it is unknown as to the form of the quantum dots found in the urine.

1.10 Aims of the thesis

Currently, environmental risk assessments are based on dissolved metals, which have led to a high level of understanding in terms of potential effects to organisms. For example, silver is very toxic to freshwater organisms (Ratte 1999), with its waterborne toxicity in the low µg/L range and dependent on the ion (Ag^+, Bury et al. 1999; Wood 2012). To fish, the specific aetiology of Ag^+ is through the blockage of Na^+/K^+-ATPase and carbonic anhydrase enzymes resulting in ion loss and causing cardiovascular collapse (Morgan et al. 1997). However, this mode of action is not observed when mammals are exposed *via* the diet to dissolved silver at such low concentrations (Hadrup and Lam 2014), presumably because of complexation with binding sites in chyme; this makes aquatic species of interest to silver exposure.

With the advent metals being incorporated into new forms (i.e., silver nanoparticles; Ag NPs), it is necessary to compare these new materials to dissolved metals. By comparison, this will allow to see if new materials are covered by the current risk assessment, or if specific modifications are required. Ag NPs have previously demonstrated toxicity to aquatic animals (e.g., Gaiser et al. 2012; Bondarenko et al. 2013; Osborne et al. 2013), and have shown to accumulate. For example, Ag NP bioconcentration factors of 37, 52, 21 and 2 for *Chlorella sp*., *Miona macrocopa*, *Chironomus spp*., and *Barbonymus gonionotus*, respectively, have been found (Ag^+ values were 102, 46, 34 and 2, respectively; Yoo-iam et al. 2014). Therefore, the interest here is to compare the ENM to the ionic form from an environmental risk assessment, rather than focus on nano-sized specific effects (i.e., comparison to bulk material for toxicological studies).

If ENMs are released into the environment, various transformations are likely to occur, meaning that released particle may not have the same surface chemistry they began

with. For higher trophic organisms, including fish, the likely route of exposure is through the diet. Ag NPs are ideal for determining bioaccumulation in fish for several reasons. They have a well characterised environmental chemistry, whereby it is known that when Ag NPs are released they will quickly become sulfidized (Kaegi et al. 2013). It is possible to synthesise sulfidized Ag NPs (as Ag_2S NPs) in the laboratory; therefore side by side testing of pristine (Ag NPs) and environmentally aged (Ag_2S NPs) can occur. Another benefit of silver chemistry is the ENM seldom dissolves to ensure particulate accumulation is compared to the equivalent dissolved metal (as $AgNO_3$). Indeed, there are some biological concerns over silver ENMs; silver is not an essential element as so queries over its bioaccumulation potential in fish need addressing. Not being an essential element means the background concentrations of silver are low; as such there is no need for radio-labelled Ag ENMs to be produced. This quality is particularly helpful for the establishing how ENMs behave in different experimental systems (e.g., *ex vivo* and *in vivo*). Equally, the low background will be beneficial for keeping determining the form of silver in tissues. Therefore, the specific objectives are:

- There is no screening test available to assess the dietary bioaccumulation of ENMs before an *in vivo* test (e.g., OECD 305). Therefore, the aim of Chapter 2 is to assess the utility of a rapid screening method for dietary bioaccumulation potential in fish. To do this, the *ex vivo* gut sac technique is used, which has been well established in dissolved metal literature. It is hypothesised that both the Ag NP and Ag_2S NP would accumulate less compared to the equivalent dissolved metal ($AgNO_3$). Additionally, it is hypothesised the intestinal regions of the gut will accumulate more compared to the upper gastrointestinal tract.
- Should the gut sac demonstrate the bioavailability of Ag-ENMs, then there is cause for further *in vivo* testing on bioaccumulation. The aim of Chapter 3 is to determine

the *in vivo* dietary bioaccumulation of ENMs compared to the equivalent dissolved metal salt. This will be done by feeding juvenile trout Ag-containing diets for an exposure period (4 weeks), followed by a depuration period on uncontaminated feed to assess excretion of Ag. It is hypothesised that the Ag NPs and Ag_2S NPs accumulate less compared to the $AgNO_3$ treatment. Also, it is hypothesised that the liver will be the central compartment of accumulation, regardless of the treatment.

- For adequate risk assessment, there is a need to extract and quantify the form of ENMs from fish tissues. Currently, the extraction protocols of ENMs from tissue matrices have not been applied to fish, or include the equivalent dissolved metal control to ensure extractions do not change the form of metal in the tissue. The aim of Chapter 4 is to develop a suitable extraction method coupled to single particle inductively coupled plasma mass spectrometry (spICP-MS) to detect ENMs. This will be done by using a series of spike tests into different matrices, with subsequent alterations to protocols, and finally by assessing the extraction of biologically incorporated Ag. For this chapter, it is hypothesised that previously used methods (TMAH or proteinase K) will be suitable to extract Ag NPs in a fish tissue matrix. Also, it is hypothesised these will be suitable for $AgNO_3$ and not alter the form of Ag present in the tissue.
- The form of material in fish tissues following chronic dietary exposure to ENMs is required for risk assessment. Equally, it is important to determine if particles can become excreted from the body after accumulation. The aim of Chapter 5 is to assess the form of Ag in fish organs following dietary exposure. To do this, the digestion method from Chapter 4 will be used to extract Ag (form unknown) from the hind intestine, liver and kidney of chronically exposed fish (4 weeks), followed by a depuration period (2 weeks). The hypotheses of this chapter was that the

$AgNO_3$ and Ag NP treatments will have accumulated dissolved Ag, whereas the Ag_2S NP treatment will accumulation particulate Ag.

- The use of rodents is mandatory in hazard assessment. It has been postulated that fish can replace rodents in immunological and oxidative stress assays in response to ENM exposure (Johnston et al. 2018). This question remains unanswered with regards to the potential for rat replacement with fish for dietary accumulation testing. The aim of Chapter 6 is to assess the gastrointestinal accumulation of ENMs in rats using the same method for fish in Chapter 2 to allow for a species comparison. Additionally, the form of Ag in the mucosa, muscularis and serosal compartment will be assessed using single particle ICP-MS. It is hypothesised that both the Ag NPs and Ag_2S NPs accumulate less compared to Ag as $AgNO_3$. Equally, it is hypothesised that any accumulation will predominantly be in the intestinal regions of the gut, and there will be some differences compared to fish accumulation.

Chapter 2 - An Assessment of the Dietary Bioavailability of Silver Nanomaterials in Rainbow Trout Using an *Ex Vivo* Gut Sac Technique

Abstract

The uptake of engineered nanomaterials (ENMs) by the gut of fishes is poorly understood. This study assessed the utility of the *ex vivo* gut sac method for measuring bioavailability following exposures to silver nanoparticles (Ag NPs) or silver sulphide nanoparticles (Ag_2S NPs). Whole gut sacs were prepared from rainbow trout and filled with saline containing: control (no added Ag), or 1 mg/L of Ag as $AgNO_3$, Ag NPs or Ag_2S NPs; then incubated for 4 h. The mucosa and muscularis were analysed for total silver concentrations. The amount of Ag associated with the gut ranged from 2-20% of the exposure dose, with the majority being associated with the mucosa. For the $AgNO_3$ treatment, the anterior, mid and hind intestine had significantly more Ag (4, 6 and 6 fold higher) compared to the oesophagus and stomach (72.4 ± 27.5 and 76.4 ± 16.3 ng/g dw tissue, respectively). For Ag NPs, there was a similar pattern of total Ag concentrations in the mucosa, with proportionally more total Ag in the mid (1506 ± 907 ng/g dw) and hind (732 ± 258 ng/g dw) intestine; but not statistically different from the equivalent $AgNO_3$ treatment. For Ag_2S NPs, there were no differences in total Ag by anatomical region, or compared to $AgNO_3$, for the mucosa. Crucially, sometimes the muscularis from the $AgNO_3$ treatment showed much higher Ag concentrations than either NP treatment. Overall, the gut sac method can determine the bioavailability of ENMs. Both NPs were less bioavailable than the metal salt, and with no material-type effects.

2.1 Introduction

The persistence, bioaccumulation potential and toxicity (PBT) of chemicals are crucial aspects of environmental risk assessment. For engineered nanomaterials (ENMs), fate and behaviour studies are informing on persistence (Fabrega et al. 2011; Lowry et al. 2012; Levard et al. 2012; Lead et al. 2018). There is also a growing body of literature on ecotoxicity (Ma et al. 2013; Khan et al. 2015), but the bioaccumulation potential of ENMs has received less attention (Selck et al. 2016; Handy et al. 2018). Dissolved silver is regarded as one of the most toxic elements in the periodic table to aquatic species (Ratte 1999), but less is known about particulate forms of silver in freshwater ecosystems and their bioaccumulation.

Computational models predict that surface waters may contain ng/L concentrations of Ag from ENMs and that sediments may contain mg/kg amounts of silver from ENMs (Sun et al. 2014). However, while commercial products often contain pristine Ag NPs, this may not be the most relevant form in the environment. A variety of biogeochemical processes may transform or modify ENMs as they are released (reviews, Lowry et al. 2012; Levard et al. 2012; Lead et al. 2018). For example, sulphur will react with silver ENMs during wastewater treatment in an exposure time- and size-dependent manner (Kaegi et al. 2013), with the formation of inert silver sulphide particles. Consequently, it is the latter form that is more persistent in the environment (Levard et al. 2012; Lead et al. 2018). The settling of ENMs from the water column is also a concern because of subsequent exposure of the sediments, associated biofilms and the benthic organisms (Li et al. 2014); with potential for trophic transfer in the case of silver to other organisms in the food web including fishes.

The bioaccumulation potential and effects of dietary exposure to metal salts are well known in freshwater fish (reviews, Clearwater et al. 2002; Handy et al. 2005) and the trophic transfer of dissolved forms of silver to fishes has been demonstrated in the laboratory (Galvez and Wood 1999; Galvez et al. 2001). In contrast, the bioaccumulation potential from dietary exposure to ENMs in fish is poorly understood and with insufficient data to reach consensus on which ENM characteristics will be important to uptake (Handy et al. 2018). For some ENMs, the dietary bioavailability to the internal organs seems minimal to fish (single walled carbon nanotubes, Bisesi et al. 2014; TiO_2, Ramsden et al. 2009), but for other ENMs some bioaccumulation of total metal in the organs may occur (ZnO NPs, Connolly et al. 2016). For Ag NPs the situation is unclear. One study with trout intestinal cell cultures showed some total Ag associated with the gut cells following exposure to citrate-coated Ag NPs (Minghetti and Schirmer 2016). However, epithelial cell cultures do not have all of the tissue layers of the intact gut, and arguably, the gut sac preparation is much closer to the *in vivo* condition for investigations on bioavailability.

In Europe, the OECD 305 test with fish is required to assess the *in vivo* bioaccumulation potential for all new substances, including ENMs. However, the *in vivo* test is not intended to reveal mechanistic details on bioavailability and the testing strategy has been criticised for not including *in vitro* tiers to identify ENMs of concern; also for not reducing the burden of animal testing (the 3 Rs; Handy et al. 2018). Some alternative approaches are therefore needed. The gut sac technique is a well-established *ex vivo* method which has been used to measure the apparent accumulation of dissolved metals in the gut tissues of fish (e.g. Cu, Handy et al. 2000; Fe, Bury et al. 2001; Hg, Hoyle and Handy 2005; Zn, Cd, Ojo and Wood 2007; Pb, Kwong and Niyogi 2009) and has been applied to pristine ENMs (TiO_2, Al-Jubory and Handy 2013). The technique involves removing the entire gastrointestinal tract of a large fish (e.g., 150 g trout), filling the gut lumen with the test

substance, and incubating this for a short period before analysing the tissue compartments for the total concentrations of the test substance. The gut sac method can also identify bioavailable fractions of metals and the media is easily manipulated to study metal speciation effects (e.g. Ag; Galvez and Wood 1999). However, the gut sac technique has not been applied to Ag-containing ENMs in fish.

This study aimed to demonstrate the utility of the gut sac technique in rainbow trout (*Oncorhynchus mykiss*) for determining the accumulation of total Ag from Ag NPs compared to $AgNO_3$. For the metal salt and any potential Ag dissolution from Ag NPs, the speciation of soluble silver will be influenced by the chloride concentration in the water (Ferguson and Hogstrand 1998), and consequently chloride concentration is also a modulating factor involved with branchial uptake of silver by fish (Bury et al. 1999), but its effect in the gut are unexplored. Therefore, an additional aim of this study was to investigate Ag accumulation in the gut tissue in the presence and absence of chloride in the media for both $AgNO_3$ and Ag NPs exposures. Silver dissolution from the Ag NPs were also measured in the gut saline used and in the presence of other ligands such as amino acids, and at low pH, to aid the interpretation of the data. Finally, the accumulation of total silver in the gut tissue from exposure to the more environmentally relevant, Ag_2S NPs, was measured to inform on whether or not this persistent material would present more hazard than the pristine (unmodified) Ag NPs.

2.2 Methodology

2.2.1 Stock animals

Adult rainbow trout (*Oncorhynchus mykiss*, triploid) were obtained from Exmoor Fisheries, weighing 212 ± 39 g (mean ± standard deviation, n = 42). The fish spent 10 days in a semi-static quarantine tank before being moved to a re-circulating system for a further 7-day period to become accustomed to the water quality (dechlorinated Plymouth tap water) and the tank environment (social hierarchy formation). During this period, fish were fed twice a day using a commercial pelleted food. Water quality was checked daily (data are mean ± S.E.M, n = 30) for pH (7.3 ± 0.1), temperature (16.7 ± 0.1^{o}C), and dissolved oxygen (96.8 ± 0.7 mg/L). The background total silver concentration of the aquarium water housing the fish over the course of the experiment was below the limit of detection for the ICP-MS (0.1 µg/L). The commercial feed contained 53.0 ± 2.1 ng/g dry weight of total Ag (mean ± S.D., n = 3 random batches of pellets). Prior to experiments, fish were unfed for 48 h to aid in evacuation of the gastrointestinal tract content and to facilitate the preparation of the gut sacs.

2.2.2 Preparation and characterization of Ag NPs and $AgNO_3$ solutions

The Ag NPs and Ag_2S NPs were provided by Applied Nanoparticles (Barcelona). The Ag NPs were supplied (manufacture's information) at a nominal size and concentration of 60 nm and 10.8 g/L, respectively. The Ag_2S NPs had a nominal size and concentration of 35 nm and 14 g/L, respectively. The Ag NP material was dispersed in 25 µM tannic acid and 5.5 mM sodium citrate, and the Ag_2S NP material was dispersed in 1 mg/mL polyvinylpyrrolidone (PVP). Transmission electron microscopy (TEM, JEOL-1200EX II) was conducted at Plymouth to confirm the primary particle diameters of the materials. Briefly, a copper grid was placed on top of a drop of the stock suspension; after which the grid was removed and allowed to dry for 10 mins at room temperature before imaging.

Nanoparticle tracking analysis (NTA) was conducted to confirm the materials could be dispersed adequately from the stocks supplied by the manufacture. Briefly, 1 mg/L dispersions of the Ag NPs were made in ultrapure by pipetting 100 µL of a secondary stock (1 in 10 dilution from stock solution supplied) and made to 100 mL with ultrapure water, or saline as appropriate. The suspension was then sonicated for 1 h and analysed in triplicate. NTA was also conducted in freshly spiked gut saline (see below) to better understand particle behaviour in a biologically relevant media. The NTA was also conducted after the Ag NPs or Ag_2S NPs had been in the gut saline for 4 hours to mimic the behaviour over the duration of the gut sac experiment (kept in the same conditions, see below).

2.2.3 Gut sac preparation

Whole gut sacs preparations were prepared according Handy et al. (2000) with slight modifications (Ojo and Wood 2007). The technique involved filling the entire gut lumen with the test solution of interest and then isolating the anatomical regions by suturing them closed. Then, the filled gut sacs can then be individually placed in a clean serosal (blood side) saline to incubate for 4 hours. The apparent metal accumulation in the tissue is then measured. Briefly, fish were euthanized by induced concussion and then pithing (schedule 1 method in accordance with ethical approvals, Home Office, U.K., and in compliance with the EU directive 2010/63/EU), and their total weight was recorded. A total of 6 fish were used per treatment (see below). This number was derived from other reports (Al-Jubory and Handy 2013) where 6 biological replicates were suitable to demonstrate statistical difference between treatments, but still low enough to not warrant unnecessary animal usage (e.g., 3 R's, reduction). The whole gastrointestinal tract was carefully removed and

then the liver and gallbladder were discarded. The whole gut was then separated into anatomical regions of the oesophagus, stomach, anterior intestine with the pyloric caeca, mid intestine and hind intestine. The gut segments were washed with a physiological gut saline (in mmol/L: NaCl, 117.5; KCl, 5.7; $NaHCO_3$, 25.0; $NaH_2PO_4.H_2O$, 1.2; $CaCl_2$, 2.5; $MgSO_4.7H_2O$, 1.2; glucose, 5.0; mannitol, 23.0; pH 7.8 from Handy et al. (2000)). The resulting portions of gut were formed into sacs by closing one end with surgical thread and then filled with the gut saline as appropriate, and then weighed.

The gut sacs for each anatomical region were inevitably of different sizes, but each gut sac was filled as much as possible, with one of four solutions: gut saline (described above, no added Ag), or gut saline spiked with 1 mg/L Ag as $AgNO_3$, Ag NPs or Ag_2S NPs. The volume of the added saline was recorded to facilitate calculation of the absolute dose in each gut sac (see below). The exposure concentration of 1 mg/L of Ag was selected as a sub-lethal concentration which would provide mechanistic information of the accumulation of different forms of Ag (i.e., not for environmental realism), and to ensure that any Ag accumulated by the tissue could be readily detected by ICP-MS, as well as enabling direct comparison with our previous gut sac studies on TiO_2 ENMs (Al-Jubory and Handy 2013). The silver speciation from the $AgNO_3$ in the gut saline above (pristine, no contact with fish tissue) was theoretically calculated using Visual MINTEQ 3.1 by J. P. Gustafsson (https://vminteq.lwr.kth.se/download/). The calculated silver species in the normal gut saline containing chloride was: Ag^+, 79.55%; AgCl (aq), 20.21%, and $AgCl_2^-$, 0.22%. For the experiments with chloride-free saline, the relevant salts of chloride-containing chemicals were substituted with equimolar concentration of $NaNO_3$, KNO_3 and $CaNO_3$ in the recipe above. The calculated silver speciation in the chloride-free saline at pH 7.8 was: Ag^+, 96.1%; $AgNO_3$ (aq), 3.91%; indicating the silver was dissolved. The

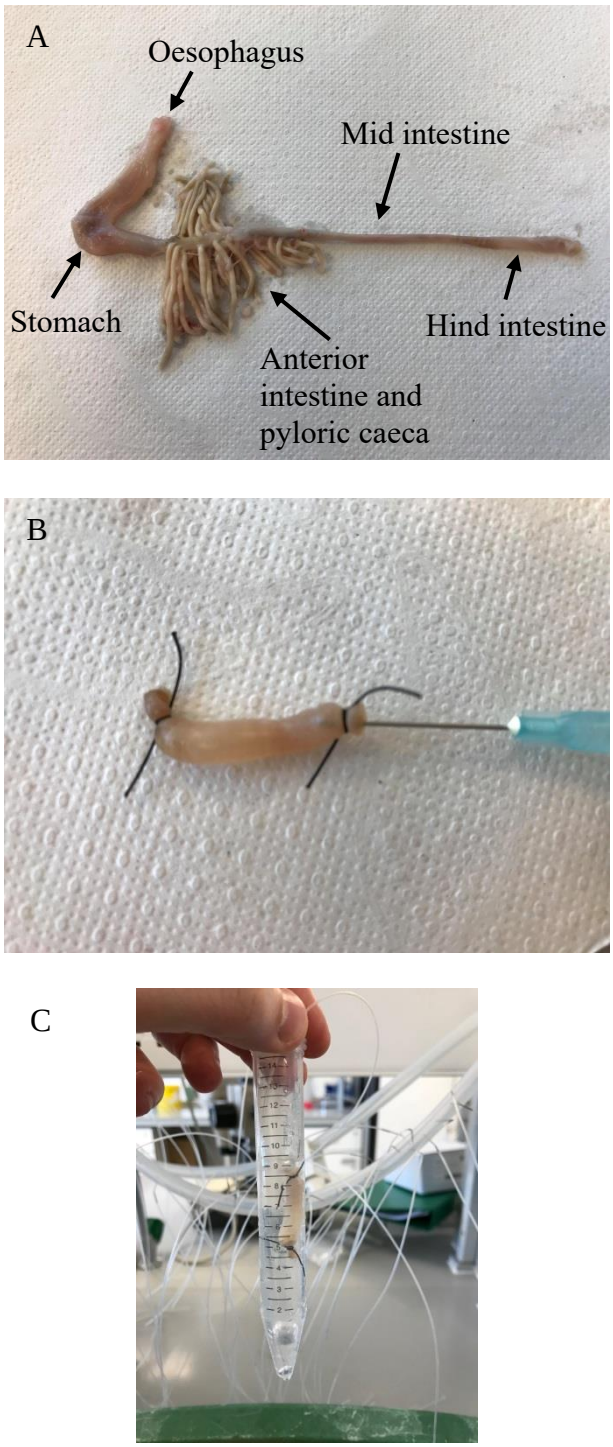

Figure 2-1. Gut sac exposures. (A) The entire gastrointestinal tract is removed from the fish followed by separation into anatomical regions. (B) One end of the gut sac is sutured shut and the opposite end filled using a syringe with test solution/suspension (i.e., control or 1 mg/L Ag as $AgNO_3$, Ag NPs or Ag_2S NPs). The hind intestine only is shown for clarity. (C) The gut sac is incubated in physiological saline for 4 h and gassed with 99.7:0.3% O_2:CO_2.

chloride-free experiment was not performed with the Ag_2S NPs as there was not expected to be an effect due to the inert nature of this material.

Tissue compartments were subsequently closed using suture thread and the tissues were carefully weighed to confirm the net mass of the exposure media added to each compartment. Tissues were individually incubated in 50 mL (stomach and anterior intestine) or 15 mL (oesophagus, mid and hind intestine) tubes containing 20 and 7.5 mL of the appropriate gut saline, respectively. The use of individual tubes for each anatomical region and piece of gut enabled collection of the serosal fluid for total Ag determination and the subsequent calculation of the apparent net transepithelial uptake of the metal. In all experiments, the serosal saline was isosmotic with that on the luminal side, but without any silver addition. The gut sacs were incubated at 15 ± 1^{o}C for 4 h and aerated with a 99.7% O_2: 0.3% CO_2 gas mixture. Samples of the serosal saline were taken after 4 h from each individual tube (n = 6 per tissue/treatment). The viability of the gut sacs is measured through calculation of the fluid flux (Handy et al. 2000; Hoyle and Handy 2005; Ojo and Wood 2007; Kwong and Niyogi 2009). The fluid flux was measured gravimetrically at the beginning and end of experiment gravimetrically (any net flux of water should be into the gut sac in freshwater fish; Handy et al. 2000). Any gut sac that showed appreciable weight loss (i.e., loss of the contents) or a high silver concentration in the serosal saline (i.e., evidence that the sutures were leaking) was discarded.

Successful gut sacs were then processed to determine the total Ag concentration by ICP-MS. For each regions of the gut, the sutures were removed and the gut rinsed in 5 mL of the appropriate clean gut saline, with these luminal washings collected into a 50 mL tube for Ag determination. Tissues were then immediately dipped into a second 5 mL of gut saline containing 1 mmol/L disodium ethylenediaminetetraacetate (EDTA) as a precautionary further rinse to aid removal of any loose surface associated material (i.e.,

particulates and cations that were labile on the surface of the tissue). Subsequently, the tissues were blotted on 25 cm^2 squares of tissue paper (two squares for oesophagus, mid intestine and hind intestine, four sheets for the stomach and anterior intestine). The tissue papers were stored in the tube with the EDTA saline rinse for later trace metal analysis (see below). The collection of these various washings and blotted papers enabled some ready estimate of the externally adsorbed silver, rather than the internally absorbed silver, during the experiments. Although, more detailed surface adsorption experiments were also performed (see below). Following the washing and blotting, the gut mucosa was stripped from the surface of the muscularis using the edge of a microscope slide and weighed and stored at -20^oC prior to subsequent metal analysis (see below).

Tissue concentrations of Ag were routinely expressed as ng/g dry weight (dw) of tissues and net accumulation rates expressed per g dw of tissue. However, it can also be useful to express fluxes across the gut epithelium on a surface area basis. For the latter, the outline of the muscularis layer was drawn onto white paper and the surface area calculated using ImageJ software. The fluid flux (µL/cm^2/h; equation 2.1), was assessed gravimetrically according to Ojo and Wood (2007).

$$Fluid\ flux = \frac{\Delta V}{SA\ x\ T} \qquad \text{Equation 2.1}$$

Where ΔV (g) is the change in volume of the gut sac lumen (based on equivalent weight of water) over the 4 h exposure, SA (cm^2) is the surface area and T (h) is time.

The apparent net accumulation of metals in the gut is rarely fixed, but usually varies with the exposure concentration; with the fraction remaining in the gut lumen or loosely attached to the exterior of the gut mucosa also changing. It is therefore useful to express the absolute amount of total Ag measured in the washings and the different tissues as a fraction of the absolute amount of Ag in the exposure; with the latter amount being the

measured concentration in ng/mL multiplied by the volume (mL x 100%). The proportions of the total Ag in the muscularis, mucosa and the EDTA wash were expressed as a percentage of the absolute amount of silver added to the gut lumen at the start of the incubation. The proportion of the total silver in the initial saline rinse to obtain the luminal washings was estimated as follows:

$$Percent\ of\ Ag\ in\ luminal\ washing = \frac{D0-(Muscularis+Mucosa+EDTA}{D0} \qquad \text{Equation 2.2}$$

Where *D*0 is the absolute amount of Ag (i.e. the dose, the absolute mass of total silver in ng) inserted into the gut lumen at the start of the experiment, *Muscularis*, *Mucosa* and *EDTA* represent the mass (ng) of Ag associated with the muscularis, mucosa and the EDTA washing, respectively.

2.2.4 Surface binding experiment using $AgNO_3$, Ag NPs and Ag_2S NPs

To quantify the amount of Ag that was surface bound to the intestine during the gut sac experiment, a separate 'rapid solution dipping' experiment was conducted following Al-Jubory and Handy (2013). The mid and hind intestines were selected for this task because these segments of the gut could be easily everted and dipped in test solutions to quantify the adsorption of Ag to the mucosa. The tissues collected were first dipped in 500 mL of clean chloride-containing saline (described above) for 30 seconds as an initial rinse. Then the tissues were dipped in 500 mL of the same saline but containing 1 mg/L of the appropriate Ag material for 30 seconds. This duration was to mimic the instantaneous exposure of the surface of the gut sacs, but also ensuring negligible uptake into the tissues

(Al-Jubory and Handy 2013). Tissues were then processed as above (i.e., with a luminal wash and an EDTA rinse), prior to measurement of the total Ag concentrations (see below).

2.2.5 Trace metal analysis

Trace metal analysis was conducted using a similar approach to Shaw et al. (2012). The total silver concentration was determined by ICP-MS in the luminal and serosal saline at the end of each experiment, and in the washings from the mucosa, as well as in the tissue samples following strong acid digestion. Samples of saline collected from the experiment were acidified and diluted prior to analysis. The washings from both the initial luminal saline rinse and the subsequent EDTA rinse of the exterior surface of the mucosa (~ 5 mL) were acidified with 2 mL nitric acid and diluted to 20 mL with ultrapure water and left over night before being analysed by ICP-MS. For the EDTA wash, this enabled time for any labile silver on the surface of the blotting paper in each tube to leach into the solution. With every set of samples, procedural blanks were also performed to account for any contamination from test tubes or reagents. For the analysis of all salines and washings, the standards were matrix matched and standard curves of $AgNO_3$, Ag NPs and Ag_2S NPs in saline were compared to commercially available elemental standards. Instrument drift was monitored by the addition of internal standards (indium and iridium) and standard checks were made every 10-15 samples. The instrument limit of detection was calculated for each set of samples by multiplying the standard deviation of the lowest standard by three. The Ag detection limit for the gut saline was around 0.54 ng/mL. Measurements of the total Ag from the working stocks were 97 ± 0.14%, 98 ± 0.24% and 95 ± 5.66% of the expected nominal total Ag concentration for $AgNO_3$, Ag NP and Ag_2S NPs, respectively (mean ± S.D., n = 5).

Tissue samples of mucosa and separated muscularis were analysed according to Shaw et al. (2012) with minor modifications. Tissues were freeze dried overnight (Lablyo freeze dryer), weighed and then digested in 0.2 mL of primer plus grade nitric acid for 4 h at 55^{o}C and diluted to 2 mL using ultra-pure water. Standards were matrix matched and instrument drift checked during the sample runs as above. A certified reference tissue (Dorm 4; National Research Council Canada) was also digested as above and analysed for total Ag. Dorm 4 gave a good recovery of 112 ± 10% (mean ± S.D., n = 3). The limit of detection for Ag in the tissue digests was 0.08 ng/mL, which equates to a tissue detection limit of (mean ± S.E.M., n = 6) 40.9 ± 7.8 and 5.1 ± 0.9 ng g^{-1} dw in the mucosa and muscularis, respectively.

2.2.6 Dialysis experiments

Dialysis experiments were conducted with the Ag NPs or Ag_2S NPs to determine any dissolution of dissolved silver from the particles. Measurements were made in both ultrapure water and the appropriate gut saline. Two pH values were selected: pH 7.8 to simulate the gut sac exposures and pH 2 (adjusted using nitric acid to ensure same chloride concentration) to mimic the acidity of the stomach (Bucking and Wood 2009). One concern for the pH experiment was that the neutral pH would drive the binding of any Ag^+ ions to the glassware, unlike acid conditions, and thus cause artefacts in the measured silver concentration in the external solution in the beaker. To check for this phenomena, a known concentration of Ag as $AgNO_3$ (100 µg/L) was spiked directly into the gut saline at pH 2 and 7.8, and its disappearance over time was monitored. Another concern for the gut is the presence of amino acids in the lumen that might chelate any dissolved silver and so drive dissolution of the Ag NPs. Dialysis experiments were therefore also conducted in the gut

saline, but in the presence of essential amino acids (0.5 mM of either L-histidine or L-cysteine). In addition, to know if the dissolution characteristics were saline-specific, a blood compartment saline (Cortland saline, in mmol L^{-1}: NaCl, 121.4; KCl, 5.1; $NaHCO_3$, 11.9; $Na_2HPO_4.H_2O$, 2.9; $CaCl_2.2H_2O$, 1.4 and $MgSO_4.7H_2O$ 1.9; pH 7.8) was also used to compare against the gut saline. These latter two experiments with amino acids or Cortland saline were only conducted with the Ag NPs, as Ag_2S material showed no appreciable dissolution in the earlier experiments with gut salines.

The dialysis experiments were performed similar to Besinis et al. (2014). Beakers (400 mL volume) were acid washed and rinsed in ultrapure water before adding 297 mL of the respective saline. Dialysis tubing (Sigma-Aldrich, 12,000 kDa cut off) was cut into 15 cm lengths and soaked overnight in water and then rinsed in ultrapure water. The tubing was sealed at one end with a knot and 3 mL of a 100 mg/L Ag NP stock added to the bag. The tubing was then sealed with another knot. Once sealed, the exterior of the dialysis bags were carefully rinsed with ultrapure water and placed in the beakers of the respective saline. The beakers were gently stirred (IKA RO 15 power Magnetic stirrer) at room temperatures for 4 h. For all dialysis experiments, water samples (1 mL) were taken at 0 (before dialysis bags were added to beakers), 0.25, 0.5, 1, 2 and 4 h (i.e., to match the duration of the gut sac experiments). The samples were acidified immediately with 1 mL of Primar Plus trace analysis grade nitric acid. Samples were further diluted with ultrapure water to a final volume of 4 mL and analysed using ICP-MS as above using matrix matched standards.

2.2.7 Statistical analysis

All data were presented using mean ± S.E.M., with curve fitting and statistical analysis conducted using SigmaPlot 13.0. Data was analysed for outliers using Grubbs test ($P <$

0.05) before checking data for normality (Shapiro-Wilk test) and equal variance (Brown Forsythe). Data that were normally distributed, or could be $\log_{10}$ transformed to a normal distribution, were analysed by either a one-way ANOVA (either for effects within saline or Ag concentrations within gut sacs from one region of the gut) or a two-way ANOVA (between treatment and tissue types and/or gut region) followed by the post hoc Holm-Sidak procedure. Where data were non-parametric and could not be transformed, the Kruskal-Wallis test was used. *P* values presented are from post hoc tests. For dialysis experiments, the dissolution curves were fitted with a rectangular hyperbole function to the mean values.

2.3 Results

2.3.1 Particle characterisation

The TEM revealed the primary particle diameter of Ag NPs and Ag_2S NPs to be 55 ± 3 nm (mean ± S.D., n = 120) and 37 ± 19 nm (mean ± S.D., n = 103), respectively (Fig. 2-2). The concentration of the total Ag in the stocks of Ag NPs and Ag_2S NPs was also measured by inductively coupled plasma mass spectrometry (ICP-MS, Thermo X-series 2 ICP-MS). The stock concentrations for (mean ± S.D., n = 4) the Ag NPs and Ag_2S NPs were 9.9 ± 0.3 and 2.3 ± 0.2 g/L. The latter stock was from a bespoke commercial synthesis undergoing validation and for understanding potential settling in the vials as supplied, emphasis was therefore on the measured, rather than nominal, concentration of silver. The mean (± S.D.) hydrodynamic diameter was 66 ± 4 nm (n = 3) for 1 mg/L Ag NPs, and a mean hydrodynamic diameter of 135 ± 7 nm (n = 3) for 1 mg/L Ag_2S NPs (Fig. 2-1). As expected, both types of Ag NPs and Ag_2S NPs tended to aggregate in the high ionic strength media

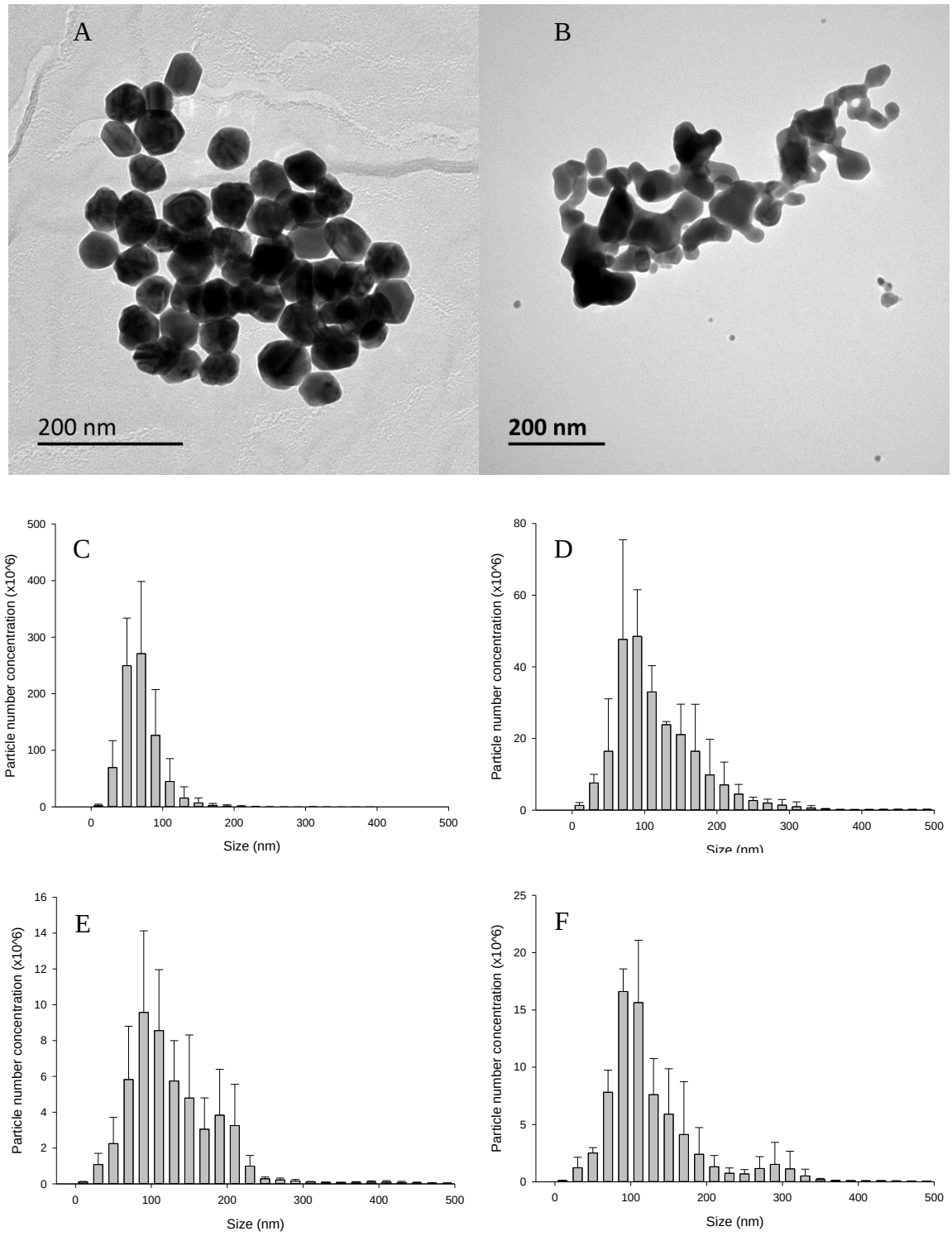

Figure 2-2. Transmission electron micrographs of Ag NPs (A) and Ag_2S NPs (B). Particle aggregation behaviour of Ag NPs and Ag_2S NPs in ultrapure water (C and E, respectively) and physiological gut saline (D and F, respectively) measured by Nanosight Tracking Analysis. Note the small percentage of particles above 300 nm in the Ag_2S NP panels only. Mean ± S.D. (n = 3).

compared to ultrapure water. Dispersions of Ag NPs in the gut saline had a mean hydrodynamic diameter of 115 ± 19 nm (n = 3). For Ag_2S NPs in saline the mean hydrodynamic diameter was 135 ± 13 nm (n = 3). The NTA could not detect a significant number of particles after 4 h, indicating that most of the particles had settled from the water column.

2.3.2 Ag exposure of gut sacs in chloride-containing media

The nominal Ag concentrations were confirmed by ICP-MS measurement in the fresh stocks before dosing. In addition to this, the gut sac lumen contents were collected at the end of the experiment and then the tissue was rinsed in clean saline to ensure as much as possible of the residual exposure media was collected (the 'luminal saline' in Table 2-1). The Ag contents of the resulting saline from this initial rinse at the end of the experiment are shown in Table 2-1. The data are expressed as ng of absolute mass as the volume of the gut sac varied between anatomical regions of the gut. Nonetheless, the amounts of Ag in the rinses from the control (unexposed) gut sacs were below the detection limit, as expected (Table 2-1). For the $AgNO_3$ exposure, the luminal saline contained around 72-100 ng of total Ag, or much higher depending on the region of the gut, at the end of the experiment; confirming that the supply of Ag in the lumen remained in excess throughout. Similarly, for the Ag NPs and Ag_2S NP exposures, readily detectable amounts of Ag remained in the lumen (Table 2-1), confirming that the exposure had persisted over the 4 h incubation.

There were also some differences in the residual Ag remaining in the gut lumen after the initial rinse according to anatomical regions of the gut (Table 2-1). Within the $AgNO_3$ treatment, there tended to be more Ag remaining in the lumen of the stomach and hind intestine compared to other regions of the gut, but these were not statistically different

Table 2-1. Confirming exposure of gut sacs to control (no added Ag) or 1 mg/L Ag as either $AgNO_3$, Ag NPs or Ag_2S NPs. Total mass (ng) of Ag found in the luminal saline (rinse 1) and EDTA wash (rinse 2).

Saline type	Treatment	Sample type	Oesophagus	Stomach	Anterior intestine	Mid intestine	Hind intestine
Chloride-containing	Control	Luminal saline	$<10.8^{A}$	$<10.8^{A}$	$<10.8^{A}$	$<10.8^{A}$	$<10.8^{A}$
		EDTA wash	$<10.8^{A}$	$<10.8^{A}$	$<10.8^{A}$	$<10.8^{A}$	$<10.8^{A}$
	$AgNO_3$	Luminal saline	71.9 ± 18.3^{A}	217.8 ± 56.2^{Aa}	$<10.8^{Aa}$	100.5 ± 42.7^{Aa}	311.6 ± 56.3^{Aa}
		EDTA wash	20.3 ± 7.2^{Ba}	143.7 ± 27.7^{Ac}	47.2 ± 17.5^{Aab}	76.4 ± 10.1^{Abc}	67.4 ± 22.4^{Babc}
	Ag NPs	Luminal saline	$53.4 \pm 25.0^{A\,ab}$	100.8 ± 28.5^{Ab}	26.11 ± 15.4^{Aa}	90.8 ± 16.7^{Ab}	378.8 ± 69.6^{Ac}
		EDTA wash	36.9 ± 7.3^{A}	66.2 ± 9.0^{Aa}	45.6 ± 10.6^{Ba}	42.97 ± 9.4^{Aa}	49.8 ± 10.8^{Ba}
	Ag_2S NPs	Luminal saline	13.2 ± 3.9^{Aabc}	378.3 ± 80.4^{Aab}	217.9 ± 77.5^{Ac}	52.4 ± 10.3^{Aab}	14.7 ± 4.9^{Ac}
		EDTA wash	16.1 ± 3.1^{Ab}	69.2 ± 14.5^{Ba}	6.3 ± 1.6^{Ba}	28.1 ± 6.1^{Ac}	5.3 ± 1.7^{Ab}
Chloride-free	Control	Luminal saline	$<10.8^{A}$	$<10.8^{A}$	$<10.8^{A}$	$<10.8^{A}$	$<10.8^{A}$
		EDTA wash	$<10.8^{A}$	$<10.8^{A}$	$<10.8^{A}$	$<10.8^{A}$	$<10.8^{A}$
	$AgNO_3$	Luminal saline	<10.8	202.8 ± 56.2^{Aa}	<10.8	85.6 ± 42.6^{Aa}	296.6 ± 56.3^{Aa}
		EDTA wash	<10.8	127.6 ± 27.7^{Aa}	52.1 ± 17.9	63.2 ± 10.1^{Aa}	61.6 ± 24.3^{Aa}
	Ag NPs	Luminal saline	<10.8	85.9 ± 28.5^{Aab}	<10.8	44.36 ± 22.6^{Aa}	363.9 ± 69.6^{Ab}
		EDTA wash	<10.8	74.6 ± 41.2^{Aa}	36.4 ± 5.7	20.8 ± 11.0^{Aa}	29.8 ± 12.0^{Aa}

Data are mean ± S.E.M (n = 5/6). Different upper case letters denote significance between rinse 1 and 2. Different lower case letters denote statistical differences between gut regions (rows; Two-way ANOVA). No difference between gut regions of the chloride-free AgNO3 and Ag NP treatments (Two-Way ANOVA). No significant difference between the gut regions of the chloride-free AgNO3 treatment (Two-Way ANOVA). The limit of detection of the instrument was 0.54 ng/mL which equates to 10.8 ng Ag in the luminal and EDTA washes.

from other regions (two-way ANOVA, P = 0.062 to 0.898). Similarly for the Ag NP exposure, the highest Ag content was found in the lumen of the hind intestine (two-way ANOVA, P = 0.001), but not in the case of Ag_2S NPs where the most residual Ag was found in the lumen of the stomach ($P < 0.001$) and anterior intestine ($P < 0.036$).

The exposure was also confirmed by measuring the total Ag concentrations in the rinsed portions of mucosa and muscularis at the end of the experiment (Table 2-2). The measured Ag concentrations in tissues from control (unexposed) gut sacs remained below the detection limit. In contrast, exposure to $AgNO_3$, Ag NPs and Ag_2S NPs resulted in readily detectable total Ag in both the mucosa and muscularis in all regions of the gut (Table 2-2).

Unsurprisingly, the gut mucosa being the uppermost external facing tissue showed much higher concentrations of total Ag than the equivalent underlying muscularis, regardless of the type of Ag exposure (Table 2-2). In most cases, two thirds or more of the accumulated Ag was associated with the mucosa, rather than the muscularis. Two-way ANOVA revealed both gut region and treatment related differences in the mucosa. For the $AgNO_3$ exposure, there was a tendency for more Ag to accumulate in the mucosa of the mid intestine, although this was not statistically significant from the other regions in the gut (P = 0.458 to 0.998). Similar observations were made for the mucosa from gut sacs exposed to Ag NPs or Ag_2S NPs. However, for the Ag_2S NP treatment, the total Ag concentration in the mid intestine was significantly higher than the anterior intestine (P = 0.022). Within treatment, the Ag associated with the mucosa of the mid intestine of Ag_2S NP (P = 0.043) treatment was significantly elevated compared to the mid intestine of the Ag NP treatment; indicating a material-type effect within the mid intestine.

The two-way ANOVA of the concentration of total Ag in the muscularis (Table 2-2) showed statistically significant differences overall for both the gut region and type of

treatment. In most cases, there was statistically more Ag in the muscularis from the $AgNO_3$ exposure than either of the nano forms; indicating the nano forms were less bioavailable to this tissue. However there were also some small, but statistically significant differences, between the total Ag accumulated in the muscularis from exposure to Ag NPs compared to the Ag_2S NPs; with generally less Ag accumulated from exposure to Ag_2S NPs (Table 2-2). Anatomical region of the gut was also important and within the muscularis of the $AgNO_3$ treatment, the anterior, mid and hind intestine showed significantly elevated total Ag concentrations compared to both the oesophagus and stomach (all values $P < 0.001$). A similar pattern was observed from the gut region effect in the Ag_2S treatment where the hind intestine was significantly higher compared to the oesophagus ($P = 0.024$) and stomach ($P = 0.049$). However, there was no significant difference between gut regions within the Ag NP treatments for the muscularis ($P > 0.05$).

2.3.3 Ag exposure of gut sacs in chloride-free media

The results of the experiments using a nominally chloride-free saline were almost identical to those with the chloride-containing saline, indicating that the exposure (Table 2-1) and Ag accumulation in the tissue (Table 2-2) were largely unaffected by the removal of chloride. In the washing from the chloride-free experiment, as expected the Ag concentrations from the unexposed controls remained below detection limit. However, silver from both $AgNO_3$ and Ag NP exposures was detected in the luminal and EDTA washes at the end of the exposure, confirming the metal was in excess in the lumen throughout the experiments (Table 2-1). Both the $AgNO_3$ and Ag NP treatments had a tendency for more Ag to be found in the washings from the stomach and hind intestine, compared to the other regions of the gastrointestinal tract; yet a two-way ANOVA revealed only the washings from the Ag NP exposure to the hind intestine was significantly higher

Table 2-2. The concentration of Ag in the tissues (ng/g dw) and the percentage of Ag in the mucosa following 4 h exposure to control (no added Ag) or 1 mg/L Ag as either $AgNO_3$, Ag NPs or Ag_2S NPs.

Saline type	Treatment	Sample type	Oesophagus	Stomach	Anterior intestine	Mid intestine	Hind intestine
Chloride-containing	$AgNO_3$	Mucosa	1303.6 ± 398.7^{Aa}	1165.6 ± 295.4^{Aa}	1301.7 ± 445.1^{Aa}	3961.7 ± 1254.5^{ABa}	1508.9 ± 375.3^{Aa}
		Muscularis	72.4 ± 27.5^{Aa}	76.4 ± 16.3^{Aa}	289.1 ± 36.1^{Ab}	457.2 ± 110.9^{Ab}	518.2 ± 66.9^{Ab}
		% in mucosa	58.0 ± 9.0^{Aa}	63.7 ± 7.6^{Aa}	63.7 ± 5.5^{Aa}	74.8 ± 4.4^{Aa}	59.3 ± 4.0^{Aa}
	Ag NPs	Mucosa	747.6 ± 317.5^{Aab}	395 ± 68.7^{Aab}	610.0 ± 155.7^{Aa}	1506.9 ± 907.5^{Bb}	732.3 ± 258.7^{Aab}
		Muscularis	32.4 ± 6.5^{ABa}	39.0 ± 5.8^{Aa}	45.3 ± 8.3^{Ba}	38.0 ± 8.2^{Ba}	57.0 ± 6.6^{Ba}
		% in mucosa	71.4 ± 5.2^{Aab}	59.5 ± 3.7^{Aa}	90.2 ± 1.7^{Bc}	84.6 ± 3.8^{Bbc}	84.4 ± 4.3^{Bbc}
	Ag_2S NPs	Mucosa	852.6 ± 330.1^{Aa}	595.0 ± 106.1^{Aa}	327.9 ± 78.1^{Aa}	5145.5 ± 1944.4^{Aa}	2610.7 ± 628.0^{Aa}
		Muscularis	13.5 ± 1.6^{Ba}	13.1 ± 2.0^{Ba}	26.7 ± 8.6^{Bba}	38.5 ± 19.5^{Bab}	42.9 ± 10.3^{Bb}
		% in mucosa	77.6 ± 5.8^{Aa}	90.2 ± 1.3^{Bab}	90.6 ± 2.1^{Bb}	98.5 ± 0.6^{Cc}	96.8 ± 0.4^{Cd}
Chloride-free	$AgNO_3$	Mucosa	954.0 ± 439.4^{Aa}	1777.8 ± 680.0^{Aa}	527.7 ± 164.0^{Aa}	3278.0 ± 1156.2^{Aa}	1629.3 ± 477.5^{Aa}
		Muscularis	86.6 ± 23.8^{Aa}	65.6 ± 8.2^{Aa}	$144.1 \pm 23.3^{Aab*}$	488.3 ± 165.8^{Ab}	641.0 ± 110.8^{Ab}
		% in mucosa	49.1 ± 9.2^{Aa}	74.4 ± 5.3^{Ab}	60.9 ± 9.4^{Ab}	82.5 ± 11.1^{Ab}	41.9 ± 8.6^{Aa}
	Ag NPs	Mucosa	416.5 ± 245.8^{Bab}	462.8 ± 182.3^{Bab}	$95.6 \pm 16.7^{Aa*}$	2729.5 ± 1016.8^{Ab}	1976.1 ± 1110.7^{Ab}
		Muscularis	19.0 ± 4.8^{Ba}	30.5 ± 9.3^{Bb}	31.1 ± 5.4^{Bb}	$88.6 \pm 21.9^{Bbc*}$	273.0 ± 117.9^{Bc}
		% in mucosa	51.8 ± 3.1^{Aa}	69.2 ± 13.5^{Aab}	72.3 ± 4.5^{Aab}	93.3 ± 1.5^{Ab}	56.6 ± 7.7^{Ba}

Data are mean ± S.E.M (n = 5/6). % in mucosa = mass in mucosa/mass in mucosa + mass in muscularis x 100. Unexposed controls are not shown due to being below the LOD of the ICP-MS. Different lower case letters denote statistical differences between regions of the gut (rows). Difference upper case letters denote statistical differences between treatment within the same sample type (but within saline type; columns). (*) denotes significant difference between same tissue but exposed to chloride-containing saline. No letters or * means no significant difference between tissues or treatments.

compared to that remaining following exposure of the mid intestine ($P = 0.027$). There was no significant difference between the amounts of total Ag recovered in the EDTA wash in either treatments with respect to anatomical regions of the gut.

The gut tissue itself also showed elevated total Ag concentrations following exposure to $AgNO_3$ or Ag NPs in chloride-free saline (Table 2-2), while the unexposed controls remained below the detection limit. Some anatomical regions of the gut also showed more total Ag accumulation from exposure to $AgNO_3$ compared Ag NP, indicating the metal salt was more bioavailable than the nanomaterial. Similar to the findings with chloride-containing saline, typically around two thirds of the Ag was associated with the mucosa rather than the underlying muscularis in chloride-free conditions, regardless of the form of Ag presented (Table 2-2). For the mucosa tissue, two-way ANOVAs revealed some overall gut anatomical region and treatment effects. However, the $AgNO_3$ treatment showed no significant difference of total Ag concentration in the mucosa with anatomical region of the gut. In contrast, the mucosa from the Ag NP treatment had significantly more total Ag in the mid ($P < 0.001$) and hind ($P = 0.004$) intestine compared to the anterior intestine. Additionally for the mucosa, there were some small, but statistical significant differences observed between the treatments in chloride-free saline with anatomical region of the gut. For example, the stomach of the $AgNO_3$ treatment had significantly more Ag compared to the Ag NP treatment ($P = 0.037$).

The muscularis of gut sacs exposed to either $AgNO_3$ or Ag NPs also showed readily measurable total Ag concentrations, albeit less than the equivalent mucosa. A two-way ANOVA showed the concentration of total Ag within the muscularis was dependent on gut region and treatment (Table 2-2) in chloride-free conditions. For example, the mid ($P = 0.001$) and hind intestine ($P < 0.001$) of the $AgNO_3$ treatment has significantly higher Ag concentrations compared to the oesophagus, or the stomach ($P < 0.001$). Similar

observations were made for anatomical region of the gut within the Ag NP exposures, with the muscularis of the mid (P <0.001) and hind (P = 0.001) intestine being significantly higher compared to the oesophagus.

Despite some treatment effects within the experiment with chloride-free saline, overall the replacement of chloride with other anions had absolutely no effect on the total amount of Ag recovered in the gut washings (Table 2-1). The removal of chloride from the saline did not increase Ag accumulation in the tissues, and mostly had no effects, except for a decrease in total Ag in the muscularis of the anterior intestine of the $AgNO_3$ treatment in chloride-free conditions (one-way ANOVA, P = 0.007). Within the muscularis of the mid intestine for Ag NP treatment, there was significantly more total Ag in tissue from the chloride-free saline compared to the chloride-containing saline (one-way ANOVA, P = 0.045).

2.3.4 Surface bound Ag and partitioning of total Ag in the gut tissue

The luminal saline rinses and EDTA washes of the gut sac tissue at the end of the main experiments (Table 2-1) was useful to demonstrate that the total Ag remained in excess in the gut lumen (i.e., the luminal contents could not be rate limiting for apparent uptake). The EDTA wash attempted to remove any labile fraction from the surface of the mucosa. This fraction (unsurprisingly) often had less total Ag than the initial rinse in luminal saline, but it did show that a surface associated EDTA-extractable fraction was present. A separate surface binding experiment was therefore conducted to investigate the phenomena in more detail in conditions where chloride was present (Fig. 2-3).

The latter experiment used the mid and hind intestine because those regions of the gut had shown the most Ag accumulation (Table 2-2). Fig. 2-3 shows the Ag remaining on

the surface of the tissue after a 30 second exposure and rinses to remove any labile or EDTA extractable fraction. The exposure time was too short for true internal uptake of Ag (regardless of form) and the Ag measured represents that which is associated with surface of the mucosa, but not easily removed by washing. The concentrations of Ag measured were low, <90 ng/g dw or much less (Fig. 2-3). There were some material-type effects on the apparent surface binding (Fig. 2-3) with more surface-bound Ag from $AgNO_3$ (unsurprising for dissolved silver) compared to the nano forms; and with Ag_2S binding the least. For example, a two-way ANOVA revealed the surface associated Ag from the $AgNO_3$ exposure to the mid intestine was significantly greater than that for both the Ag NP (P <0.001) and Ag_2S NP (P <0.001) treatments. The surface associated Ag from the $AgNO_3$ exposure to the hind intestine was significantly elevated.

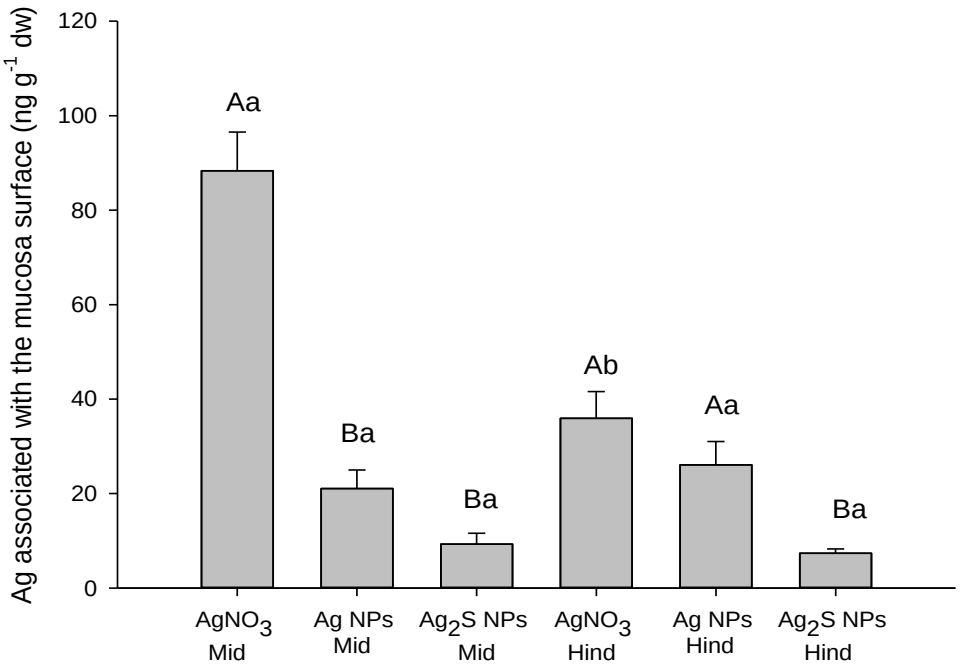

Fig. 2-3. The concentration of total Ag associated with the surface of the mid and hind intestine following the surface binding experiment (a 30 second exposure to saline containing control [no added Ag] or 1 mg/L Ag as either $AgNO_3$, Ag NPs or Ag_2S NPs). Data are mean ± S.E.M (n = 5). Upper case letters denotes statistical differences within same tissue type. Different lower case letters denotes statistical differences between gut regions within the same treatment.

Regardless of any treatment effects on surface binding, the values (Fig. 2-3) are in contrast to the hundreds of ng/g dw measured in the tissues from the main experiments (Table 2-2). This indicates that only a small fraction (<5%) of the total Ag measured in the gut sacs from the main experiments (Table 2-2) is surface associated, and that most of the Ag was inside the mucosa. The apparent net Ag accumulation rates into the mucosa are shown in Table 2-3 for the main experiments. The values reflect the original measured concentrations of Ag in the gut tissue (Table 2-2; or surface area; Table 2-4), with apparent net Ag uptake rates of a few nmol/g/h (Table 2-3). The apparent Ag accumulation rates were not attributed to passive water movement (i.e., solvent drag) as the water fluxes were small and sometimes in the opposite direction to the Ag flux (Table 2-3).

The partitioning of the exposure dose of Ag is shown in Table 2-5. The majority of the dose on a percentage basis remained in the lumen, or was removed by the EDTA wash; leaving only a few percent of the original dose in the mucosa, and even less in the muscularis (Table 2-5). This demonstrates the bioavailability of Ag is only a few percent of the exposure dose, regardless of the form of Ag used; and with the mid and hind intestine being more important that other regions of the gastrointestinal tract (Table 2-5). There is perhaps one exception, where the mucosa of the mid intestine was calculated to contain 19.7% of the Ag from Ag_2S (Table 2-5). Also, the anterior intestine contain the pyloric caeca, where between 30-54% of the total dose was localised. One-way ANOVA revealed no significant difference between the concentration of Ag associated with the caeca by treatment (P = 0.061). The pyloric caeca are blind-ending tubes and these values for the caeca likely contain some Ag that was impossible to rinse out of the tissue, reflecting the lower fractions of Ag also recovered from the luminal rinse of the anterior intestine (Table 2-5).

Table 2-3. Fluid flux and rate of accumulation into the mucosa of all materials in either chloride-containing or chloride-free saline.

		Oesophagus	Stomach	Anterior intestine	Mid intestine	Hind intestine
Fluid flux (mL/g/h)						
Chloride-containing	Control	0.05 ± 0.12^{a}	$-0.04 \pm 0.01^{a*}$	1.61 ± 1.49^{a}	0.03 ± 0.18^{a}	-0.12 ± 0.06^{a}
	$AgNO_3$	0.19 ± 0.24^{a}	-0.02 ± 0.02^{a}	0.81 ± 0.57^{a}	0.22 ± 0.13^{a}	-0.11 ± 0.04^{a}
	Ag NPs	0.13 ± 0.06^{a}	0.16 ± 0.09^{a}	2.79 ± 1.23^{a}	$0.03 \pm 0.28^{a*}$	0.12 ± 0.36^{a}
	Ag_2S NPs	-0.03 ± 0.10^{a}	-0.06 ± 0.04^{a}	0.27 ± 0.58^{a}	0.91 ± 0.41^{a}	0.59 ± 0.45^{a}
Chloride-free	Control	-0.07 ± 0.07^{a}	0.03 ± 0.02^{a}	0.03 ± 0.06^{a}	-0.19 ± 0.08^{a}	-0.16 ± 0.19^{a}
	$AgNO_3$	0.11 ± 0.07^{a}	0.05 ± 0.02^{a}	0.12 ± 0.24^{a}	-0.19 ± 0.09^{a}	-0.10 ± 0.25^{a}
	Ag NPs	-0.03 ± 0.08^{a}	0.05 ± 0.02^{a}	0.28 ± 0.20^{a}	-0.17 ± 0.09^{a}	-0.17 ± 0.14^{a}
Accumulation rate into mucosa (nmol g^{-1} h^{-1})						
Chloride-containing	Control	ND	ND	ND	ND	ND
	$AgNO_3$	2.31 ± 0.75^{Aa}	2.72 ± 0.69^{Aa}	3.04 ± 1.04^{Aa}	9.26 ± 2.93^{ABa}	3.53 ± 0.88^{Aa}
	Ag NPs	4.08 ± 2.40^{Aa}	0.92 ± 0.16^{Aa}	$1.43 \pm 0.36^{Aa*}$	3.52 ± 2.12^{Ba}	1.71 ± 0.60^{Aa}
	Ag_2S NPs	1.99 ± 0.77^{Aab}	1.39 ± 0.25^{Aab}	0.77 ± 0.18^{Aa}	12.02 ± 4.07^{Ab}	6.10 ± 1.47^{Aab}
Chloride-free	Control	ND	ND	ND	ND	ND
	$AgNO_3$	2.23 ± 0.93^{Aa}	4.15 ± 1.59^{Aa}	1.23 ± 0.38^{Aa}	7.66 ± 2.70^{Aa}	3.73 ± 1.12^{Aa}
	Ag NPs	0.97 ± 0.57^{Bab}	1.08 ± 0.43^{Bab}	0.20 ± 0.03^{Aa}	7.48 ± 2.57^{Ab}	5.36 ± 3.05^{Ab}

Data are mean ± S.E.M (n = 5/6). ND indicates an accumulation rate cannot be determined due to tissue concentration being below the LOD of the ICP-MS. No significant difference in the fluid fluxes between treatments. Lower case letters denotes statistical difference between gut regions in the same treatment (rows). Upper case letters denote statistical differences between treatments (columns). (*) denotes significant effect between saline (One-Way ANOVA). Significant Difference between saline of the control stomach, $AgNO_3$ mid (one way ANOVA).

Table 2-4. The moisture content, fluid flux and total Ag accumulation rates of all $AgNO_3$, Ag NPs and Ag_2S NPs into the mucosa, either in the chloride-containing or chloride-free saline.

	Control	$AgNO_3$	Ag NPs	Ag_2S NPs
Moisture (%)				
Chloride-containing				
Oesophagus	78.2 ± 1.08	77.4 ± 2.34	80.0 ± 1.68	80.1 ± 0.84
Stomach	80.7 ± 1.27	81.2 ± 0.77	80.5 ± 0.51	80.5 ± 0.65
Anterior	76.9 ± 1.51	76.2 ± 1.45	75.9 ± 1.71	74.8 ± 2.49
Mid intestine	80.9 ± 1.80	81.8 ± 1.72	79.9 ± 1.66	83.0 ± 1.86
Hind intestine	81.0 ± 1.81	82.3 ± 1.68	81.8 ± 1.30	81.7 ± 1.43
Chloride-free				
Oesophagus	78.5 ± 1.35	80.5 ± 1.02	80.2 ± 1.60	N/A
Stomach	80.2 ± 0.52	82.1 ± 1.23	80.1 ± 0.79	N/A
Anterior	73.9 ± 2.20	74.7 ± 2.20	69.7 ± 1.76	N/A
Mid intestine	78.0 ± 3.05	80.4 ± 2.03	81.5 ± 1.80	N/A
Hind intestine	83.0 ± 2.07	78.6 ± 5.90	79.1 ± 3.39	N/A
Fluid flux (µL/cm^2/h)				
Chloride-containing				
Oesophagus	1.37 ± 2.39	-1.06 ± 0.85	3.06 ± 1.23	-0.30 ± 1.26
Stomach	-1.46 ± 0.58	-0.76 ± 0.99	3.40 ± 2.10	-1.43 ± 0.92
Anterior	4.84 ± 4.51	1.52 ± 2.37	7.31 ± 2.71	0.78 ± 1.17
Mid intestine	0.34 ± 1.67	2.07 ± 1.23	0.70 ± 2.48	5.03 ± 1.62
Hind intestine	-2.26 ± 0.33	-1.34 ± 0.72	1.54 ± 5.05	3.55 ± 1.92
Chloride-free				
Oesophagus	-2.63 ± 2.32	4.41 ± 1.96	-0.57 ± 1.44	N/A
Stomach	1.63 ± 0.80	2.08 ± 0.90	1.32 ± 1.39	N/A
Anterior	0.33 ± 2.73	5.50 ± 11.82	12.13 ± 9.46	N/A
Mid intestine	-1.94 ± 0.74	-2.17 ± 0.46	-1.54 ± 0.88	N/A
Hind intestine	-2.44 ± 1.46	-3.67 ± 3.62	-4.14 ± 2.22	N/A
Accumulation rate into the mucosa (pmol/cm^2/h)				
Chloride-containing				
Oesophagus	ND	5.87 ± 1.92^{Aa}	7.70 ± 4.92^{Aa}	7.02 ± 2.09^{Aa}
Stomach	ND	13.08 ± 4.08^{Aa}	4.58 ± 0.68^{Aa}	11.63 ± 1.09^{Aa}
Anterior	ND	28.04 ± 7.77^{Aa}	13.32 ± 3.94^{Aa}	12.07 ± 2.86^{Aa}
Mid intestine	ND	23.05 ± 5.20^{Aa}	8.39 ± 4.55^{Ba}	63.45 ± 22.44^{Aa}
Hind intestine	ND	19.74 ± 7.23^{Aa}	7.01 ± 1.99^{Aa}	23.66 ± 7.88^{Aa}
Chloride-free				
Oesophagus	ND	6.13 ± 3.06^{Aa}	1.39 ± 0.55^{Aa}	N/A
Stomach	ND	28.84 ± 11.49^{Aa}	4.58 ± 3.26^{Bab}	N/A
Anterior	ND	11.14 ± 2.80^{Aa}	5.26 ± 1.34^{Aab}	N/A
Mid intestine	ND	27.31 ± 8.04^{Aa}	14.07 ± 4.39^{Ab}	N/A
Hind intestine	ND	12.88 ± 4.61^{Aa}	13.44 ± 5.27^{Aab}	N/A

Data are mean ± S.E.M (n = 5/6). Data are expressed as surface area of tissue (cm^2) for comparability to other published literature. There was no transepithelial uptake of Ag to the serosal saline. ND, not determined as the measured tissue concentration of total Ag was below detection limit. N/A, not applicable to Ag_2S experiments. Different lower case letters denotes statistical difference between gut regions in the same treatment (column). Different upper case letters denote statistical differences between treatments. There was no significant difference between fluid fluxes. The effect of saline had no statistically significant effects in the fluid flux or between the uptake rates in the mucosa (One-Way ANOVA).

Table 2-5. Partitioning of Ag distribution throughout the gut sac following exposure to saline containing control (no added Ag) or 1 mg/L Ag as either $AgNO_3$, Ag NPs or Ag_2S NPs. The rinse 1, rinse 2, the mucosa and muscularis expressed as the percentage of Ag dosed at the start of the 4 h incubation.

Treatment	Region of gut	Luminal rinse	EDTA wash	Cecae	Mucosa	Muscularis
$AgNO_3$	Oesophagus	80.5 ± 5.4 ^{a}	13.7 ± 6.0 ^{ab*}	-	3.8 ± 1.9 *	2.1 ± 0.7 *
	Stomach	76.6 ± 4.2 ^{a}	17.7 ± 3.6 ^{Aa*}	-	3.8 ± 1.1 $^{*\#}$	1.8 ± 0.4 $^{*\#}$
	Anterior	41.5 ± 2.4 ^{Ab}	4.5 ± 1.5 ^{Ab}	48.1 ± 3.3 $^{\#\wedge>}$	3.7 ± 0.7	2.2 ± 0.6 ^{A*}
	Mid	65.8 ± 3.3 ^{a}	22.4 ± 2.5 ^{Aa}	-	8.9 ± 1.9 $^{A*\#}$	2.9 ± 0.7 $^{A*\#}$
	Hind	82.1 ± 3.4 ^{a}	9.4 ± 2.3 ^{Aab*}	-	5.3 ± 1.2 *	3.2 ± 0.5 ^{A*}
Ag NPs	Oesophagus	69.9 ± 9.3 ^{a}	23.1 ± 6.0 ^{a*}	-	1.8 ± 0.5 $^{*\#}$	1.2 ± 0.4 $^{ab*\#}$
	Stomach	81.8 ± 5.1 ^{a}	14.8 ± 5.1 ^{ABab}	-	2.1 ± 0.7 *	1.4 ± 0.4 ^{a*}
	Anterior	39.4 ± 8.1 ^{Ab}	4.1 ± 0.8 ^{Ab}	54.0 ±7.9 $^{\#\wedge>}$	2.1 ± 0.6	0.4 ± 0.2 $^{Bb*\wedge}$
	Mid	78.0 ± 4.9 ^{a}	18.2 ± 3.8 ^{Ab}	-	3.5 ± 1.9 ^{B}	0.3 ± 0.1 ^{Bb*}
	Hind	88.8 ± 1.9 ^{a}	7.6 ± 2.1 ^{Aab*}	-	3.1 ± 1.1 $^{*\#}$	0.5 ± 0.2 $^{Bab*\wedge}$
Ag_2S NPs	Oesophagus	78.1 ± 3.8 ^{ab}	12.3 ± 1.7 ^{a*}	-	7.8 ± 2.5 ^{ab*}	1.8 ± 0.6 $^{a*\#}$
	Stomach	87.6 ± 1.7 ^{ab}	5.6 ± 1.2 ^{Bab}	-	6.1 ± 0.8 ^{ab}	0.7 ± 0.1 ^{ab*}
	Anterior	67.0 ± 8.0 ^{Ba}	0.3 ± 0.1 ^{Bc}	30.3 ± 7.4 $^{\#\wedge>}$	2.0 ± 0.6 ^{a*}	0.2 ± 0.1 $^{Bc*\wedge}$
	Mid	75.6 ± 6.3 ^{ab}	4.5 ± 1.2 ^{Bb}	-	19.7 ± 6.3 ^{Ab}	0.2 ± 0.1 ^{Bc*}
	Hind	90.9 ± 2.6 $^{b\#}$	0.5 ± 0.1 ^{Bc}	-	8.3 ± 2.7 ^{ab}	0.2 ± 0.0 $^{Bbc*\wedge}$

Data are mean ± S.E.M (n = 5/6). Upper case differences between treatments within the same gut region (columns). Lower case between gut regions in the same fraction and treatment (columns). For significant differences between fractions within rows, (*) denotes different to rinse 1, (#) denotes different to rinse 2, (^) different to mucosa and (>) different to muscle. There was no Ag detected in the serosal saline (transepithelial uptake). -, not applicable to this anatomical region of the gut.

2.3.5 Dialysis experiments in pure water and physiological salines

These experiments were conducted to explore the possibility of dissolved silver release from the Ag NPs and Ag_2S NPs. For the Ag_2S NPs no silver could be detected in the external compartment of the beakers, for either pure water or salines at pH 7.8 or pH 2. The instrument detection limit for Ag_2S was 0.2 µg/L as silver. However, dissolution curves could be constructed for the Ag NPs (Fig. 2-4), but the dissolution was only a few µg/L of dissolved silver (< 1% of the silver added) in most cases. For example, in ultrapure water at pH 7.8 there was a steady time-dependent rise in Ag concentration in the beaker over 4 hours that fitted a rectangular hyperbola (Fig. 2-4A), and reaching a silver concentration of 1.8 ± 1.5 µg/L by the end of the experiment. This represents dissolution of 0.18 % of the total Ag present in the dialysis bag, and the maximum rate of dissolution during the first few minutes of the experiment was 0.03 µg/min. There was a similar response for ultrapure water at pH 2 (Fig. 2-4B), although the curve reach a plateau within the first hour (0.9 ± 0.5 µg/L), representing 0.09% dissolution of the Ag NPs and with a maximum dissolution rate of 0.53 µg/min.

At pH 7.8, the concentration of dissolved Ag released into the normal gut saline (containing chloride) over 4 h was 6.2 ± 0.8 µg/L (Fig. 2-4C) and not statistically different to that in ultrapure water at neutral pH (P = 0.093). The dissolution in the gut saline was 0.87% of the Ag added to the dialysis bag, and with a maximum dissolution rate of 0.03 µg/min at pH 7.8. However, the dissolution was greater in the gut saline in acid condition (pH 2, Fig. 2-4D). A one-way ANOVA revealed some significant differences between the final concentration of Ag released Ag NPs in media after 4h, and for gut saline at pH 2 this was significantly higher (21.3 ± 10.0 µg/L) compared to that of ultrapure water at the same pH (P = 0.002). However, even this greater Ag release represented only 2.13% and with

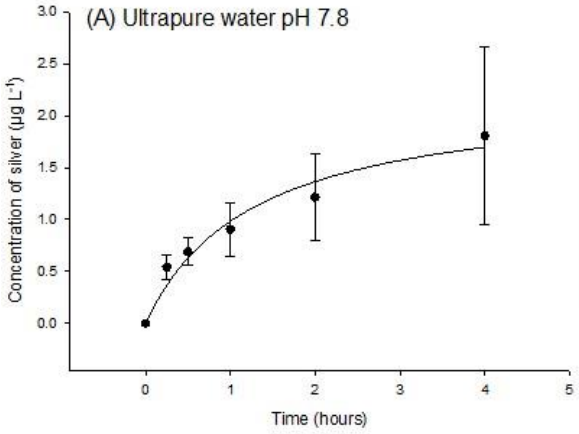
(A) Ultrapure water pH 7.8
Concentration of silver (µg L-1)
Time (hours)

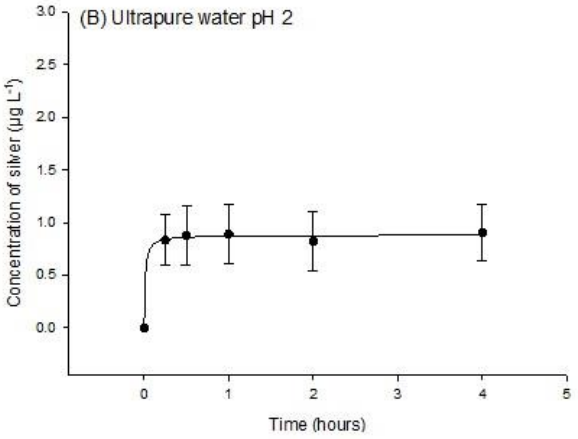
(B) Ultrapure water pH 2
Concentration of silver (µg L-1)
Time (hours)

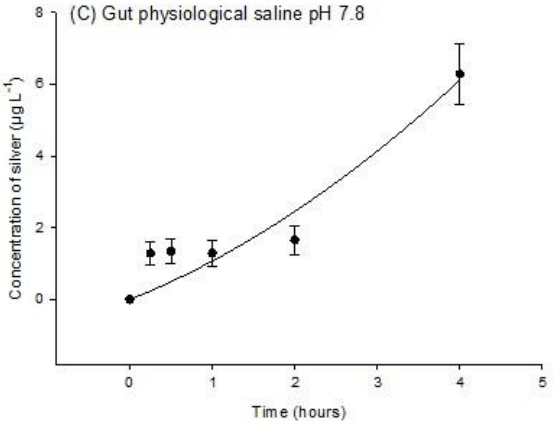
(C) Gut physiological saline pH 7.8
Concentration of silver (µg L-1)
Time (hours)

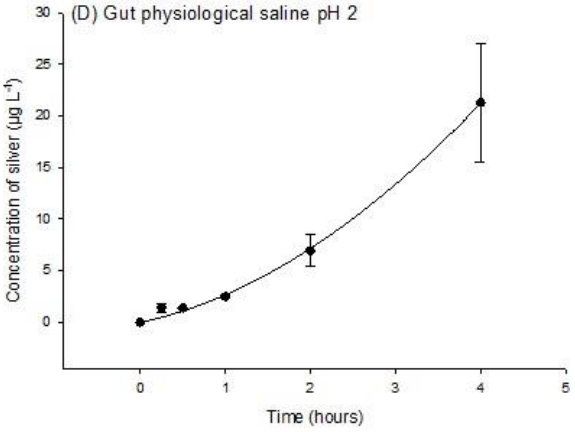
(D) Gut physiological saline pH 2
Concentration of silver (µg L-1)
Time (hours)

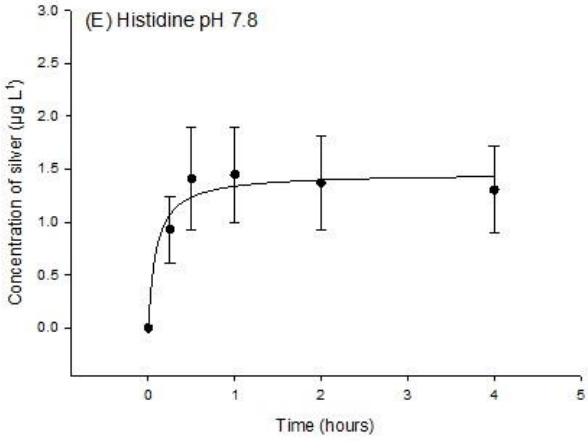
(E) Histidine pH 7.8
Concentration of silver (µg L-1)
Time (hours)

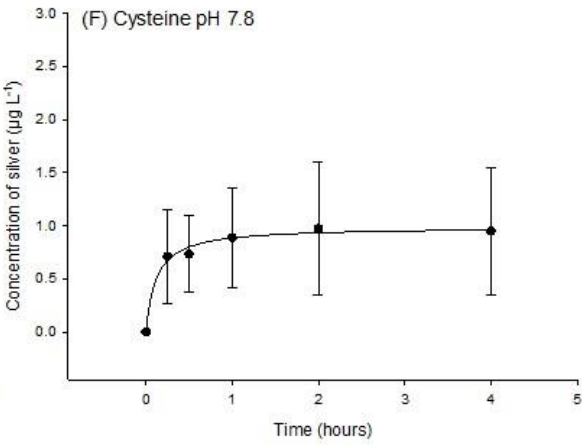
(F) Cysteine pH 7.8
Concentration of silver (µg L-1)
Time (hours)

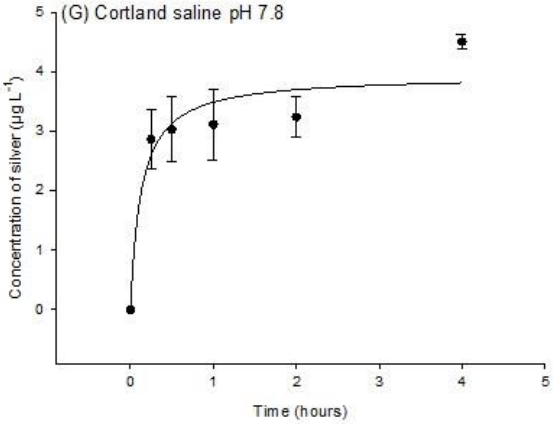
(G) Cortland saline pH 7.8
Concentration of silver (µg L-1)
Time (hours)

Fig. 2-4. Dialysis curves for the release of total dissolved silver from Ag NPs in ultrapure water at pH 7.8 (A) and 2 (B), gut physiological saline at pH 7 (C) and 2 (D), gut physiological saline + histidine (E), gut physiological saline + cysteine (F), and Cortland's saline (G). Data are mean ± S.E.M (n = 3). Curves were fitted with the equations y=a*x/(b+x). The values for a and b, as well as R^2 value were (A) 2.23, 1.27 and 0.96, (B) 0.88, 0.01 and 0.99, (C) -8.25, -9.3 and 0.90, (D) -19.22, -7.61 and 0.99, (E) 1.46, 0.09 and 0.95, (F) 0.99, 0.12 and 0.99, and (G) 3.93, 0.12 and 0.92., respectively.

a maximum dissolution rate 0.09 µg/min at pH 2 in gut saline. These differences in pH effects could not be attributed to artefacts such as the pH-dependent binding of dissolved Ag to the glassware because time course controls spiked with $AgNO_3$ directly into the beakers showed 104% recovery at both pH 7.8 and 2.

The presence of amino acids in the gut saline did not enhance silver dissolution. Additions of histidine (Fig. 2-4E) had no effect of the release of dissolved silver compared to the gut saline without histidine (P = 0.058); resulting in 1.3 ± 0.4 µg/L of dissolved Ag in the beakers at the end of the experiment. This was 0.13% of the initial Ag present, with a maximum dissolution rate of 0.23 µg/min in the presence of histidine. In contrast, the presence of cysteine caused a significant reduction in the concentration of Ag released compared to the same saline without amino acids (P = 0.010). The cysteine containing saline had a silver concentration of 0.9 ± 0.6 µg/L by the end of the experiment (Fig. 2-4F), representing 0.09% dissolution and a maximum rate of dissolution of 0.12 µg/min.

Cortland saline was also tested (Fig. 2-4G) as a fluid that represents the serosal compartment (i.e., the blood). There was 2.1 ± 1.0 µg/L release of Ag from Ag NPs after 4 h (not statistically different from the gut saline, P = 0.863); representing 0.45 % dissolution and with a maximum rate of 0.45 µg/min.

2.4 Discussion

This study has demonstrated the utility of the gut sac method and found that the mid and hind intestines are especially important to total Ag accumulation in the gut, regardless of the form of silver added. In most cases, the metal salt showed slightly more total Ag accumulation than either ENM. However, regardless of material added, the bioavailability was mostly only a few percent of the exposure dose, as expected for the gut as a biological barrier. Dialysis experiments showed very low or negligible dissolution of Ag NPs and Ag_2S NPs in gut physiological saline used, indicating that the NPs remained in the particulate form in the gut lumen.

2.4.1 Bioavailability of the metal salt and nanomaterials in the gut lumen

The first step in dissolved metal, or ENM uptake, is the presentation of the test substance in the gut lumen. For $AgNO_3$ at neutral pH in the presence of the millimolar concentrations of chloride found in the saline, a sparingly soluble AgCl complex is spontaneously formed (AgCl particles about 25 nm, see Besinis et al. 2014). The presence of AgCl was also predicted from chemical speciation calculations with Visual MINTEQ. Consequently, much of the silver would precipitate onto the mucus covering the gut surface and be readily washed off (as observed, Table 2-1). Thus, the bioavailability of Ag from $AgNO_3$ exposure was very modest (<9% of the exposure dose, Table 2-5).

In the case of the ENMs, a similar situation may apply. Reasonable dispersions were formed in ultrapure water, but the high ionic strength of the gut saline caused some particle settling (Fig. 2-2). Nonetheless, the freshly made gut saline used for dosing contained particles (Fig. 2-2). The particle size distribution in gut saline was also measured after 4

hours (no tissue present), but the particle number concentrations were too low to obtain reliable tracks by NTA. This showed that both types of silver NPs would settle quickly from the gut saline and therefore be delivered to the surface of the tissue (measured as total Ag, Table 2-1), and as previously observed with TiO_2 NPs (Al-Jubory and Handy 2013).

One concern for the gut lumen is whether or not the ENMs remain as particles, or simply dissolve in the gut saline. Silver sulphide particles are regarded as persistent in environmental matrices (Lead et al. 2018). This was the case in the gut lumen over 4 h. In the dialysis experiments, there was no detectable dissolved Ag released from the Ag_2S NPs, not even at the acidic pH 2 representative of the stomach. The Ag NPs showed some dissolution, but it was only a few µg/L of dissolved Ag, and represented < 1% of the total silver present at neutral pH (Fig. 2-4). This is consistent with previous findings for Ag NPs in salines (Besinis et al. 2014). Increasing the acidity to pH 2 caused only small further increases in dissolved Ag (Fig. 2-4, <3% of the silver), indicating the Ag NPs remained as particles. In any event, the µg/L amounts of dissolved Ag released would be partly complexed with the excess chloride (as above) or bind to the mucus layer (see review on fish mucus, Handy and Maunder 2009). Mucus was observed, as expected, in the gut sacs during the experiments.

Silver ions also bind avidly to the –SH groups on proteins and free amino acids (Smith et al. 2002), and one concern is that any residual amino acids in the gut sacs might drive silver dissolution from the Ag NPs. There were no amino acids in the gut saline used for the exposures, and the gut sacs were carefully washed and from unfed fish, so the problem is unlikely. The dialysis experiments also showed no effect of histidine on particle dissolution, but the presence of cysteine caused dissolution to decrease, contrary to expectations (Gondikas et al. 2012). It is possible that the saline conditions used here could mask the effects of the cysteine, although the mechanism is unclear. Alternatively, cysteine

might covalently bond to the surface of the particles to form a stable layer that reduces further dissolution (Mandal et al. 2001). Regardless of the details of the gut lumen chemistry, together the observations from all the dialysis experiments (Fig. 2-4) and the particle aggregation in gut saline (Fig. 2-2) indicate that particles would have been presented to the gut lumen. However, the bioavailability was low with most of the total Ag being removed in the luminal and EDTA washings (Table 2-1) and only a few percent of the dose remaining in the mucosa (Table 2-5).

2.4.2 Total silver accumulation in the gut tissue

This study attempted to show total Ag accumulation in the tissue (form unknown inside the cells) under physiological conditions, and to differentiate the apparent accumulation in the gut tissue from any surface-associated fraction. The gut sacs were viable and showed normal water fluxes (Table 2-3) and moisture content (Table 2-4); comparable to our previous reports with trout gut (Al-Jubory and Handy 2013). The luminal and EDTA washing procedure attempted to remove most of the surface-associated fraction (Table 2-1); but with the convoluted topography of the gut, the presence of mucus, and the polyanionic nature of the epithelial surface, some external total Ag inevitably would remain. This was quantified in the rapid solution dipping experiment (Fig. 2-3) and shows 88 ± 8 ng/g dw or less of surface-associated total Ag on the mid and hind intestine. For $AgNO_3$ exposure to the mucosa of the mid intestine this equates maximally to ~2% of the apparent accumulation in the tissue (3962 ± 1255 ng/g dw, Table 2-2). For Ag NPs the 21 ± 4 ng/g dw of surface associated Ag equates to <2% of the apparent accumulation in the tissue (1507 ± 908 ng/g dw, Table 2-2). Similarly, for Ag_2S NPs in the mucosa of the mid

intestine (< 1%). It is therefore possible to interpret the measured total Ag concentrations in the tissue (Table 2-2) as mainly accumulation into, not on, the mucosa.

The apparent accumulation for $AgNO_3$ would involve the diffusion of any dissolved silver present into the epithelial cells from the gut lumen and with the electrochemical gradient. It is likely to be physiological uptake through a carrier-mediated pathway because the water flux was in the opposite direction to the highest rates of Ag accumulation (Table 2-3). Solvent drag with incidental passive uptake of soluble metal is therefore excluded. It was also hoped to demonstrate a dissolved silver involvement in uptake by removing the chloride from the physiological saline. This would, in theory, do two things: (i) increase the dissolved Ag^+ fraction in the gut lumen as AgCl formation would be less likely, and (ii) demonstrate the competitive NaCl-dependent nature of silver uptake (through apical Na^+ channels, Bury and Wood 1999). However, the removal of chloride failed to show any appreciable effects on either the amounts of total Ag recovered in the luminal and EDTA washing (Table 2-1), or on the Ag accumulation in the tissue (Table 2-2). With the benefit of hindsight, this manipulation failed because the intact epithelium is secretory and a few millimoles of chloride ion activity will always be present in the mucus layer (Shephard et al. 1984). Any Ag^+ would therefore be rapidly converted to AgCl in the microenvironment at the gut surface. The facilitated diffusive uptake of Ag^+ through epithelial ion channels is also dependent on the overall inward electrochemical gradient; but the transepithelial potential across the gut remains unchanged with symmetrical removal of chloride from both the luminal and serosal solutions (Handy et al. 2000). Interestingly, without the complexity of the real tissue, trout gut epithelial cell cultures do show the expected chloride-dependence (Minghetti and Schirmer 2016). This highlights the importance of cell cultures for illuminating details of uptake mechanisms in

individual cell types, while the gut sac approach can show the integrated effect at tissue and organ level.

Nevertheless, the accumulation rates in the gut for total Ag from $AgNO_3$ exposure were around a few nmols/g/h; and with some of the highest rates in the mid intestine (Table 2-3). Considering the gut sac is a closed system where concentrations will come into equilibrium more quickly, these values are not inconsistent with previous reports on the net uptake rates of metals into the blood across perfused intestines (Cu, 1 µmol/g/h or less, Handy et al. 2000; Hg, 1-2 µmol/g/h, Hoyle and Handy 2005). The accumulation rates for gut from the present study were also calculated on the basis of tissue surface area (Table 2-4). Ojo and Wood (2007) report tissue accumulation rates of around 250-100 pmol/cm^2/h in the mid and hind intestine for additions of 5.3 mg/L of dissolved Ag over 4 h. Considering, the concentration was more than five times that used here, the values 23.05 ± 5.20 and 19.74 ± 7.23 pmoles/cm^2/h for the mid and hind intestine with $AgNO_3$, respectively (Table 2-3) are not that dissimilar.

There are few reports of ENM accumulation rates in the gut tissue of fish. Al-Jubory and Handy (2013) reported an accumulation of around 0.02 ± 0.01 µmol/g of Ti for TiO_2 NPs over 4 hours in the mid and hind intestine of trout; equivalent to a total Ti accumulation rate into the mucosa of 5 nmols/g/h, and in keeping with the accumulation rates for Ag in the mucosa here (Table 2-3). Interestingly, the values (Table 2-3) are also consistent with the maximum influx rates for the estuarine snail, *Peringia ulvae*, exposed to Ag NPs of around 90 nmol/g/day (Khan et al. 2012); equivalent to about 4 nmol/g/h. The accumulation rates of Ag NPs are also broadly in the nanomolar range in rainbow trout gut cell lines (Minghetti and Schirmer 2016).

Notably, the amount of total Ag accumulated by the gut from exposure to Ag_2S NPs was much higher in the mucosa of the mid intestine than any other treatment (Table 2) and

with the highest accumulation rate (12.02 ± 4.07 nmol/g/h, Table 2-3). This suggests the mucosa of the mid intestine has a particular affinity for Ag from Ag_2S. The reasons for this observations requires further investigation, but it could imply the uptake pathways for Ag NPs and Ag_2S are different in this region of the gut. Khan et al. (2015) found both amantadine- and nystatin-dependent uptake of Ag NPs in estuarine snails, suggesting at least two pathways may exist (clathrin- and caveolae-mediated endocytosis, respectively). The pyloric caeca of the anterior intestine also had high silver concentrations, leading to them containing an estimated 30-54% of the silver dose (Table 2-4). However, this data is not interpreted as substantial internal uptake of total Ag (form unknown) into the mucosa. The pyloric caeca are extremely difficult to dissect open and separate from the surrounding mesentery. The high values for the caeca are therefore likely an artefact of Ag that could not be washed from the lumen in this portion of the gut. Dietary metal concentrations in the anterior intestine that include the pyloric tissue are rarely reported, but the values with the pyloric caeca included tend to be higher than the mid intestine *in vivo* (e.g. copper, Kamunde and Wood 2003), and likely for the same reasons of difficulty in washing excess metal out of the caeca.

Some metal accumulation is also reported in the muscularis, regardless of the type of silver exposure (Table 2-2), which represents 1-2% of the dose (Table 2-4). In this experiment, the muscularis is essentially all the tissue remaining after the mucosa has been stripped from the surface and will therefore include blood vessels and the lymphatics. For dissolved silver, the measured total Ag in the muscularis may therefore represent ions that has been exported from the mucosal cells into the serosal side (i.e., into the capillaries), or Ag^+ ions that have permeated into the muscularis via a paracellular route through the mucosa. The latter is unlikely given net water fluxes are often in the opposite direction, but active export from the mucosal cell into the blood against the electrochemical gradient is

regarded as the rate limiting step in trace metal uptake (Handy and Eddy 2004). The presence of some total Ag in the muscularis from the Ag NPs and Ag_2S NP exposures needs further investigation, but might imply vesicular serosal export of Ag from the epithelial cells, as is known for Cu (Handy et al. 2000).

2.5 Conclusions and regulatory perspective

In conclusion, the gut sac technique has been used for decades to investigate the dietary accumulation potential of the dissolved metals including silver, and here the method is demonstrated for two different types of silver-containing ENMs. The data show both dissolved and nano forms of Ag have limited bioavailability to the gut mucosa, with only a few percent of the dose being accumulated in the epithelium and even less being transferred to the serosal side. This might predict modest or negligible bioaccumulation potential *in vivo*. In the present study, Ag from $AgNO_3$ was accumulated more than the equivalent nano forms, with only a couple of exceptions. Therefore, from a regulatory toxicology perspective, the existing data sets on dissolved silver should be protective of the nano forms. The gut sac method has utility as a screening tool to identify materials of accumulation concern as well as the anatomical regions of the gut involved in uptake. A tiered approach for the measurement of bioaccumulation potential of ENMs has already been proposed (Handy et al. 2018), and the current data adds to the weight of evidence that the *ex vivo* gut sac approach can be used to reduce the burden of regulatory work as well as the use of animals for *in vivo* testing.

Chapter 3 - Dietary Exposure to Silver Nitrate Compared to Two Forms of Silver Nanoparticles in Rainbow Trout: Bioaccumulation Potential with Minimal Physiological Effects

Abstract

The trophic transfer of silver to fishes in aquatic food chains is a concern, but little is known about the dietary accumulation of pristine (Ag NPs) and modified (Ag_2S NPs) forms of silver-containing nanoparticles. The aim of the current study was to assess the bioaccumulation potential of these materials following dietary exposure to 100 mg/kg Ag as either $AgNO_3$, Ag NPs or Ag_2S NPs and compared to no added Ag controls. The experiment consisted of a 4 week uptake phase, followed by 2 weeks placed onto the control diet (total 6 weeks). Fish were sampled for total Ag analysis (weeks 1-4 and 6), as well as haematology, biochemistry and histology. The highest concentrations of Ag were in the liver > hind intestine > gallbladder > kidney > and mid intestine, regardless of the type of silver exposure. Overall, there was significantly more Ag accumulation from $AgNO_3$ and Ag NP exposure compared to the Ag_2S NP treatment, indicating a lower bioavailability of the latter. Following the 4 week exposure, the highest concentration of Ag (from $AgNO_3$, Ag NPs and Ag_2S NPs, respectively) was in the hind intestine (140 ± 22, 90 ± 14, 0.5 ± 0.1 µg/g), liver (122 ± 10, 129 ± 17 and 11 ± 1 µg/g) and gallbladder (19 ± 3, 40 ± 14 and 0.9 ± 0.3 µg/g) in all Ag treatments. The liver concentration represented 38-44% of the body burden of Ag in all Ag treatments. Following the depuration period (week 6), the concentration of Ag in the tissues showed some transient changes. Notably, there was a significant increase in the liver Ag body burden (65.9 ± 5.1, 62.9 ± 2.2 and 98.9 ± 0.4% for $AgNO_3$, Ag NPs and Ag_2S NPs, respectively) in the post-exposure phase. An *in chemico* digestibility assay simulating low pH in the stomach indicated some dissolution of silver, but there were equal orders of Ag release from both the $AgNO_3$ and Ag NP diets, and none from the Ag_2S NPs. There were no treatment-dependent differences in cumulative food intake or intestinal morphology, and only minor transient changes in plasma ions, total

glutathione and TBARS in the organs. Overall, the dietary bioaccumulation potential of the nano forms of silver was equal to, or less than the metal salt, and with minimal toxicological effects following 4 weeks exposure.

3.1 Introduction

The persistence in the environment, bioaccumulation potential and toxicity (PBT) are key triggers of concern for the environmental risk assessment of chemicals, including engineered nanomaterials (ENMs); but of these processes, bioaccumulation has received little attention (review, Handy et al. 2018). Dissolved silver is very toxic to aquatic species (review, Ratte 1999). The uptake of total Ag from food exposures of silver salts have been reported for freshwater fish with dietary bioavailability typically being a few percent of the exposure concentration (Galvez and Wood 1999; Galvez et al. 2001); in keeping with other studies on dietary metal salts in fish (reviews, Clearwater et al. 2002; Handy et al. 2005). However, less is understood about the dietary uptake and bioaccumulation potential of ENMs in fish (Handy et al. 2018).

The ecological concern is that the propensity of ENMs to settle from the water column will lead to exposure of the sediments and benthic species that comprise the base of food webs; leading to subsequent dietary exposure of higher trophic levels (Klaine et al. 2008; Cross et al. 2015; Selck et al. 2016). This is an issue for Ag-containing ENMs, but pristine Ag NPs can be transformed in the environment to stable, persistent Ag_2S NPs (Levard et al. 2012; Lowry et al. 2012; Lead et al. 2018). Indeed, sulfidation is regarded as the primary transformation of Ag NPs during wastewater treatment (Kaegi et al. 2013), such that Ag_2S NPs are likely the main form of release to the aquatic environment.

There are only a few reports of dietary exposures to ENMs in freshwater fish. For single walled carbon nanotubes (Bisesi et al. 2014) and TiO_2 NPs (Ramsden et al. 2009), the dietary bioavailability to the internal organs appears to be small or negligible. However, this is not the case with some other ENMs. For example, Connolly et al. (2016) fed rainbow trout with food containing 300 or 1000 mg/kg ZnO, and after 12 days the intestine and gill

tissue concentrations of total Zn were greater than the controls, and the elevated Zn concentrations persisted in those tissues for some weeks during a depuration phase. Interestingly, there were only transient changes in the plasma and liver Zn concentrations (Connolly et al. 2016). Zebrafish (*Danio rerio*) exposed for 60 days to 0.8% body weight of 4 mg/kg of two sizes of cadmium quantum dots (CdS NPs; 8 or 50 nm diameter) showed elevated total Cd concentrations in the livers from both sizes of the material compared to the unexposed controls (Ladhar et al. 2014). However, a key concern for risk assessment is whether the nano form is more hazardous than the equivalent concentration of a metal salt. In sea bream (*Pargus major*) at least, animals fed diets containing 4 mg/kg of Cu as Cu NPs or $CuSO_4$ for 60 days showed similar increases in total Cu concentrations in the whole carcass and liver; although Cu dissolution and particle characterisation was not reported (El Basuini et al. 2016).

Recently, our laboratory explored the potential bioavailable fraction of total Ag released from fish food using a sequential extraction procedure that simulated the digestion of food in the gut of fish (Handy et al. 2018). This *in chemico* digestibility assay showed that both $AgNO_3$ and Ag NPs have an extractable fraction of Ag between 1-4% of the dose, depending on the region of the gut being simulated; and less for Ag_2S NPs. This raises the concern that ingested Ag-containing ENMs could be available via the gut to fish and that the hazard will depend on the chemical form of the ENM. The aim of the present study was therefore to explore the *in vivo* dietary bioaccumulation potential of total Ag from exposures to diets containing $AgNO_3$, Ag NPs or Ag_2S NPs compared to unexposed controls for rainbow trout (*Oncorhynchus mykiss*). In addition, a post-exposure phase was included to inform on the clearance of any apparent Ag accumulation by the fish. The *in chemico* digestibility assay was also used to access any apparent dissolved Ag release from the food pellets at the acidic pH of the stomach. Finally, it is also critical to link any

apparent bioaccumulation with biological effects, consequently the health of the animals was monitored in terms of food intake and intestinal morphology. Given the known interferences of dissolved Ag with sodium homeostasis, plasma and tissue electrolytes were also measured along with biomarkers of oxidative stress in the tissues (total glutathione, GSH, and thiobarbituric acid reactive substances, TBARS).

3.2 Methodology

3.2.1 Experimental design

Juvenile triploid rainbow trout weight ~10g (n = 350) were obtained from Exmoor Fisheries and held for 14 days in a quarantine tank prior to the experiment. Fish were graded and transferred into a flow through systems containing 12 glass tank aquaria (70 L; 26 fish per tank). Water turnover was 0.52 ± 0.07 L/min (n = 12) and did not statistically differ (one way ANOVA, $P = 0.328$) between treatments. Fish were left in the tanks for two days prior to the experiment to settle and form social hierarchies. Treatments were randomly assigned to tanks (3 tanks per treatment). Fish were fed one of four diets for four weeks: a control diet (no added Ag), or 100 mg/kg Ag as $AgNO_3$, Ag NP or Ag_2S NPs. This concentration was used to allow a mechanistic investigation of the accumulation of different forms of Ag, and not for environmental relevance. Following this, a two-week depuration period occurred where all treatments were fed the control diet. Fish were fed a 2% body weight ration per day whereby the amount of food was altered each week based on the tank biomass. This ration was selected as a mid-point of reported values for dietary exposures (see Clearwater et al. 2002), and to ensure faecal material would not deteriorate water quality through nitrogen waste (e.g., Handy and Poxton 1993) or silver leaching. Equally,

this ration reduced the chance of feed intake decreasing in the presence of high contamination loads (e.g., Glavez and Wood 1999), which would confound growth results. Fish were fed carefully at approximately 9 am, 1 pm and 5 pm each day and observed to ensure the daily ration was eaten immediately. There were no residual food pellets in the water after each feed. The photoperiod was set to 12 h light:12 h dark. The tanks were also cleaned periodically, with careful siphoning of any residual faecal matter from the tanks to ensure water quality.

Water samples were taken daily for oxygen, temperature, pH and ammonia. Water samples for measuring total silver concentration were collected once a week. There was no consistent detectable Ag in the control or Ag_2S NP treatments (<0.10 ng/mL; LOD). Despite monitoring the cleanliness of the fish tanks, the $AgNO_3$ and Ag NP treatments showed a trace amount of total silver in the tanks that was just above the LOD of 0.40 ± 0.04 and 0.47 ± 0.04 ng/mL (mean ± S.E.M., n = 24 per treatment), respectively. No Ag was detected during the depuration period.

Six of the stock fish were sampled at the start of the experiment for reference and to determine the background tissue Ag concentrations in the animals. Subsequently, fish from the experimental tanks were sampled at weeks 1, 2, 3 and 4 during the exposure phase and at the end of the depuration phase on clean food (week 6) for trace metal analysis. Samples for biochemistry and histology were taken at week 4. Blood samples were also collected at weeks 2, 4 and 6 (see below). From each tank, n = 2 fish were taken, giving a total of 6 fish per treatment for each end point (see section 2.2.3 for details). The entire experiment was conducted with ethical approval from the UK Home Office via a Project Licence held at Plymouth University under the Animals (Scientific Procedures) Act (1986), and its amendments, in compliance with Directive 2010/63/EU. In order to facilitate dissection and to ensure animal welfare during anaesthesia (see below), fish were not fed

on the morning of the sampling days. The last feed of the fish was the evening before sampling, allowing time for evacuation of the gut contents (~15 h).

3.2.2 Nanoparticles and diet formulation

The ENMs were supplied as part of the EU NanoFase project, and the characterisation of batches of the same materials used here are reported elsewhere (Baccaro et al. 2018). Briefly, the Ag NPs and Ag_2S NPs were provided by Applied Nanoparticles (Barcelona). The Ag NPs were supplied (manufacture's information) at a nominal size and concentration of 50 nm and 10.4 g/L, respectively. The Ag_2S NPs had a nominal size and concentration of 20 nm and 9.6 g/L, respectively. The Ag NPs were dispersed in 25 µmol/L tannic acid and 5.5 mmol/L sodium citrate, and 1 mg/mL polyvinylpyrrolidone (PVP), and the Ag_2S NPs were dispersed in 1 mg/mL PVP only. Transmission electron microscopy (TEM, JEOL-1200EX II) was conducted at Plymouth to confirm the primary particle diameters of the materials. Briefly, a copper grid was placed on top of a drop of the stock suspensions; after which the grid was removed and allowed to dry for 10 mins at room temperature before imaging. The concentration of the total Ag in the stocks of Ag NPs and Ag_2S NPs was also measured by inductively coupled plasma mass spectrometry (ICP-MS, Thermo X-series 2 ICP-MS). The stock concentrations for (mean ± S.D., n = 4) the Ag NPs and Ag_2S NPs were 9.5 ± 0.4 and 1.4 ± 0.1 g/L.

The diet used throughout the study was a commercial fish food (Aller Futura, EX, Kaliningrad, Russia), with a pellet size of 1.5 mm. The proximate composition of the diets was (% dry weight from manufacturer's guidelines): lipid, 17; protein, 58; ash, 10.1; fibre, 0.9. The intact food pellets were supplemented with stock dispersion of the relevant nanomaterial or $AgNO_3$ that was allowed to soak into the pellets and this was then sealed

with a topcoat of 10% gelatine; similar to the method used in our previous dietary studies on ENMs (Fraser et al. 2011). The dosing dispersion for mixing with the diets were prepared by sonicating (FB15048 ultrasonic bath, 35W, Thermo Fisher) 100 mL of a nominal stock concentration of 1 g/L of Ag as either $AgNO_3$, Ag NPs and Ag_2S NPs prepared in ultrapure water for 1 h (i.e., a 1:10 dilution of the stock supplied by the manufacturer). Nanoparticle tracking analysis (NTA) was conducted to confirm the materials could be dispersed adequately in these stocks. The stocks were slowly added to 900 g of the diet and thoroughly, but gently mixed with a commercial food mixer (Kenwood KM810/KM816, 2004). A solution of 10 g of porcine gelatine (>98% purity, Sigma-Aldrich) in 100 mL of ultrapure water was prepared by gentle heating to 40^{o}C, allowed to cool for 10 mins, and then gently poured over the diet and mixed in for 15 minutes. The unexposed control diet was prepared in exactly the same way, but ultrapure water without any silver was added. The diets were then placed in an incubator at 45^{o}C and left to dry overnight. The expected nominal concentration in the silver-supplemented diets was 100 mg of total Ag/kg dry weight of food. The total Ag concentrations of the diets were measured by inductively coupled plasma mass spectrometry (ICP-MS, see below) with 0.72 ± 0.22, 92.35 ± 7.33, 96.19 ± 11.49 and 88.16 ± 23.16 mg/kg dry weight (mean ± S.E.M., n = 8) in the control, $AgNO_3$, Ag NP and Ag_2S NP treatments respectively. There was no significant difference between the Ag concentrations in the exposure diets (one way ANOVA, $P > 0.05$).

3.2.3 Tissue collections and blood sampling

Blood sampling and dissection followed Shaw et al. (2012). The experimental fish were blood sampled at weeks 2-6 (the animals were too small at week 1). For blood sampling,

(n = 2 fish per tank, n = 6 per treatment) were anaesthetised using buffered ($NaHCO_3$) MS222, pithed (to destroy the brain) and the whole blood removed via the caudal vein into heparinised syringes. Then 50 µL of whole blood was digested in 0.2 mL of concentrated nitric acid at 60^oC for 4 hours, allowed to cool and diluted to 2 mL with ultrapure water prior to analysis for total Ag by ICP-MS (see below). The remaining whole blood was centrifuged, and the plasma removed and stored at -20^oC until required. The plasma Na^+ and K^+ concentrations were analysed by flame photometry (Sherwood Model 420 Flame Photometer).

After blood sampling, the fish were dissected for the mid intestine, hind intestine, liver (following gallbladder removal), kidney, gill and brain (n = 2 fish/tank, n = 6 per treatment). The mid and hind intestine were rinsed in ultrapure water and blotted before wet weight determination. Care was taken to avoid cross-contamination between fish with clean, acid-washed instruments. Tissues (0.001-0.363 g) and carcasses (7-38 g) were freeze dried (Lablyo freeze dryer) for 24 h and weighed. Once dried, the hind intestine, kidney and liver, of week 2, 4 and 6 only, were cut in half; one half was used for total Ag concentrations (and electrolytes) reported here, and the other half for particulate analysis (reported in Chapter 5).

3.2.4 Trace metal analysis

Tissue metal analysis was similar to Shaw et al. (2102) with modifications for silver. Tissues were freeze dried, weighed and digested using 200 µL of analytical grade (primer plus) nitric acid and heated using a water bath to 60^oC for 4 h. With every analysis, procedural blanks were analysed to check for leaching from the test tubes or other incidental contamination from the reagents (not observed, blanks remained below the limit

of detection of the instrument). Following digestion, the samples were diluted to 2 mL using 22.2 µg/L indium and iridium spiked ultrapure water (for use as internal standards) before being analysed by ICP-MS. Drift was monitored using the indium and iridium signals and standards were checked after every 15 samples. The samples were matrix-matched with the standards. The ^{107}Ag isotope signal was used to determine total Ag concentration. However, both ^{107}Ag and ^{109}Ag isotopes were measured to aid interpretation of results from values near the limit of detection of the ICP-MS. The limit of detection of the ICP-MS ranged between 0.04 and 0.18 ng/mL depending on the same type, which equates to between 1 and 50 ng/g tissue dw. In addition to Ag determination, tissue samples from week 4 (the end of the exposure phase) were diluted (0.5 mL sample diluted to 2.5 mL) and analysed by ICP-OES for the tissue electrolyte composition (Cu, Zn, Mn, Na, Ca and K) according to Shaw et al. (2012).

3.2.5 Histology examination

Fish were sampled at week 4 for histological examination according to Al-Bairuty et al. (2013). Animals were randomly selected (n = 2 per tank/ n = 6 per treatment), euthanized (as above) and carefully dissected to collect the second gill arch, mid intestine, hind intestine and liver. Tissues were immediately placed in 10% buffered formal saline for at least one week for fixation. Tissues were processed using an automated tissue processor (Leica TP1020 semi-enclosed benchtop) where samples were taken from the formal saline into industrial methylated spirit (50-100%), followed by clearing using histolene and then taken to wax (~20 h total time). Tissues were then embedded in wax blocks (Leica EG 1150H) and sectioned at 6 µm intervals (Leica RM2235 microtome) and dried overnight. For the mid and hind intestinal morphology, slides were stained with 0.5% haematoxylin

and counter-stained with 1.1% van Gieson's to differentiate the connective tissues, followed by 1.0% alcian blue for the mucocytes in the epithelium. Malory's trichrome was used for gill morphology. Tissues were viewed and photographed using a Leica microscope (DMD108) with a built in camera.

3.2.6 Biochemistry

The mid intestine, hind intestine, liver, kidney, gill and brain were sampled at week 4 for biomarkers of oxidative stress including the thiobarbituric acid reactive substances (TBARS) assay and total GSH according to Smith et al. (2007). Following dissection, tissues were snap frozen in liquid nitrogen and stored at -80^{o}C until required for analysis. Tissues (approximately 0.2 g) or the whole brain were thawed on ice and homogenised (Cat X520D with a T6 shaft, medium speed, Bennett & Co., Weston-Super-Mare) into 1 mL of ice-cold isotonic buffer [in mmol/L; 300 sucrose, 0.1 ethylenediamine tetraacetic acid (EDTA), 20 (4-(2-hydroxyethyl)piperazine-1-ethane sulfonic acid (HEPES)), adjusted to pH 7.8 with a few drops of Tris (2-amino-2-hydroxylmethyl-1,3-propanediol)]. Following centrifugation (2 mins at 13,000 rpm), the supernatant from the crude tissue homogenates were stored at -80^{o}C until required. The samples were analysed (in triplicate) for TBARS and total GSH.

For the TBARS assay, 130 µL of sample or standard was added to an Eppendorf tube followed by 32.5 µL of 1 mmol/L butylated hydroxytoluene (2,6-Di-O-tert-butyl-4-methylphenol or BHT) to prevent oxidation, 455 µL of phosphate buffer (100 mmol/L potassium phosphate and 5 mmol/L EDTA) and then 162.5 µL of 50% (w/v) trichloroacetic acid (TCA) to precipitate excess protein. The samples were then centrifuged for 2 mins at 13,000 rpm. Following this, 150 µL of the supernatant was added to 3 wells in a 96-well

plate, followed by the addition of 75 µL of 1.3% TBA (in 0.3% NaOH). The plate was covered and incubated for 60 mins at 60ºC, allowed to cool to room temperature and the absorbances measured at 530 nm against standards (0.5-25 mmol/mL 1,1,3,3-tetraethoxypropane).

For total glutathione, 20 µL of sample homogenate and 140 µL of mixture containing 0.714 mmol/L DTNB (5,5'-Dithiobis(2-nitrobenzoic acid)), 100 mmol/L phosphate buffer and 0.357 U/mL glutathione reductase into a 96-well plate. To start the reaction, 40 µL of 1 mmol/L NADPH was added to each well. The rate of change of the absorbance of each sample were read at 412 nm for 15 mins with readings every 15 seconds, and compared to GSH standards. TBARS and GSH were normalised to the protein concentration of each homogenate. Protein was determined in the triplicate using of 25 µL of sample using a commercially available kit (Pierce BCA protein assay kit 23227, Thermo Fisher). To check for interferences, the assays were run with the appropriate amount of Ag spiked into the samples at their respective tissue concentrations of total Ag. No interferences were found.

3.2.7 *In vitro* digestibility

To aid data interpretation over the bioavailability and form of Ag in the gut lumen of rainbow trout, an *in chemico* digestibility assay was used (Handy et al. 2018). Two compartments of gastrointestinal tract were simulated with artificial solutions: the stomach (0.1 M HCl, 0.9% NaCl, pH 2) and the intestine (0.9% NaCl, pH 7.8). The experimental diets (described above) were placed into 15 cm sections of clean dialysis tubing (typical pore size < 2 nm) and tied closed (1 g food per bag, n = 4 replicates). Samples were then incubated in 20 mL of the respective artificial gut fluid for 4 h in rotating tubes at 30 rpm

(Stuart tube roller SRT6) to mimic peristalsis movements. Afterwards, the external fluid was collected for total Ag determination by ICP-MS (as above).

3.2.8 Calculations

The average body weight of fish in each tank was calculated each week as:

$$\frac{Tank\ biomass\ (g)}{Number\ of\ fish\ per\ tank} \quad \text{Equation 3.1}$$

To determine the body distribution, the absolute mass of Ag in the organ was calculated as:

$$(concentration\ in\ tissue\ analysed\ x\ weight\ in\ tissue\ analysed) +$$
$$(concentration\ in\ tissue\ analysed\ x\ weight\ of\ spare\ tissue) \quad \text{Equation 3.2}$$

3.2.9 Statistical analysis

Data analysis were performed in SigmaPlot 13.0. Data were checked for outliers using Grubb's test, following which they were assessed for normality (Shapiro-Wilk test) and equal variance (Brown Forsythe). Statistical differences were assessed using either a one-way ANOVA (growth, cumulative feed, tissue moisture and electrolyte composition, mucin size, biochemical endpoints) or two-way ANOVA for analysis treatment and time (tissue Ag concentrations, Ag body distribution and *in chemico* digestibility). For non-normal data, they were $\log_{10}$ transformed. Where data were non-parametric and could not be transformed, the Kruskal-Wallis test was used. *P* values presented are from post hoc tests.

3.3 Results

3.3.1 Particle characterisation

The TEM revealed the primary particle diameter of Ag NPs and Ag_2S NPs to be 55 ± 3 nm (mean ± S.D., n = 120) and 37 ± 19 nm (mean ± S.D., n = 103), respectively (as reported in Chapter 2). The mean (± S.D.) hydrodynamic diameter was 73 ± 2 nm (n = 3) for 1 mg/L Ag NPs and a mean hydrodynamic diameter of 124 ± 31 nm (n = 3) for 1 mg/L Ag_2S NPs.

3.3.2 Tissue total Ag concentration in the organs and percent Ag assimilation

The initial stock fish were analysed for total Ag by ICP-MS and showed trace amount of Ag in the liver tissue only (0.43 ± 0.06 µg/g Ag, mean ± S.E.M., n = 6). The remaining tissues Ag concentrations were below the limit of detection of the instrument (<50 ng/g dw). Over the 6 week experiment, the organs of the unexposed control fish including the spleen, brain, gills, gallbladder, kidney, mid intestine and carcass had no detectable total Ag concentration. Trace amounts of Ag were found in the hind intestine and liver of the unexposed fish, which remained low but with some transient time-dependent changes (Table 3-1).

During the 4 week exposure phase to dietary $AgNO_3$, there were elevated total Ag concentrations in all the organs compared to the unexposed controls, with persistent increases of total Ag concentrations found in the mid and hind intestine in keeping with the route of exposure. The liver as a central compartment in metal accumulation also showed a gradual elevation of Ag with the highest total Ag concentration at week 4 of $AgNO_3$ diet compared to week 1 (two-way ANOVA; P <0.001). There were also especially elevated Ag concentrations in the gallbladder, whole blood and kidney compared to the unexposed

controls (Table 3-1). In contrast, the gills of fish fed $AgNO_3$ diet showed a steady total Ag concentration of 0.73-1.30 µg/g dw, in keeping with the organ being perfused with Ag-containing blood rather than incident Ag exposure *via* the water. Two-way ANOVA's revealed the brain (P <0.05) and spleen (P <0.05) had very modest time-dependent increases in total Ag, not exceeding 2 µg/g dw, by the end of the exposure phase. The whole blood Ag concentrations remained constant throughout the exposure phase (two-way ANOVA; P >0.05).

The $AgNO_3$ and Ag NP treatments showed a very similar profile of total Ag concentrations in the organs and whole blood, with no statistically significant differences between these two treatments over the 4 weeks (Table 3-1). For example, the livers of fish from both treatments at week 4 showed total Ag concentrations around 122-129 µg/g dw. However, both the $AgNO_3$ and Ag NP treatments showed statistically significantly higher total Ag concentrations compared to the Ag_2S NP treatments in all tissues from week 1 to 4 (Table 3-1). For example, the livers (two-way ANOVA; P <0.001) of fish from the Ag_2S NP treatment showed only 10.9 ± 1.0 µg/g dw of total Ag; an order of magnitude less Ag than either the Ag NP or $AgNO_3$ dietary treatments. Crucially, the mid (P <0.001) and hind (P <0.001) intestine of fish from the Ag_2S NP treatment accumulated 0.17-0.24 and 0.46-1.92 µg/g, respectively, of total Ag (two-way ANOVA; Table 3-1), which was 10-100 fold less than the intestine of the other Ag treatments and indicating that Ag from Ag_2S form was the least available for uptake by the gut. Within the Ag_2S NP treatment, there were no time-dependent changes in the gallbladder, brain or carcass concentration (P >0.05), with values of 0.02-1.01 µg/g; although there were some transient increases in the total Ag in the kidney (P <0.03) and hind intestine (P <0.001) during the exposure to the Ag_2S diet (two-way ANOVA's; Table 3-1).

Table 3-1. The concentration of total silver in the tissues (µg/g dw) and blood (ng/ml) of rainbow trout following 4 weeks of exposure to a control or 100 mg/kg Ag as either $AgNO_3$, Ag NPs or Ag_2S NPs.

Tissue	Week 1	Week 2	Week 3	Week 4	Week 6
Mid intestine					
Control	<LOD	<LOD	<LOD	<LOD	<LOD
$AgNO_3$	6.33 ± 1.80^{Aab}	8.31 ± 1.04^{Aab}	11.86 ± 2.52^{Aa}	12.77 ± 3.30^{Aab}	4.79 ± 1.72^{Ab}
Ag NPs	3.24 ± 0.51^{Aa}	5.65 ± 1.15^{Aab}	12.48 ± 3.13^{Ab}	10.08 ± 1.60^{Aab}	12.19 ± 4.15^{Aab}
Ag_2S NPs	0.24 ± 0.04^{Ba}	0.17 ± 0.03^{Ba}	0.22 ± 0.05^{Ba}	0.21 ± 0.05^{Ba}	< LOD
Hind intestine					
Control	0.05 ± 0.01^{Aa}	0.04 ± 0.01^{Aa}	0.04 ± 0.00^{Aa}	0.02 ± 0.01^{Aa}	0.04 ± 0.01^{Aa}
$AgNO_3$	61.38 ± 6.12^{Bab}	62.35 ± 6.62^{Bab}	85.59 ± 10.37^{Bab}	140.02 ± 22.38^{Ba}	52.88 ± 10.55^{Bb}
Ag NPs	35.55 ± 5.20^{Ba}	65.15 ± 3.19^{Ba}	70.43 ± 7.16^{Ba}	89.87 ± 13.61^{Ba}	46.36 ± 8.19^{Ba}
Ag_2S NPs	1.92 ± 0.29^{Ca}	1.15 ± 0.22^{Ca}	1.12 ± 0.26^{Ca}	0.46 ± 0.09^{Cb}	0.04 ± 0.01^{Ac}
Liver					
Control	0.28 ± 0.02^{Aab}	0.23 ± 0.01^{Aa}	0.45 ± 0.06^{Ab}	0.44 ± 0.03^{Ab}	0.53 ± 0.06^{Ac}
$AgNO_3$	7.27 ± 1.02^{Ba}	79.76 ± 11.52^{Bb}	89.43 ± 5.93^{Bb}	121.77 ± 9.58^{Bb}	113.33 ± 23.66^{Bb}
Ag NPs	5.65 ± 0.57^{Ba}	64.50 ± 6.40^{Bb}	85.03 ± 11.86^{Bbc}	128.63 ± 17.41^{Bc}	87.67 ± 4.08^{Bbc}
Ag_2S NPs	1.98 ± 0.31^{Ca}	4.46 ± 0.68^{Cb}	7.71 ± 0.94^{Cc}	10.93 ± 0.95^{Cc}	10.41 ± 2.15^{Cc}
Gallbladder					
Control	<LOD	<LOD	<LOD	<LOD	<LOD
$AgNO_3$	10.60 ± 3.18^{Aa}	34.08 ± 9.18^{Aa}	20.66 ± 3.56^{Aa}	19.13 ± 3.25^{Aa}	6.62 ± 2.31^{Aa}
Ag NPs	15.60 ± 4.11^{Aa}	14.64 ± 1.69^{Aa}	22.84 ± 4.97^{Aa}	39.79 ± 14.41^{Aa}	10.37 ± 4.02^{Aa}
Ag_2S NPs	0.17 ± 0.06^{Ba}	0.64 ± 0.11^{Ba}	1.01 ± 0.20^{Ba}	0.94 ± 0.33^{Ba}	0.26 ± 0.13^{Ba}
Kidney					
Control	<LOD	<LOD	<LOD	<LOD	<LOD
$AgNO_3$	2.17 ± 0.31^{Aa}	8.68 ± 1.54^{Abc}	8.32 ± 1.07^{Ab}	23.59 ± 3.76^{Abc}	24.77 ± 4.95^{Ac}
Ag NPs	3.24 ± 0.75^{Aa}	7.16 ± 1.80^{Aab}	8.87 ± 1.95^{Abc}	23.01 ± 6.59^{Acd}	31.16 ± 8.05^{Ad}
Ag_2S NPs	0.12 ± 0.04^{Ba}	0.19 ± 0.04^{Bab}	0.76 ± 0.26^{Bb}	0.37 ± 0.11^{Bb}	0.14 ± 0.06^{Ba}

Spleen					
Control	<LOD	<LOD	<LOD	<LOD	<LOD
$AgNO_3$	0.28 ± 0.05^{Aa}	0.54 ± 0.09^{Aab}	0.68 ± 0.07^{Aab}	1.24 ± 0.21^{Ab}	0.64 ± 0.10^{Aab}
Ag NPs	0.24 ± 0.00^{Aa}	0.49 ± 0.11^{Aa}	0.71 ± 0.17^{Aab}	1.94 ± 0.57^{Ab}	2.31 ± 0.80^{Bb}
Ag_2S NPs	< LOD	< LOD	< LOD	< LOD	< LOD
Gill					
Control	<LOD	<LOD	<LOD	<LOD	<LOD
$AgNO_3$	0.73 ± 0.32^{Aa}	0.75 ± 0.12^{Aa}	0.83 ± 0.11^{Aa}	1.30 ± 0.28^{Aa}	0.35 ± 0.09^{Aa}
Ag NPs	0.55 ± 0.06^{Aa}	0.63 ± 0.10^{Aa}	0.92 ± 0.12^{Aa}	1.66 ± 0.30^{Aa}	0.63 ± 0.08^{Aa}
Ag_2S NPs	0.14 ± 0.06^{Bab}	0.05 ± 0.01^{Ba}	0.77 ± 0.43^{Bb}	0.03 ± 0.01^{Ba}	< LOD
Brain					
Control	<LOD	<LOD	<LOD	<LOD	<LOD
$AgNO_3$	0.46 ± 0.06^{Aa}	0.84 ± 0.12^{Aab}	1.08 ± 0.19^{Abc}	1.53 ± 0.13^{Ac}	1.08 ± 0.20^{Abc}
Ag NPs	0.43 ± 0.06^{Aa}	0.57 ± 0.05^{Aab}	1.02 ± 0.11^{Abc}	1.57 ± 0.28^{Ac}	1.05 ± 0.14^{Abc}
Ag_2S NPs	< LOD	0.04 ± 0.00^{Ba}	0.07 ± 0.02^{Ba}	0.02 ± 0.00^{Ba}	0.04 ± 0.01^{Ba}
Carcass					
Control	<LOD	<LOD	<LOD	<LOD	<LOD
$AgNO_3$	1.01 ± 0.21^{Aa}	1.11 ± 0.17^{Aa}	1.19 ± 0.14^{Aa}	2.02 ± 0.35^{Aa}	0.17 ± 0.02^{Ab}
Ag NPs	1.21 ± 0.42^{Aa}	1.01 ± 0.17^{Aa}	1.33 ± 0.23^{Aa}	2.05 ± 0.23^{Aa}	0.26 ± 0.07^{Ab}
Ag_2S NPs	0.08 ± 0.03^{Ba}	0.16 ± 0.05^{Ba}	0.26 ± 0.08^{Ba}	0.17 ± 0.04^{Ba}	<LOD
Blood					
Control	N/A	<LOD	N/A	<LOD	<LOD
$AgNO_3$	N/A	249.76 ± 29.71^{Aa}	N/A	268.59 ± 17.28^{Aa}	36.93 ± 4.18^{Ab}
Ag NPs	N/A	225.33 ± 13.70^{Aa}	N/A	260.61 ± 20.97^{Aa}	54.97 ± 5.74^{Ab}
Ag_2S NPs	N/A	9.57 ± 2.21^{Ba}	N/A	21.39 ± 11.78^{Ba}	<LOD

% assimilation					
Control	N/A	N/A	N/A	N/A	N/A
$AgNO_3$	2.91 ± 0.43^{Aa}	3.29 ± 0.26^{Aa}	1.78 ± 0.12^{Aa}	2.02 ± 0.27^{Aa}	N/A
Ag NPs	3.52 ± 0.92^{Aa}	2.58 ± 0.43^{Aa}	2.07 ± 0.26^{Aa}	2.15 ± 0.28^{Aa}	N/A
Ag_2S NPs	0.25 ± 0.05^{Ba}	0.25 ± 0.05^{Ba}	0.31 ± 0.08^{Ba}	0.18 ± 0.03^{Aa}	N/A

Data mean ± S.E.M (n = 5/6). Limit of detection (LOD) of organs ranged from 0.8 to 25 ng/g dry weight. The LOD in whole blood samples was 5.2 ng/mL. N/A indicates no sampling at that time point occurred. Within the % assimilation, the control values are not reported due to only trace amounts being present. Equally, week 6 is not reported as the interest is in accumulation only. Different upper case letter denotes statistical difference between treatments within the same week (columns). Different lower case letters denotes statistical difference between weeks within the same treatment (rows). Data were analysed using a two-way ANOVA.

The percent of Ag assimilated from the diets were calculated over the 4 weeks uptake phase. There was no significant difference in any treatment over time. However, the $AgNO_3$ and Ag NP treatment assimilated a significantly higher amount of Ag compared to the Ag_2S NP treatment. For example, after 4 weeks, the percent of Ag assimilated into the fish was 2.02 ± 0.27, 2.15 ± 0.28 and 0.18 ± 0.03% for the $AgNO_3$, Ag NP and Ag_2S NP treatments, respectively.

After the 4 weeks of exposure to the Ag-containing diets, there was a two-week depuration phase where the fish from all treatments were fed the unexposed control diet. In the animals fed the $AgNO_3$ diet, a two-way ANOVA revealed there were statistically significant decreases in the total Ag concentrations in the hind intestine (P <0.001) and carcass (P <0.001) at the end of the depuration phase compared to the values at the end of the exposure phase (week 4, Table 3-1). However, there was no appreciable clearance of Ag from the other internal organs of fish from the $AgNO_3$ treatment, including the liver (Table 3-1). An identical pattern of decreasing, or unaltered, total Ag concentrations were found in the organs of fish from the Ag NP treatment in the post exposure phase. Despite some evidence of clearance, none of the organs that had shown elevated total Ag concentrations recovered to control levels, with at least one third or more of the total Ag remaining in the organs of fish both the $AgNO_3$ and Ag NP treatments (Table 3-1). The Ag_2S treatment showed a similar pattern of decreasing total Ag concentrations in the organs in the post exposure phase, but with a few crucial differences. Unlike the other treatments, the and kidney (P = 0.029) showed statistically significant decreases in the total Ag concentrations at week 6 (two-way ANOVA); and in the case of the gill, carcass and the blood, the total Ag returned to control levels (below the detection limit); likely because these compartments had only accumulated a small amount of total Ag in the first place.

3.3.3 Body distribution of Ag for $AgNO_3$, Ag NP and Ag_2S NP treatments

The calculated body distribution in the animals at the end of the exposure and the end of the depuration phase are shown (Table 3-2). The Ag body distribution for the control treatment was not calculated because several organs were below the limit of detection. At the end of the 4 week exposure, the Ag body distribution in the $AgNO_3$ treatment was as expected with the organs containing a percentage of body burden (BB) in the following order carcass > liver > hind intestine > kidney > gallbladder > mid intestine > gill > brain > spleen. Critically, the liver contained around two fifths of the BB. For the Ag NP treatment, the profile of the BB was similar to the $AgNO_3$ treatment and in the order: carcass > liver > hind intestine > kidney > gallbladder > mid intestine > gill > brain > spleen. There was no significant difference between the BB of any organ in the $AgNO_3$ and Ag NP treatments (two-way ANOVA; P >0.05). Small changes were found in the order of BB in the Ag_2S NP treatment; carcass > liver > kidney > hind intestine > gallbladder > gill > mid intestine > brain > spleen. However, the main organs of BB remained the carcass, liver, kidney and hind intestine (>99 % of the total), similar to the $AgNO_3$ and Ag NP treatments (98 and 97% of the total, respectively).

After the depuration period (week 6), there was some evidence of redistribution of the BB in the $AgNO_3$ treatment (Table 3-2). For example, there was a 4-fold reduction in proportion of the BB associated with the carcass (two-way ANOVA; P <0.001); this was complemented by a significant rise in the kidney (2.4-fold; P = 0.003) and liver (1.7-fold; P <0.001). The predominant organ of Ag contamination became the liver (68 ± 5% of the BB). This pattern of re-distribution of the BB from the carcass to the kidney and liver was also observed in the Ag NP and Ag_2S NP treatments.

Table 3-2. Total absolute amount of total Ag and the percentage of body burden within each organ after 4 weeks exposure to either 100 mg Ag/kg as $AgNO_3$, Ag NPs or Ag_2S NPs, and followed by 2 week depuration.

		Week 4		Week 6	
Tissue	Treatment	Amount Ag (ng)	% body burden	Amount Ag (ng)	% body burden
Mid intestine	$AgNO_3$	126.1 ± 46.6	0.47 ± 0.18 ^{Aa}	188.5 ± 77.5	1.51 ± 0.38 ^{Aa}
	Ag NPs	81.6 ± 18.0	0.35 ± 0.04 ^{Aa}	266.4 ± 85.4	2.30 ± 0.81 ^{Aa}
	Ag_2S NPs	2.2 ± 0.7	0.13 ± 0.05 ^{Aa}	0.2 ± 0.0	0.02 ± 0.00 ^{Bb}
Hind intestine	$AgNO_3$	2022.7 ± 760.8	9.80 ± 3.98 ^{Aa}	1591.1 ± 213.2	11.52 ± 2.59 ^{Aa}
	Ag NPs	1295.7 ± 413.4	5.27 ± 1.31 ^{Aa}	1601.8 ± 275.8	12.20 ± 2.16 ^{Aa}
	Ag_2S NPs	17.4 ± 9.6	0.90 ± 0.37 ^{Ba}	1.8 ± 0.6	0.17 ± 0.03 ^{Bb}
Liver	$AgNO_3$	7343.5 ± 515.5	38.25 ± 3.05 ^{Aa}	10615.4 ± 2407.4	65.90 ± 5.10 ^{Ab}
	Ag NPs	8327.7 ± 947.5	38.38 ± 4.07 ^{Aa}	9200.4 ± 1033.8	62.89 ± 2.16 ^{Ab}
	Ag_2S NPs	907.2 ± 68.4	44.44 ± 5.34 ^{Aa}	937.8 ± 180.2	99.88 ± 0.37 ^{Bb}
Gallbladder	$AgNO_3$	137.8 ± 68.7	0.84 ± 0.50 ^{Aa}	78.7 ± 32.7	0.51 ± 0.16 ^{Aa}
	Ag NPs	194.9 ± 20.0	0.95 ± 0.18 ^{Aa}	88.6 ± 28.1	0.64 ± 0.22 ^{Aa}
	Ag_2S NPs	10.5 ± 4.7	0.59 ± 0.34 ^{Aa}	4.6 ± 3.4	0.39 ± 0.26 ^{Aa}
Kidney	$AgNO_3$	760.9 ± 132.9	3.88 ± 0.62 ^{Aa}	1096.8 ± 266.3	9.01 ± 1.63 ^{Ab}
	Ag NPs	966.1 ± 190.1	4.16 ± 0.65 ^{Aa}	1517.1 ± 317.5	9.25 ± 0.90 ^{Ab}
	Ag_2S NPs	59.2 ± 45.3	3.11 ± 2.16 ^{Aa}	5.4 ± 2.3	0.46 ± 0.12 ^{Ba}
Spleen	$AgNO_3$	8.2 ± 1.5	0.04 ± 0.01 ^{Aa}	5.4 ± 1.0	0.05 ± 0.01 ^{Aa}
	Ag NPs	10.6 ± 4.1	0.04 ± 0.01 ^{Aa}	16.7 ± 5.5	0.09 ± 0.02 ^{Aa}
	Ag_2S NPs	<LOD	<LOD	<LOD	<LOD
Gill	$AgNO_3$	67.9 ± 29.6	0.33 ± 0.12 ^{Aa}	12.8 ± 2.4	0.11 ± 0.02 ^{Aa}
	Ag NPs	89.5 ± 45.3	0.34 ± 0.14 ^{Aa}	32.5 ± 12.1	0.28 ± 0.15 ^{Aa}
	Ag_2S NPs	3.7 ± 2.7	0.19 ± 0.13 ^{Aa}	<LOD	<LOD
Brain	$AgNO_3$	21.4 ± 2.5	0.11 ± 0.01 ^{Aa}	22.0 ± 4.4	0.19 ± 0.03 ^{Aa}
	Ag NPs	25.2 ± 6.6	0.11 ± 0.02 ^{Aa}	18.3 ± 1.9	0.13 ± 0.02 ^{Aa}
	Ag_2S NPs	0.9 ± 0.1	0.05 ± 0.01 ^{Aa}	0.7 ± 0.1	0.09 ± 0.02 ^{Ab}
Carcass	$AgNO_3$	10606.8 ± 2053.5	46.28 ± 3.77 ^{Aa}	1442.0 ± 256.9	11.21 ± 1.48 ^{Ab}
	Ag NPs	11663.8 ± 1739.9	50.41 ± 2.80 ^{Aa}	1968.2 ± 378.6	12.23 ± 1.20 ^{Ab}
	Ag_2S NPs	942.1 ± 225.7	50.58 ± 4.92 ^{Aa}	<LOD	<LOD

Data are mean ± S.E.M. (n = 5/6). Blood Ag was not included in body distribution % (not taken from the same individual fish so not valid comparison). Control fish are excluded for clarity due to small signals in the hind intestine and liver tissues. Statistical analysis was only performed on the % body burden (Two-way ANOVA) for treatment and time. Different lower case letters denotes statistical difference between weeks within the same treatment (rows). Different upper case letter denotes statistical difference between treatments within the same week (columns). Statistical analysis not performed on the mass of Ag in the tissue as this is not standardised data with respect to organ weight.

3.3.4 Growth and fish health

The fish weighed around ~10 g at the start of the experiment and growth was steady with around a 4-fold increase in weight over the 6 week period. At the start of each week, there was no significant difference (one-way ANOVA's) between the average fish weight per treatment (P >0.05), or the weekly cumulative food intake (P >0.05; Fig. 3-1). Over the course of the study, there was a total loss of seven fish. Due to the mortalities being spread over five tanks across all treatment, and the presence of fin lesions from observable bullying; these were not attributed to treatment related effects.

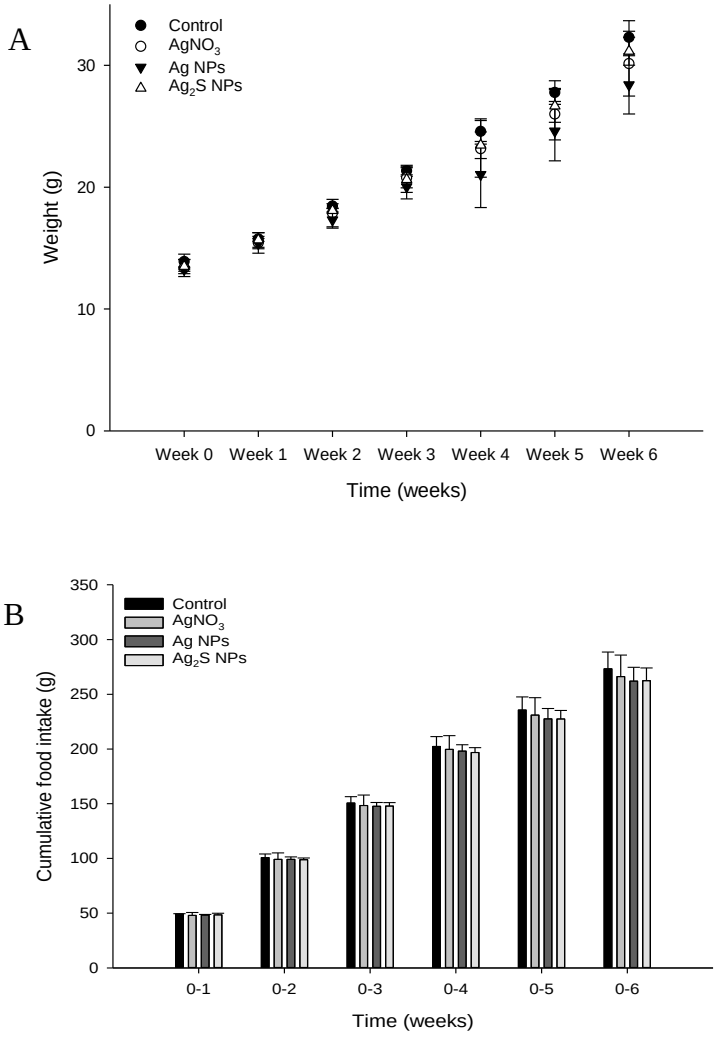

Figure 3-1. Average body weight (A) and cumulative food intake (B) in rainbow trout fed a control diet (no added Ag) or diets containing 100 mg/kg of Ag as either $AgNO_3$, Ag NPs or Ag_2S NPs. There was no statistical difference between treatments within weeks (one-way ANOVA).

3.3.5 Blood plasma and tissue electrolyte concentration

The plasma Na^+ and K^+ concentration were measured from all treatments (Table 3-3). The plasma Na^+ showed a transient decrease at week 4 in the $AgNO_3$ treatment, but this was within the normal physiological range, and overall there was no statistically significant differences from the other treatments (P >0.05). There were some time and treatment related effects in the plasma K^+ concentrations (two-way ANOVA; Table 3-3), but these were also transient and within the normal range. For example, after 4 weeks of exposure, the plasma K^+ concentrations in the Ag_2S NP treatment was significantly elevated 2.8 mmol/L compared to the control only (1.8 mmol/L, P = 0.014). However, overall there was no nanomaterial-type effects on either Na^+ or K^+ concentrations, and after the depuration period there was no significant differences between treatments (two-way ANOVA; Na^+, P >0.05, K^+, P >0.05).

The tissue electrolyte concentrations showed only small transient changes between treatments (one-way ANOVA or Kruskal-Wallis; Table 3-4). For example, the $AgNO_3$

Table 3-3. Plasma Na^+ and K^+ concentrations (mmol/L) over the six week experiment.

Treatment	Week 2	Week 4	Week 6
Na^+			
Control	155.4 ± 2.4^{Aa}	148.0 ± 14.2^{ABa}	127.6 ± 12.2^{Aa}
$AgNO_3$	148.4 ± 6.0^{Aa}	122.3 ± 16.3^{Aa}	132.5 ± 4.1^{Aa}
Ag NPs	163.6 ± 3.0^{Aa}	142.1 ± 11.1^{ABa}	145.1 ± 4.4^{Aa}
Ag_2S NPs	154.9 ± 2.7^{Aa}	161.1 ± 5.6^{Ba}	140.3 ± 1.3^{Aa}
K^+			
Control	1.2 ± 0.2^{Aa}	1.3 ± 0.2^{Aa}	0.8 ± 0.4^{Aa}
$AgNO_3$	3.3 ± 0.4^{Ba}	2.4 ± 0.3^{ABab}	1.6 ± 0.2^{Ab}
Ag NPs	2.7 ± 0.4^{BCa}	1.8 ± 0.3^{ABb}	0.9 ± 0.1^{Ab}
Ag_2S NPs	1.9 ± 0.4^{ACab}	2.8 ± 0.5^{Ba}	1.6 ± 0.2^{Ab}

Data are means ± S.E.M., n = 5/6. Data were analysed by a two-way ANOVA. Upper case denotes significant difference between treatments (columns). Lower case denotes statistical difference over time (rows). Vertical dashed line represents the end of exposure at week 4 where all treatments were placed on the control diet for a further two weeks.

treatment hind intestine Na concentration was significantly lower (1.83 ± 0.27 mg/g) compared to the control (3.13 ± 0.23 mg/g; P = 0.032), Ag NP (3.59 ± 0.39 mg/g; P = 0.004) and Ag_2S NP treatments (2.99 ± 0.20 mg/g; P = 0.041). There was no nanomaterial-type effects.

Table 3-4. Tissue concentrations of sodium, potassium, calcium, zinc, manganese and copper at week 4.

Tissue	Na^+ (mg/g)	K^+ (mg/g)	Ca^{2+} (mg/g)	Zn^{2+} (mg/g)	Mn^{2+} (µg/g)	Cu^{2+} (µg/g)
Mid						
Control	4.07 ± 0.26	13.73 ± 1.74	0.64 ± 0.03	2.00 ± 0.74	3.3 ± 0.5	3.81 ± 0.38
$AgNO_3$	2.97 ± 0.42	9.83 ± 0.57	0.50 ± 0.11	1.46 ± 0.46	2.9 ± 0.7	4.72 ± 0.35
Ag NPs	3.46 ± 0.31	10.29 ± 1.02	0.49 ± 0.08	1.86 ± 0.55	2.7 ± 0.7	5.87 ± 0.81
Ag_2S NPs	3.52 ± 0.19	10.98 ± 1.12	0.68 ± 0.08	2.07 ± 0.52	4.4 ± 1.0	5.64 ± 0.43
Hind						
Control	3.13 ± 0.23^{A}	13.05 ± 0.56	0.39 ± 0.06	1.89 ± 0.69	6.2 ± 2.2	7.37 ± 1.74
$AgNO_3$	1.83 ± 0.27^{B}	7.41 ± 0.48	0.16 ± 0.07	0.56 ± 0.27	2.8 ± 1.1	9.92 ± 1.12
Ag NPs	3.59 ± 0.39^{A}	10.98 ± 1.14	0.42 ± 0.12	1.42 ± 0.36	1.9 ± 0.6	8.38 ± 1.40
Ag_2S NPs	2.99 ± 0.20^{A}	11.48 ± 0.72	0.44 ± 0.07	1.43 ± 0.30	4.0 ± 1.0	7.57 ± 0.97
Liver						
Control	3.18 ± 0.13	12.68 ± 0.53	0.23 ± 0.03	0.09 ± 0.00	5.3 ± 0.3	127.39 ± 8.24
$AgNO_3$	2.91 ± 0.12	11.59 ± 0.35	0.22 ± 0.03	0.09 ± 0.00	5.2 ± 0.4	93.08 ± 9.23
Ag NPs	2.84 ± 0.11	12.11 ± 0.52	0.26 ± 0.06	0.10 ± 0.01	5.2 ± 0.2	93.37 ± 15.52
Ag_2S NPs	2.70 ± 0.12	10.92 ± 0.43	0.20 ± 0.02	0.08 ± 0.00	4.7 ± 0.2	159.00 ± 11.78
Gallbladder						
Control	22.67 ± 2.77	7.99 ± 0.97	1.20 ± 0.15	0.09 ± 0.02	1.6 ± 0.6	23.36 ± 7.07^{A}
$AgNO_3$	20.76 ± 3.70	6.27 ± 0.99	0.82 ± 0.28	0.07 ± 0.02	0.7 ± 0.3	11.98 ± 1.64^{B}
Ag NPs	24.51 ± 6.12	8.14 ± 1.16	1.18 ± 0.41	0.08 ± 0.02	2.5 ± 0.9	17.70 ± 5.7^{AB}
Ag_2S NPs	19.29 ± 2.55	4.99 ± 1.20	0.95 ± 0.12	0.04 ± 0.02	1.3 ± 0.3	15.82 ± 4.16^{AB}
Kidney						
Control	4.76 ± 0.29	9.53 ± 0.55^{A}	0.71 ± 0.23	0.12 ± 0.01	2.7 ± 0.2	4.31 ± 0.57^{A}
$AgNO_3$	5.94 ± 0.55	12.51 ± 0.95^{AB}	1.06 ± 0.32	0.15 ± 0.01	3.5 ± 0.4	7.01 ± 0.45^{B}
Ag NPs	6.51 ± 0.22	12.71 ± 0.63^{B}	2.08 ± 0.34	0.14 ± 0.02	3.3 ± 0.4	5.62 ± 0.72^{AB}
Ag_2S NPs	6.79 ± 3.79	12.77 ± 0.92^{B}	1.51 ± 0.67	0.17 ± 0.05	3.9 ± 0.3	6.61 ± 0.47^{B}
Spleen						
Control	2.16 ± 0.19	16.42 ± 1.38	0.14 ± 0.03	0.15 ± 0.02	2.7 ± 0.2	2.10 ± 0.74
$AgNO_3$	2.19 ± 0.15	16.62 ± 0.97	0.09 ± 0.02	0.17 ± 0.03	2.6 ± 0.2	3.62 ± 0.29
Ag NPs	2.29 ± 0.18	16.94 ± 1.52	0.07 ± 0.02	0.19 ± 0.03	2.2 ± 0.2	4.39 ± 0.38
Ag_2S NPs	2.10 ± 0.18	16.79 ± 2.14	0.07 ± 0.03	0.20 ± 0.03	2.2 ± 0.2	3.89 ± 0.35
Gill						
Control	7.37 ± 0.33	17.15 ± 0.56	5.19 ± 1.77	1.16 ± 0.26	6.8 ± 1.0	3.51 ± 0.29
$AgNO_3$	6.71 ± 0.80	14.84 ± 1.36	5.38 ± 1.82	1.30 ± 0.16	6.1 ± 0.5	3.27 ± 0.12
Ag NPs	7.70 ± 0.60	14.74 ± 1.09	6.13 ± 1.03	1.32 ± 0.26	7.1 ± 1.1	3.51 ± 0.17
Ag_2S NPs	6.82 ± 1.40	13.79 ± 2.78	2.99 ± 0.80	1.10 ± 0.19	6.7 ± 0.5	3.68 ± 0.10
Brain						
Control	8.55 ± 0.94	15.68 ± 1.53	16.96 ± 8.04	0.10 ± 0.01	2.6 ± 0.1	5.89 ± 0.43
$AgNO_3$	9.01 ± 0.74	18.99 ± 1.36	12.38 ± 10.25	0.08 ± 0.01	2.7 ± 0.3	5.58 ± 0.17
Ag NPs	9.45 ± 0.60	16.56 ± 1.68	24.25 ± 14.56	0.09 ± 0.01	2.7 ± 0.2	5.58 ± 0.42
Ag_2S NPs	9.55 ± 1.25	16.24 ± 0.88	18.85 ± 10.93	0.09 ± 0.01	2.5 ± 0.3	6.64 ± 0.77
Carcass						
Control	2.22 ± 0.10	8.68 ± 0.16	11.57 ± 0.99	2.77 ± 0.12	4.03 ± 0.43	1.61 ± 0.05
$AgNO_3$	2.28 ± 0.11	8.34 ± 0.21	12.00 ± 1.53	3.02 ± 0.20	4.57 ± 0.57	1.94 ± 0.16
Ag NPs	2.24 ± 0.06	8.46 ± 0.16	12.39 ± 0.47	3.06 ± 0.12	4.17 ± 0.42	1.63 ± 0.13
Ag_2S NPs	2.23 ± 0.11	8.36 ± 0.46	12.22 ± 0.90	2.82 ± 0.10	3.81 ± 0.22	1.67 ± 0.09

Data are mean ± S.E.M., n = 5/6. Data were analysed by one-way ANOVA or Kruskal-Wallis. Different upper case letters within columns denote statistical differences between treatments (columns). Data points with no letters indicate no statistically significant effect in that organ.

The moisture content of the tissue (data not shown) ranged between 69 and 84%, and was dependent on the tissue. There was no significant difference between the treatments (one-way ANOVA or Kruskal-Wallis; $P > 0.05$).

3.3.6 Histological examination and biochemical alterations

There were no major changes to the mid and hind intestine after 4 weeks of exposure (Fig 3-2). The mucous epithelium showed normal morphology. There was no evidence of erosion of the tips of the villi and the tissue showed normal columnar epithelial cells without foci of necrosis or reactive hyperplasia. The mucocytes in the epithelial also appeared normal, with no evidence of mucocyte proliferation. The average size of the mucocytes in the mid intestine were 19.2 ± 1.2, 19.8 ± 1.5, 19.8 ± 1.8 and 17.5 ± 0.9 µm in the control, $AgNO_3$, Ag NP and Ag_2S NP treatments, and there was no significant difference (one-way ANOVA) between treatments ($P = 0.733$). Additionally, there was no evidence of pathology to the gills of the Ag treatments or controls, with the absence of oedema in the tips of the secondary lamellae and no evidence of necrosis in the epithelium, or evidence of mucocyte proliferation. The vasculature in the gill appeared normal without aneurisms or evidence of swollen red blood cells. Overall, the normal gill morphology indicated the absence of waterborne exposure to silver.

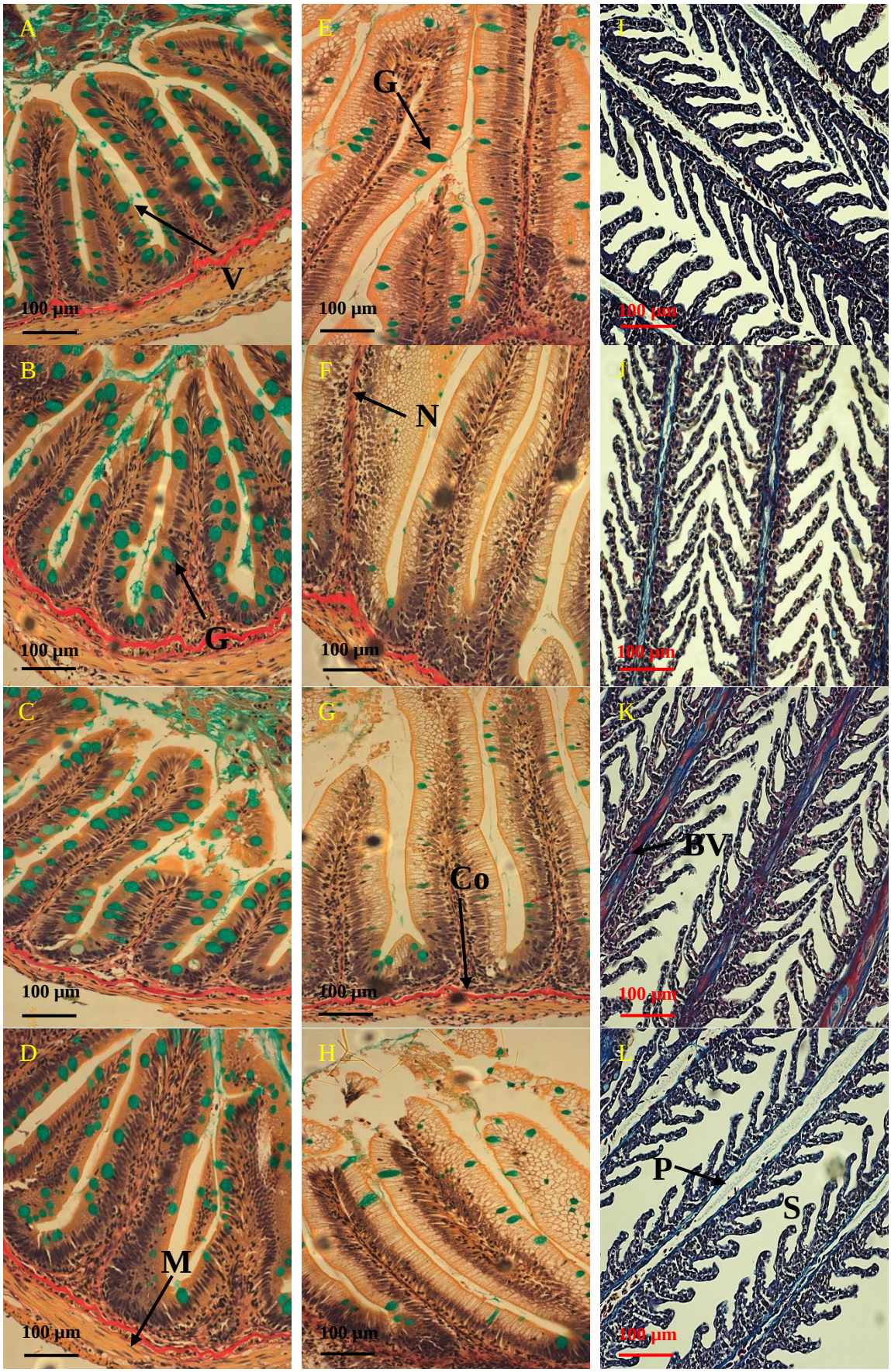
A
V
100 µm
E
G
100 µm
I
100 µm
B
G
100 µm
F
N
100 µm
J
100 µm
C
100 µm
G
Co
100 µm
K
BV
100 µm
D
M
100 µm
H
100 µm
L
P
S
100 µm

Figure 3-2. Histological structure of the mid intestine (left) hind intestine (central) and gill (right) following 4 weeks exposure to control (no added Ag; A, E, I), or 100 mg/kg of Ag as $AgNO_3$ (B, F, J), Ag NPs (C, G, K) or Ag_2S NPs (D, H and L). The intestines were stained using haematoxylin/ alcian blue/ van Gieson. In both the mid and hind intestine, the muscularis (M) surrounds the collagen (Co) which is attached to the base of the villi (V). The microvilli contain nucleated cells (N) and mucous-containing goblet cells (G). The gills were stained with Mallory's trichrome. The blood vessels (BV) can be seen within the primary gill filament (P), and the secondary lamellae (S) attached at a 45 degree angle.

There were no treatment-related differences in the total GSH concentration of the liver, brain, mid intestine, hind intestine or kidney by the end of the exposure (one-way ANOVA or Kruskal-Wallis; Fig. 3-3). However, there was a small, but statistically significant decrease in total GSH concentration in the gill in the $AgNO_3$ treatment compared to the Ag NP treatment only ($P = 0.023$), but these effects were not significantly difference from the control fish. There were no differences in total GSH between the Ag NP and Ag_2S NP treatments at the end of the exposure phase.

There was no change to TBARS concentration of the gill, brain, kidney or liver tissues at the end of the exposure phase (one-way ANOVA or Kruskal-Wallis; Fig. 3-3). However, some small changes were observed in the intestine (Kruskal-Wallis). The mid intestine of the control fish had a TBARS concentration of 3.1 ± 0.3 nmol TBARS/mg protein, whereas the Ag NP and Ag_2S NP treatments had 1.4 ± 0.1 and 1.3 ± 0.2 nmol TBARS/mg protein. A one-way ANOVA revealed the Ag_2S NP treatment was significantly lower compared to the control ($P = 0.030$) but the Ag NP treatment was not ($P = 0.057$). Within the hind intestine, there was a trend of decreasing TBARS concentration in all the Ag treatments compared to the controls (the latter, 2.1 ± 0.4 nmol TBARS/mg protein), but of these only the Ag NP treatment was significantly reduced compared to the controls ($P < 0.001$). There were no material-type effects.

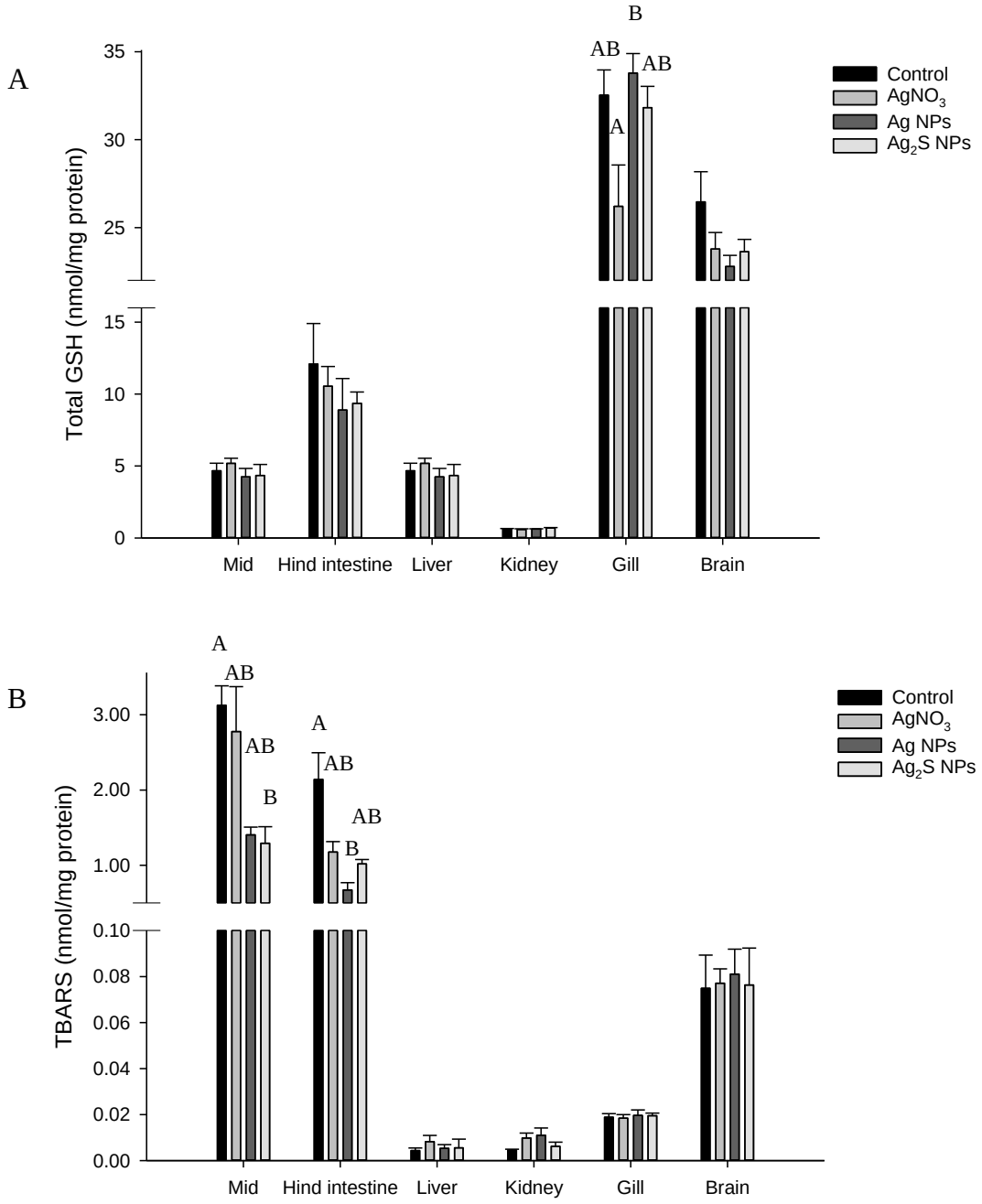

Figure 3-3. Total GSH (A) and TBARS (B) concentrations following 4 week exposure to the control (no added Ag) or 100 mg/kg Ag as either $AgNO_3$, Ag NPs or Ag_2S NPs. Data are mean ± S.E.M (n = 5/6). Different upper case letters denote statistical difference between treatments within the same organ. Data points with no letters indicate no statistically significant effect in that organ (one-way ANOVA or Kruskal-Wallis).

3.7 *In chemico* digestibility assay

The *in chemico* digestibility assay was used to identify any potential labile fraction of dissolved silver from the experimental diets (Fig. 3-4). There was no detectable dissolution from the control or Ag_2S NPs (below the procedural LOD of 2.3 ng/g). However, there was some release of dissolved Ag from the $AgNO_3$ and Ag NP diets with both time- and treatment-related differences (two-way ANOVA). There was a rapid elevation of dissolved Ag appearing in the external compartment of the test vessel over the 4-hour incubation, with the ng of total Ag released per g of food approximately doubling between each time point, in both treatments (Fig. 3-4). There was significantly more total Ag released from the food pellets containing Ag NPs compared to those with $AgNO_3$ after 1 h (P = 0.040), 2 h (P <0.001) and 4 h (P <0.001). There was no detectable dissolution in the intestine (<LOD).

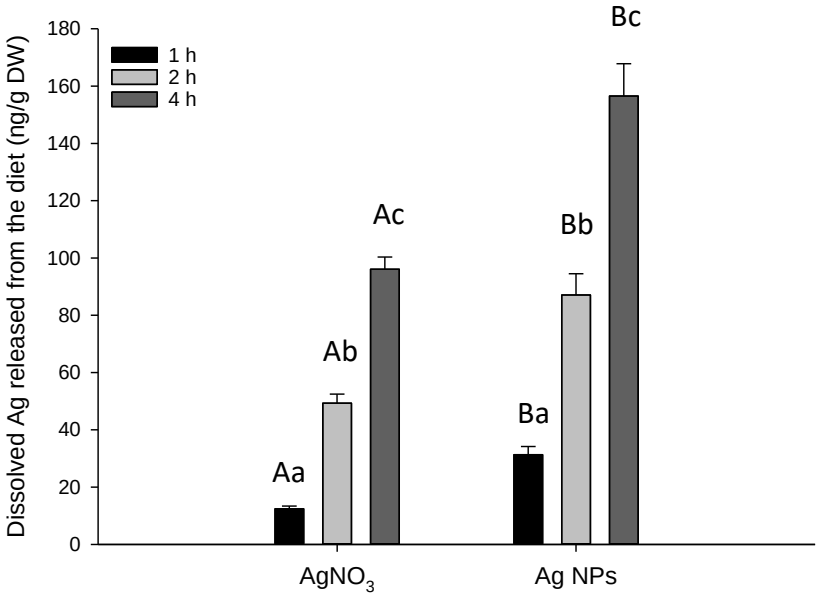

Figure 3-4. Concentration of dissolved silver released from the diet under acidic stomach conditions (pH 2). Data are means ± S.E.M., (n = 4). Different upper case letters denote statistical difference between Ag treatments. Different lower case letters denote statistical difference between time points (two-way ANOVA). Note the control and Ag_2S NP treatments had no apparent release of total Ag (the procedural LOD was 2.3 ng/g dw). Also, the intestinal simulation (pH 7.8) did not release any Ag.

3.4 Discussion

This study has demonstrated that rainbow trout will eat diets contaminated with a nominal 100 mg/kg of Ag as $AgNO_3$, Ag NPs or Ag_2S NPs without effects on growth or overt toxicity. The ingested silver subsequently caused total silver accumulation (form unknown) in the internal organs including the liver, kidney, brain, and the blood supply. Where accumulation was observed, the internal organs generally showed a gradual increase in accumulation over time, and with either partial or negligible decreases in the organ concentrations during the depuration phase, suggesting only a slow clearance from the body. As a proportion of the body burden, the liver showed the greatest organ accumulation for all treatments, and in keeping with the organ's role as a central compartment in processing metals. While the target organs and pattern of total Ag accumulation was broadly similar for dietary exposure to $AgNO_3$ and Ag NPs, the Ag_2S often caused less total Ag accumulation in the internal organs, suggesting the latter nanomaterial was less bioavailable.

3.4.1 Dietary Exposure and Total Silver Accumulation

It is well known that fish will eat food contaminated with metals (review, Handy et al. 2005), including Ag (Galvez et al. 2001), usually without mortality. This was also the case in the present study where only a few fish mortalities were observed (in random tanks), and regardless of the form of Ag added to the food, the animals continued to feed and gain body weight (Fig. 3-1). Dietary Ag exposure was confirmed by the measured total Ag in the food and by carefully monitoring the food intake during the experiment. Incidental waterborne exposure is unlikely because the measured total metal concentrations in the water were at

trace levels or below the detection limit and there was no evidence of the gill pathology (e.g., oedema, epithelial lifting) that is normally associated with dissolved metal toxicity. There was also no overt pathology in the intestines (Fig. 3-2), and overall the exposure can be regarded as a sub-lethal event leading to a physiologically relevant pattern of total Ag accumulation in the internal organs.

The unexposed control fish showed either trace amounts of total Ag in the organs (< 1 µg/g dw) or were below detection, in keeping with previous reports of background Ag in trout (Galvez et al. 2001). The dietary exposure to food containing $AgNO_3$ also resulted in the expected pattern of Ag accumulation, with the total Ag accumulating primarily in the intestine and liver compared to unexposed controls, and consistent with the route of exposure. While some total Ag was also detected in the kidney and blood, but not much in the gills of fish fed food containing $AgNO_3$; similar to Galvez et al. (2001). There appears to be no *in vivo* reports of dietary exposure to Ag NPs in rainbow trout. The present study showed a pattern of total Ag accumulation (form unknown) in the organs which was very similar to that of the $AgNO_3$ treatment; both in terms of the target organs and the total Ag concentrations achieved in those organs at the end of the exposure phase (Table 3-1). The distribution of the Ag body burden was also identical between $AgNO_3$ and Ag NP treatments. This suggests the bioaccumulation hazard from dietary $AgNO_3$ and Ag NPs are the same. Recently, Kleiven et al. (2018) exposed Atlantic salmon to ~60 mg Ag/kg as either $^{110}AgNO_3$ or as citrate-coated or uncoated ^{110}Ag NPs in a slurry, administered by oral gavage. After two days of exposure, the radioactivity from the $AgNO_3$ and citrate-coated Ag NPs oral treatment, was associated with the liver, but not the gills (Kleiven et al. 2018); similar to the findings in the present study with total Ag.

However, Kleiven et al. (2018) also noticed that radioactivity from the uncoated Ag NPs was transferred less to the liver than the citrate-coated Ag NPs. This suggests the form

of the nanomaterial is important to the accumulation pattern. In the present study, the Ag_2S treatment generally showed less total Ag accumulation in the internal organs than that of the Ag NPs after four weeks of exposure (Table 3-1). An *in chemico* digestibility assay on the same food used in the present study (Handy et al. 2018), showed that total Ag from the Ag_2S-containing pellets was less extractable and therefore would have lower bioavailability in the gut lumen. This is in keeping with the *in vivo* findings here. However, bioavailability in the gut lumen may not be the only factor to consider. Interestingly, Kleiven et al. (2018) found that the radioactivity in the intestine (~700, 900 and 700 corrected counts per minute/g wet weight tissue, for $AgNO_3$, coated Ag NPs and uncoated Ag NPs, respectively) were similar and yet less of the radioactivity associated with uncoated Ag NPs was found in the liver.

There are only a few reports of depuration following Ag exposures in fish, and these are for waterborne exposures (Wood et al. 2002; Hogstrand et al. 2003). Nonetheless, these studies show, for dissolved silver at least, that the uptake is relatively rapid over hours or a few days and that depuration is slower, over weeks. The depuration phase has an initial exponential decrease in body silver concentrations and then a much slower fraction that persists and is never cleared entirely (Wood et al. 2002). For dietary exposure to $AgNO_3$, there are some differences. Notably, apart from some clearance from the blood and intestines, there is no appreciable clearance of the body burden after two weeks on normal food (Table 3-1). On the other hand, there does seem to be some redistribution of the total Ag towards the liver and kidney, presumably to facilitate eventual excretion and/or inert storage of the total Ag.

There have been reports of dietary uptake of metal-containing ENMs in fish (TiO_2, Ramsden et al. 2009; ZnO, Connolly et al. 2016; CdS particles, Ladhar et al. 2014; Gold particles, Geoffrey et al. 2012; quantum dots, Lewinski et al. 2011). Unfortunately, these

studies did not necessarily aim to profile all the internal organs, or may not have measured the remaining carcass to enable body distribution calculations. At least one study with Ag NPs on marine Medaka (*Oryzias melastigma*) showed retention of Ag from Ag NP dietary exposure (Wang and Wang 2014), but comparisons with freshwater-adapted trout are problematic because of the very different osmoregulatory strategies, renal function, and gut chemistries of marine and freshwater fish. In the present study, the fish fed the Ag NP diet showed a very similar response in the depuration phase to those on the $AgNO_3$ diet; with negligible clearance from the internal organs and much of the body burden remaining in the liver and carcass (Table 3-1), with evidence of redistribution to the liver as a central compartment (Table 3-2). The presence of at least some Ag in the gallbladder (Table 3-1) suggests at least some incidental Ag excretion (form unknown) into the bile from the Ag NP dietary exposure, although the fraction was less than 1% of the body burden (Table 2). Alternatively, the proportion of the body burden in the kidney increased from 4 ± 1% to 9 ± 1% in the depuration phase for the Ag NP treatment (Table 3-2). This might imply some renal excretion of total Ag, or more likely, that the normal macrophage activity in the kidney is resulting in some Ag precipitation in the organ, as is known for Cu NPs (Al-Bairuty et al. 2013). The renal perfusion as a proportion of blood flow is also relatively high in freshwater-adapted trout, so the apparent retention by the kidney in the post-exposure phase will inevitably include some total Ag that is in the blood inside the organ. Similar arguments of macrophage activity and blood flow may also apply to the spleen where some total Ag remains (Table 3-1). Interestingly, van der Zande et al. (2012) also found that dietary Ag NP exposures in rodents resulted in total Ag accumulation in the internal organs with the most blood flow, such as the liver, spleen, kidney, lung and brain. The rodents also showed some clearance from the blood post-exposure, but with a

persistent residual of total Ag in the internal organs, similar to the present study on trout (Tables 3-1 and 3- 2).

The internal organs of fish fed with Ag_2S showed much less total Ag accumulation than either of the other Ag treatments. Consequently, the smaller amounts present were sometimes cleared. For example, at the end of the experiment, the blood and the gills were at the detection limit for total Ag (Table 3-1); but otherwise the pattern for the depuration phase was similar to the Ag NPs. However, on a proportion of body burden basis, there was a tendency of more of the residue total Ag remaining (albeit a small amount) to be redistributed to the carcass from the Ag_2S treatment compared to the others (Table 3-2).

3.4.2 Growth, health and sub-lethal effects

One concern for dietary exposure to metals is the potential for adverse effects on growth, nutritional performance or on the integrity of the gut epithelium. In the present study, there were no effects of any of the Ag-containing treatments on cumulative food intake or growth (Fig. 3-1). The intestines showed some reductions in TBARS in the animals fed with nanomaterials, but without total glutathione depletion in any treatment (Fig. 3-3), and the intestinal morphology was normal (Fig. 3-2). Together, this suggests the gut remained healthy, despite the potential for some dissolved silver release in the acidic conditions of the stomach (Fig. 3-4). There are only a few *in vivo* reports of nutritional performance in rainbow trout few diets containing added silver salts. Galvez and Wood (1999) fed trout diets containing up to 3000 mg/kg of Ag as Ag_2S for 58 days with no significant differences in food intake, specific growth rate or food conversion efficiency; despite clear Ag accumulation in the intestines. Galvez et al. (2001) made similar observations on growth

and food intake with trout fed 3.1 mg/kg of Ag over 126 days, where the Ag has been biologically incorporated into trout meal used to make the food pellets.

The absence of intestinal pathology with dietary $AgNO_3$ (Fig. 3-2) is perhaps not surprising. The gut is well-defined with intact mucous cells (Fig. 3-2), and the tissue depending on the region of the gut in trout, typically contains between 100-500 µg/g wet weight of metallothionein (Chowdhury et al. 2005); which together might readily chelate the maximum total Ag of 140 ± 22 µg/g found in the hind intestine (Table 3-1). There appear to be no reports of *in vivo* intestinal morphology in trout fed dietary Ag NPs, but in zebrafish fed 500 mg/kg of Ag NPs for 14 days there was no loss of integrity of the gut epithelium or any damage to the microvilli on the apical surface of the gut cells (Merrifield et al. 2013). Rats receiving a daily administration of 3.6 mg/kg by gavage of cubic or spherical Ag NPs (20 ml/kg body weight) for 14 days also showed no evidence of histological disturbance to the stomach, small intestine, cecum or colon (Javurek et al. 2017).

Exposure to dissolved silver *via* the water is known to interfere with branchial sodium homeostasis in trout (Grosell et al. 2002). However, dietary silver generally does not. Galvez et al. (2001) found no effects of dietary Ag on Na^+ influx or plasma Na^+ in trout. Similarly for the $AgNO_3$ diet in the present study, there were no effects on the total glutathione or TBARS in the gill (Fig. 3-3), indicating negligible oxidative stress. There were no effects on plasma Na^+, and only small changes in plasma K^+ within the physiological range, compared to controls (Table 3-3). The major electrolytes in the internal organs was also unaffected (Table 3-4). The same observations were made for dietary exposure to Ag NPs or Ag_2S NPs (Tables 3-3 and 3-4). There were some statistically significant disturbances to Cu concentrations in some organs (Table 3-4), and this was observed previously in dietary studies with TiO_2 NPs in trout (Ramsden et al.

2009), although the biological importance of small changes in tissue Cu is unclear. In the present study, there was no evidence of oxidative stress in the internal organs (Fig. 3-3).

3.4.3 Conclusions and perspective on environmental hazard assessment

In conclusion, the present study has demonstrated dietary accumulation of total Ag in trout arising from exposures to food containing $AgNO_3$, Ag NPs or Ag_2S NPs. The data is interpreted as a sub-lethal, with physiologically relevant uptake and without pathology to the gut or biochemical disturbances to the internal organs. A key concern for environmental regulation is whether ENMs present a different hazard to their nearest equivalent metal salt. The present study showed the dietary bioaccumulation of $AgNO_3$ and Ag NPs to be equal, with total silver from both of these materials (from unknown in the tissue) being more bioavailable than total Ag arising from the Ag_2S NP treatment. The bioaccumulation potential ranking would therefore be $AgNO_3$ = Ag NPs > Ag_2S NPs. However, there is also a desire to reduce the use of animals in the bioaccumulation testing strategy (Handy et al. 2018). Recently, an alternative *ex vivo* gut sac technique for assessing the total Ag accumulation by the gut in 4 hour incubations (Chapter 2) using the same ENMs as the present study. The gut sac approach is intended as a screening tool in a tiered approach to bioaccumulation testing (Handy et al. 2018) and correctly identified a bioaccumulation concern for both $AgNO_3$ and Ag-containing ENMs in the gut tissue. The *ex-vivo* gut sac results gave a slightly different ranking of $AgNO_3$ > Ag NPS = Ag_2S NPs (Chapter 2). Regardless, both the *in vivo* and *ex vivo* findings on these materials suggest the existing risk assessment for dissolved silver would encompass the bioaccumulation potential risk of the nano forms (i.e., no additional risk from nano). In both studies, the most likely of the nano forms to be released into the environment, the Ag_2S NPs, was identified as less hazardous

than $AgNO_3$. However, further work is needed to understand how the food matrix can effect dietary bioavailability of ENMs and to determine if ENMs can become 'biologically incorporated' into the tissues in a similar fashion to dissolved metals. The human health risk from the total silver accumulated in the carcass (i.e., mostly the edible flesh) also needs to be considered, and work is underway to validate a detection method for nano forms and particle size distributions in the internal organs of trout.

Chapter 4 - Development of a Suitable Extraction Protocol for Silver Nanoparticles and Silver Nitrate from Fish Tissues Using Single Particle ICP-MS

Abstract

For adequate environmental risk assessment, suitable methods to extract and quantify engineered nanomaterials (ENMs) from fish tissues following exposures are required. Currently, single particle (sp) ICP-MS is being increasingly used to measure ENMs, giving information on particle mass concentration, particle number concentration, and mean particle size and particle size distributions. Previous reports of digestion methods have focussed solely on ENM testing, with no consideration for the equivalent dissolved metal. Here, using spICP-MS, a step-wise process of assessing the suitability of enzymatic (proteinase K) and alkali (TMAH) methods are assessed using fish livers, the main site of chemical storage. A total of four different digestion matrices were used: proteinase K either in the presence or absence of $CaCl_2$ or TMAH, either in the presence or absence of $CaCl_2$. A series of spike tests of equal mass concentrations (50 ng/L) Ag NPs and $AgNO_3$ were conducted fresh into the matrix. All digestion matrices spiked with Ag NPs showed recovery similar to ultrapure deionised water (95-105%). When spiked in TMAH alone, the $AgNO_3$ precipitated to form small particles; therefore it is not a suitable extraction matrix without changing the form of Ag. The second series of experiments looked at the recovery of Ag NPs and $AgNO_3$ in the appropriate extraction matrix with tissues. Proteinase K, both in the presence and absence of $CaCl_2$, did not result in complete digestion of the tissues, rendering both of these extraction methods obsolete. Only TMAH + $CaCl_2$ demonstrated the ability to solubilise the tissue. Ag NPs were spiked onto liver tissues and analysed 24 h later, showing no significant change in particle size distribution or particle mass concentration. The particle number concentration fell significantly to around 80% of freshly spiked Ag NPs. To assess the suitability of this method, samples from an *in vivo* dietary study where fish were fed nominally 100 mg/kg Ag as either $AgNO_3$

or Ag NPs were analysed to represent biologically incorporated Ag. There was no significant difference between the particle number concentration, mean particle size or particle mass concentration between the *in vivo* $AgNO_3$ and Ag NP treatment liver tissues. For example, the particle number concentrations were 68.3 ± 33.1 and 76.9 ± 51.6 $x10^9$ particle/g dw liver in the $AgNO_3$ and Ag NPs, respectively. This *in vivo* liver tissue data indicating potential transformative processes in the gut lumen or tissue.

4.1 Introduction

There are now numerous reports on the ecotoxicity of engineered nanomaterials (ENMs) to aquatic organisms (reviews, Handy et al. 2008; Kahru et al. 2010; Baker et al. 2014; Lead et al. 2018), including metal-containing ENMs (Shaw and Handy 2011). However, metallic ENMs, depending on their physico-chemical properties, can partially dissolve in the environment (e.g., ZnO in seawater, Wong et al. 2010; Cu NPs in freshwater, Al-Bairuty et al. 2016). Consequently, aquatic organisms may take up the substance in the particulate form, or as dissolved metal, or both (Shaw and Handy 2011). There is also the potential for the dissolution of metallic ENMs inside the tissues of the test organism. Therefore, a central question for the hazard assessment is whether the toxicity arises from the particle themselves or metal ions released from them. There is also a lack of suitable techniques for the routine environmental monitoring of ENMs in biota (Klaine et al. 2012). Thus, robust methods for detecting ENMs in the tissues of aquatic organisms are desirable, especially fishes as important species in aquatic food webs that are also consumed by humans.

Silver is especially of concern as one of the most toxic elements to aquatic species (review, Ratte 1999). Aqueous exposure to dissolved silver in rainbow trout (*Oncorhynchus mykiss*) causes total Ag accumulation in the internal organs, especially the liver as a central compartment in the handling of metals (Hogstrand et al. 1996). The accumulation of total Ag (form unknown) in the tissues of trout has also been demonstrated for waterborne exposures to silver nanoparticles (Ag NPs, Scown et al. 2010), and in *ex-vivo* gut sacs (Chapter 2). The total Ag concentration in the tissue is usually determined after strong acid digestion of sample, with subsequent analysis by inductively coupled plasma optical emission spectroscopy (ICP-OES) or mass spectrometry (ICP-MS). For Ag

NPs at least, this approach assumes that all the ENM in the sample is digested to the dissolved form. Consequently, acid digestion methods are not suitable for the detection of intact Ag NPs inside the tissue.

The available methods for detecting and characterising ENMs in environmental samples have been documented (reviews, Handy et al. 2012; von der Kammer et al. 2012; Meermann and Nischwitz 2018). For tissue samples, the approaches for metallic particles have been mainly concerned with the *in situ* detection of the presence or absence of particles, such as scanning or transmission electron microscopy (SEM or TEM) coupled with energy dispersive X-ray measurements for elemental composition (EDX, see Handy et al. 2012). For example, the detection of TiO_2 NPs in Caco-2 cells (Gitrowski et al. 2014). Anti-Stokes Raman Scattering (CARS) microscopy has also been used to identify metallic ENMs in or on fish gills (Johnston et al. 2010). While such methods can successfully identify ENMs in cells, microscopy is often only semi-quantitative in terms of measuring particle number concentration, and is laborious.

Alternative approaches include attempts to extract the ENM from the tissue into a liquid samples. For example, toluene extraction of C_{60} from *Daphnia magna* (Tervonen et al. 2010), or acid-extraction of (acid resistant) TiO_2 NPs from fish tissues (Shaw et al. 2013). However, any subsequent attempt to quantify the particle number concentration or size distribution in the extracted sample by light scattering methods [i.e., Nanoparticle Tracking Analysis (NTA) or Dynamic Light Scattering (DLS)] are compromised by several factors. These include the corrosive nature of the sample that may damage the instrument, interferences from other colloids in the sample (e.g., salt crystals or proteins), and/or a modest detection limit for light scattering methods (around 10 mg/L, see Handy et al. 2012).

The development of single particle (sp) ICP-MS, has allowed the measurement of both particle mass and number concentration, and particle size distributions in liquid

samples. The approach relies on aspirating a dispersion of intact particles into the plasma of the instrument. The extremely high temperature of the plasma atomises each particle to produce an ion 'cloud' of ionised atoms that arrives at the detector together (i.e., within one time period or dwell time). The resulting signal at the detector is proportional to the size of the particle, and the signal frequency proportional to the particle number concentration in the sample (see Montaño et al. 2016). The spICP-MS technique was first demonstrated in ultrapure water (Degueldre and Favarger 2003) and has been used to demonstrate its capability to detect silver nanoparticles in ultrapure water (Laborda et al. 2011). The technique has also been applied to enzymatic digestions of plant materials (tomato plants, Dan et al. 2016; rice plants, Deng et al. 2017).

There are two approaches that have been reported for animal tissues, but none of these have been applied to fish. The first is a strong alkali digestion using tetramethylammonium hydroxide (TMAH), that has been used to release Ag NPs and Au NPs from Daphnia after waterborne exposure to these ENMs (Gray et al. 2013). This study demonstrated the ability to extract and measure particle size distributions of Ag NPs from organisms, which were comparable in primary particle size to the original Ag NPs in the exposure media. The second reported method used an enzymatic digestion with proteinase K to extract Ag NPs, which had been spiked at relatively high concentrations (5-25 mg/kg) into a chicken meat matrix. The resulting samples were then diluted up to 100,000-fold and analysed by spICP-MS (Peters et al. 2014b).The latter method was intended for the food industry, but also has the potential to be applied to fish tissue from ecotoxicity studies.

However, there are some technical challenges to overcome to routinely apply either the TMAH or proteinase K digestion methods to the determination of Ag NPs in fish tissues. Firstly, it is expected that environmentally-relevant exposures will have modest bioavailabilites (typically only a few percent of the exposure dose, Chapter 2 and 3), and

so the first challenge would be to routinely detect low concentrations of Ag NPs in fish without suffering interferences from the chemical matrix of the sample. Secondly, it is expected that fish will have a low concentration of silver 'naturally' occurring in the tissue, and this dissolved silver background will influence both the detection limit and the minimum particle size that can be detected by spICP-MS, as well as the ratio of dissolved to particulate silver in the sample with respect to toxic mechanisms. Finally, spike recovery tests for dissolved metals in conjunction with the analysis of certified reference tissues for total metal is widely applied to the validation of measurements of dissolved metals in fish (e.g., Lemes and Wang 2009). However, the validation of particle number concentrations for ENMs in tissue remains challenging because there are, as yet, no certified reference tissues for ENMs and arguably spike-recovery test with dissolved silver (e.g. silver nitrate) may not represent the recovery of the nano form.

The present study aimed to tackle these challenges and to develop a robust method to extract Ag NPs from fish tissues, using modified versions of the proteinase K or TMAH digestions outlined above to determine the particle number concentration and particle size distributions in liver tissue from rainbow trout by spICP-MS. The specific objectives included digesting the livers from normal (unexposed trout) and then determining the effect of spiking the digested matrix with either Ag NPs or $AgNO_3$ (i.e., the effect of the digestion matrix on the detection of each form of Ag). Then, experiments were performed by spiking normal liver tissues prior to digestion in order to investigate the overall procedural recovery of the entire digestion and measurement protocol. Finally, attempts were made to establish the dissolved versus nanoparticulate fractions of Ag from the fish intestine and livers that had been previously exposed *ex vivo* and *in vivo*, respectively, to either $AgNO_3$ or Ag NPs. This was to determine if the tissue matrix affected the process. This latter experiment was aimed at determining if the method could detect 'biologically incorporated' Ag NPs in a

tissue sample compared to artificial processes of directly spiking liver samples with Ag NPs. It also enabled some appreciation of the likely ratio of dissolved to particulate silver in exposed fish *in vivo*.

4.2 Methods

4.2.1 Nanomaterial characterisation, materials and reagents

Reagents were analytical grade or higher (proteinase K [lyophilized powder from *Tritirachium album*], TMAH [25% in H_2O], calcium chloride, triton X-100, calcium acetate, Triz buffer) and were obtained from Sigma-Aldrich (UK). High purity water (HPW) was used throughout (18.2 MΩ cm; Elga Ltd, High Wycombe, UK). The Ag NPs were obtained from Applied Nanoparticles (Barcelona, Spain) and the characterisation of the same batch used here has been reported elsewhere (Chapter 3). Briefly, the manufacturer's specifications were a primary particle diameter of 50 nm diameter and a mass concentration of 10.4 mg Ag/mL suspended in 5.5 mmol/L of sodium citrate and 25 µmol/L tannic acid. The actual total Ag concentration in the stock supplied by the manufacturer at the time of these experiments was 9.5 ± 0.4 mg/mL. A daily working suspension of 1 mg/L Ag NPs was freshly made for the experiments (see below) spike tests. Gold nanoparticles (Au NPs) were used for reference to help optimise the initial settings of the spICP-MS and were obtained from BBI Solutions (UK), with a nominal size of 60 nm at a total Au concentration of 56.8 mg/L. The Au NPs were prepared by taking 1 mL of the stock suspension and transferring to a 2 mL centrifuge tube (Eppendorf, UK), and centrifuged at 13,000 rpm for 20 mins. After this, the supernatant was removed, and 20 µL sample was used for TEM analysis. The mass concentration of total Au as 49.4 mg/L by

acid digestion and analysed by ICP-MS. A commercially available dissolved Ag standard (QMX Laboratories Ltd, UK) at a concentration of 1000 ± 5 µg/mL in 2% HNO_3 was used for routine instrument calibration after dilution to appropriate concentrations. All suspensions and solutions were prepared fresh for each day of analysis.

4.2.2 Animal husbandry and tissue collection

Adult rainbow trout (*Oncorhynchus mykiss*, triploid, n = 10) weighing ~150 g were obtained from Exmoor fisheries. Fish were kept in a recirculating system until sampling and fed a commercially available diet (Aller Futura, Kaliningrad, Russia). Trace amounts of Ag was present in the normal animal diet. Batches of the food pellets were digested in primer plus grade nitric acid, diluted and analysed using ICP-MS (Handy et al. 2018), with a total Ag concentration in the animal feed of 0.52 ± 0.02 µg/g dw (mean ± S.E.M., n = 5). Liver tissue, as a key target organ for metals in fish, was selected for the analytical work. For liver tissue collection, fish were euthanised by induced concussion followed by pithing of the brain (schedule 1 method in accordance with ethical approvals, Home Office, UK and in compliance with the EU directive 2010/63/EU). For the gut sac experiments (see below, n = 9), food was withheld from the fish for 48 h prior to tissue collection to aid the evacuation of the gastrointestinal tract, in compliance with ethical approval from the UK Home Office (Project Licence held at Plymouth University under the Animals (Scientific Procedures) Act (1986)).

4.2.3 Experimental work

Initial experiments were aimed at simply optimising the ICP-MS for the detection of particle suspensions made in ultrapure water. For this initial work, 25 ng/L dispersions of the Au NPs were used for reference and transport efficiency (see below) and compared to the Ag NPs from Applied Nanoparticles (Barcelona). These experiments involved observing the effect of different dispersion concentrations on the particle number concentration and particle size distribution. This allowed optimum concentration of 50 ng/L for Ag NPs to be found where double particle events do not occur (i.e. 2 particles entering the plasma at the same time).

The next series of experiments using either the proteinase K or TMAH digestion matrices alone, without any liver tissue, to determining the effect of spiking the digested matrix with either Ag NPs or $AgNO_3$ in order to understand how the digestion matrix influenced the detection of each form of Ag. The proteinase K extraction method was conducted as previously reported (Peters et al. 2014b), but with minor modifications. A digestion buffer was made containing 10 mmol/L Tris buffer, 1% Triton X-100 and 1 mmol/L calcium acetate, adjusted to pH 9.5 with NaOH). A working stock solution of proteinase K (one unit will hydrolyse urea-denatured haemoglobin to produce colour equivalent to 1.0 µmole of tyrosine per min ay pH 7.5 at 37^{o}C) was also prepared. To ultrapure deionised water, 6 mg of proteinase K was added, giving a concentration of 6 mg/mL. From this working stock solution of enzyme, 0.57 mL of proteinase K solution was added to 4 mL of the digestion buffer. An additional experiment was conducted whereby proteinase K (1 mg/mL) was added to 5 mmol/L $CaCl_2$ with 50 mmol/L Tris-HCl (as per manufacturer's specifications).

For the TMAH extraction 2 mL of 25% TMAH was added to a 15 mL centrifuge tube. The effect of added Ca and Cl on the extraction was also tested with the TMAH digestion. For the TMAH + $CaCl_2$ matrix, a stock of 25 mmol/L $CaCl_2$ was made (0.183 mg into 50 mL of ultrapure water). The two digestion matrices were spiked with 50 µL of 100 µg/L Ag NP stock to contain a final total silver concentration of 2.5 µg/L. The samples of Ag-spiked matrix were immediately vortexed for 1 min and then diluted 50-fold using ultrapure deionised water to a final concentration of 50 ng/L before analysis by spICP-MS. Samples were also spiked with 50 µL of 100 µg/L Ag as silver nitrate. The samples were immediately vortexed for 1 min and then diluted 50-fold using deionised water to a final concentration of 50 ng/L. To measure the within sample variability, one sample was measured five consecutive times, and a measurement of between sample variability was made by measuring five independently made sample.

The next series of experiments involved digesting the livers from normal (unexposed trout) in the proteinase K, TMAH and TMAH + $CaCl_2$ matrices (as above). For each method, 50 mg (dry weight) of fish liver was used as a representative tissue. For both proteinase K extraction protocols, 4 mL of extraction buffer was added to the tissue. The samples were vortexed for 1 min, sonicated for 5 mins and then incubated in a water bath at 35^{o}C for 3 hours (Peters et al. 2014b). For the TMAH-based extractions, 2 mL of extraction solution was added. The samples were left for 24 h (Gray et al. 2013).

The next experiments involved spiking normal liver tissues prior to digestion in order to investigate the overall procedural recovery of the entire digestion plus the measurement protocol. This was conducted for the TMAH + $CaCl_2$ digestion matrix only. The 50 mg liver tissue, plus the 2 mL of extraction solution was fortified with 50 µL of 1 mg/L Ag as Ag NPs or $AgNO_3$. The samples were left for 24 hours before being diluted 50-fold with deionised ultrapure water and analysed using spICP-MS.

Finally, attempts were made to establish the dissolved versus nanoparticulate fractions of Ag in the mucosa of the mid intestine following an *ex vivo* gut sac experiment or from fish livers that had been previously exposed *in vivo* to either $AgNO_3$ or Ag NPs via the diet. This latter experiment was aimed at determining if the method could detect 'biologically incorporated' Ag NPs in a tissue sample compared to the artificial process of directly spiking liver samples with Ag NPs.

4.2.4 Gut sac experiment

For fish, there is an interest in ENM uptake across the gut epithelium, particularly the intestine (e.g., Al-Jubory et al. 2013). Chapter 2 demonstrated the utility of the gut sac method to screen for the accumulation potential of the Ag NPs used here. After food withdrawal for 48 h, adult triploid rainbow trout (n = 9) weighing ~200 g were euthanised (as described above) and the mid intestine was removed. To minimise potential Ag from residual food particles, the tissue was rinsed with a physiological gut saline (in mmol/L: NaCl, 117.5; KCl, 5.7; $NaHCO_3$, 25.0; $NaH_2PO_4.H_2O$, 1.2; $CaCl_2$, 2.5; $MgSO_4.7H_2O$, 1.2; glucose, 5.0; mannitol, 23.0; pH 7.8, from Handy et al. 2000) and then weighed. One end of the intestine was sutured closed with surgical thread before insertion of the gut physiological saline spiked with either ultrapure deionised water (control) or 1 mg/L Ag as $AgNO_3$ or Ag NPs made up in gut physiological saline. The mid intestine gut sacs were closed with suture thread and incubated in gut physiological saline gassed with 99.7:0.3% O_2:CO_2 for 4 h at 15 ± 1°C. After incubation, the gut sacs were removed, cut open and rinsed with fresh physiological gut saline (5 mL) followed by the same saline but containing 1 mmol/L EDTA (5 mL) to aid removal of the surface bound fraction of Ag. The mucosa was then separated from the muscularis using the edge of a glass microscope slide. The

tissues were stored at -20^{o}C until required for analysis. Subsequently, the tissues were thawed and used wet. The presence of Ag NPs in the tissues were then determined following digestion (described above, n = 3 mid intestine mucosa/treatment).

4.2.5 *In vivo* fish exposure to silver nanoparticles and silver nitrate for determination of biogenically incorporated Ag

The diet production and *in vivo* dietary exposure is described in detail in Chapter 3. Briefly, diets were made to contain no added Ag (control) or 100 mg/kg Ag as either $AgNO_3$ or Ag NPs. This was made by 'top dressing' a commercially available diet with the material of interest (ultrapure deionised water was used in the control).

Juvenile triploid rainbow trout (~10 g, n = 18) were graded into flow through tanks (n = 3/treatment). Fish were fed the diets for 2 weeks before being sampled for spICP-MS analysis. The fish were euthanized, the liver removed and weighed. The liver was dried in a freeze drier, weighed and digested using TMAH + $CaCl_2$, diluted and analysed using spICP-MS.

4.2.6 Instrumentation

An iCAP RQ ICP-MS (Thermo Fisher) was operated in collision cell mode, with He as the cell gas, and a micromist nebuliser (nominal uptake rate) and quartz cyclonic spray chamber cooled to 2^{o}C. The plasma power was 1550 Watts and the plasma, nebulizer and auxiliary flow rates were 14.0, 1.0 and 0.8 L/min. A nickel plated sampler and high matrix skimmer cones were used throughout this work. A dwell time of 3 msec was used throughout this work, and a total sampling time was 60 seconds. Before analysis, the ICP-

MS was tuned such that it performed to the manufacturer's installation specifications using 1 µg/L ^{115}In for maximum sensitivity and minimum oxide (CeO/Ce) formation below 0.01% (as per manufacturer's specification) as an indication of polyatomic interferences. In spICP-MS, only one m/z charge can be measured at a time. Silver has two m/z ratios (107 and 109), with the data presented here being 107. The sample wash time was set to 60 seconds. The sample uptake flow rate was determined gravimetrically by difference in weight by aspirating deionised ultrapure water over 2 mins (n = 5) and remained between 0.2 and 0.3 mL/min in all experiments. The transport efficiency was calculated daily and according to Pace et al. (2011). A 60 nm Au NP standard was purchased from BBI Solutions (UK). The transport efficiency was calculated in each matrix used, as well as in ultrapure water (n = 5). The instrument was calibrated using a series of dissolved Ag standards from 0 to 4 µg/L. The dissolved standards were made up in each relevant matrix. Quality control measures of procedural blanks and checks every 10-15 samples were included.

4.2.7 Data processing and statistics

For a 60 second time scan, with a dwell time of 3 msec, a total of 20,000 data points are generated per sample. The raw data file for each sample was exported from the instrument and pasted into a bespoke Excel spreadsheet (Peters et al. 2014b) which calculates the signal distribution (Fig. 4-1) and particle size distribution (Fig. 4-2). This spreadsheet has been used for spike recovery tests (Grombe et al. 2015; Peters et al. 2015; Weigel et al. 2017). A large proportion of the sample aspirated into the uptake tube is lost from the spray chamber. Due to ENM suspensions being heterogeneous, there is a need to calculate the amount of suspension reaching the detector, and is termed the transport efficiency (or

nebulisation efficiency; modified from Pace et al. 2011). First, the particle number concentration is calculated as (Peters et al. 2014b):

$$PNC = \frac{Particle\ no.}{TE}\ x\ \frac{1000}{V} \qquad \text{Equation 4.1}$$

Where PNC = particle number concentration (L^{-1}), Particle no. = number of particles in a time scan (min^{-1}), and v = sample flow rate into the instrument (mL/min). Rearrangement of this equation is used to calculate the transport efficiency from well characterised materials (e.g. Au NPs). The individual particle mass is calculates using the response to ionic silver:

$$Particle\ mass = \frac{P.I.x\ 3}{Response} x\ \frac{V\ x\ TE}{60} \qquad \text{Equation 4.2}$$

Where P.I. = the signal from an individual particle (CPS), 3 = the dwell time (ms), response = the slope of the dissolved calibration curve (CPS/µg/L). This is then used to calculate the particle mass concentration using the sum of particle masses:

$$Particle\ mass\ concentration = \frac{\Sigma\ particle\ mass}{TE\ x\ V\ x\ 1000} \qquad \text{Equation 4.3}$$

Finally, the particle diameter can be expressed as:

$$Particle\ diameter = \sqrt[3]{\frac{6\ x\ particle\ mass}{\pi\ x\ \rho}}\ x\ 10^4 \qquad \text{Equation 4.4}$$

These individual particle sizes contribute to the size distribution graph.

The average transport efficiency of the Au NPs in the appropriate matrix was used for spike and unknown samples. The limit of detection (LOD) for determining particle events was set as the standard deviation of the blank (n = 3) multiplied by 3, which equated to 18 particles.

Statistical analysis were performed in SigmaPlot 13.0, unless specified. Data were checked for normality and equal variance (Shapiro-Wilk and Brown Forsythe tests, respectively). Statistical differences were highlighted using either a one-way ANOVA

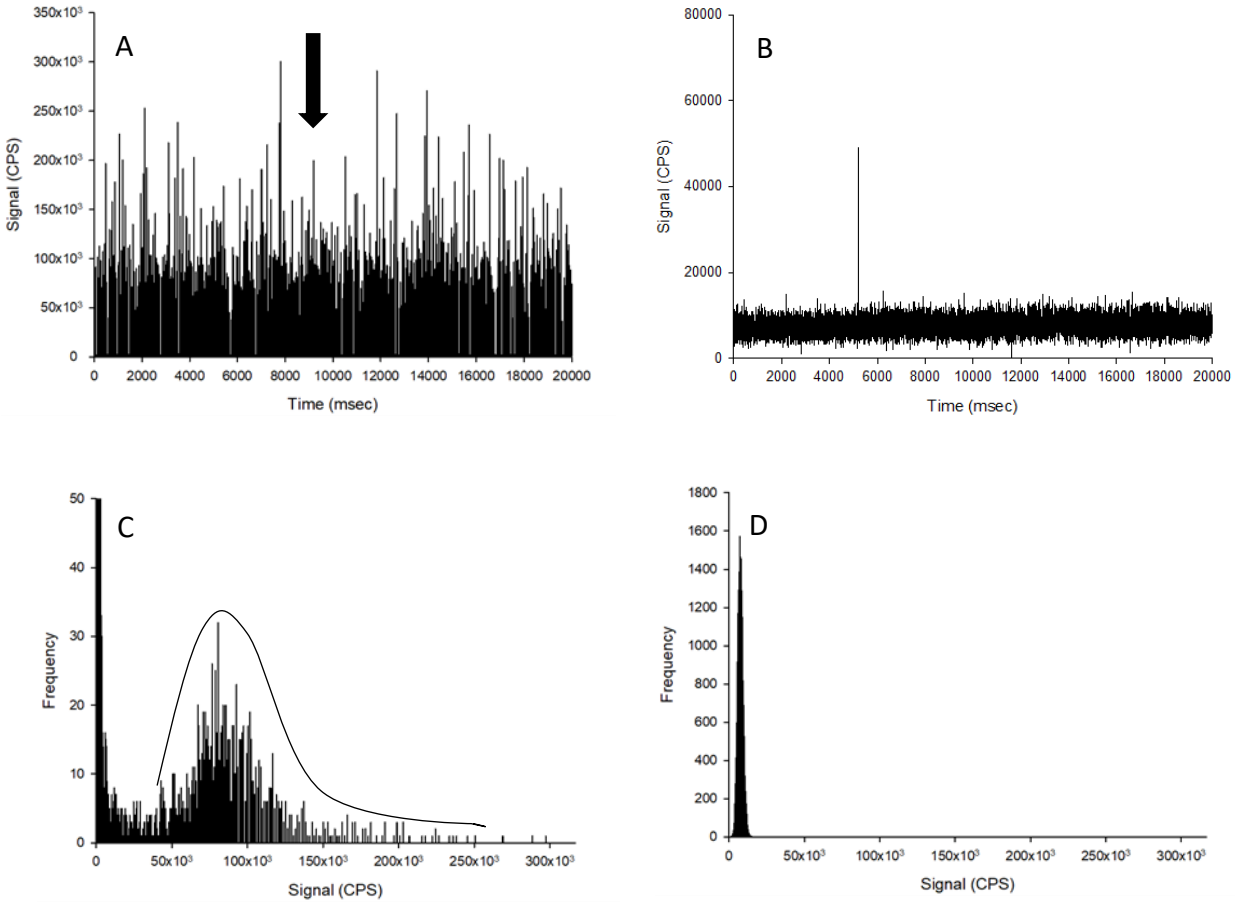

Figure 4-1. Time scan of 50 ng/L Ag NPs (A) or 50 ng/L as $AgNO_3$ (B). The Ag NP (C) and $AgNO_3$ (D) time scans are converted into signal distributions. The dissolved signal is characterised by high frequency of a low number of counts. The dissolved signal is subtracted from the intensity signal of the particles to produce a size distribution. The black arrow indicates individual particles detected in a dwell time. The black line (C) indicates the particle distribution.

(between day variability, $AgNO_3$ spiked into TMAH and *in vivo* data) a two-way ANOVA (between/within sample variation and matrix). For non-parametric data, the Kruskal-Wallis test was used. The normality of the size distributions were checked using a Kolmogorov-Smirnov test (spiked liver versus *in vivo* data) and was conducted in SPSS.

4.3 Results and discussion

4.3.1 Analysis of Au NPs and Ag NPs using spICP-MS

To determine the accuracy of spICP-MS, the mean particle sizes of both Au NPs and Ag NPs were compared to TEM (Fig. 4-2). The Au NP size determination is required for calculating the transport efficiency and is reported here for comparison. The mean values of the Au NPs and Ag NPs (n = 100 and 120, respectively) measured by TEM were 59 ± 6 and 56 ± 9 nm, respectively. The mean value of particle size using spICP-MS was 59 ± 0.1 and 57 ± 0.5 nm for the Au NPs and Ag NPs, respectively (n = 5 and 5, respectively). Generally, the two methods are comparable, giving similar information on particle size.

The purpose of this experiment was to determine if the instrument could routinely report the expected particles number concentration and median particle size of Ag NPs in simple dispersions. Table 4-1 shows these data on three consecutive days of independent sample preparation. There was no difference between the particle number concentrations, mean particle size or particle mass concentration reported on the three different days (one-way ANOVA, $P > 0.05$).

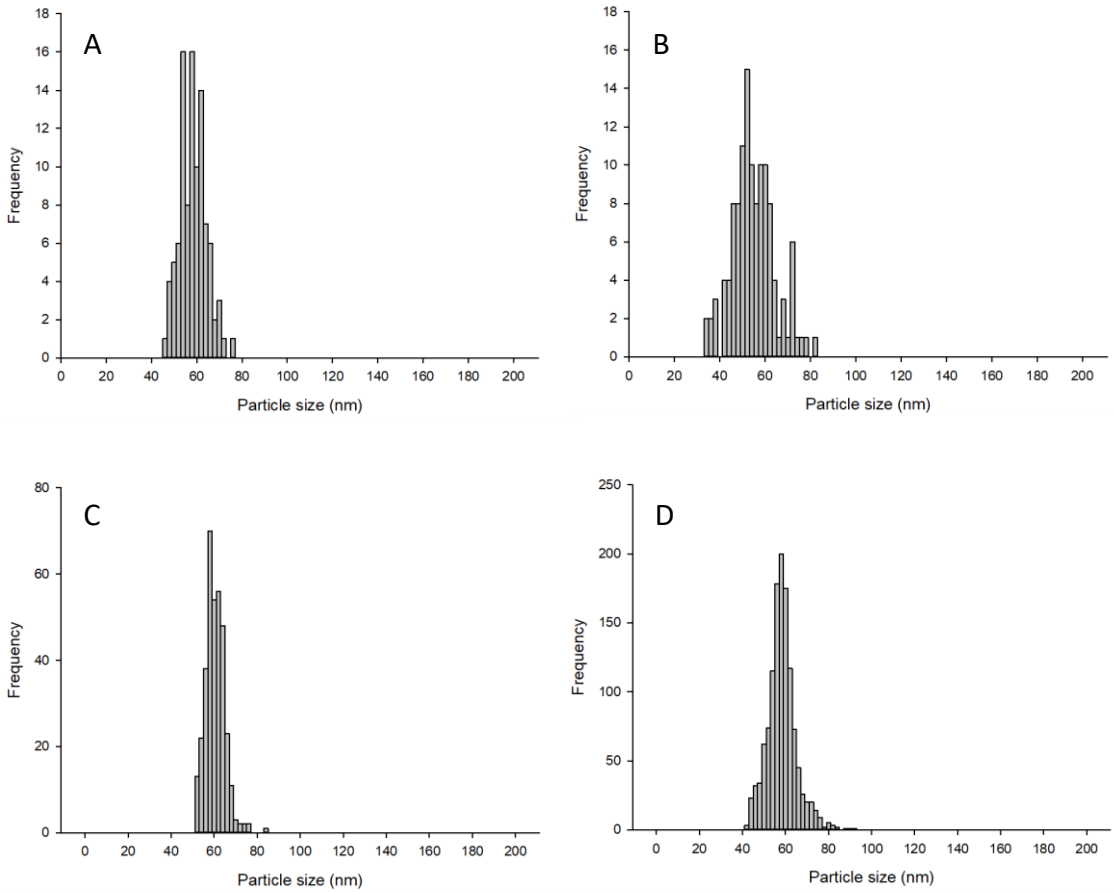

Figure 4-2. Example particle size distribution of Au NPs (left panels) by transmission electron microscopy (A) compared to 25 ng/L samples by spICP-MS (C), and Ag NPs (right panels) using transmission electron microscopy (B) compared to 50 ng/L samples by spICP-MS (D). For spICP-MS, the dissolved signals of Au or Ag were 2000 counts or below and were taken away from the mass before calculation of the particle size.

Table 4-1. The determination of particle parameters by spICP-MS in 50 ng/L dispersions of Ag NPs made in ultrapure deionised water on three independent data.

Time (days)	Particle mass concentration (ng/L)	Coefficient of variation (%)	Particle number concentration ($x10^7$/L)	Coefficient of variation (%)	Average particle size (nm)	Coefficient of variation (%)
1	42.7 ± 1.5	3.56	4.23 ± 0.13	3.07	56.7 ± 0.2	0.37
2	46.2 ± 4.0	8.67	4.51 ± 0.13	2.91	56.6 ± 1.2	2.16
3	47.1 ± 2.6	5.42	4.46 ± 0.09	1.91	57.2 ± 0.7	1.17

Data are means ± S.D., n = 3 replicate measurements on each day. There was no statistical difference between the particle mass concentration, particle number concentration or median particle size. For reference, the median particle size as measured by TEM was 58 nm and the expected particle number concentration for a 1 mg/L suspension is 171 $x10^9$/L as measured by Nanosight Tracking Analysis.

4.3.2 Spiking silver nanoparticles and $AgNO_3$ into extraction matrices alone

The aims of the first experiment were to determine whether the measurements reported by spICP-MS for ionic silver and/or Ag NPs were altered due to the extraction reagents (i.e. TMAH or proteinase K digestion). Data were presented as % recoveries of the expected particle mass concentration, particle number concentration and mean particle size based on the results by spICP-MS of the equivalent dispersions made in ultrapure deionised water rather than TEM analysis of the primary particle size distributions. The reason for doing this was that the measurement artefacts in TEM (e.g., dried samples, difficulty in seeing every individual particle) are not the same as those for spICP-MS (e.g., variability in sampling rate, the apparent dissolved metal background). Thus with two different assumptions being made in the two detection procedures, it is preferred to use the particle distributions in ultrapure water by ICP-MS for reference (see discussion in Pace et al. 2012).

The recovery of Ag NPs in proteinase K without additions of 5 mmol/L $CaCl_2$ showed no appreciable loss of particle mass concentration, particle number concentration or mean particle size (96-103%; Table 4-2). However, proteinase K in the presence of 5 mmol/L $CaCl_2$ caused a significant increase in the particle mass concentration (140-150%) and mean particle size to (111-112%) and compared to suspensions in deionised ultrapure water for within and between sample variation. When Ag NPs were spiked into proteinase K either in the presence or absence of $CaCl_2$, there was no change in the particle size distribution (Fig. 4-3). Equally, when $AgNO_3$ was added to proteinase K in either the presence or absence of $CaCl_2$, there was no unwanted reaction from the reagents (Fig. 4-4).

Table 4-2. Particle mass concentration, particle number concentration and mean particle size of Ag NPs and $AgNO_3$ spiked into different extraction matrices.

Extraction method	Form of silver	Sample type	Particle mass concentration (ng/L)	% recovery	Coefficient of variation (%)	Mean particle number concentration/L ($x10^7$)	% recovery	Coefficient of variation (%)	Mean particle size (nm)	% recovery	Coefficient of variation (%)
Ultrapure deionised water	Ag NPs	Within samples	47.66 ± 2.06^{Aa}	100 ± 4.32	4.32	4.51 ± 0.09^{Aa}	100 ± 0.00	1.98	57.21 ± 0.57^{Aa}	100 ± 0.00	1.00
		Between samples	51.83 ± 2.90^{Ab}	100 ± 5.59	5.59	4.85 ± 0.19^{Ab}	100 ± 0.00	3.98	57.65 ± 0.53^{Aa}	100 ± 0.00	0.92
	$AgNO_3$	Within samples	<LOD	N/A	N/A	<LOD	N/A	N/A	<LOD	N/A	N/A
		Between samples	<LOD	N/A	N/A	<LOD	N/A	N/A	<LOD	N/A	N/A
Proteinase K (without 5 mmol/L $CaCl_2$)	Ag NPs	Within samples	49.48 ± 1.38^{Aa}	103.84 ± 2.89	2.78	4.54 ± 0.13^{Aa}	100.67 ± 2.86	2.84	58.29 ± 0.23^{Ba}	101.90 ± 0.41	0.40
		Between samples	50.74 ± 1.66^{Aa}	97.90 ± 3.20	3.27	4.66 ± 0.13^{Aa}	96.15 ± 2.62	2.73	58.09 ± 0.20^{Ba}	100.00 ± 0.35	0.35
	$AgNO_3$	Within samples	<LOD	N/A	N/A	<LOD	N/A	N/A	<LOD	N/A	N/A
		Between samples	<LOD	N/A	N/A	<LOD	N/A	N/A	<LOD	N/A	N/A
Proteinase K (with 5 mmol/L $CaCl_2$)	Ag NPs	Within samples	70.79 ± 3.67^{Ba}	148.54 ± 7.71	5.19	4.70 ± 0.21^{Aa}	104.19 ± 4.59	4.40	64.58 ± 0.33^{Da}	112.89 ± 0.58	0.52
		Between samples	72.87 ± 3.54^{Ba}	140.58 ± 6.83	4.86	4.87 ± 0.17^{Aa}	100.52 ± 3.42	3.40	64.38 ± 0.39^{Da}	111.68 ± 0.67	0.60
	$AgNO_3$	Within samples	<LOD	N/A	N/A	<LOD	N/A	N/A	<LOD	N/A	N/A
		Between samples	<LOD	N/A	N/A	<LOD	N/A	N/A	<LOD	N/A	N/A

TMAH (without 5 mmol/L $CaCl_2$)	Ag NPs	Within samples	50.16 ± 1.27 ^{Aa}	105.25 ± 2.66	2.66	4.43 ± 0.13 ^{Aa}	98.26 ± 2.84	2.89	59.06 ± 0.22 ^{Ca}	103.24 ± 0.38	0.37
		Between samples	54.72 ± 3.75 ^{Ab}	105.58 ± 7.24	7.24	4.86 ± 0.46 ^{Ab}	100.32 ± 9.56	9.53	58.98 ± 0.51 ^{Ca}	102.30 ± 0.88	0.86
	$AgNO_3$	Within samples	0.85 ± 0.11 ^{Aa}	N/A	13.52	0.30 ± 0.03 ^{Aa}	N/A	10.54	34.34 ± 0.25 ^{Aa}	N/A	0.73
		Between samples	0.67 ± 0.27 ^{Aa}	N/A	39.58	0.23 ± 0.07 ^{Aa}	N/A	33.25	34.04 ± 0.72 ^{Aa}	N/A	2.12
TMAH (with 5 mmol/L $CaCl_2$)	Ag NPs	Within samples	51.04 ± 0.78 ^{Aa}	107.09 ± 1.65	1.54	4.48 ± 0.05 ^{Aa}	99.24 ± 1.12	1.13	59.05 ± 0.17 ^{Ca}	103.22 ± 0.31	0.30
		Between samples	53.30 ± 2.08 ^{Aa}	102.83 ± 4.02	3.91	4.70 ± 0.16 ^{Aa}	96.86 ± 3.23	3.33	59.09 ± 0.11 ^{BCa}	102.50 ± 0.20	0.19
	$AgNO_3$	Within samples	<LOD	N/A	N/A	<LOD	N/A	N/A	<LOD	N/A	N/A
		Between samples	<LOD	N/A	N/A	<LOD	N/A	N/A	<LOD	N/A	N/A

Data are means ± S.D., n = 5. Recovery was based on the particle number concentration as measured in ultrapure deionised water at the same concentration suspension (50 ng/L). The LOD was 20 particles per scan, which equates to 1.25 x10^5 particles/L. N/A indicates does not apply due to no particles detected, or cannot be calculated as was a false positive (e.g. $AgNO_3$ in TMAH only). Different uppercase letters denotes significant difference between same sample and silver type compared to different matrix (two-way ANOVA). Different lower case letters denote significant difference between sample types within the same matrix (two-way ANOVA). There was no significant difference in any measurements of the $AgNO_3$ in TMAH (one-way ANOVA or Kruskal-Wallis).

For the TMAH digestion (without $CaCl_2$), the particle mass concentration and particle number concentration recovery was within generally accepted limits of 100 ± 5%, and did not significantly differ from those measurements in ultrapure deionised water (Table 4-2, Fig. 4-3). However, there was a slight but significant increase in the mean particle size to 59 nm (two-way ANOVA, P <0.001). When $AgNO_3$ was spiked into TMAH, there was formation of particle-like events (Table 4-2, Fig. 4-4), with no difference between the within and between sample variation (one-way ANOVA or Kruskal-Wallis, P >0.05). Therefore, TMAH alone is not suitable to extract Ag NPs when there is a potential background of dissolved Ag in the original sample (e.g. from particle dissolution or the incidental occurrence of dissolved silver salts in the original sample). The cause of this apparent particulate signal with TMAH is likely to be precipitation as Ag_2O under the high pH conditions (Liu et al. 2009; Yang et al. 2016).

For the TMAH digestion, Ag NPs in the present of 5 mmol/L $CaCl_2$, there was no effect on the between and within sample variation particle number concentration (Table 4-2) or size distribution (Fig. 4-3). However, similarly for TMAH alone, there was a slight but statistically significant increase (~103%) in the mean size particle, both between and within samples (two-way ANOVA, P <0.001). This is within acceptable limits for the analysis of even dissolved metals in complex matrices (i.e., within 10%), and while acceptable limits of deviation for measurements with ENMs are not generally agreed (Handy et al. 2012), the percent deviation for an 'ideal' suspension by spICP-MS has been suggested to be 100 ± 25% or less (Gray et al. 2013). The results here (Table 4-2) for TMAH + $CaCl_2$ are all within the suggested limit offered by Gray et al. (2013). When $AgNO_3$ was spiked into the sample, there was no presence of particle-like events.

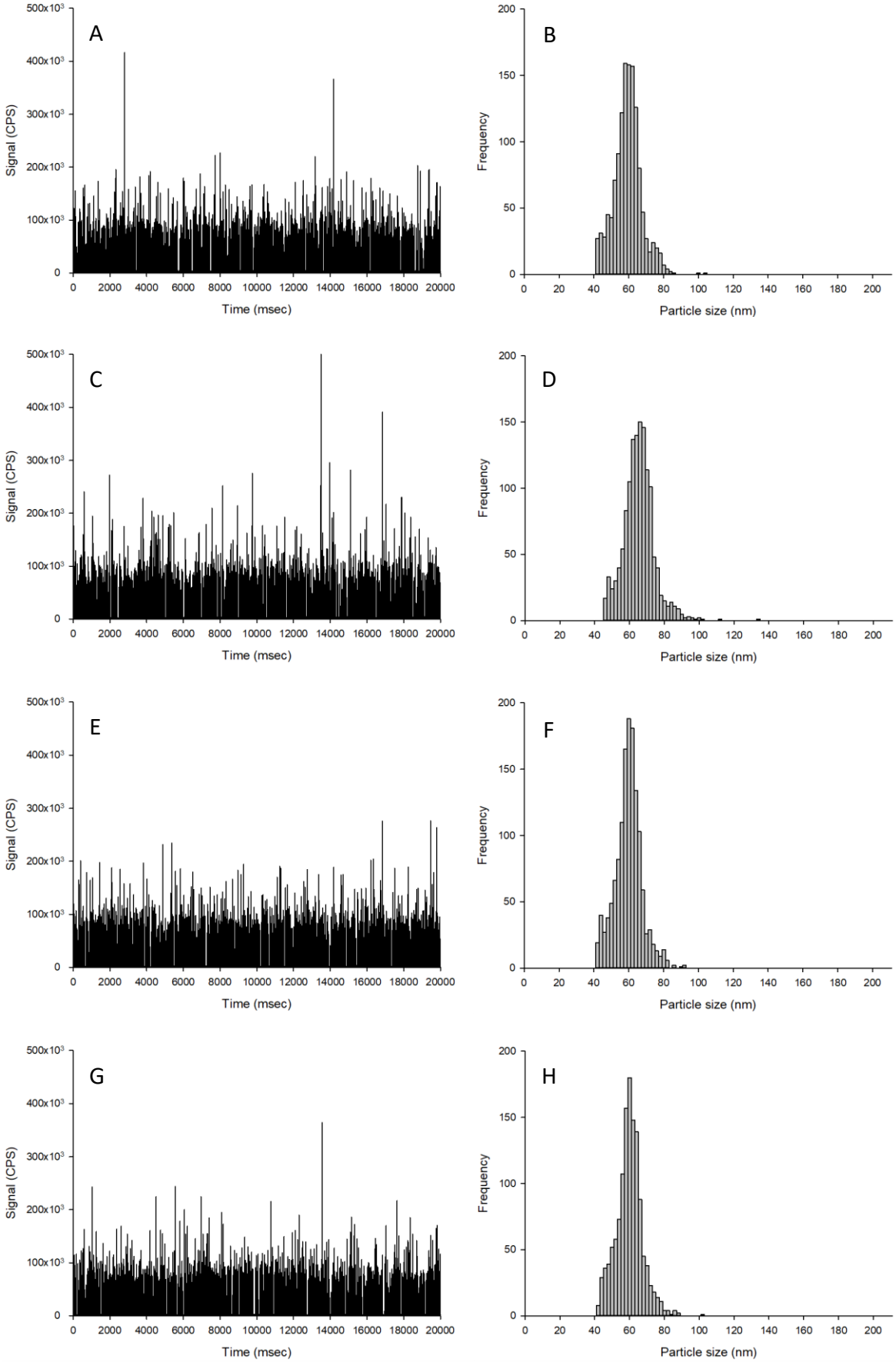
A
B
C
D
E
F
G
H
Signal (CPS)
Time (msec)
Frequency
Particle size (nm)

Figure 4-3. Time scans (left panels) and size distributions (right panels) of Ag NPs spiked into proteinase K without $CaCl_2$ (A and B), proteinase K with $CaCl_2$ (C and D), TMAH without $CaCl_2$ (E and F) or TMAH with $CaCl_2$ (G and H).

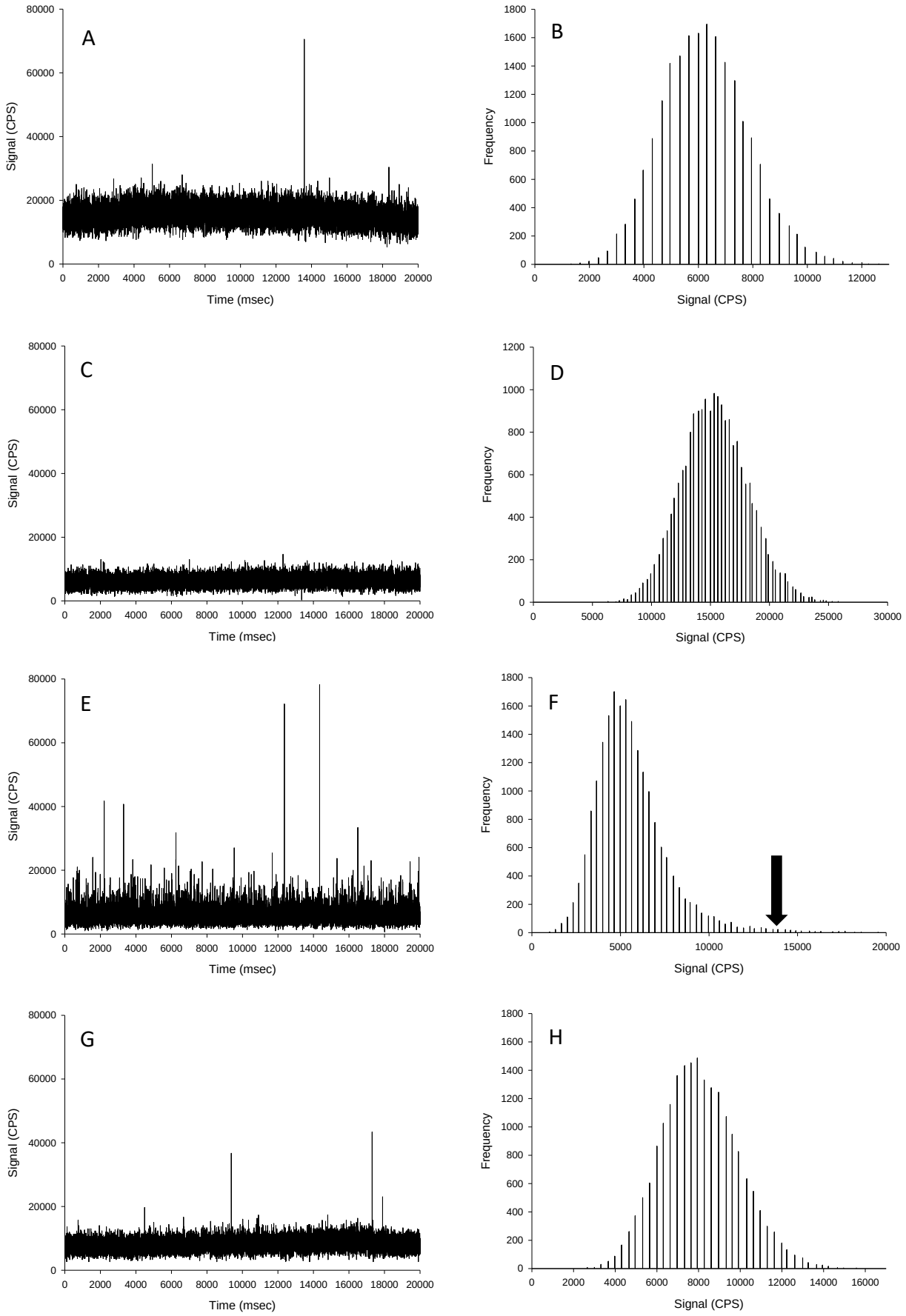
A
Signal (CPS)
Time (msec)
B
Frequency
Signal (CPS)
C
Signal (CPS)
Time (msec)
D
Frequency
Signal (CPS)
E
Signal (CPS)
Time (msec)
F
Frequency
Signal (CPS)
G
Signal (CPS)
Time (msec)
H
Frequency
Signal (CPS)

Figure 4-4. Time scans (left panels) and signal distributions (right panels) of $AgNO_3$ spiked into proteinase K without $CaCl_2$ (A and B), proteinase K with $CaCl_2$, (C and D), TMAH without $CaCl_2$ (E and F), and TMAH with $CaCl_2$ (G and H). Black line indicates loss of normal distribution through presence of particles being formed in TMAH matrix without the presence of chloride.

4.3.3 Spiking silver nanoparticles on liver tissues

The proteinase K method, both in the absence and presence of 5 mmol/L $CaCl_2$, was not suitable for breaking down the liver tissues, and resulted in only partially digested samples that could not be analysed. One reason for this observation is the potentially higher lipid content of the liver compared to the lean chicken used elsewhere (Peters et al. 2014b). Therefore, tests using proteinase K did not proceed any further.

The TMAH in the presence of 5 mmol/L $CaCl_2$ was the only suitable matrix to continue spiking experiments with liver tissues. Spiking Ag NPs onto liver tissue and left for 24 h caused no appreciable change in particle size distribution compared to freshly spiked (Fig. 4-5). For the liver tissue spiking tests, TMAH + $CaCl_2$ was spiked with Ag NPs or $AgNO_3$ in either the presence or absence of liver tissue and left for 24 h (Table 4-3). The liver tissue presence did not alter the particle mass concentration (two-way ANOVA, $P > 0.05$). However, presence of the liver did cause a significant decrease in mean particle number concentration and an increase in mean particle size. For example, the between sample variation decreased from 4.6 to 3.6 $x10^7$ particle/L in the absence and presence of liver, respectively (Table 4-3).

Table 4-3. Particle mass concentration, particle number concentration and mean particle size of Ag NPs or $AgNO_3$ spiked into TMAH + $CaCl_2$ extraction matrix in the absence or presence of liver tissue for 24 h.

TMAH + CaCl2	Sample type	Particle number concentration (ng/L)	% recovery	Coefficient of variation (%)	Mean particle number concentration/ L (x10^7)	% recovery	Coefficient of variation (%)	Mean particle size (nm)	% recovery	Coefficient of variation (%)
Spiked with Ag NPs	Within sample	49.07 ± 2.49 ^{Aa}	96.14 ± 4.88	5.07	4.12 ± 0.18 ^{Aa}	91.93 ± 4.06	4.42	59.30 ± 0.18 ^{Aa}	100.43 ± 0.30	0.30
	Between samples	52.98 ± 2.36 ^{Aa}	99.40 ± 4.43	4.45	4.68 ± 0.49 ^{Ab}	99.57 ± 10.39	10.44	59.26 ± 0.45 ^{Aa}	100.28 ± 0.77	0.77
Spiked with $AgNO_3$	Within sample	<LOD	N/A	N/A	<LOD	N/A	N/A	<LOD	N/A	N/A
	Between samples	<LOD	N/A	N/A	<LOD	N/A	N/A	<LOD	N/A	N/A
Liver spiked with Ag NPs	Within sample	54.60 ± 2.03 ^{Aa}	106.98 ± 3.98	3.72	3.76 ± 0.12 ^{Ba}	83.96 ± 2.95	3.15	63.42 ± 0.65 ^{Ba}	107.41 ± 1.10	1.03
	Between samples	53.38 ± 4.85 ^{Aa}	100.15 ± 9.11	9.09	3.60 ± 0.20 ^{Ba}	76.77 ± 5.58	5.58	63.46 ± 1.81 ^{Ba}	107.39 ± 3.06	2.85
Liver spiked with $AgNO_3$	Within sample	<LOD	N/A	N/A	<LOD	N/A	N/A	<LOD	N/A	N/A
	Between samples	<LOD	N/A	N/A	<LOD	N/A	N/A	<LOD	N/A	N/A

Data are means ± S.D., n = 5. Recovery was based on the particle number concentration as measured in freshly spiked TMAH + $CaCl_2$ at the same concentration solution (50 ng/L). Both $AgNO_3$ treatments showed no particle presence (<LOD). Different upper case letters denote statistical difference between the presence and absence of liver tissue with TMAH + $CaCl_2$ matrix within the same sample type (two-way ANOVA). Different lower case letters denote statistical difference between sample types (two-way ANOVA).

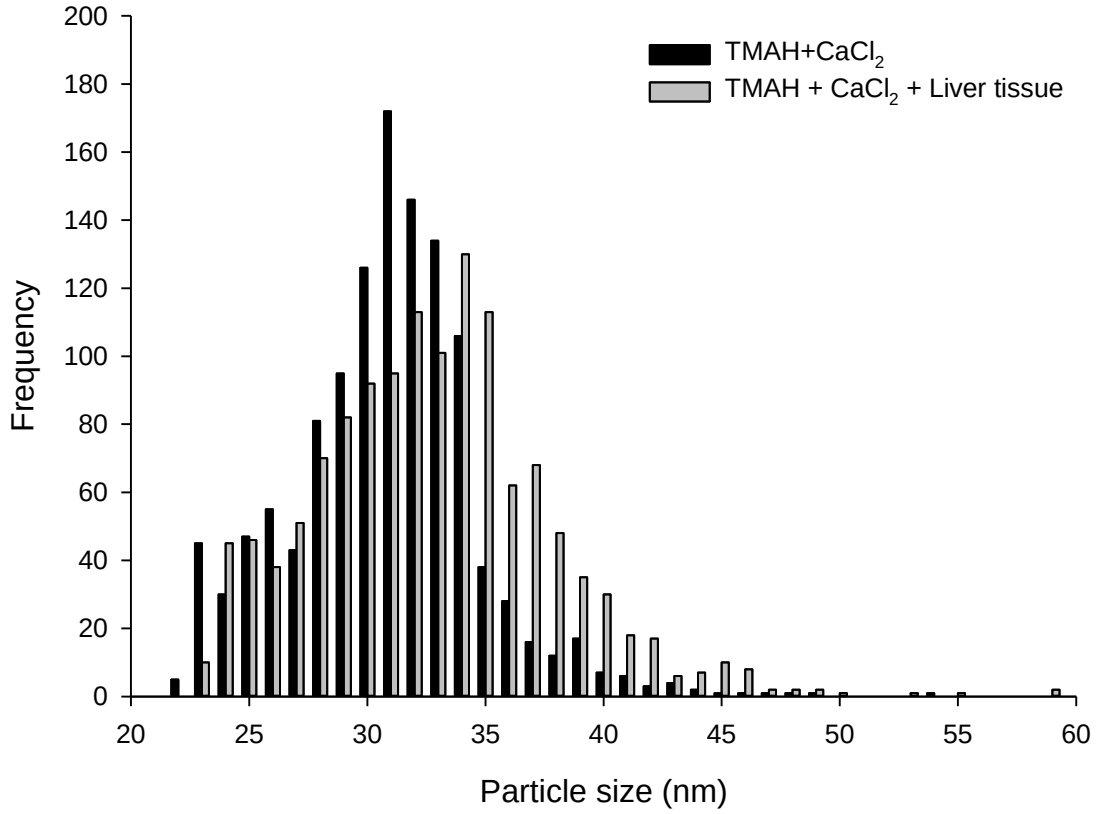

Figure 4-5. Particle size distribution of Ag NPs in TMAH + $CaCl_2$ either freshly into the extraction matrix, or onto a piece of liver tissue and allowed to solubilise overnight (representing extraction protocol).

4.3.4 Extraction methods for tissue samples containing biologically incorporated silver

The challenge for determining the Ag NP particle number concentration in living tissues that had been exposed to silver (either from *ex vivo* or *in vivo* exposure) is that the tissue may contain an incidental natural concentration of silver (forms unknown), plus any Ag that may have incorporated into the tissue during uptake in the exposure. Thus any digestion protocol with subsequent spICP-MS would need to detect potentially both any apparent dissolved Ag and particulate Ag in the tissue; and to do that without causing changes in the ratio of dissolved to particulate metal in the sample. The gut sac mucosa showed no background Ag signal (Fig. 4-6). The time scan of the mucosa from the $AgNO_3$ treatment

shows a typical dissolved signal, with no particles present. As expected, particles were detected in the mucosa of the Ag NP treatment, which showed a size distribution of particles in higher bin sizes (Fig 4-6). The gut sac mucosa samples were analysed using spICP-MS to confirm that Ag as $AgNO_3$ incorporated into a tissue matrix is not altered by the extraction protocol (Fig. 4-6). Therefore, the next step is to analyse the form of Ag in livers from chronically exposed fish.

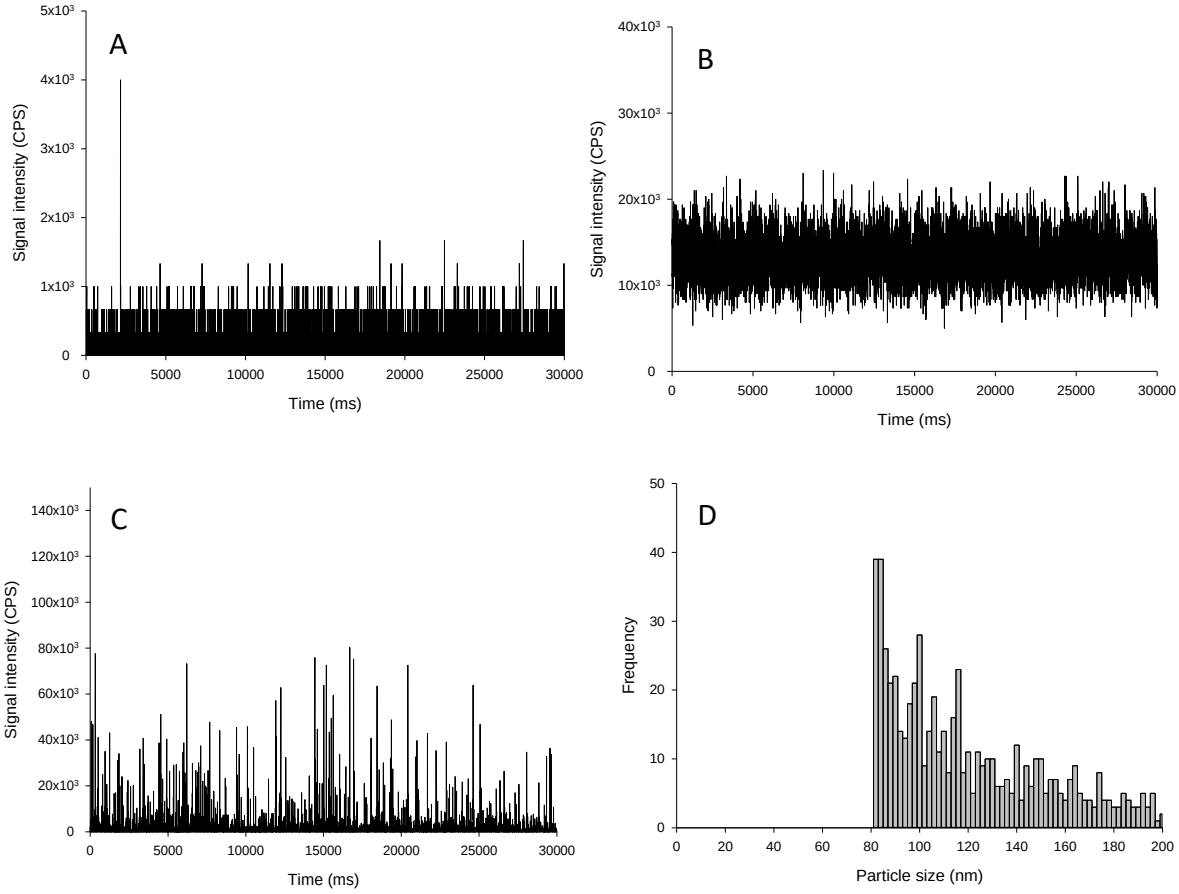

Figure 4-6. Example time scan of Ag removed from the mucosa of the mid intestine following exposure to a control (no added Ag; A), or 1 mg/L Ag as either $AgNO_3$ (B) or Ag NPs (C). The corresponding size distribution of Ag NPs is shown (D). There were no particles extracted from the control or $AgNO_3$ treatments.

Of the livers from fish exposed via the diet, the control organs had some incidental particulate silver above the LOD threshold, but most of the silver in the control fish was in the dissolved form (Fig. 4-7). The particles in the control liver equated to around 7 $x10^6$ particle/g dw tissue, which was 10,000-fold lower compared to the exposed tissues.

The particles found in the control did not significant differ in mean size compared to both of the Ag treatments (Table 4-4). In the Ag NP treatment, there was a significantly elevated number of particles compared to the controls (Fig 4-7 and Table 4-4) as well as a significant increase in particulate mass concentration. The particles in the Ag NP treatment were very similar to those in the $AgNO_3$ treatment (Fig 4-7) as there was no significant difference between any particle-based measurements between the two treatments (Table 4-4). The relative standard deviation of the *in vivo* livers is at least 7-fold higher compared to spike tests in the same matrix (Table 4-2) or in the presence of uncontaminated liver tissue (Table 4-3), highlighting the potential biological variability between fish and importance of including exposure data in methods. The presence of Ag particles in all treatments suggest apparent transformations within the gut or tissue, but these were possible to measure using the TMAH + $CaCl_2$ digestion matrix. All of the particle size distributions from the *in vivo* livers were significantly different from those of Ag NPs spiked into the matrix (Kolmogorov-Smirnov, P <0.001). The presence of particles in all treatments suggests the potential for biogenic nano-sized Ag formation.

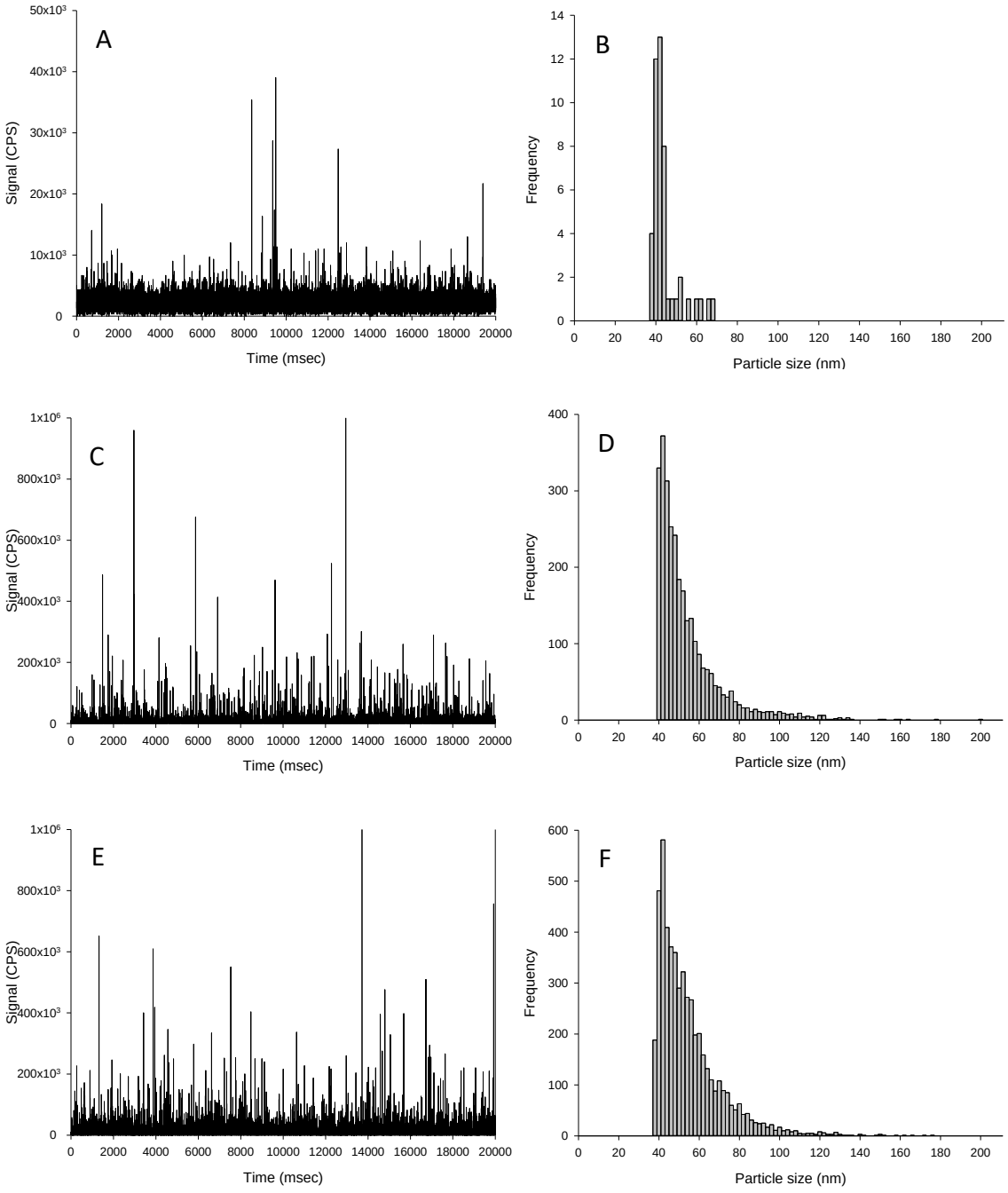

Figure 4-7. Time scan (left panels) and corresponding particle size distributions (right panels) of biologically incorporated Ag material extraction from the liver of fish exposed to either control (no added Ag; A and B), or 100 mg/kg Ag as $AgNO_3$ (C and D) or Ag NPs (E and F) for 2 weeks.

Table 4-4. The particle mass concentration, particle number concentration and mean particle size of Ag particles extracted from the livers of fish exposed to either a control (no added Ag), or 100 mg/kg Ag as either $AgNO_3$ or Ag NPs.

Measurement	Treatment	Liver 1	Liver 2	Liver 3	Liver 4	Liver 5	Liver 6	Mean ± S.D	Coefficient of variation
Tissue particle mass concentration (µg/g)	Control	0.002	0.005	0.002	0.006	0.002	0.004	0.003 ± 0.001 ^{A}	45.3
	$AgNO_3$	43.8	200.0	309.9	23.1	90.0	57.9	120.8 ± 111.74 ^{A}	92.5
	Ag NP	84.5	0.3 *	184.8	155.7	111.3	54.1	98.4 ± 67.4 ^{A}	68.4
Particle number concentration ($x10^9$/g)	Control	0.0123	0.0017	0.0155	0.0005	0.0029	0.0009	0.007 ± 0.004 ^{A}	61.9
	$AgNO_3$	32.4	67.4	51.1	53.2	12.8	78.0	49.2 ± 23.6 ^{B}	48.0
	Ag NP	39.2	26.6	65.8	14.0	92.1	12.2	41.7 ± 31.6 ^{B}	75.9
Mean particle size (nm)	Control	61.2	44.7	43.7	43.5	42.8	39.0	45.8 ± 7.8. ^{A}	17.0
	$AgNO_3$	61.8	76.6	93.6	42.7	53.2	49.2	62.9 ± 19.1 ^{A}	30.4
	Ag NP	66.1	26.7	72.8	54.0	54.7	41.5	52.7 ± 16.7 ^{A}	31.7

Data are n = 5/6. (*) denotes a significant outlier from Grubbs test and removed from further calculations. Different upper case letters denotes significant difference between treatments (columns; one-way ANOVA).

4.4 Conclusions and regulatory perspective

There is a regulatory need requirement to confirm the exposure in ecotoxicity tests, and the need for monitoring tools to measure ENMs exposure of biota in the wild. Such analytical methods need to be robust, preferably inexpensive and reproducible with a coefficient of variation less than 10%, and with a detection limit relevant to wildlife. Here, the spICP-MS method works for the liver tissue from fish, and meets the above needs. To the author's knowledge, this is the first report of developing a suitable extraction protocol for Ag NPs and $AgNO_3$ from fish tissues, emphasising the importance of checking suitability on dissolved metal controls. The next steps are to trial the method with a broader range of fish tissues and in different organisms for Ag NPs, further standardisation of the protocol and then, with inter-laboratory testing to demonstrate/validate the protocols for regulatory use.

Chapter 5 - Determination of particulate silver in fish following *in vivo* exposure to $AgNO_3$, Ag NPs or Ag_2S NPs using spICP-MS

Abstract

The toxicity of nanomaterials may partly arise from their physico-chemical characteristics, such as the particle size, but also the particle number concentration present in the tissue which represents the internal concentration. Single particle ICP-MS (spICP-MS) has gained a lot of interest for determining the latter. Here, data following an *in vivo* dietary exposure to $AgNO_3$, Ag NPs or Ag_2S NPs are shown. Fish were fed an Ag-supplemented diet (100 mg total Ag/kg) for 4 weeks, followed by 2 weeks depuration. At weeks 2, 4 and 6, the hind intestine, kidney and liver were collected from the fish. An alkali based extraction method was developed to remove the particles from the tissue matrix and with subsequent analysis of the liquid sample by spICP-MS. Particulate Ag was found in the hind intestine of all treatments, including the $AgNO_3$ treatment and trace amounts in the controls. At week 4, the particle number concentration (per g dw) in the hind intestine was 0.07 ± 0.03, 318.17 ± 116.71, 119.51 ± 33.00 and $0.60 \pm 0.22 \times 10^9$, for the control, $AgNO_3$, Ag NPs and Ag_2S NPs, respectively. In the Ag treatments, the particle number concentrations for both the $AgNO_3$ and Ag NPs were significantly higher compared to the Ag_2S NP treatment, indicating a lower bioavailability of the latter material. The presence of particles in the $AgNO_3$ treatment indicates that particulate Ag can be made in either the gut lumen or within the intestinal tissue. There was no difference in the mean particle size within the hind intestine or kidney of any Ag treatment (30-50 nm), suggesting that the particles did not dissolved inside the body and that intact particles circulated in the blood to other organs. Interestingly, in the liver of week 4 fish, the average particle size of the $AgNO_3$ and Ag NP treatments significantly increase to 77 ± 7 and 82 ± 11 nm, respectively, compared to the controls (47 ± 2 nm). Such increases in particle size suggests an agglomerative process or more complex ionic deposition to particles. TEM analysis of

intact tissues could not confirm the presence of particles, but a few were imaged in the liver tissue following digestion using TMAH +$CaCl_2$. In conclusion, there was detection of particles in the hind intestine, liver and kidney following exposure to both dissolved and particulate forms of Ag, with only small difference between tissues. These data also indicate possible transformative processes of Ag particles in the liver of exposed fish.

5.1 Introduction

The gastrointestinal tract is a dynamic physical and chemical environment that can vary in terms of pH, alkalinity, ionic strength and the types of organic matter in the lumen (Loretz 1995). Consequently, the behaviour and form of engineered nanomaterials (ENMs) may alter during their passage through the gut. Under acidic conditions, dissolution of some metal ENMs will cause decreases in primary particle size through the release of ions (e.g. Cu NPs, pH 5; Al-Bairuty et al. 2016). Acidic conditions will be found in the stomach of fish, with values as low as pH 2 (Bucking and Wood 2009) and subsequent dissolution of metal containing ENMs will occur (e.g. dialysis experiments using Ag NPs; Chapter 2). Complete dissolution of ENMs within the stomach can potentially aid data interpretation, since all the metal will be in the dissolved form and taken up by well-known solute transporters. In these situations, the accumulation profiles from exposure to particulates may be very similar to the equivalent dissolved metal control (e.g. $AgNO_3$ and Ag NPs; Chapter 3, $CuSO_4$ and Cu NPs; El Basuini et al. 2016). The intestine is widely regarded as the site of adsorption of dissolved metals (Ag; Chapter 2; Hg, Hoyle and Handy 2005, Cu, Zn, Cd, Pb and Ni; Ojo and Wood 2007). However, one aspect of the gastrointestinal tract environment that is often overlooked is the effect of the alkali pH of the intestine (7.5-9.5; Bucking and Wood 2009) on the dissolved metals. This is of particular importance where dissolved metals (or ions released from metallic ENMs) could potentially precipitate under alkali conditions, thus becoming particulate (e.g. Ag; Liu et al. 2009; Yang et al. 2016, Cu, Cd, Zn and Pb; Zirino and Yamamoto 1972).

Whether the pH of the intestine can precipitate dissolved metals into particulate material is unknown. If dissolved metals are precipitated as insoluble metal complexes by the alkali pH, fundamental aspects of dietary bioaccumulation modelling may need to be

revised. Typically, Michaelis-Menten kinetic parameters are used to describe the kinetics of dissolved metal accumulation (and solutes in general), whereby solute kinetics are incorporated, yet this will not be appropriate for the dynamic nature of ENMs (Handy et al. 2012). Consequently, for inert ENMs such as Ag_2S NPs that are unlikely to dissolve, confirmation of particle uptake, or the internal concentration as the nano form, requires the presence of the particles in the tissue to be measured.

The aim of this experiment was to assess the form of Ag in the organs on rainbow trout following a dietary exposure to either $AgNO_3$, Ag NPs or Ag_2S NPs. In Chapter 3, the $AgNO_3$ and Ag NPs treatments demonstrated a similar pattern of total Ag accumulation, which were generally higher compared to the Ag_2S NP treatment. It was hypothesised that this discrepancy between the bioaccumulation of total Ag from the Ag NP and Ag_2S NP exposures was due to dissolution of the Ag NPs (*in chemico* digestibility; Chapter 3), while the unreactive Ag_2S NP remained particulate. Therefore, the aim of this study was to determine the form of the Ag in the hind intestine, kidney and liver following exposure to $AgNO_3$, Ag NPs or Ag_2S NPs using spICP-MS, and to contrast that with the total Ag concentration reported in Chapter 3.

5.2 Methodology

5.2.1 Size distribution of silver and silver sulphide nanoparticles by spICP-MS

Stock suspensions of Ag NPs and Ag_2S NPs were supplied by Applied Nanoparticles (Barcelona) and the characterisation is reported in Chapter 3 (primary particle size [TEM], hydrodynamic diameter [NTA] and total metal concentration [ICP-MS]). To determine the Ag NPs and Ag_2S NPs particle size distributions, stock suspensions were diluted using

ultrapure deionised water to 50 ng/L and analysed using spICP-MS (n = 3) and calculated as reported in Chapter 4. These stock solutions were used for diet preparation for the dietary exposure.

5.2.2 Exposure and tissue collection

The use of animals in this experiment was under a project licence held at Plymouth University under the Animals (Scientific Procedures) Act (1986) in compliance with the Directive 2010/63/EU. The dietary exposure of fish to the Ag materials is described in Chapter 3. Briefly, juvenile triploid rainbow trout (~10 g, n = 84) were fed diets containing no added Ag (control) or nominally 100 mg/kg of Ag as $AgNO_3$, Ag NPs or Ag_2S NPs for 4 weeks. Following this, they were all placed on the control diet for a depuration period of 2 weeks (total 6 weeks). Fish were euthanized by an overdose of buffered MS222, with confirmation via pithing (schedule 1 method in accordance with ethical approvals, Home Office, U.K., and in compliance with the EU directive 2010/63/EU), weighed and dissected for their hind intestine, liver and kidney at weeks 2, 4 and 6 (n = 2/tank, n = 6/treatment, total 72 fish). The hind intestine was chosen as a 'positive control' for the dietary exposure (i.e., the route of exposure), while the liver was selected as central compartment for internal Ag accumulation (Chapter 3). The kidney was also chosen as an organ that does not typically accumulate material from dietary exposures. The tissues were dried and weighed before being cut in half. One half was used for total Ag determination (Chapter 3), and one half was used for spICP-MS analysis (see below). Additionally, liver tissues were taken (n =3/treatment) and fixed for TEM imaging (see below).

5.2.3 Extraction protocol

The extraction of Ag ENMs was as reported in Chapter 4. A stock of 25 mmol/L $CaCl_2$ (Sigma-Aldrich, CAS Number 10035-04-8) was made in deionised ultrapure water and diluted with 25% TMAH (Sigma-Aldrich, CAS Number 75-59-2) to make an extraction solution of 20% TMAH containing 5 mmol/L $CaCl_2$. Of this stock, 2 mL of this was added to each sample of tissue (21 ± 13 mg, mean ± S.D.). The samples were left overnight in a dark, dry storage cupboard and analysed the next day.

5.2.4 Single particle ICP-MS

For all sample analysis, a RQ iCAP ICP-MS (Thermo Fisher) was operated in standard mode, and a micromist nebuliser with a quartz cyclonic spray chamber cooled to 2^{o}C. The plasma power was 1550 Watts and the plasma, nebulizer and auxiliary flow rates were 14.0, 1.0 and 0.8 L/min. A nickel plated sampler and high matrix skimmer cones were used throughout this work. A dwell time of 3 msec was used throughout this work, and a total sampling time was 60 seconds. Before analysis, the ICP-MS was tuned such that it performed to the manufacturer's installation specifications using 1 µg/L ^{115}In for maximum sensitivity and minimum oxide (CeO/Ce) formation below 0.01% (as per manufacturer's specification) as an indication of polyatomic interferences. Data was acquired over a 60 second period using the ^{107}Ag m/z ratio, with a sample wash out time of 60 seconds. The sample wash time was set to 60 seconds. The sample uptake flow rate was determined gravimetrically by difference in weight by aspirating deionised ultrapure water over 2 mins (n = 5) and remained between 0.2 and 0.3 mL/min in all experiments. The transport efficiency was calculated daily and according to Pace et al. (2011). A 60 nm Au NP standard was purchased from BBI Solutions (UK). The transport efficiency was calculated in each matrix used, as well as in ultrapure water (n = 5). The instrument was calibrated

using a series of dissolved Ag standards from 0 to 4 µg/L. The dissolved standards were made up in each relevant matrix. Quality control measures of procedural blanks (n = 3) and checks every 10-15 samples were included.

It is well known that metals bind to glassware and can cause background contamination in instruments. These concerns also apply to ENMs. Prolonged use of samples containing ENM may result in some of the material being deposited on the internal workings of the instrument (e.g. tubing, spray chamber etc.). When the instrument is left overnight, there will be some solution left within the tubing, unless the tubing is thoroughly cleaned at the end of a sample run. Figure 5-1 shows the results of a procedural blank run the day after where the instrument was not cleaned properly the night before (other than aspirating 2% nitric acid before shutting the instrument down). Particle events are apparent on the trace even though there were none in the sample being analysed. This effect was ameliorated when the spray chamber was cleaned before use in 10% nitric acid and the peristaltic tubing is replaced. Therefore, the spray chamber was cleaned in this manner before each analysis, as well as changing the peristaltic tubing.

The limit of detection for particle size was calculated by using the lowest signal possible in a dwell time (333 CPS) and calculating the particle size for this signal. The result was a particle size LOD of 14 nm.

5.2.5 Transmission electron microscopy (TEM) on liver extracts and liver tissues

It is usual to validate any new analytical method by comparing it against an established alternative technique. In this case, TEM was used to confirm the presence of particles in the digested tissue samples and as an attempt to measure primary particle diameter of any particles that were observed. Following digestion (as above), the samples were diluted 100-

fold using ultrapure water (n = 3/treatment). The diluted samples were pre-concentrated by centrifugation at 4000 rpm for 30 mins. After this, the supernatant, with no particles, was removed and the pellet was re-suspended in a smaller volume to avoid tissue presence in the sample. After, a copper grid was placed on top of a drop of the sample. Following this, the grid was removed and allowed to dry at room temperature before imaging.

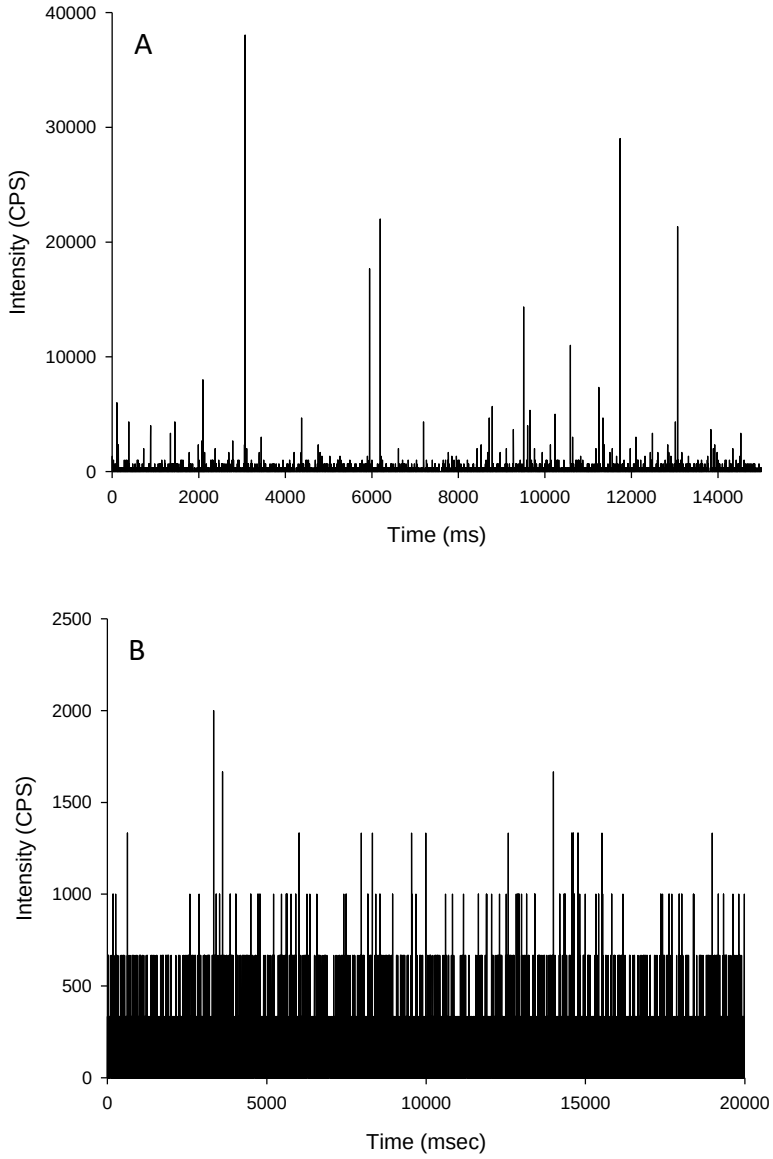

Figure 5-1. Time scan of a (A) procedural blank the following day after prolonged Ag NP introduction and (B) a procedural blank following the spray chamber being incubated in 10% nitric acid for 30 mins.

Liver samples were prepared according to Gitrowski et al. (2014), with modifications. The liver samples (n = 3/treatment, total = 12 fish) were fixed in glutaraldehyde (2.5%, pH 7.2) for at least 1 hour. Following this, tissues were rinsed twice in 100 mmol/L sodium cacodylate buffer (pH 7.2) for 15 mins. The livers were then secondarily fixed with 1% osmium tetroxide for 1 hour. Tissues were rinsed and then dehydrated through a series of alcohol solutions (30, 50, 70, 90 and 100% ethanol; 15 mins each), with the 100% being repeated to ensure dehydration. Following this, the 100% ethanol was replaced with low viscosity agar resin by placing tissues in increasing concentrations of resin (30:70, 50:50, and 70:30% for resin to ethanol percentages, respectively) until 100% resin. The tissues were left in each concentration of resin for 12 hours, with the 100% resin step being repeated twice and left over night. The tissues were placed in Beem capsules, and subsequently into an embedding oven and the resin polymerised at 60^{o}C overnight. The resulting blocks were sectioned with a Leica Ultracut E ultra-microtome using a diatome diamond knife. Sections were stained using a saturated solution of uranyl acetate in 70% ethanol (15 mins) and Reynold's 3% lead citrate (15 mins). Sections were also made with no staining for comparison. Photographs were taken by systematically taking photos of each grid section. All sections were then analysed using a JEOL 1400 TEM. Particles sized from TEM images were calculated using ImageJ software.

5.2.6 Calculations

Size-based calculations. The particle mass concentration, particle number concentration, mean particle size and particle size distributions were calculated as reported in Peters et al. (2014b) and Chapter 4.

% particulate Ag. The fraction of Ag that was dissolved compared to particulate in the liver was calculated in each sample by:

$$\frac{Sum\ of\ counts\ in\ dissolved\ fraction + sum\ of\ counts\ in\ particulate\ fraction}{Sum\ of\ counts\ in\ particulate\ fraction}\ x\ 100 \qquad \text{Equation 5.1}$$

Where the "sum of counts" refers to the sum of all counts recorded in the 60 s sampling period.

5.2.7 Statistics

Statistical analysis were performed using SigmaPlot 13.0. Data were checked for outliers using Grubbs test, following which they were assessed for normality (Shapiro-Wilk test) and equal variance (Brown Forsythe). Statistical differences were assessed using a one-way ANOVA (particle size of TEM images of extracts only) or a two-way ANOVA for analysis (time and treatment as factors). The Holm-Sidak post-hoc test for normally distributed data. For non-normal data, they were $\log_{10}$ transformed. Where data were non-parametric and could not be transformed, the Kruskal-Wallis test was used. *P* values presented are from post hoc tests. The association between organ total Ag concentrations (from Chapter 3) and particle mass concentrations were assessed using the Spearman rank order correlation.

5.3 Results

5.3.1 Particle characterisation in ultrapure deionised water using spICP-MS

As expected, the particle size distribution of Ag NPs in ultrapure water was similar to those in Chapter 4, with a normal distributions (Fig. 5-2) consistently produced (n = 3). The size distribution of Ag_2S NPs showed a constant skewed distribution in water (n = 3, Fig. 5-2), with a minimum particle size of 40 nm and a long tail of larger particle diameters. This tailing effect was not observed in the Ag NPs.

5.3.2 Organ particle mass concentration

There were no particles detected in the kidney samples from control (unexposed) fish (Table 5-1). However, in the hind intestine and liver of control fish, traces of particles were found. Throughout the dietary exposure and depuration, only the liver showed a time dependent change, whereby there was a significant increase in particle mass concentration from week 4 compared to week 2 (two-way ANOVA, $P = 0.012$). Regardless, each organ

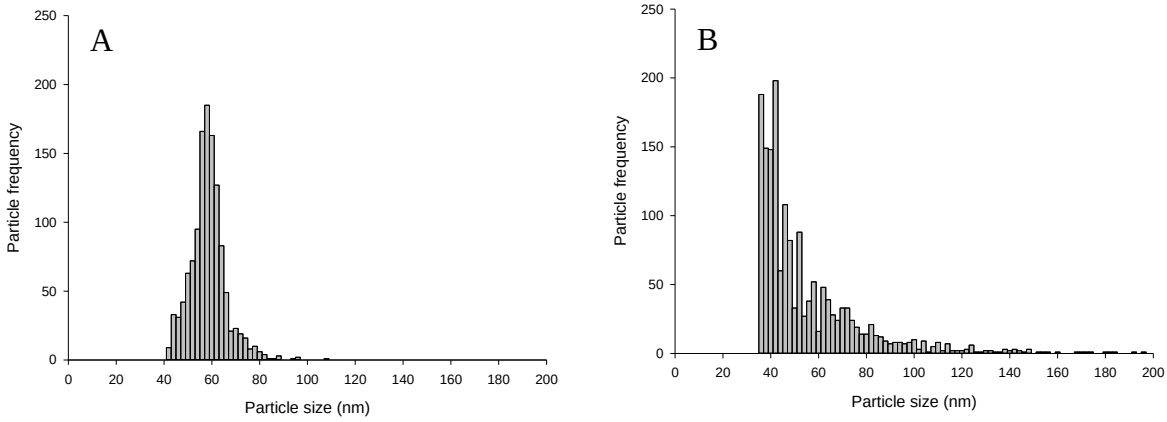

Figure 5-2. Example size distribution of (A) Ag NPs and (B) Ag_2S NPs in deionised ultrapure water that were subsequently added to the fish diet.

showed a significantly lower particle mass concentration than all of the Ag material exposed fish.

Within the $AgNO_3$ treatment, all organs at all-time points throughout the study were significantly elevated by around 60- to 200-fold compared to the controls (Table 5-1). In general, the organs particle mass concentration appears to increase between weeks 2 and 4, but this was not significant (two-way ANOVA, $P > 0.05$). For example, the liver particle mass concentration increased from 121 ± 46 µg/g at week 2 to 268 ± 43 µg/g at week 4. The Ag NP treatment showed a very similar trend compared to the $AgNO_3$, showing no statistical difference between the $AgNO_3$ and Ag NP treatment in any organ at any time point. However, some time-dependent changes were observed in the Ag NP treatment kidney, whereby the particle mass concentration significantly increased 7-fold from week 4 compared to week 2 (Table 5-1). Time-dependent changes were not observed in the other organs. Compared to the $AgNO_3$ and Ag NP treatment, the particle mass concentration within the Ag_2S NP treatment was significantly lower (10-200 fold) in all organs (Table 5-1). For example, at week 4 the hind intestine particle mass concentrations were 193 ± 36, 103 ± 19 and 1.2 ± 0.6 µg/g in the $AgNO_3$, Ag NP and Ag_2S NP treatments, respectively (two-way ANOVA, $P < 0.001$).

After the 4 week exposure, fish were placed on the control diet with no additional Ag for 2 weeks. The organ particle mass concentrations fell up to 10-fold over this 2 week depuration (Table 5-1). Generally, these reductions at week 6 in organ particle mass concentration were not statistically different from week 4, indicating the organs were not clearing the particles. One exception to this was the kidney from the Ag_2S NP treatment which significantly reduced from 2.6 ± 0.8 to 0.3 ± 0.1 µg/g (two-way ANOVA, $P < 0.001$).

5.3.3 Organ particle number concentration

There were no particles found in the kidney samples from control (unexposed) fish (Table 5-2). However, a small number of particles were found within the hind intestine and liver of the control fish. These concentrations equate to 25-40 particles in a time scan, which was above the LOD of ~15 particles per scan. At each week during the dietary exposure, the three orders of magnitude lower than all of the Ag treatments within the same organ.

Within the $AgNO_3$ treatment, the organs from fish at 4 week of exposure showed a significantly elevated particle number concentration compared to the controls (Table 5-1). Generally, the organ particle number concentration in all three organs appears to increase from week 2 to 4, but not in a statistically significant manner (two-way ANOVA, $P > 0.05$). The Ag NP treatment showed a very similar pattern of particle number concentration

Table 5-1. The particle mass concentration (µg/g dw) within the hind intestine, liver and kidney of rainbow trout exposed to control (no added Ag) or 100 mg/kg Ag as $AgNO_3$, Ag NPs or Ag_2S NPs *via* the diet for 4 weeks and with 2 weeks recovery.

Treatment	Organ	Week 2	Week 4	Week 6
Control	Hind	0.027 ± 0.008 ^{Aa}	0.018 ± 0.006 ^{Aa}	0.015 ± 0.004 ^{Aa}
$AgNO_3$	intestine	40.7 ± 16.9 ^{Ba}	192.9 ± 35.6 ^{Bb}	110.7 ± 53.4 ^{Bab}
Ag NPs		31.4 ± 10.4 ^{Ba}	102.7 ± 18.7 ^{Ba}	113.7 ± 25.6 ^{Ba}
Ag_2S NPs		0.8 ± 0.2 ^{Ca}	1.2 ± 0.6 ^{Ca}	2.0 ± 1.3 ^{Ca}
Control	Liver	0.003 ± 0.001 ^{Aa}	0.061 ± 0.039 ^{Ab}	0.011 ± 0.003 ^{Aab}
$AgNO_3$		120.8 ± 45.6 ^{Ba}	267.5 ± 42.5 ^{Ba}	174.5 ± 55.0 ^{Ba}
Ag NPs		98.4 ± 27.5 ^{Bab}	315.5 ± 69.5 ^{Ba}	96.9 ± 31.4 ^{Bb}
Ag_2S NPs		3.2 ± 1.00 ^{Ca}	5.3 ± 1.9 ^{Ca}	7.6 ± 2.1 ^{Ca}
Control	Kidney	<LOD	<LOD	<LOD
$AgNO_3$		10.0 ± 1.3 ^{Aa}	30.2 ± 9.6 ^{Aa}	34.3 ± 6.9 ^{Aa}
Ag NPs		5.2 ± 1.0 ^{Aa}	34.5 ± 7.4 ^{Ab}	64.0 ± 19.2 ^{Ab}
Ag_2S NPs		0.5 ± 0.3 ^{Ba}	2.6 ± 0.8 ^{Bb}	0.3 ± 0.1 ^{Ba}

Data are mean ± S.E.M. (n = 5/6 fish). Upper case letters denote significant difference between treatments (two-way ANOVA, columns). Lower case letters denotes significant difference between time points (two-way ANOVA, rows). The number of decimal places in the controls are shown for clarity between treatments. The LOD was 35.5 ng/g dw.

compared to the $AgNO_3$ treatment and there was no significant difference between the Ag NP and $AgNO_3$ treatments in any organs at any time point (Table 5-1). For example, the livers from fish at week 4 has particle number concentrations of around 83 ± 20 and 73 ± 17 $x10^9$ particle/g dw for the $AgNO_3$ and Ag NP treatments, respectively (two-way ANOVA, P >0.05). Compared to both the livers in the $AgNO_3$ and Ag NPs treatments, the livers from the Ag_2S NP treatment had significantly lower particle number concentrations at each time point during the exposure (two-way ANOVA, P <0.001).

Between week 4 and 6, all treatments were placed on the control diet with no added Ag. During this depuration phase on normal food, all the fish that had been fed the Ag-containing treatments showed a tendency for the particle number concentration to fall up to 8-fold at week 6 compared to week 4 (Table 5-1), but there was no significant difference between the weeks. For example, in the kidney from fish exposed to Ag_2S NP, the particle

Table 5-2. The particle number concentration ($x10^9$ per g dw) within the hind intestine, liver and kidney of rainbow trout exposed to control (no added Ag) or 100 mg/kg Ag as $AgNO_3$, Ag NPs or Ag_2S NPs via the diet for 4 weeks and with 2 weeks recovery.

Treatment	Organ	Week 2	Week 4	Week 6
Control	Hind	0.022 ± 0.006 ^{Ab}	0.070 ± 0.031 ^{Aa}	0.009 ± 0.004 ^{Ab}
$AgNO_3$	intestine	135.5 ± 45.2 ^{Bab}	318.2 ± 116.7 ^{Ba}	72.1 ± 31.5 ^{Bb}
Ag NPs		172.1 ± 58.7 ^{Ba}	119.5 ± 33.0 ^{Ba}	81.8 ± 16.8 ^{Ba}
Ag_2S NPs		0.6 ± 0.2 ^{Ca}	0.6 ± 0.2 ^{Ca}	0.4 ± 0.2 ^{Ca}
Control	Liver	0.007 ± 0.001 ^{Aa}	0.006 ± 0.003 ^{Aa}	0.002 ± 0.001 ^{Aa}
$AgNO_3$		68.3 ± 13.5 ^{Ba}	83.4 ± 20.2 ^{Ba}	54.5 ± 11.3 ^{Ba}
Ag NPs		76.9 ± 21.0 ^{Ba}	72.6 ± 17.0 ^{Ba}	51.7 ± 8.9 ^{Ba}
Ag_2S NPs		6.6 ± 1.4 ^{Ca}	5.4 ± 1.6 ^{Ca}	6.9 ± 2.2 ^{Ca}
Control	Kidney	<LOD	<LOD	<LOD
$AgNO_3$		27.3 ± 8.6 ^{Aa}	67.1 ± 20.4 ^{Aa}	47.2 ± 15.7 ^{Aa}
Ag NPs		26.6 ± 5.2 ^{Aa}	41.6 ± 14.2 ^{Aa}	85.8 ± 19.3 ^{Aa}
Ag_2S NPs		0.1 ± 0.1 ^{Ba}	0.5 ± 0.1 ^{Bb}	0.1 ± 0.01 ^{Ba}

Data are mean ± S.E.M. (n = 5/6 fish). Upper case letters denote significant difference between treatments (two-way ANOVA, columns). Lower case letters denotes significant difference between time points (two-way ANOVA, rows). The number of decimal places in the controls are shown for clarity between treatments. The LOD was 0.0007 $x10^9$/g dw.

number concentration was 0.50 ± 0.10 and 0.1 ± 0.01 x10^9 particles/g dw at week 4 and 6, respectively. However, this downward trend was not significantly lower at week 6 compared to week 4 (two-way ANOVA, P >0.05), indicating that particles were not cleared from the organs post-exposure.

5.3.4 Particle size distribution and mean particle size

The particle size distributions in the samples from the hind intestine can be seen in Figure 5-3. The size distribution profile of the hind intestine from the control fish consisted of a reduced number of particles compared to the Ag treatments as expected, with the particle sizes ranging from 25 to 60 nm in the controls. Within the hind intestine from the $AgNO_3$ treatment, the size distribution showed a skewed distribution with a long tail of larger particles, and the particles varied from 50 to 200 nm. The Ag NP size distribution is very similar to the $AgNO_3$ treatment. However, the Ag_2S NP treatment has a narrower size distribution ranging from 40 to 80 nm.

The particle size distributions in the livers showed a similar trend to the hind intestine of fish at the end of the 4 weeks exposure (Fig. 5-4). There were trace amounts of particles in the liver of fish from the control treatment, with a particle size of around 55 nm. Livers from the $AgNO_3$ treatment showed a long tail of larger particle sizes, and the size ranged from 60 to 200 nm. A similar profile was also displayed in the Ag NP treatment. Within the Ag_2S NP treatment, there were fewer particles in larger bin sizes, and similar to the hind intestine from the Ag_2S NP treatment at week 4.

The mean particle size is the central value of the particle size distributions. The mean particle size in the hind intestine, liver and kidney is shown in Table 5-3. No particles were observed in the kidney of control fish. The mean size of the control particles in the hind intestine of control fish were around 27 ± 5 nm and the liver was 47 ± 2 nm at week 4 of the exposure. There was no change in the mean size of particles from the hind intestine or liver over the 6 week experiment (Table 5-3). Within the $AgNO_3$ treatment, there were no statistically significant time-related changes in mean particle size in any organ (P >0.05).

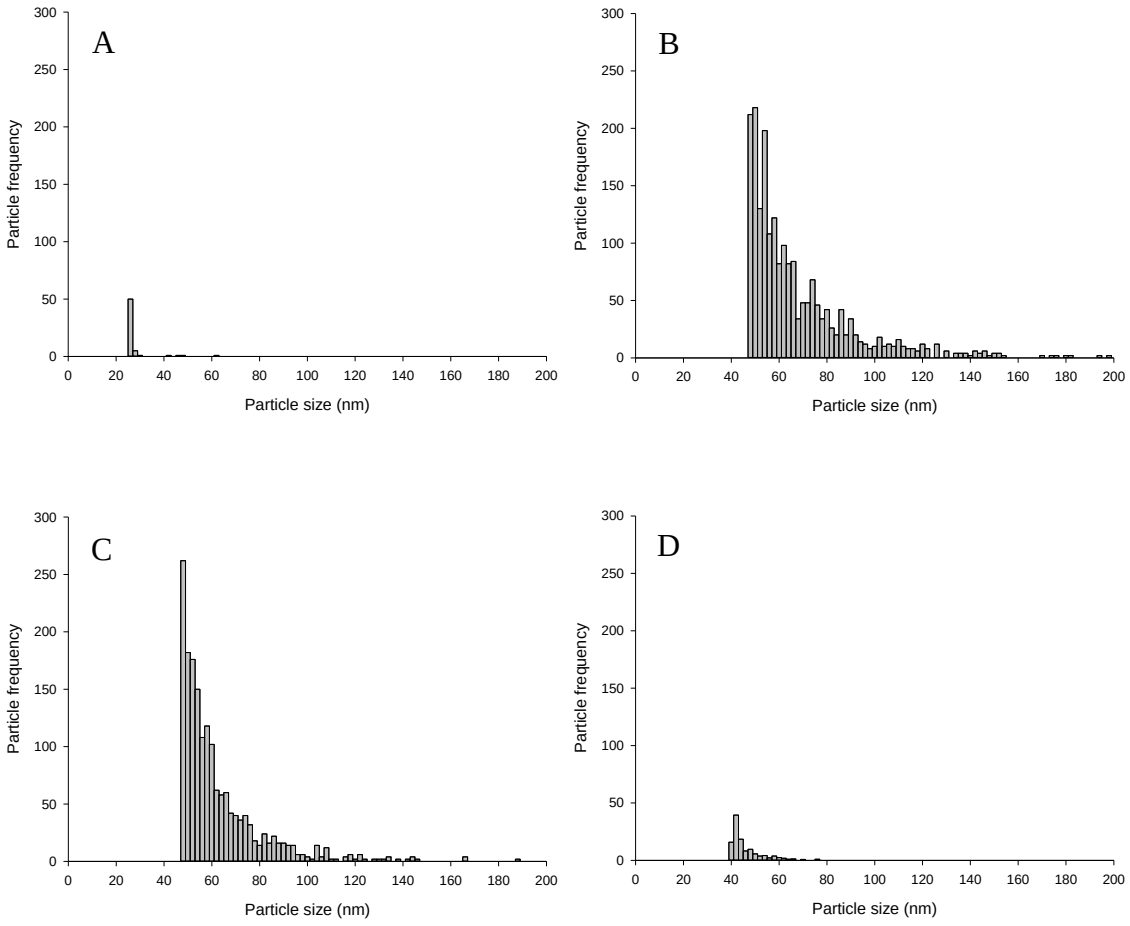

Figure 5-3. Example particle size distributions in the hind intestine of rainbow trout after 4 weeks of dietary exposure to a control (normal diet; A), or 100 mg/kg Ag as $AgNO_3$ (B), Ag NP (C) or Ag_2S NP(D).

However, the livers from the $AgNO_3$ treatment at week 4 had a mean particle size (two-way ANOVA, P <0.001) that was significantly higher compared to the control (P = 0.049). The same pattern was observed in the livers from the Ag NP treatment, with a significant increase in mean particle size compared to the control (P = 0.022). Some transient changes were observed within the Ag NPs treatment. For example, there was a significant increase in mean size at week 4 compared to week 2 (two-way ANOVA, P = 0.015). However, this returned to normal at week 6. Within the Ag_2S NP treatment, there was no time-dependent change in the mean particle size, and was not significantly different from the controls in any organ at any time point. At week 4, the liver mean particle size was significantly reduced compared to both the $AgNO_3$ (P = 0.040) and Ag NP (P = 0.013) treatments.

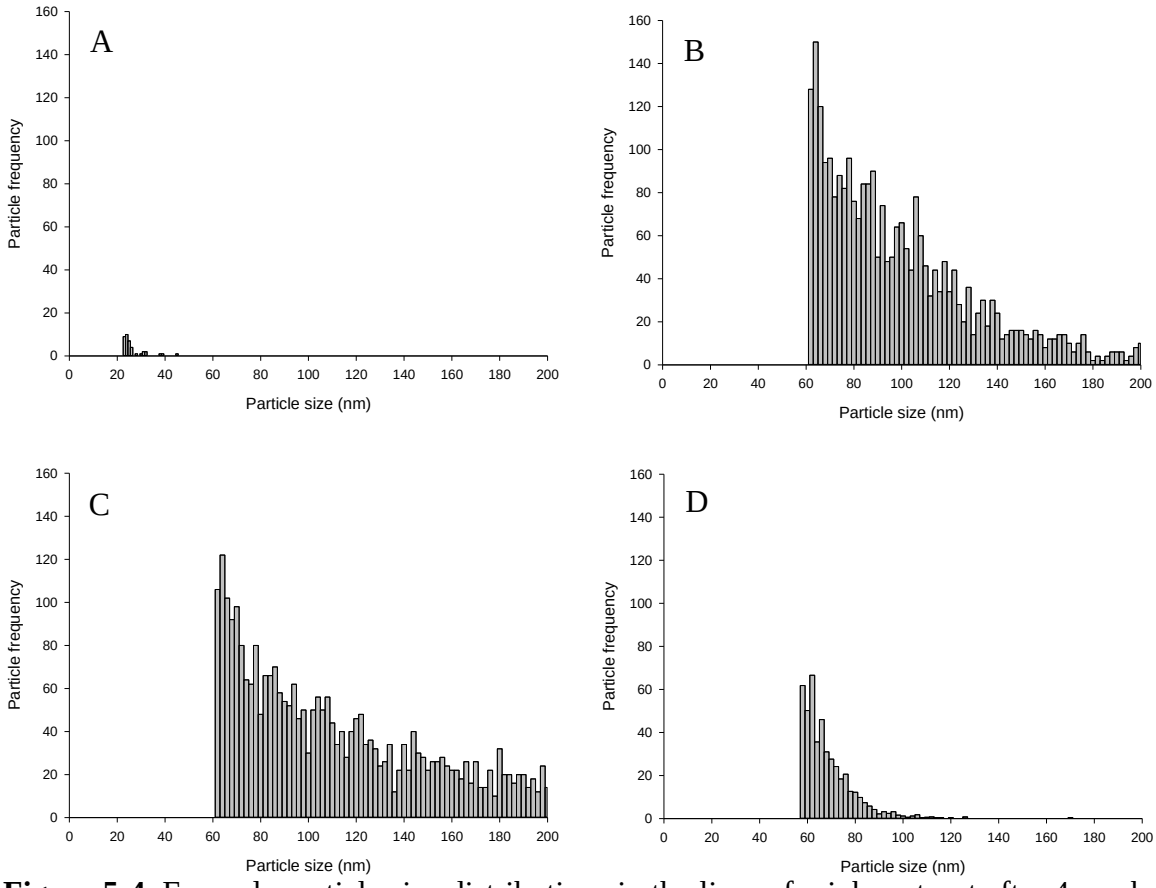

Figure 5-4. Example particle size distributions in the liver of rainbow trout after 4 weeks of dietary exposure to a control (normal diet; A), or 100 mg/kg Ag as $AgNO_3$ (B), Ag NP (C) or Ag_2S NP (D).

Table 5-3. The mean particle size (nm) within the hind intestine, liver and kidney of rainbow trout exposed to a control (no added Ag) or 100 mg/kg Ag as $AgNO_3$, Ag NPs or Ag_2S NPs diet for 4 weeks and with 2 weeks recovery.

Organ	Treatment	Week 2	Week 4	Week 6
Hind intestine	Control	32.4 ± 1.7 ^{Aa}	26.8 ± 5.3 ^{Aa}	33.4 ± 3.9 ^{Aa}
	$AgNO_3$	41.5 ± 5.8 ^{Aa}	41.3 ± 6.3 ^{Aa}	46.7 ± 7.4 ^{Aa}
	Ag NPs	42.0 ± 3.7 ^{Aa}	42.7 ± 2.6 ^{Aa}	46.8 ± 4.9 ^{Aa}
	Ag_2S NPs	38.8 ± 3.3 ^{Aa}	31.3 ± 4.0 ^{Aa}	33.7 ± 2.6 ^{Aa}
Liver	Control	45.8 ± 3.2 ^{Aa}	46.9 ± 2.0 ^{Aa}	59.1 ± 7.7 ^{Aa}
	$AgNO_3$	62.9 ± 7.8 ^{Aa}	76.8 ± 6.7 ^{Ba}	73.7 ± 10.2 ^{Aa}
	Ag NPs	52.7 ± 6.8 ^{Aa}	82.2 ± 10.9 ^{Bb}	60.3 ± 5.1 ^{Aa}
	Ag_2S NPs	41.9 ± 1.6 ^{Aa}	53.2 ± 0.9 ^{Aa}	57.3 ± 4.4 ^{Aa}
Kidney	Control	N/A	N/A	N/A
	$AgNO_3$	36.2 ± 2.6 ^{Aa}	43.1 ± 9.4 ^{Aa}	44.9 ± 5.7 ^{Aa}
	Ag NPs	31.0 ± 2.1 ^{Aa}	46.8 ± 7.2 ^{Aa}	39.2 ± 2.3 ^{Aa}
	Ag_2S NPs	33.1 ± 2.4 ^{Aa}	39.7 ± 4.0 ^{Aa}	35.1 ± 3.2 ^{Aa}

Data are mean ± S.E.M. (n = 5/6 fish). Upper case letters denote significant difference between treatments within columns. Lower case letters denotes significant difference between time points within treatments.

5.3.5 Confirmation of particles in liver extract sample by TEM of liver

The use of spICP-MS confirmed the presence of particle-like events in the fish organs (Fig. 5-3 and 5-4). The TMAH + $CaCl_2$ extraction process was intended to allow the release of intact Ag particles from the liver tissue matrix into a liquid sample. The liquid samples were also observed by TEM to confirm the presence of particles. Within the control treatment, no particles-like events were observed by TEM. Within the $AgNO_3$ treatment (Fig 5-5), only a few particle-like images were found (n = 4 particles). The mean particle size was 36.9 ± 31.2 nm (± S.D.). A similar number of particle-like events were found within the Ag NP treatment by TEM (n = 4 particles), with a mean size of 110.8 ± 54.7 nm (± S.D.). There was no significant difference between the size of particles found in the livers from $AgNO_3$ and Ag NP treatments (one-way ANOVA, P >0.05). Unfortunately, no particles were found within the Ag_2S NP treatment by TEM. The particles in the $AgNO_3$ and Ag NP treatments were morphologically similar to the Ag NPs added to the diet

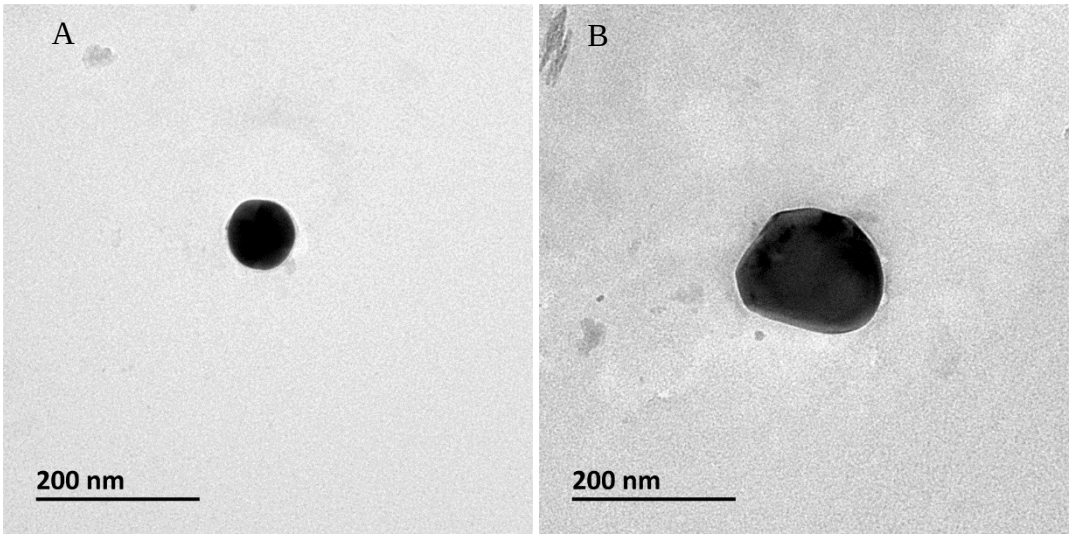

Figure 5-5. Transmission electron micrograph of the particles isolated from rainbow trout liver following the TMAH + $CaCl_2$ extraction in the $AgNO_3$ (A) and Ag NP (B) treatment. No particles were observed in the control or Ag_2S NP treatment (data not shown).

(Chapter 2, Fig. 5-5). The particle sizes found were similar to those reported using spICP-MS (Fig. 5-3).

Samples of intact livers from week 4 were also viewed using TEM, either stained or unstained. The presence of particles in the liver of any treatment could not be found, using a systematic approach to visualise particles (n = 3 livers/treatment, n = 24 images). The stained liver samples showed some precipitates from the use of metal salts. These were absent in unstained samples.

5.3.6 Percent of particulate Ag in the liver verses the dissolved fraction

The time scan of spICP-MS can be used to determine the presence of both dissolved and particulate Ag. There was no consistent dissolved form of Ag in the hind intestine or the kidney (Fig. 5-6). The livers of the control fish showed a relatively small amount of

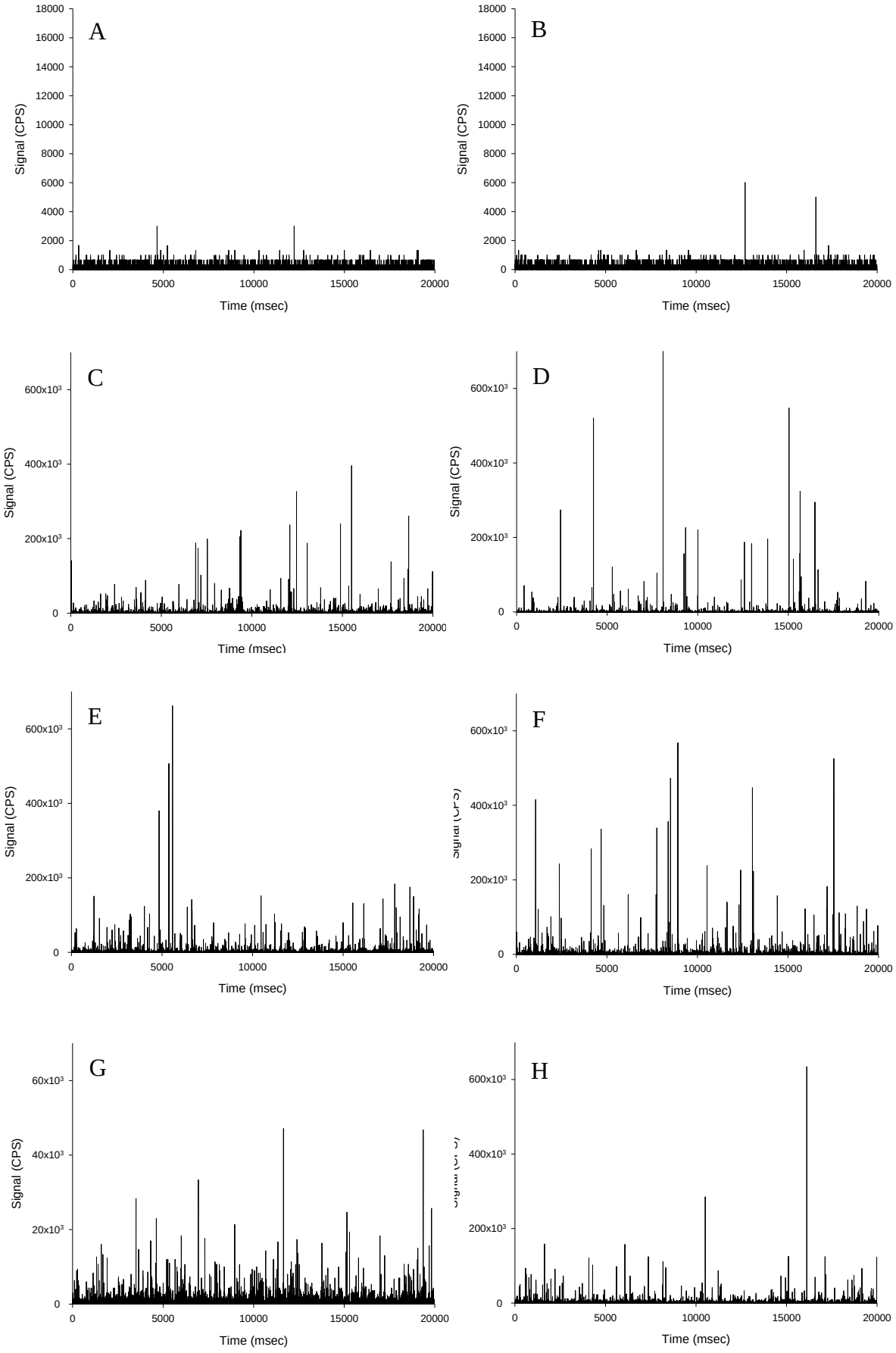
A
B
C
D
E
F
G
H
Signal (CPS)
Time (msec)
18000
16000
14000
12000
10000
8000
6000
4000
2000
0
600x10³
400x10³
200x10³
60x10³
40x10³
20x10³
5000
10000
15000
20000

Figure 5-6. Example traces of the hind intestine (left panels) or kidney (right panels) at 4 weeks from the control (A and B), or 100 mg/kg Ag as $AgNO_3$ (C and D), Ag NP (E and F) or Ag_2S NP (G and H) treatments. Note the Ag_2S NP hind intensity is smaller due to different day analysis and a different sensitivity of the instrument.

particulate Ag in them (1-4% of the total Ag as particles). Compared to the livers from controls fish at week 2 (two-way ANOVA), livers from the $AgNO_3$ (P <0.001), Ag NPs (P <0.001) and Ag_2S NP treatments (P <0.001) had significantly more Ag as the particulate form. For example, the $AgNO_3$, Ag NP and Ag_2S NP treatments had 42, 54 and 27% of the total Ag as particulate Ag at week 2. There was no difference between the $AgNO_3$ and Ag NP treatment at any time point (P >0.05). At week 4, an Ag treatment effect was observed; the $AgNO_3$ (P = 0.007) and Ag NP treatments (P = 0.007) had a significantly higher percentage of the total Ag as particulates compared to the Ag_2S NP treatment (Fig. 5-6).

5.3.7 Particle mass concentration versus total Ag concentration

One question that arises for the practical application of spICP-MS in ecotoxicology is whether or not the total Ag measured by routine ICP-MS might be predictive of the particle mass concentration, especially where it is expected that the particle will not appreciably dissolve by dissolution inside a tissue. Figure 5-8 shows the correlations between the total Ag in the tissues (data from Chapter 3) compared to the particle mass concentration measured here for the $AgNO_3$, Ag NP and Ag_2S NP treatments. The controls were omitted from this because of the scaling of the graphs. In each organ, there was a positive correlation between the amount of total Ag and the number of particles present. However, the correlations were, at best, with an r^2 of 0.705 in the liver, and so are not robust enough from an analytical chemistry view point.

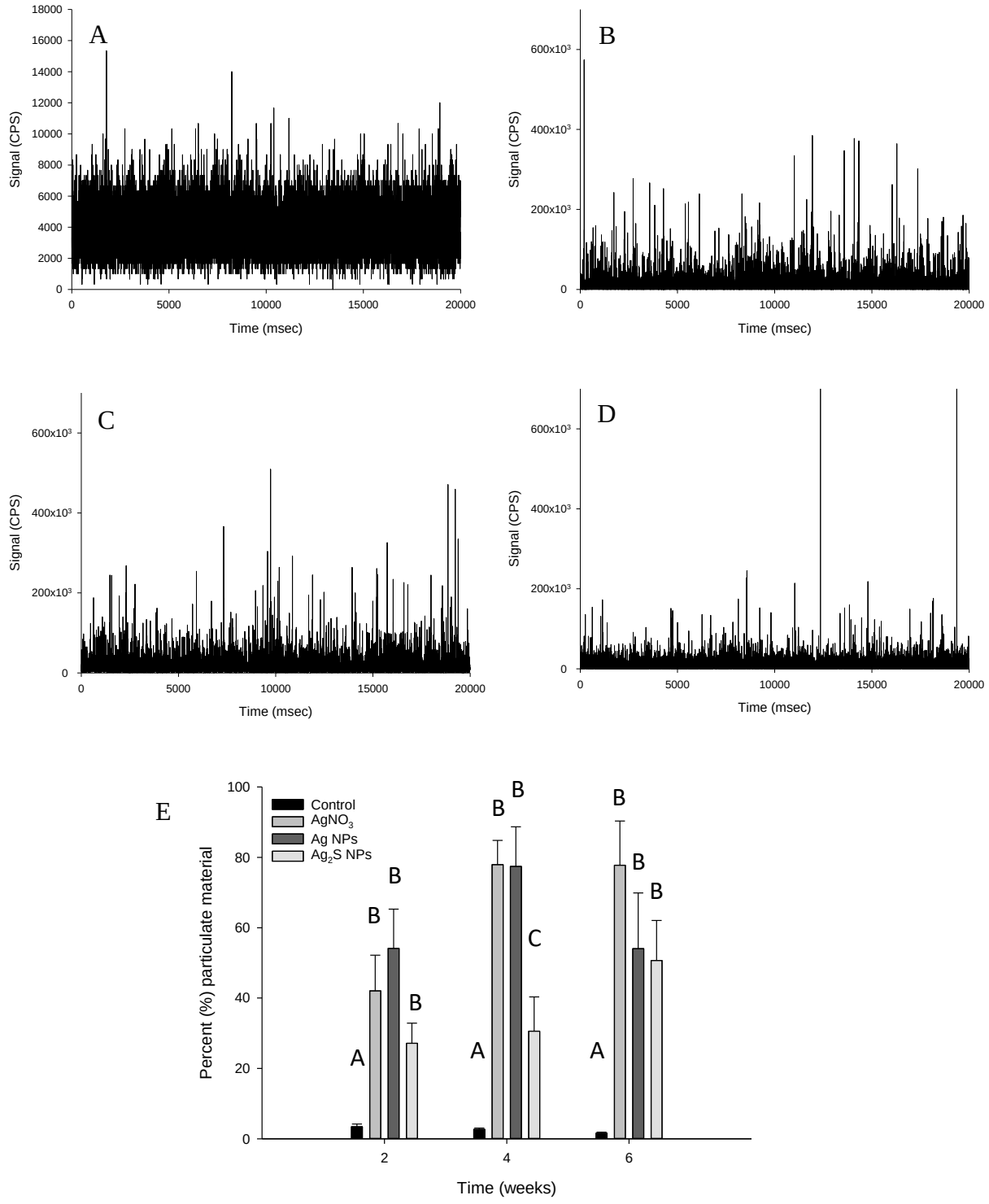

Figure 5-7. Example time scans of the liver at week 4 from the control (A), or 100 mg/kg Ag as $AgNO_3$ (B), Ag NP (C) or Ag_2S NP (D). From the raw time scans, the percentage of particulate material in the liver is calculated (E). Different upper case letters denote significant difference between treatments within the same time point. There was no time dependent changes. There was no appreciable dissolved signal within the hind intestine or kidney of any treatment.

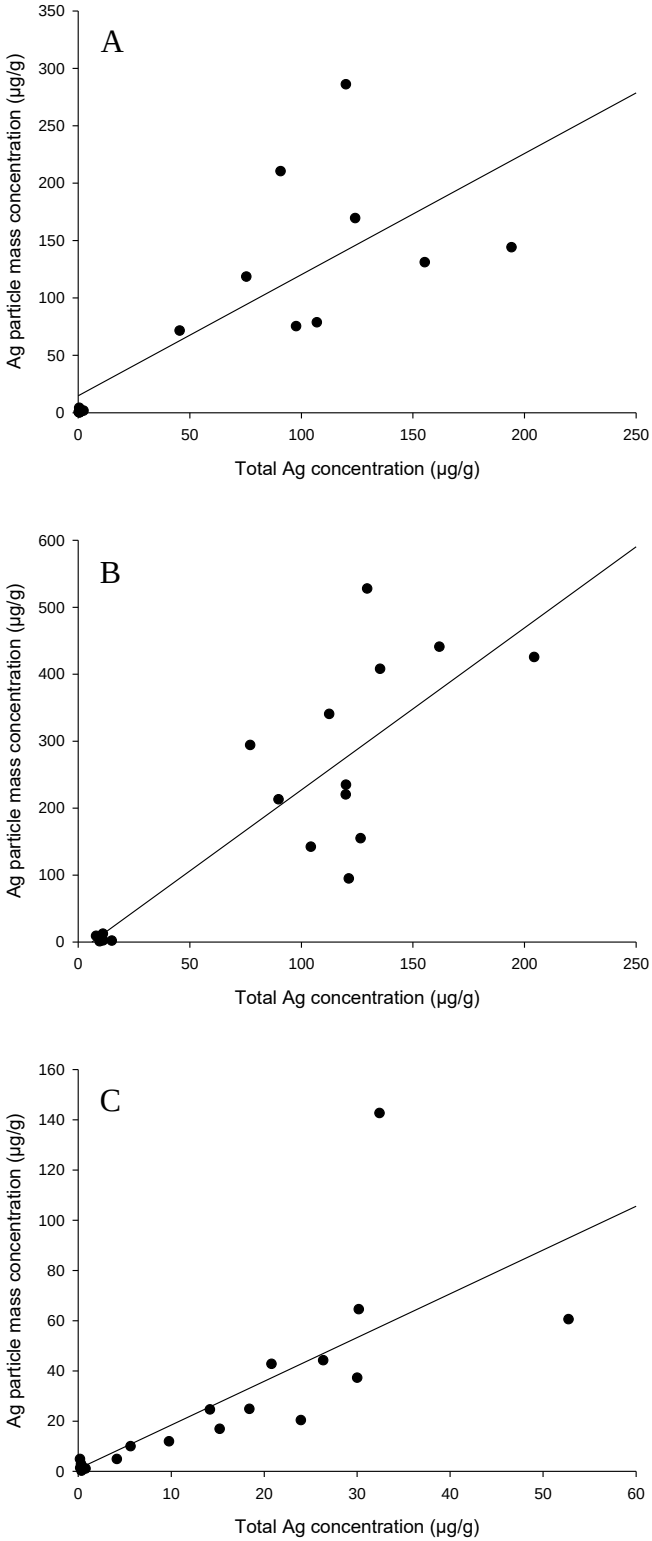

Figure 5-8. Correlation of total Ag concentration against particle mass concentration in the hind intestine (A), liver (B) and kidney (C) of fish fed 100 mg/kg Ag as $AgNO_3$, Ag NP and Ag_2S NP for 4 weeks. Black lines show the line of best fit. The r^2 values for the hind intestine, liver and kidney were 0.594, 0.705 and 0.545, respectively.

5.4 Discussion

This study has demonstrated that following exposure to $AgNO_3$, Ag NPs and Ag_2S NPs, the internal organs will contain particulate material. The target organs of particle accumulation in the $AgNO_3$ treatment was the hind intestine and liver. This target organ profile was the same in the Ag NP and Ag_2S NP, despite the Ag_2S NP treatment showing a lower bioavailability compared to the other Ag treatments. During the 4 week dietary exposure, particles were retained in the organs. Following the 2 week recovery phase on the control diet, there was no depuration of particles from the organs.

5.4.1 Detecting particles in tissues by spICP-MS

The analytical approach used here involved careful checks on procedural blanks, spike recovery tests with liver samples (Chapter 4), and to consider the matrix of the samples during instrument calibrations. The Ag NPs size distribution in deionised ultrapure water that was calculated using spICP-MS showed a normal distribution as expected (e.g. Chapter 4). The Ag_2S NPs also showed good dispersions in deionised ultrapure water. Both of these materials were used to contaminate the food. Before setting up the ICP-MS for analysis, the spray chamber was washed in 10% nitric acid to remove contamination which was successful as demonstrated during analysis where there was no contamination from the vessels or instrument 'wash out'. Digestion of the organs demonstrated low background of dissolved Ag in the hind intestine and kidney, with traces found in the liver.

5.4.2 Particulate Ag in the organs

Particles were found in the hind intestine and liver of control fish. These were not attributed to contamination from the reagents because the procedural blanks did not contain this signal. The particles are therefore likely a background of naturally occurring Ag that has been incorporated into the tissue, either as part of a metal-containing granule in the case of trout liver (e.g., for Cu, Lanno et al. 1987), or simply as sparingly soluble AgCl (Nocchetti et al. 2013). Interestingly, particles were not found in the kidney of control fish, and this is consistent with no detectable total Ag in the organ (Chapter 3). This suggests that any incidental AgCl particulate requires the presence of some trace Ag in the tissue to form. The absence of appreciable Ag in the kidney is also consistent with the protective role of the liver in preventing Ag absorbed *via* the gut from distributing to the rest of the body. The presence of particles in control samples have been reported in tomato plants (*Solanum lycoperiscum*; Au NPs, Dan et al. 2015; CeO, Dan et al. 2016).

Dietary exposure to the $AgNO_3$ treatment resulted in a significantly higher particle mass concentration µg/g and particle number concentration/g dw in all the organs measured compared to the controls (Table 5-1 and 5-2). The particle mass concentration and particle number concentrations in the organs at weeks 2 and 4 of the exposure were similar, suggesting the organs had reached a steady state during the exposure, and apart from the kidney there was no statistically significant clearance of particle number concentration from the organs during the two week depuration phase at the end of the exposure (Table 5-1 and 5-2). The presence of particles in the hind intestine is consistent with route of exposure for $AgNO_3$. It is probable that the particles were initially formed in the gut lumen from $AgNO_3$, where the millimolar concentrations of chloride could drive AgCl particle formation (e.g. Wu et al. 2013). This would imply that Ag from $AgNO_3$ was taken up in

the particulate form, although formation of AgCl particles in the tissues cannot be excluded. Any dissolved and/or particulate Ag taken up at the gut would pass into the hepatic portal vein on route to the liver. The particle number concentrations in the liver from the $AgNO_3$ treatment were generally lower than the hind intestine, indicating the gut barrier offered some protection from the exposure. Nonetheless, the particle number concentration in the liver was readily detected from the $AgNO_3$ treatment, and consistent with the liver as a central compartment in metabolism. However, the liver could not sequester all of the Ag particles internalised as some were found in the kidney that were similar in size to those in the hind intestine (Table 5-3).

There appears to be no reports of dietary exposure of Ag NPs in fish where the form of material (dissolved versus particulate) is determined. The present data shows the particulate profile for the organs in terms of particle mass concentration (Table 5-1) and particle number concentration in each organ (Table 5-2). The profile is the same as for the $AgNO_3$ treatment, and for each target organ also consistent with total Ag measurements from the animals (Chapter 3). Kleiven et al. (2018) made similar observations from Ag accumulation in Atlantic salmon exposed to ~60 mg/kg Ag as either $^{110}AgNO_3$ or ^{110}Ag NPs (the latter either citrate coated or uncoated) using a slurry for administration via oral gavage. After 2 days, the intestine radioactivity was similar for both the metal salt and the ENMs (Kleiven et al. 2018) yet the form of Ag was not determined. Baccaro et al. (2018) used exactly the same ENMs as in the present study and exposed earthworms to 15 mg/kg $AgNO_3$ or Ag NPs for 28 days, with both treatments showing very similar accumulation patterns of 8 and 9 mg/kg particle mass concentration in the $AgNO_3$ and Ag NP treatment, respectively.

The Ag_2S NP treatment had a significantly higher particle mass concentration and particle number concentration in each organ compared to the control (Table 5-1 and 5-2),

indicating there was some uptake of this material. However, each organ also contained significantly fewer particles than all the other Ag treatments (Table 5-1); suggesting the particles in the Ag_2S form were the least bioavailable. For example, the particle number concentration in the livers of fish from the Ag_2S NP treatment was an order of magnitude less than that in the equivalent $AgNO_3$ and Ag NP treatments (Table 5-1). Similar observations were made when earthworms were exposed to the same materials where particles from the Ag_2S NP treatment showed the least accumulation in the tissue (Baccaro et al. 2018). Despite the lower accumulation of Ag_2S NPs here, the target organs in trout were the same as the other silver treatments, and with no evidence of particle clearance from the organs in the post-exposure phase (Table 5-1).

Due to the similar average size of particles between tissues (Table 5-3), it suggests that once they are released into the blood from the hind intestine, they are distributed around the body. Internalisation of particles into the kidney and liver could result from endocytotic mechanism (see Treuel et al. 2013), with the differential partitioning between organs relating to the activity of transport systems at the organ cell surfaces to incorporate particulate material (i.e., ADME). While accumulation is typically reported, the elimination of silver is less studied. In one study (Wood et al. 2002) the elimination of Ag^+ and AgCl from rainbow trout following acute exposure was assessed. The higher elimination of AgCl over Ag^+ was attributed to simple diffusion out of the gills or sloughing of the mucous (Wood et al. 2002). Here, with the confirmed presence of particles, elimination was reduced. While a variety of biological processes could be occurring (e.g. tissue shunting), the lack of elimination could simply be due to the fish tolerating the presence of non-toxic silver particles.

The $AgNO_3$ and Ag NP treatments have a higher incidence of larger particles compared to the control and Ag_2S NP treatments (Fig. 5-3 and 5-4). Any apparent

difference in the distributions are not likely due to the matrix causing artefacts in agglomeration within the tissue, because the matrix was the same. One might also expect that Ag dissolution from the particles would be a function of the total surface area of all the particles in the tissue (i.e., a low concentration of monodispersed particles would dissolve more quickly). However, this is not the case inside the organs. Despite the presence of particles, neither hind intestine nor the kidney had an appreciable dissolved silver signal (Fig. 5-5). In contrast, the liver appeared to be the only organ to have an appreciable dissolved Ag signal at the end of the exposure (Fig. 5-7). This dissolved fraction was about 20% of the signal for the $AgNO_3$ and Ag NP treatments, indicating some potential dissolution of Ag particles. Notably, there was a much bigger dissolved fraction from the Ag_2S treatment (Fig. 5-7). This finding was not expected because factors such as low pH have minimal influence on Ag_2S NP dissolution (e.g. Baccaro et al. 2018, Chapter 2, and Chapter 3). One possible explanation for this difference is the internal handling of different concentrations of Ag in the body. This apparent dissolution (Fig. 5-5) with a tendency for the Ag_2S NPs to have a slightly smaller primary particle diameter in the liver, suggests the possibility of an internal organ process where Ag is being cycled between dissolved and particulate phases. How and why this might occur requires further investigation.

The particle mass concentration does not reflect the same statistical differences that was shown over time with total Ag measurements (Chapter 3, Table 3-1). This may be due to differences in how the sample is prepared and the Ag is measured. For total Ag, the organ sample containing Ag is dissolved in strong acid, and then diluted before measurement. The ICP-MS will measure the continuous arrival of ions, which will relate to the total ions present. However, in spICP-MS, discrete events are that are counted.

5.4.3 Possible explanations for the formation of particulate Ag

There are several possibilities for the formation of Ag particles present in the tissue: (1) complexation of Ag with other elements/compounds such as chloride or sulphur in the gut lumen, (2) precipitation of Ag to form hydroxides under alkali conditions in the gut lumen, (3) formation in the liver only, or (4) another nanoscale process yet to be identified.

It is well known that dissolved Ag is highly reactive, with particular affinity for chloride or sulphur resides. The presence of mmol/L concentrations in the chyme of the lumen, in the mucosa and intracellular spaces suggests that complexation is likely and will occur rapidly. Equally, the high pH of the gut lumen could cause Ag precipitation as Ag_2O (Liu et al. 2009, Yang et al. 2016) or AgOH. Early work into the rodent GIT has demonstrated that in the absence of sufficient quantities of ligands certain metals (e.g. Al, Cu, Fe, Mn and Zn) can precipitate under alkali conditions found in the intestine (Powell et al. 1999a,b). Dissolved Ag (as $AgNO_3$) has shown to produce 20-40 nm particles in simulated intestinal juices (pH 8.2) that were not shown in the simulated saliva (pH 6.8) or stomach (pH 1.3; Walczak et al. 2013). For the Ag NPs, dissolution in the stomach in the presence of secreted HCl and subsequent precipitation of dissolved Ag in the gut lumen as Ag_2O or AgCl seems logical. It might also explain why there are close similarities between the accumulation pattern of $AgNO_3$ and Ag NP treatments. The presence of some incidental background silver in the animal feed might also explain the low fraction of particulate material found in the liver in the controls (Fig. 5-5). The Ag_2S NPs are sparingly soluble (dialysis experiments; Chapter 2 and *in chemico* digestibility; Chapter 3) and from the size distribution (Fig. 5-1), it suggests the possibility of this material being accumulated directly into the tissue, rather than transformed. Although determination of particulate accumulation is rare in vertebrates, one study has demonstrated the possibility of TiO_2 to transverse the gut epithelium. For instance, 2 h following ingestion (100 mg), TiO_2 particles could be detected within the blood of participants using dark field microscopy (Pele et al. 2015).

Biogenically made particles have been documented in the liver from dissolved copper exposure in rainbow trout. For example, fish fed 730 mg/kg Cu for 24 weeks had particles present in the liver which were observed in histological sections, but were not observed in the hind intestine or kidney (Lanno et al. 1987). The authors attributed this to synthesis within the liver, although the size limit for detecting of particles by histology will have easily 'missed' any nanoscale material. In the present study, the Ag particles would need to be synthesised in the liver, released into the circulatory system and deposited into the hind intestine and kidney. Furthermore, highly organised starch granules show alternating rings of amorphous and semi-crystalline ring structures (Pérez and Bertoff 2010). Such structures were not observed here, indicating a less regulated synthesis.

Some particles were observed using TEM from the $AgNO_3$ and Ag NP treatments, but not seen from the control or Ag_2S NPs treatment. The 10 to 100 fold lower concentration of particles in the tissues of the control and Ag_2S NPs may explain why these treatments did not have any observable particles. Or rather, 100 fold more TEM grids would be need to be observed to find them (not practical). Interestingly, the TEM images of the all treatment livers could not confirm the presence of particles. This could be an artefact of the sectioning process; the tissue can be dragged, rather than cut, using the microtome. Indeed, this problem may be associated more with tissues opposed to cell culture studies (e.g. Gitrowski et al. 2014), given the differences in sample preparation. While there are some *in vivo* exposures to Ag NPs where the particles have been localised in the gut tissue with TEM (e.g. *Nereis diversicolor*; García-Alonso et al. 2011), they require electron dense areas for elemental analysis by EDS to confirm chemical composition of the particles. Carp were nominally exposed to 100 mg/L CuO NPs for 30 days, with TEM analysis showing some particle-like Cu deposits in the gill, intestine and liver (Zhao et al. 2011). EDS confirmed there was 2-24% of copper present in these particles (Zhao et al. 2011), which

does not match the CuO NPs used during the exposure of 79.9%. Equally, they stained the images with uranyl acetate, which can result in salt artefacts, which appear similar to colloidal material. Presently, the particles found in the TMAH-based extracts did not have a high enough number for the EDS to confirm the elemental composition. For these reasons, the use of spICP-MS may be more beneficial for tissue analysis compared to TEM.

5.5 Conclusions

This study demonstrated the presence of particles in the organs of fish exposed to $AgNO_3$, Ag NPs or Ag_2S NPs, with the Ag_2S NPs being less bioavailable. These are either produced in the gut lumen or within the tissues, but the current data cannot determine which. The potential for the stomach to dissolve Ag NPs, which can subsequently precipitate in the gut lumen suggests the role of the stomach may not protect fish, or human, of the gut exposed to Ag particles. The presence of particles suggest a revision of modelling parameters is needed for fish from dietary exposure of Ag. For risk assessment, the use of pristine materials (Ag NPs) may overestimate the particle exposure from environmentally relevant forms (Ag_2S NPs). Regardless, the current dissolved metal regulations will cover the risk of pristine and environmentally relevant Ag ENMs.

Chapter 6 - Dietary bioaccumulation potential of silver nanoparticles, silver sulphide nanoparticles and silver nitrate in Wistar rats using an *ex vivo* gut sac technique

Abstract

Chronic dietary bioaccumulation tests with rodents are required for new substances, including engineered nanomaterials (ENMs), in order to inform on the potential hazards to human health. However, screening tools are needed to manage the diversity of ENMs and alternative methods are desirable with respect to animal welfare. Here, an *ex vivo* gut sac method is used to estimate the dietary bioaccumulation potential of silver nanomaterials. The entire gastrointestinal tract (except the caecum) was removed and filled with a gut saline containing 1 mg/L Ag as either $AgNO_3$, Ag NPs or Ag_2S NPs, and compared to controls with no added Ag. The gut sacs were incubated for 4 h, rinsed to remove excess media, and the total Ag determined in the mucosa and muscularis. Particle number concentrations in tissue was determined by single particle ICP-MS. The duodenum demonstrated serosal accumulation in both the $AgNO_3$ (~10 ng/mL) and Ag NP (~3 ng/mL) treatments. As such, further tests were conducted assessing the form of the Ag material in the tissue and serosal saline using spICP-MS. Nanoscale Ag particles were found in mucosa of all Ag treatments, with particle number concentrations of 40, 130 and 70 $x10^6$ particles/g ww tissue in the $AgNO_3$, Ag NP and Ag_2S NP treatments, respectively. The duodenum showed some of the highest Ag accumulation with 41 ± 4, 61 ± 4 and 57 ± 4% of the total Ag in the mucosa compared to the muscularis for the $AgNO_3$, Ag NP and Ag_2S NP treatments, respectively. In terms of particle number concentration 35 ± 20, 51 ± 6 and 49 ± 4% of the particles were in the mucosa of the $AgNO_3$, Ag NP and Ag_2S NP treatments, respectively. In conclusion, the *ex vivo* gut sac method demonstrates the uptake of Ag as particles in all Ag treatments, with the duodenum the site of highest accumulation.

6.1 Introduction

Engineered nanomaterials (ENMs) are being incorporated into food and food-based products (reviews, Chaudhry et al. 2008; Tiede et al. 2008; Bouwmeester et al. 2014) and inevitably there is the potential for human exposure of the gastrointestinal tract (GIT); yet the subsequent accumulation of ENMs across the mammalian GIT remains unclear. There are also concerns that ENMs can be incidentally incorporated into the human food chain from agriculture (e.g. nano pesticides) as well as from food processing (e.g. anti-caking agents; review Martirosyan and Schneider 2014). Indeed, ENMs are also intended for direct consumption in health foods and nutritional supplements (review Katouzian and Jafari 2016), and of course in oral medicines (review Bobo et al. 2016). The measured concentrations of ENMs in food remains uncertain because reliable methods for detecting nanoparticulate material in food are only now being established (e.g. chicken meat, Peters et al. 2014b; confectionary, Peters et al. 2014a). Some attempts have also been made to determine ENMs in drinks (e.g., sports drinks, Reed et al. 2014). Regardless, the inclusion of metal-containing ENMs can be a few µg/kg of food (e.g., TiO_2, Weir et al. 2012) to mg/L concentration in sports drinks (e.g., silver; Reed et al. 2014). Metal-containing ENMs may partially or completely dissolve during acid digestion in the stomach (Vassello et al. 2019) and the concern for hazard assessment is whether the ENM is taken up by the gut in particulate form or as dissolved metal. For the nutritionally required metals such as Cu, the solute transport pathways are well described, and the export of metal from the gut epithelial cell to the blood is the rate limiting step in absorption (Handy et al. 2000; Linder 2002). Non-essential metals, such as Hg may also use some of these pathways (Hoyle and Handy 2005), but the situation for dissolved Ag is less clear. Alternatively, ENMs may be taken up in the particulate form. The apical uptake of intact particles has been demonstrated in

cultures of intestinal epithelial cells and the uptake may also be dependent on the crystal structure of the material (e.g., TiO_2, Gitrowski et al. 2014). For the mammalian gut, *in vivo*, the M cells of the Payers patches are especially associated with the uptake of iron particles (Powell et al. 2010) and one concern is that these specialised structures could be a route for the preferential accumulation of particulates across the gastrointestinal tract. However, so far, data shows that only a small fraction of the ingested dose is taken up as particles *in vivo* (e.g., TiO_2 in rodents, Kreyling et al. 2017). Human volunteers who ingested a single 100 mg dose of TiO_2 in capsules with 250 mL water showed that 6 h post ingestion around 10 µg/L of total titanium was found in the blood of participants. Dark field examination of blood smears from the volunteers showed the presence of particulate material (Pele et al. 2015), suggesting that intact particles were absorbed into the blood.

Although there have been oral gavage studies with rodents showing that ENMs can be taken up (form unknown) via the gut into the internal organs (e.g., Folkmann et al. 2009; Geraets et al. 2014), the precise mechanisms of uptake for Ag NPs is unclear. Silver NPs may show some dissolution in the acid conditions found in the stomach (Chapter 2 and 3), but any Ag could form a sparingly soluble AgCl complex (see discussion in Chapter 2). Thus in any case, particulate Ag will be presented to the mucous epithelium of the intestine. Earlier dietary studies with Ag NPs in rodents show that total Ag accumulation occurs in the internal organs, notably the liver (van der Zande et al. 2012; Elle et al. 2013). Unfortunately, single particle inductively coupled plasma mass spectrometry (spICP-MS) was not available then to confirm if the Ag accumulation was a dissolved or particulate silver. Pristine Ag NPs may also be transformed into sparingly soluble Ag_2S NPs by sulfidation reactions (Lead et al. 2018). In the gut lumen, Ag NPs will inevitably be in close association with the food matrix which is enriched with sulphur residues (see Peters et al. 2014b), and in the reducing environment of the lumen, silver sulphide nanoparticles will

form. Consequently, the sulfurized form of Ag should also be included in the hazard assessment.

In Europe, oral toxicity tests with rodents are a mandatory part of hazard assessment of new substances, including ENMs, and especially when oral exposure to humans is a route of concern (e.g., OECD 407, 408 and 420 tests). However, with a myriad of forms and chemistries of ENMs, there are too many to test each one as a new substance, and so screening methods are needed to identify ENMs that present a bioaccumulation concern (Handy et al. 2018). From the perspective of animal welfare, there is also a need to reduce the use of animals in regulatory toxicity testing the 3 R's reduction, refinement, replacement. There is a test of bioaccumulation in fish (OECD 305 test); the concern is can we reduce the use of mammals by using fish instead (e.g., Johnston et al. 2018), but also use alternative to *in vivo* studies with any vertebrate animal. However, the cross species extrapolation from mammals to fish for bioaccumulation potential following dietary exposure to ENMs should consider species differences in the gut lumen chemistry, the anatomy of the gastrointestinal tract, the molecular biology of the absorptive mechanisms, and the body temperature. Handy et al. (2018) proposed a tiered testing approach to bioaccumulation testing with respect to environmental hazard assessment using fish. This approach included an *ex vivo* tier where rainbow trout gut sac technique was used to estimate the dietary bioaccumulation hazard, which has been successfully applied to Ag NPs (Chapter 2 and Chapter 3). The use of isolated perfused gut segments and/or gut sacs from rodents has been long established for investigating gastrointestinal physiology (Wilson and Wiseman 1954) and the uptake of metals (Cu, Wapnir and Stiel 1987, Cd Hoadley and Johnson 1987), but not so far applied to ENMs.

The present study aimed to determine the bioavailability of Ag to the different anatomical regions of the rodent gastrointestinal tract when presented as either $AgNO_3$, Ag

NPs or Ag_2S NPs. Crucially, in addition to measuring total Ag, attempts were made to determine particulate fraction in the tissue using spICP-MS in order to understand the physical form of each material taken up by the gut. The serosal solution was also explored for evidence of any transepithelial uptake of Ag materials. The experimental approach used the same methodology as previously reported in fish (Chapter 2) to enable a direct cross-species comparison between fish and rodents for exactly the same batches of nanomaterial.

6.2 Methodology

6.2.1 Stock animals

Wistar rats (*Rattus norvegicus*) were bred in house at Plymouth University and kept until 7 weeks old (100-150g). Rats (n = 45), weighing 100-150 g were housed in cages maintained at 20 ± 2^{o}C and humidity 55 ± 10% with free access to drinking water and food. Rats were fed a commercially available diet (RM3A [P], 9.5 mm pellets, Special Diet Services, England), containing crude fat, protein, fibre and ash of 4.2, 22.4, 4.2 and 7.6%, respectively. Prior to the experiments, food was withheld for 24 h to aid in the evacuation of the gastrointestinal tract and faecal material was continuously removed to prevent coprophagic behaviour. Despite these efforts to clear the gastrointestinal tract, the caecum still contained food material and so this part of the tissue was excluded from the experiment to minimise the risk of uneaten food particulates confounding the results.

6.2.2 Preparation and characterization of silver nanomaterials and silver nitrate

The same batch of Ag NPs and Ag_2S NPs were used here as reported in Chapter 2.

6.2.3 Gut sac preparation

The gut sac technique was described in Chapter 2 (page 59) with minor modifications for the physiological differences between fish and rodents. Rats were weighed and then euthanized by exposure to a rising concentration of CO_2 followed by cervical dislocation, an approved Schedule 1 method (in accordance with ethical approval from the U.K. Home Office and in compliance with the European directive 2010/63/EU). The entire GIT was removed and separated into the following anatomical regions: oesophagus, stomach, duodenum, jejunum, ileum, caecum and hind intestine. Due to their large size, the intestinal regions (duodenum, jejunum, ileum and hind intestine) were dissected into smaller three inch sections to facilitate the preparation of the gut sac (Wilson and Wiseman 1954; Dixon and Mizen 1977). This approach also allowed the uniform filling of the anatomical regions of the gut to equal fullness with the test media and thus helped standardise the exposure (see below). A total of 6 rats were used per treatment (see section 2.2.3 for rationale).

The gut regions were washed in a gut physiological saline (in mmol/L: NaCl, 117.5; KCl, 5.7; $NaHCO_3$, 25.0; $NaH_2PO_4.H_2O$, 1.2; $CaCl_2$, 2.5; $MgSO_4.7H_2O$, 1.2; glucose, 5.0; mannitol, 23.0; pH 7.5) and weighed. Each gut sac was closed at one end using surgical suture thread and filled with the relevant saline solution containing either no added Ag (as above), or 1 mg/L Ag as $AgNO_3$, Ag NPs or Ag_2S NPs. This concentration was chosen to match that in Chapter 2 (see section 2.2.3 for rationale). The silver speciation from the $AgNO_3$ in the gut saline above (pristine, no contact with fish tissue) was theoretically calculated using Visual MINTEQ 3.1 by J. P. Gustafsson (https://vminteq.lwr.kth.se/download/). The calculated silver species in the normal gut saline containing chloride was: Ag^+, 0.172%; AgCl (aq), 13.187%, $AgCl_2^-$, 80.663%, and $AgCl_3^{2-}$; 5.976. The sacs were then subsequently closed with suture thread, and weighed to

calculate the volume of respective saline solution added. The gut sacs were then incubated in the gut physiological saline for 4 h at 37^{o}C.

Following the 4 h incubation, the gut sacs were removed and weighed for fluid flux to assess the viability of each preparation (according to Chapter 2). Then, the gut sacs were carefully cut open and rinsed into 5 mL of clean gut physiological saline to collect the luminal contents. Tissues were then rinsed in a second 5 mL of solution containing gut physiological saline with 1 mmol/L EDTA and blotted with 25 cm^2 pieces of tissue paper (4 pieces for the stomach and 2 for the oesophagus and intestinal regions) to remove surface bound material (~5% adsorbed; see surface binding experiment in Chapter 2). This blotting paper was kept in the EDTA rinse and processed as described below. The rinse solutions were frozen at -20^{o}C until processing for metal analysis.

Following the rinse solutions, the mucosa was separated from the muscularis by using a glass microscope slide, both parts of the tissue were weighed and stored at -20^{o}C. The tissues were then freeze dried and reweighed before acid digestion for total Ag and electrolyte analysis (see below).

6.2.4 Total Ag, Na and K analysis

Analysis of the luminal saline and EDTA rinse solutions was performed according to Chapter 2. Briefly, the samples were thawed, acidified with 2 mL of primer plus grade nitric acid, diluted with ultrapure water (containing 20 µg/L internal standards of indium and iridium) to 20 mL and left over night before analysing for total Ag concentration using an ICP-MS (iCAP RQ Thermo Fisher). All samples were analysed using matrix matched standards and procedural blanks to account for trace elements from tubes and reagents.

Tissue samples (mucosa and muscularis) were analysed as reported in Chapter 2. Each tissue was digested in 0.2 mL of analytical grade nitric acid (0.5 mL for the muscularis of the stomach) and incubated at 60^{o}C for 4 h. The tissues were then diluted to a final volume of 2 mL (3 mL for the muscularis of the stomach) with 22.2 µg/L indium and iridium spiked ultrapure water. The limit of detection for total Ag of the ICP-MS was around 0.2 ng/mL of tissue digest, which equates to 10.6 ng/g dry weight (dw) of tissue.

The Na^+ and K^+ concentrations were also measured in the tissue digests. Following Ag analysis, 0.5 mL of the sample was taken and diluted to 2.5 mL using yttrium (internal standard) spiked ultrapure water and analysed using an iCAP 7000 ICP-OES for Na^+ and K^+.

6.2.5 Single particle ICP-MS in tissues and saline

Based on the total Ag results, two additional sets of experiments were conducted on the duodenum region of the GIT only to determine the physical form of Ag. The first set was to determine the form of Ag in the tissues in all Ag treatments (n = 3/treatment; total 12 rats). The experiment was performed exactly as described above and the tissues were stored at -20^{o}C until prepared for analysis by spICP-MS as described in Chapter 4.

Total Ag was detected in the serosal saline around the duodenum (i.e., transepithelial uptake) for the $AgNO_3$ and Ag NP treatments. Consequently, a third set of experiments was conducted to determine if particulate material was present in the serosal compartment. The gut sac experiment was performed exactly as described above, but for the duodenum region only. Following the 4 h incubated, a serosal saline sample was taken, diluted 100-fold using ultrapure water only and analysed immediately without storage or acidification (see below) by spICP-MS. Dissolved Ag standards were used for instrument

calibration and matrix matched to the samples. The analysis for spICP-MS was conducted as described in Chapter 4.

6.2.6 Statistical analysis

All data are presented as mean ± S.E.M., unless otherwise stated. Graphs and statistical analysis conducted in SigmaPlot 13.0. Data (n = 5/6 gut sacs per treatment) were analysed for outliers using Grubbs test. Data were check for normality (Shapiro-Wilk test) and equal variance (Brown Forsythe). Data that were normally distributed, or could be $\log_{10}$ transformed to become normally distributed, were analysed by either a one-way ANOVA (fluid flux, tissue electrolytes, gut partitioning [within the same gut sac], % particulate Ag in the mucosa and spICP-MS data) or two-way ANOVA (saline rinse solutions, tissue and serosal Ag concentrations, % total Ag in the mucosa, accumulation rate, partition through the gut sac [treatment and gut region]). Where data were not parametric, the Kruskal-Wallis test was used. *P* values presented are from post hoc tests.

6.3 Results

6.3.1 Ag exposure of gut sacs

Following the 4 h exposure, the gut sacs were cut open and the contents collected for total Ag analysis. This was followed by an EDTA wash to ensure loosely bound Ag was removed from the surface of the mucosa. The presence of Ag in these washes confirmed that the Ag was in excess throughout the exposure and ensured that any apparent accumulation by the tissue was not limited by the supply of Ag in the lumen. As expected,

most of the Ag was labile and within the luminal rinse, as opposed to the EDTA wash (Table 6-1).

The washes from the control gut sacs contained no detectable Ag (Table 6-1). Within the $AgNO_3$ treatment, the absolute mass of Ag in the luminal wash ranged from 40 to 300 ng, depending on the gut region. The highest absolute mass of Ag was in the jejunum (P = 0.025) and hind intestine (P = 0.003), with both being significant elevated compared to the oesophagus (2-5 fold lower). The pattern of Ag content in the washings from both the Ag NP and Ag_2S NP treatments were similar to the $AgNO_3$ treatment; with the absolute mass of Ag in the luminal washes between 20 and 300 ng for the nanomaterials. Within the luminal wash of the Ag NP treatment, there was significantly more Ag associated with the stomach, jejunum and hind intestine (all values P <0.001) compared to the oesophagus. Similarly, within the Ag_2S NP treatment, the stomach (P = 0.002), jejunum (P = 0.023) and hind intestine (P = 0.001) had more Ag compared to the oesophagus.

There were also some differences in the residual Ag in the EDTA wash (Table 6-1). In the $AgNO_3$ treatment, there was no significant difference between gut regions, but the tendency was to have higher concentrations in the EDTA wash associated with the intestinal regions. In the EDTA wash from the Ag treatment, the most was associated with the stomach (P = 0.003) and jejunum (P = 0.039) compared to the oesophagus. There was no significant difference between the gut regions in the Ag in the EDTA wash of the Ag_2S NP treatment.

The exposure was also confirmed by the measured concentrations of total Ag in the gut tissues (Table 6-2). The control tissues (both mucosa and muscularis) contained no detectable Ag, regardless of gut region (LOD = 10.6 ng/g). Within the Ag treatments there

Table 6-1. Mass of Ag (total) found in the luminal saline (rinse 1) and EDTA wash (rinse 2) to confirm exposure to the control (no added Ag), or 1 mg/L Ag as either AgNO3. Ag NPs or Ag2S NPs of the rodent gut sacs.

Treatment	Sample type	Oesophagus	Stomach	Duodenum	Jejunum	Ileum	Hind intestine
Control	Luminal saline	<10.4	<10.4	<10.4	<10.4	<10.4	<10.4
	EDTA wash	<10.4	<10.4	<10.4	<10.4	<10.4	<10.4
$AgNO_3$	Luminal saline	46.1 ± 12.6^{Aa}	160.5 ± 52.2^{Aab}	132.2 ± 15.4^{Aab}	207.3 ± 36.7^{Ab}	137.1 ± 32.6^{Aab}	283.3 ± 34.4^{Ab}
	EDTA wash	14.4 ± 1.2^{Ba}	60.6 ± 15.5^{Aa}	36.2 ± 3.9^{Ba}	46.2 ± 7.1^{Ba}	40.6 ± 8.2^{Ba}	49.0 ± 5.7^{Ba}
Ag NPs	Luminal saline	39.9 ± 5.0^{Aa}	287.5 ± 95.2^{Ac}	128.7 ± 19.0^{Abc}	186.2 ± 39.0^{Ac}	74.8 ± 15.9^{Aab}	199.9 ± 45.3^{Ac}
	EDTA wash	15.0 ± 3.0^{Ba}	51.9 ± 14.5^{Bb}	27.3 ± 1.3^{Bab}	35.9 ± 4.1^{Bb}	22.9 ± 1.4^{Bab}	33.0 ± 5.5^{Bab}
Ag_2S NPs	Luminal saline	19.0 ± 2.8^{Aa}	162.8 ± 55.0^{Ab}	87.7 ± 19.4^{Ab}	100.6 ± 34.9^{Ab}	60.2 ± 16.5^{Aab}	136.2 ± 38.7^{Ab}
	EDTA wash	15.4 ± 0.8^{Aa}	37.0 ± 6.6^{Ba}	23.3 ± 2.2^{Ba}	26.8 ± 4.3^{Ba}	28.6 ± 5.9^{Aa}	25.7 ± 4.9^{Ba}

Data are mean ± S.E.M. (n = 5/6). Different upper case letters denote significance between rinse 1 and 2 (columns). Different lower case letters denote statistical differences between gut regions (rows; Two-way ANOVA). The limit of detection of the instrument was 0.52 ng/mL which equates to 10.4 ng Ag in the luminal and EDTA washes.

Table 6-2. The concentration of total Ag in the tissues and the serosal saline of gut sacs from rodents after 4 h of exposure to unexposed controls (no added Ag) or 1 mg/L Ag as either $AgNO_3$, Ag NPs or Ag_2S NPs.

Treatment	Sample type	Oesophagus	Stomach	Duodenum	Jejunum	Ileum	Hind intestine
Control	Mucosa (ng/g)	<10.6	<10.6	<10.6	<10.6	<10.6	<10.6
	Muscularis (ng/g)	<10.6	<10.6	<10.6	<10.6	<10.6	<10.6
	% in mucosa	N/A	N/A	N/A	N/A	N/A	N/A
	Serosal concentration	<1.25	<1.25	<1.25	<1.25	<1.25	<1.25
$AgNO_3$	Mucosa (ng/g)	3055.8 ± 968.0^{Aab}	638.6 ± 128.3^{Aa}	4282.4 ± 574.6^{Ab}	7087.2 ± 1650.5^{Ab}	6431.0 ± 1700.5^{Ab}	3639.5 ± 631.9^{Ab}
	Muscularis (ng/g)	1045.3 ± 324.9^{Aab}	112.1 ± 31.0^{Ac}	2513.8 ± 267.2^{Ad}	3577.6 ± 644.9^{Ad}	2584.1 ± 553.1^{Aad}	638.4 ± 77.6^{Ab}
	% in mucosa	48.1 ± 11.5^{ABa}	47.7 ± 4.8^{Aa}	41.0 ± 3.5^{Aa}	47.5 ± 3.0^{Aa}	48.2 ± 8.0^{Aa}	57.7 ± 7.4^{Aa}
	Serosal concentration	<1.25	<1.25	10.4 ± 2.5^{Aa}	7.6 ± 2.7^{a}	8.1 ± 1.4^{a}	2.1 ± 0.6^{b}
Ag NPs	Mucosa (ng/g)	1313.8 ± 486.8^{Aab}	369.4 ± 116.8^{Aa}	1730.5 ± 462.9^{Aab}	3635.7 ± 1246.7^{Ab}	5364.8 ± 1500.6^{Ab}	2189.3 ± 394.5^{ABb}
	Muscularis (ng/g)	713.3 ± 321.6^{Aa}	20.3 ± 5.1^{Bb}	906.6 ± 284.1^{Bc}	685.0 ± 120.0^{Bc}	599.1 ± 152.7^{Bc}	313.6 ± 184.2^{Ba}
	% in mucosa	51.9 ± 8.2^{Aa}	69.3 ± 4.3^{Aa}	60.8 ± 4.0^{Aa}	71.3 ± 3.0^{Ba}	67.8 ± 8.2^{ABa}	70.6 ± 4.7^{ABa}
	Serosal concentration	<1.25	<1.25	2.7 ± 1.0^{B}	<1.25	<1.25	<1.25
Ag_2S NPs	Mucosa (ng/g)	3972.7 ± 1387.2^{Aa}	313.6 ± 89.9^{Ab}	2613.4 ± 1843.3^{Aa}	3174.2 ± 1099.2^{Aa}	2534.2 ± 539.6^{Aa}	1278.2 ± 379.2^{Bab}
	Muscularis (ng/g)	705.8 ± 141.4^{Aab}	32.5 ± 12.9^{Bd}	1482.2 ± 668.0^{Ba}	278.8 ± 66.1^{Cbc}	336.3 ± 88.1^{Bbc}	141.2 ± 52.6^{Bc}
	% in mucosa	29.8 ± 12.7^{Ba}	64.5 ± 8.2^{Abc}	57.3 ± 4.1^{Ab}	83.9 ± 2.9^{Bc}	83.4 ± 3.2^{Bc}	70.5 ± 10.4^{Bbc}
	Serosal concentration	<1.25	<1.25	<1.25	<1.25	<1.25	<1.25

Data are mean ± S.E.M. (n = 5/6). Different upper case letters denote significant difference between treatments for the same sample type (two-way ANOVA, columns). Lower case letters denote difference between gut regions within treatments (two-way ANOVA, rows). The limit of detection of the instrument was 0.17 ng/mL which equates to 10.6 ng/g in tissue samples. The limit of detection for the serosal solution was 0.25 ng/mL which equates to 1.25 ng/mL.

was some material-type and gut region effects on the concentration of total Ag found in the mucosa following the exposure. Within the $AgNO_3$ treatment, the duodenum (P = 0.006), jejunum (P <0.001), ileum (P = 0.002) and hind intestine (P = 0.017) all had significantly higher total Ag concentrations compared to the stomach. For example, the intestinal regions contained 7-12 fold higher Ag compared to the stomach (638.6 ± 128.3 ng/g). Similar observations were made by anatomical region of the gut within the Ag NP and Ag_2S NP treatment, with the jejunum (P <0.001 and P <0.001, respectively) and ileum (P <0.001 and P = 0.003, respectively) being significantly higher compared to the stomach. Between the Ag treatments, there was very little difference except the hind intestine of the Ag_2S NP treatment which contained around a third of the Ag compared to the $AgNO_3$ treatment (3639.5 ± 631.9 ng/g). Regardless of the treatment, only a few percent was in the tissue (Table 6-3). Between the nanomaterials, there was no significant difference in the total Ag concentration within the mucosa.

There were statistical differences by both treatment and gut region with respect to the concentration of total Ag in the muscularis (Table 6-2). In all the Ag treatments, the four anatomical regions of the intestine regions were significantly elevated compared to the stomach. For example, in the $AgNO_3$ treatment, the muscularis of the stomach contained around 112.1 ± 31.0 ng/g dw whereas the intestinal regions ranged from 600 to 3500 ng/g dw (all values P <0.001). Additionally, between treatments, the stomach, duodenum, jejunum, ileum and hind intestine (all values P <0.001) were all significantly elevated compared to their respective gut regions from both the Ag NPs and Ag_2S NPs treatments. For example, the duodenum of the $AgNO_3$, Ag NP and Ag_2S NP treatments contained around 2513.8 ± 267.2, 906.6 ± 284.1 and 1482.2 ± 668.0 ng/g dw, respectively. The only exception was the muscularis of the oesophagus where the total Ag concentration in the tissue were the same for the $AgNO_3$ treatment

Table 6-3. Partitioning of Ag distribution throughout the gut sac. The rinse 1, rinse 2, the mucosa and muscularis expressed as the percentage of Ag dosed with 1 mg/L Ag as either $AgNO_3$, Ag NPs or Ag_2S NPs at the start of the 4 h incubation.

Treatment	Region of gut	Luminal rinse	EDTA wash	Mucosa	Muscularis	Serosal saline
$AgNO_3$	Oesophagus	82.2 ± 2.0^{Aab}	$9.7 \pm 1.0^{Aa*}$	$3.5 \pm 1.0^{Aab*\#}$	$4.7 \pm 1.7^{Aab*}$	N/D
	Stomach	88.9 ± 3.8^{Ab}	8.8 ± 3.7^{Aa}	$1.1 \pm 0.2^{Aa*}$	$1.2 \pm 0.2^{Aa*}$	N/D
	Duodenum	77.5 ± 2.1^{Aabc}	$5.6 \pm 0.7^{Aa*}$	$3.0 \pm 0.6^{Aab*\#\wedge}$	$4.3 \pm 0.4^{Ab*\wedge}$	$9.7 \pm 1.5^{Aa*}$
	Jejunum	73.9 ± 4.1^{Abc}	$6.6 \pm 1.1^{Aa*}$	$4.8 \pm 1.7^{Aab*}$	$5.1 \pm 1.0^{Ab*}$	$9.6 \pm 3.1^{a*}$
	Ileum	67.3 ± 5.1^{Ac}	10.6 ± 2.7^{Aa}	$3.8 \pm 1.1^{Aab*}$	$3.9 \pm 1.1^{Aab*}$	14.4 ± 1.9^{a}
	Hind intestine	84.4 ± 2.6^{Aab}	5.2 ± 0.7^{Aa}	$5.6 \pm 2.0^{Ab*}$	$3.2 \pm 0.6^{Aab*}$	1.6 ± 0.4^{b}
Ag NPs	Oesophagus	80.8 ± 1.9^{Aabc}	14.4 ± 1.2^{Aab}	$2.6 \pm 0.7^{ABab*}$	$2.2 \pm 0.6^{Aa*}$	N/D
	Stomach	91.6 ± 1.1^{Aab}	7.1 ± 0.9^{Aabc}	$1.0 \pm 0.2^{Aa*}$	$0.4 \pm 0.0^{Bb*\#}$	N/D
	Duodenum	78.3 ± 2.5^{ABc}	8.9 ± 0.9^{Aabc}	$3.5 \pm 0.4^{Ab*}$	$2.2 \pm 0.4^{Aa*}$	7.2 ± 2.0^{A}
	Jejunum	88.2 ± 0.8^{Babc}	6.8 ± 0.9^{Ac}	$3.5 \pm 0.4^{Ab*}$	$1.4 \pm 0.2^{Ba*\#}$	N/D
	Ileum	80.1 ± 5.2^{Bc}	13.5 ± 4.1^{Aab}	$4.9 \pm 1.6^{Ab*}$	$1.5 \pm 0.3^{Ba*}$	N/D
	Hind intestine	91.2 ± 1.9^{ABab}	4.7 ± 1.0^{Ac}	$2.7 \pm 0.9^{ABab*}$	$1.4 \pm 0.7^{Bab*}$	N/D
Ag_2S NPs	Oesophagus	83.1 ± 1.7^{Aa}	$12.0 \pm 1.5^{Aa*}$	$1.3 \pm 0.6^{Ba*\#}$	$3.6 \pm 1.0^{Aa*\#}$	N/D
	Stomach	94.4 ± 0.7^{Aa}	$4.2 \pm 0.6^{Abc*}$	$1.0 \pm 0.3^{Aa*\#}$	$0.5 \pm 0.1^{Bb*\#}$	N/D
	Duodenum	87.6 ± 3.5^{Ba}	6.5 ± 1.5^{Aab}	$3.2 \pm 1.0^{Aa*}$	$2.7 \pm 1.2^{Aa*}$	N/D
	Jejunum	92.4 ± 1.3^{Ba}	4.1 ± 0.6^{Abc}	3.0 ± 0.9^{Aa}	$0.4 \pm 0.1^{Cb*}$	N/D
	Ileum	88.3 ± 1.9^{Ca}	$8.7 \pm 1.8^{Aac*}$	$2.5 \pm 0.2^{Aa*\#}$	$0.5 \pm 0.1^{Cb*\#}$	N/D
	Hind intestine	94.9 ± 0.9^{Ba}	$3.4 \pm 0.9^{Ab*}$	$1.3 \pm 0.4^{Ba*}$	$0.4 \pm 0.1^{Cb*\#}$	N/D

Data are mean ± S.E.M. (n = 5/6). Different upper case letters denote statistical difference between gut regions of different treatments (two-way ANOVA; columns). Different lower case letters denotes statistical difference between gut regions within the same treatment (two-way ANOVA; columns). One-way ANOVA or Kruskal-Wallis was used for significant differences within each gut sac where (*) denotes significant difference from luminal rinse, (#) denotes significant difference compared to EDTA wash and (^) denotes significant difference compared to the serosal saline. Note N/D equates to 0% as no total Ag was detected – the statistical notation included is only for positive values for clarity.

compared to both the Ag NP and Ag_2S NP treatments. The only effect between nanomaterials was observed in the jejunum where the Ag_2S NP treatment had around half the total Ag concentration compared to the Ag NPs treatment (the latter 685 ± 120 ng/g dw, $P = 0.021$).

Table 6-2 also shows the transepithelial accumulation of total Ag across the gut into the serosal compartment. Only a few regions of the gut showed the ability for transepithelial accumulation of Ag and they were limited to the $AgNO_3$ and Ag NP treatments. In the $AgNO_3$ treatment, the duodenum, jejunum, ileum and hind intestine showed transepithelial accumulation of total Ag, with there being significantly more in the serosal saline from the duodenum ($P = 0.005$), jejunum ($P = 0.038$) and ileum ($P = 0.017$) compared to that from the hind intestine. The only gut region to show transepithelial accumulation in the Ag NP treatment was the duodenum with the serosal saline having a significantly lower total Ag concentration compared to the same region of the $AgNO_3$ treatment ($P = 0.043$). There was no evidence of transepithelial accumulation of total Ag into the serosal saline of the Ag_2S NP treatment.

6.3.2 Tissue fluid flux, moisture and electrolyte composition

There was no treatment-related effects in the fluid flux (Table 6-4) or tissue moisture (data not shown). There were some significant changes in the tissue electrolyte composition (Table 6-4). Throughout the gastrointestinal tract, the Na^+ concentration ranged from 400 to 1000 µmol/g dw, depending on gut region, and did not significantly alter between treatments. However, there were some significant changes in the tissue K^+ concentration. In general, the Ag NP treatment had a more variable K^+ concentration which resulted in some significant differences compared to other treatments. For example, the K^+

Table 6-4. Fluid flux, accumulation rate of total Ag into the mucosa and tissue electrolyte concentration in the rodent gut sac.

Measurement	Treatment	Oesophagus	Stomach	Duodenum	Jejunum	Ileum	Hind intestine
Fluid flux (mL/g/h)	Control	0.01 ± 0.02^{A}	0.00 ± 0.01^{A}	0.06 ± 0.02^{A}	0.00 ± 0.01^{A}	0.03 ± 0.01^{A}	0.00 ± 0.00^{A}
	$AgNO_3$	-0.02 ± 0.00^{A}	0.00 ± 0.00^{A}	0.03 ± 0.01^{A}	-0.02 ± 0.03^{A}	0.00 ± 0.03^{A}	-0.01 ± 0.00^{A}
	Ag NPs	-0.01 ± 0.00^{A}	-0.01 ± 0.00^{A}	0.01 ± 0.01^{A}	-0.03 ± 0.02^{A}	0.00 ± 0.01^{A}	-0.01 ± 0.00^{A}
	Ag_2S NPs	-0.01 ± 0.00^{A}	-0.01 ± 0.00^{A}	0.03 ± 0.02^{A}	0.00 ± 0.01^{A}	0.03 ± 0.01^{A}	-0.01 ± 0.01^{A}
Ag accumulation rate into mucosa (nmol/g/h)	Control	N/A	N/A	N/A	N/A	N/A	N/A
	$AgNO_3$	7.1 ± 2.3^{Aab}	1.5 ± 0.3^{Aab}	10.0 ± 1.3^{Ab}	16.6 ± 3.9^{Ab}	15.0 ± 4.0^{Ab}	8.5 ± 1.5^{Ab}
	Ag NPs	3.1 ± 1.1^{Aab}	0.9 ± 0.3^{Aa}	4.0 ± 1.1^{Aab}	8.5 ± 2.9^{Ab}	12.5 ± 3.5^{Ab}	5.1 ± 0.9^{ABb}
	Ag_2S NPs	9.3 ± 3.2^{Aa}	0.7 ± 0.2^{Ab}	6.1 ± 4.3^{Aa}	7.4 ± 2.3^{Aa}	5.0 ± 1.2^{Aa}	3.0 ± 0.9^{Bab}
Na^+ concentration (µmol/g dw)	Control	514.1 ± 35.2^{A}	565.8 ± 32.4^{A}	1035.4 ± 98.4^{A}	940.3 ± 110.0^{A}	1030.8 ± 133.6^{A}	606.7 ± 46.0^{A}
	$AgNO_3$	482.0 ± 34.5^{A}	490.9 ± 51.7^{A}	883.2 ± 170.3^{A}	1047.7 ± 189.1^{A}	896.1 ± 184.6^{A}	634.1 ± 72.3^{A}
	Ag NPs	619.7 ± 48.7^{A}	501.4 ± 26.4^{A}	743.3 ± 88.6^{A}	857.2 ± 74.6^{A}	1065.9 ± 182.9^{A}	719.7 ± 59.3^{A}
	Ag_2S NPs	532.5 ± 76.6^{A}	408.1 ± 121.3^{A}	976.0 ± 210.2^{A}	704.5 ± 91.6^{A}	658.0 ± 151.7^{A}	573.1 ± 106.9^{A}
K^+ concentration (µmol/g dw)	Control	316.6 ± 12.3^{A}	145.4 ± 12.8^{AB}	155.3 ± 20.6^{AB}	180.5 ± 23.4^{AB}	161.3 ± 28.8^{AB}	192.3 ± 19.0^{A}
	$AgNO_3$	301.7 ± 31.0^{A}	127.7 ± 10.5^{A}	129.4 ± 17.6^{A}	88.0 ± 14.6^{A}	178.5 ± 25.3^{AB}	137.8 ± 17.3^{A}
	Ag NPs	370.1 ± 26.9^{A}	186.2 ± 15.6^{B}	292.3 ± 54.2^{B}	258.2 ± 48.0^{B}	265.5 ± 27.8^{A}	219.5 ± 31.9^{A}
	Ag_2S NPs	364.4 ± 41.5^{A}	121.2 ± 11.8^{A}	180.0 ± 34.4^{AB}	187.6 ± 20.8^{AB}	117.8 ± 30.4^{B}	168.0 ± 17.8^{A}

Data are mean ± S.E.M. (n = 5/6). Different upper case letters denote significant difference between treatments (columns). Different lower case letters denote significant difference between gut regions (rows). There was no significant difference in the fluid flux between treatments (one-way ANOVA or Kruskal-Wallis). A two-way ANOVA was used to analyse the accumulation rate into mucosa only (treatment and gut region). A one-way ANOVA or Kruskal-Wallies was used to analyse the fluid flux, Na^+ and K^+ concentrations (treatment).

concentration in the duodenum of the Ag NP treatment was around 292.3 ± 54.2 µmol/g dw, twice that of the $AgNO_3$ treatment which had 129.4 ± 17.6 µmol/g dw of K^+ (P = 0.021). Despite some variability in the K^+ concentrations, none of the Ag treatments were significantly elevated compared to the controls.

6.3.3 Form of Ag materials within the mucosa and muscularis of the duodenum

Samples of the duodenum were analysed by spICP-MS to determine if Ag-containing particles were present in the tissue. The measurements included the particle number concentration per gram wet weight of tissue, the absolute total number of particles in the tissue and the mean particle diameter. Procedural blanks produced a clean time scan with no particles detected, but particle events were found in each tissue from all treatments (Table 6-5). A trace amount of particle events were found in the unexposed controls (20-40 particle per sample), equating to a concentration of 0.9 ± 0.6 and 2.7 ± 1.4 $x10^6$ particles/g tissue (ww) in the mucosa and muscularis, respectively. These particles already present in the tissue contributed a background of between 1.6 and 4.2% of the particles found in the Ag treatments, indicating the particles present in the latter tissues were predominantly from the exposure.

Particles were found in both the mucosa and muscularis of the duodenum of the $AgNO_3$ treatment (Table 6-5). There was significantly more particles (both the absolute total particle number and concentration) in the muscularis from the $AgNO_3$ treatment compared to the equivalent tissues in the control gut sacs (all values P = 0.001 or less). Additionally, the $AgNO_3$ treatment showed a significantly higher particle number concentration in the muscularis compared to the mucosa (P = 0.009), with the mucosa

Table 6-5. The average particle diameter (nm), particle number concentration per gram (ww) and total number of particles in the tissue of rat duodenum gut sacs exposed to the control (no added Ag) or 1 mg/L Ag as either AgNO3, Ag NPs or Ag2S NPs for 4 h.

Parameter	Control	$AgNO_3$	Ag NPs	Ag_2S NPs
Particle number concentration ($x10^6$/g ww)				
Mucosa	0.9 ± 0.6 ^{Aa}	39.2 ± 32.6 ^{Aa}	125.2 ± 46.2 ^{Ba}	68.5 ± 22.1 ^{ABa}
Muscularis	2.7 ± 1.4 ^{Aa}	126.5 ± 53.7 ^{Bb}	109.9 ± 49.1 ^{Ba}	70.6 ± 35.7 ^{ABa}
Total number of particles in tissue ($x10^6$)				
Mucosa	0.12± 0.05 ^{Aa}	3.23 ± 2.69 ^{Ba}	7.46 ± 2.18 ^{Ba}	4.92 ± 0.35 ^{Ba}
Muscularis	0.17 ± 0.03 ^{Aa}	4.10 ± 2.30 ^{Ba}	7.26 ± 1.74 ^{Ba}	5.11 ± 0.61 ^{Ba}
% in mucosa	39.13 ± 8.94 ^{A}	35.15 ± 19.81 ^{A}	50.55 ± 5.93 ^{A}	49.09 ± 3.93 ^{A}
Average particle size (nm)				
Mucosa	52 ± 5 ^{Aa}	54 ± 10 ^{Aa}	65 ± 20 ^{Aa}	64 ± 14 ^{Aa}
Muscularis	48 ± 4 ^{Aa}	55 ± 19 ^{Aa}	65 ± 10 ^{Aa}	56 ± 8 ^{Aa}

Data are means ± S.D (n = 3). Different upper case letters denote significant difference between treatments (two-way ANOVA, rows). Different lower case letters denote significant difference between gut regions (two-way ANOVA, columns). A one-way ANOVA was used for the percent in the mucosa only. The average particle diameter of the controls, $AgNO_3$ and Ag NPs are based on the density of Ag (10.49 g/mL), and for the Ag_2S NP treatment they are based on Ag_2S (7.23 g/mL).

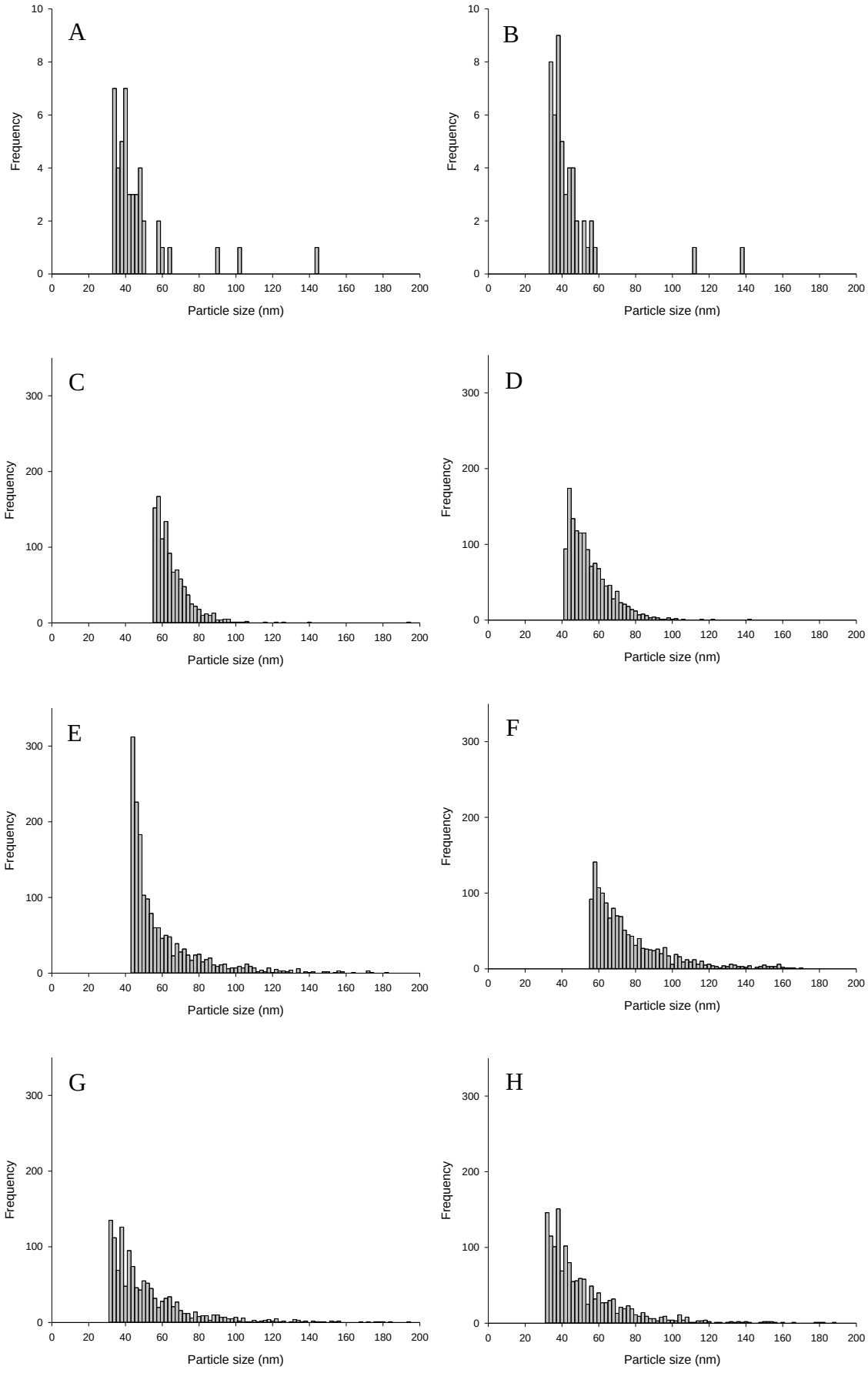
A
B
C
D
E
F
G
H
Frequency
Particle size (nm)

Figure 6-1. Example size distributions of duodenum analysed in the control (A and B), $AgNO_3$ (C and D), Ag NPs (E and F) and Ag_2S NPs (G and H) treatments for the mucosa (left) and muscularis (right). Note the size distributions of the control, $AgNO_3$ and Ag NP treatments are calculated using the density of Ag (10.49 g/mL), and the Ag_2S NP treatment is calculated suing the density of Ag_2S (7.23 g/mL).

containing around 35.15 ± 19.81% of the total particles (Table 6-5). The particle size distribution ranged from 40 to 140 nm in the mucosa and muscularis (Fig. 6-1).

In the Ag NP treatment, both the absolute total number of particles present and particle number concentration per gram of tissue was significantly elevated compared to the control tissues (all values $P = 0.01$ or less). Within the Ag NP treatment, there was no difference between the mucosa and muscularis for any particle-based parameter. There was a tendency for a higher (~1.5 fold) of particles to be associated with the mucosa compared to the equivalent tissue from the $AgNO_3$ treatment (35%), but this was not significantly different (one-way ANOVA, $P = 0.340$). The particle size distributions showed some particles in the bin sizes of the Ag NPs put into the gut lumen at the start, but also the presence of particles in larger bin sizes (Fig. 6-1).

Similarly to the other Ag treatments, the Ag_2S NP treatment showed a trend of higher number of particles both as both the absolute total particle number and concentration, but only the former was significantly elevated (both $P < 0.001$). Similarly to the Ag NP treatment, the Ag_2S NP treatment showed no significant difference in any particle-based parameter between the mucosa and muscularis within duodenum of the Ag_2S NP treatment. The mean particle diameter ranged from 50 to 70 nm, and a two-way ANOVA did not result in any significant difference between tissue ($P = 0.600$) or treatments ($P = 0.210$). The particle size distributions in the Ag_2S NP treatment ranged from 30 to 200 nm (Fig. 6-1).

6.3.4 The form of Ag in the serosal compartment following exposure to $AgNO_3$ and Ag NPs in the duodenum

There were no detectable total Ag in the serosal compartment of the control gut sacs or those from the Ag_2S NP treatment in earlier experiments (Table 6-2), so only the $AgNO_3$ and Ag NP treatments were used here for determining the form of Ag in the serosal compartment by spICP-MS. Both of the $AgNO_3$ and Ag NP treatments showed accumulation of particulate material into the serosal compartment (Table 6-6). Interestingly, there was no significant difference between any of the particle based parameters between the Ag treatments. The serosal compartment from both treatments contained around 4-5 $x10^6$ particles/mL (Table 6-6). This was a relatively modest particle number concentration and so the percent of particulate Ag relative to the dissolved fraction in the compartment was also estimated. Of the total Ag in the serosal compartment, 4 ± 1 and 17 ± 5% was present in the particulate form for the $AgNO_3$ and Ag NP treatments, respectively (one-way ANOVA; P = 0.016); indicating that most of the Ag was in the dissolved form.

Table 6-6. Particle parameters in the serosal compartment of gut sacs from the duodenum following 4 h exposure to 1 mg/L Ag as $AgNO_3$ and Ag NPs.

Parameter	$AgNO_3$	Ag NPs
Total number of particles ($x10^7$)	3.9 ± 0.8^{A}	3.1 ± 0.9^{A}
Particle number concentration ($x10^6$/mL)	5.2 ± 1.0^{A}	4.1 ± 1.2^{A}
Mean particle size (nm)	28.4 ± 8.7^{A}	26.6 ± 1.1^{A}
Percent particulate Ag (%)	4.3 ± 0.9^{A}	17.0 ± 5.4^{B}

Data are means ± S.D. (n = 3). Different upper case letter denote significant difference between treatments (one-way ANOVA, rows). Note there was no detected total silver concentration in the serosal compartment of the control or Ag_2S NP treatments in earlier experiments, so only the serosal solution from the $AgNO_3$ and Ag NP-exposed gut sacs were determined by spICP-MS here.

6.4 Discussion

This study is the first to demonstrate the utility of the rodent gut sac technique for the accumulation of different forms of silver, including ENMs. The highest accumulation of $AgNO_3$, Ag NPs and Ag_2S NPs were in the duodenum, jejunum and ileum. Specifically, the $AgNO_3$ and Ag NPs showed evidence of transepithelial accumulation in the duodenum. Regardless of the material added, the biologically incorporated Ag (i.e., the mucosa, muscularis and serosal saline) was 22% or less of the dose administered into the gut lumen. Using spICP-MS, the presence of particles in the duodenum was confirmed in all treatments, and transepithelial accumulation of particles in the $AgNO_3$ and Ag NPs was observed (<17% was particulate). The serosal compartment from the Ag_2S NP treatment did not show any Ag presence, suggesting this treatment has a lower bioavailability compared to the pristine Ag NPs.

6.4.1 Bioavailability of the metal salt and nanomaterials in the gut

The first step in dissolved metal or ENM uptake is the presentation of test materials in the gut lumen. The chemical speciation of $AgNO_3$ was calculated using Visual MINTEQ, showing most of the Ag was dissolved. The bioavailable fraction of the Ag from $AgNO_3$ exposure was 22% or less of the exposure dose (Table 6-4).

The same Ag ENM and $AgNO_3$ solution preparation was used here as in Chapter 2, which produced reasonable dispersions despite the high ionic concentration of the gut saline (Chapter 2, Fig. 2-2). For both Ag ENMs, it is known that under similar conditions, they are sparingly soluble and settling is likely to occur (Chapter 2). Any surface bound Ag

is readily washed off from the mucosa as evidenced from the higher concentrations of Ag in the luminal and EDTA washes (Table 6-4).

6.4.2 Total silver accumulation in the gut tissue

This study attempted to show total Ag accumulation into the gastrointestinal tract of rats under physiologically relevant conditions. The gut sacs were viable through the normal water fluxes (Table 6-4) and comparable to previous reports of these materials in vertebrates (Chapter 2). The luminal and EDTA washes were fruitful in removing surface bound Ag as evidenced by the highest percentages of the exposure dose (Table 6-3).

The accumulation of Ag from the $AgNO_3$ treatment would involve diffusion from any dissolved silver present in the gut lumen down the electrochemical gradient into the mucosa of the gut epithelium. Such tissue accumulation is likely to be the result of active uptake as the water flux was negligible (Table 6-3), excluding this as a reason for the apparent Ag concentrations. The resultant tissue accumulation rates in the gut for Ag from $AgNO_3$ were a few nmol/g/h (Table 6-3), with the highest rate in the jejunum and ileum (17 ± 4 and 15 ± 4 nmol/g/h, respectively). These are slightly higher compared to those in the mid intestine of fish (9 ± 3 nmol/g/h; Chapter 2). However, the uptake rates here are consistent with other reports in rodents. The intestine has been known to be important for essential metal accumulation in rodents (e.g. Zn, Oberleas et al. 1966). Rats can assimilate Ca and Mg rapidly in the duodenal mucosa from the gut lumen at rates of ~5 and 2 nmol/cm^2/h, respectively (O'Donnell and Smith 1972). Mice given a single dose of 5 µmol/kg Hg, 2 µmol/kg Cd or 30 µmol/kg Zn showed 2, 2.7, 4 nmol in the mucosa of the duodenum (no standardised to weight; Andersen et al. 1994). Equally, rats administered a dose of 0.4 µmol $CdCl_2$/kg in a volume of 4 mL/kg saline caused the duodenum

concentration of nearly 100 ng/g ww compared to the other intestinal regions (10 ng/g ww or less) following 2 days exposure (Park et al. 2002). Compared to the Cd results (Park et al. 2002), Ag as $AgNO_3$ may have a higher accumulation rate.

Despite the accumulation rates of Ag NPs into the mucosa being higher in the jejunum and ileum, transepithelial accumulation was demonstrated in the duodenum only (Table 6-6). However, in the Ag_2S NP treatment there was no total Ag signal, indicating this material was less bioavailable. This is the first study to use metallic ENMs to show intestinal accumulation. The duodenum has shown an increase in simvastatin loaded lipid nanoparticles compared to the jejunum (Zhang et al. 2010a). Additionally, the duodenum has been shown to preferentially accumulate 11.5 μm sized particles after 2 h compared to the jejunum and ileum (da Silva et al. 2009), indicating this region as important for accumulation following particulate exposure.

6.4.3 Particulate silver accumulation in the duodenum

Particles were found in the controls when the procedural blanks showed no presence of particles, demonstrating a natural presence of particles in the rat tissues (Fig. 6-1). The presence of these particles was close to the detection limit, so it is uncertain how big this contribution is compared to the dissolved fraction in control tissues. Other authors have reported particle-like events in control samples. For example, CeO_2 and Au NPs were observed in reagent blanks and controls (Dan et al. 2015; 2016).

Attempts were made in previous work (Chapter 2) to characterise the materials in physiological gut matrices; therefore, the aim here was to focus on detecting the different forms of Ag in the tissues. For the Ag treatments, the total Ag (Table 6-2) and particle number concentrations (Table 6-5) were expressed as the percent found in the mucosa.

Interestingly, when expressed as this, both methods give similar results, indicating that the total Ag measurements are from particulate Ag. Also, in all Ag treatments, there was no significant difference in total particle number or particle number concentration, including the $AgNO_3$ treatment. The data presented here is assumed to be made completely out of Ag, but if AgCl formation either in the gut lumen or inside the tissue, the altered density of AgCl would change the mean size to 75.8 ± 25.0 and 63.4 ± 11.0 in the mucosa and muscularis, respectively.

The particle size distributions of the Ag NPs and Ag_2S NPs extracted from the duodenum (Table 6-5) were similar to those of the same particles in ultrapure water (Chapter 5). The corresponding size distributions in the tissues here show a 40 nm cut off, similar to other reports of Ag NPs in tissues. For example, Makama et al. (2016) exposed earthworms to 250 mg Ag/kg of soil for 28 days with worm size distributions ranging from 40 to 190 nm.

The serosal accumulation of $AgNO_3$ has a lower particulate content compared to the Ag NP treatment (Table 6-6). This indicates dissolution in the former treatment, suggesting the potential for endogenously made nano silver to potentially dissolve in the blood compartment of a rodent. Silicon dioxide particles (70 nm) accumulated through the gut of the small intestine (region not specified), ranging from 6 to 10 µg (not standardized) following 45 min exposure to 12.5 mg/mL (Yoshida et al. 2014). If such changes occur in the serosal compartments, it may suggest that a corona is forming that could enhance the dissolution rate (e.g., Chapter 2). It may also have an effect on using Ag NPs as drug delivery systems; the nano form could potentially not reach its target organ before releasing the compound it encapsulates.

6.4.4 Rat and fish gut comparison

In the present study, exactly the same gut sac methods was used for fish and rodents. Consequently, any differences observed would be due to the biology, not the method itself. Absolute tissue concentrations of materials and accumulation rates in gut sacs are seldom useful for comparison due to anatomical differences and tissue densities. For example, in fish the gut sac uptake rates for fish range from 2 - 10, 1 - 4 and 1 - 12 nmol/g/h for $AgNO_3$, Ag NPs and Ag_2S NPs, respectively (Chapter 2). While broadly similar to values here for rat gut sacs, some regions are nearly double the accumulation rate and likely reflect either the difference in temperature for uptake kinetics (15^{o}C versus 37^{o}C) and/or the thickness of the gut epithelium. Furthermore, anatomical differences in gut regions can influence gut lumen loading. For example, in fish, the rate of Ag accumulation into the mucosa for the pyloric caeca is difficult to measure due to the anatomy, but because of their contribution to the total surface area of the gut, the caeca are likely to be important for metal and ENM accumulation (e.g. Farag et al. 1994).

The partitioning of Ag distribution throughout each gut sac from all treatments is similar for both rat (Table 6-4) and fish (Table 2-5). The tendency for 2/3 of the exposure dose to remain in the luminal rinse, and up to 15% surface bound to the mucosa of rats is broadly similar with the findings on fish (Table 2-5). Some small differences can be seen within the tissues; for example, the rodent model has less total Ag from exposure to Ag_2S NP in the mucosa than the equivalent tissue in the trout. In general, the percent of exposure dose associated with the tissues is lower for fish compared to rodents which may be attributed to the 20^{o}C difference between the body temperatures, hence incubation temperatures. However, by using the muscularis total Ag concentration in gut sacs (Chapter

2) shows good correlation with *in vivo* bioaccumulation data in fish, as shown by the accumulation profiles in trout nominally fed 100 mg/kg of these Ag materials (Chapter 3).

Interestingly, Ag particles were detected in the $AgNO_3$ treatment mucosa of rats. Such findings were not observed in the fish (Chapter 4). The reason for these to be endogenously made in the tissue is that the fish mucosa accumulates dissolved Ag from the saline; therefore as the same saline is used in both experiments it suggests tissue made particles. Indeed, exposure of earthworms to $AgNO_3$ caused nano Ag to biogenically form, constituting around 10% of the total Ag concentration (Baccarro et al. 2018). The presence of particles from $AgNO_3$ exposure has consequences for systemic exposure and indicates that mammalian systems at least have undergone nano-sized exposure before. The cause of the mucosa-produced particles is unknown, but suggests subtle micro-environment differences between fish and rat are the cause. Therefore, if fish are to replace the use of rodent models, there is a need to incorporate additional tests such as behaviour of materials at the appropriate temperature (e.g. 37^{o}C for mammals).

6.5 Conclusions and future work

In conclusion, the gut sac technique using rats can demonstrate the accumulation of different Ag materials. The bioavailability, based on the duodenum, ranks the silver materials in the order $AgNO_3$ > Ag NPs > Ag_2S NPs, showing the framework for dissolved metal accumulation is protective over nano forms of silver. Overall, only a few percent of the dose accumulated into the gut tissue, similar to those in fish. If fish are to replace, or reduce, the need for mammals in animal testing, characterisation of dissolved metals also needs assessing at the appropriate temperature. The data here suggest further investigation

of dietary exposure is required to determine if these materials can bioaccumulate *in vivo* and show some similarities towards fish accumulation.

Chapter 7 - General discussion

This thesis aimed to address several key questions surrounding the lack of data on ENM bioaccumulation testing in vertebrates, specifically fish. The first aim was to determine if a short term gut sac experiment (Chapter 2) can predict the *in vivo* dietary bioaccumulation of ENMs (Chapter 3), with the aid of appropriate particle characterisation in both experiments. The second aim was to develop a suitable method for extracting dissolved silver and silver nanoparticles from fish tissues, with subsequent characterisation using single particle ICP-MS (Chapter 4), and apply this to determine the form of Ag in fish tissues following *in vivo* dietary exposure (Chapter 5). Finally, this thesis aimed to determine the gastrointestinal accumulation of the same Ag materials in rats and compare it to fish to see if fish could replace rodents in bioaccumulation testing (in agreement with the 3 R's), through a side by side experimental comparison using the gut sac technique (Chapter 6).

7.1 *Ex vivo* gut sac versus *in vivo* dietary exposure

The work in Chapter 2 had two elements: to determine where the silver materials were accumulated, and to determine the order of their accumulation. The dissolved Ag (as $AgNO_3$) was preferentially accumulated in the intestinal regions. For the two Ag ENMs, the Ag NPs had uniform accumulation throughout the gastrointestinal tract, and the Ag_2S NPs had the highest accumulation in the hind intestine. Between all Ag treatments, there was no difference between the total Ag concentrations in the mucosa. However, significant differences, and hence the potential for *in vivo* bioaccumulation, were found in the muscularis. For example, in the muscularis of the mid and hind intestine, the concentration of total Ag in the $AgNO_3$ treatment was 10-fold higher compared to the Ag NP and Ag_2S NP treatments. There was no difference between the Ag-containing ENMs; therefore, the order of magnitude of accumulation in the muscularis was $AgNO_3$ > Ag NPs = Ag_2S NPs.

Thus, with the use of 24 fish (including controls, n = 6/treatment), this gave evidence of a potential hazard to fish, and therefore additional *in vivo* testing was required.

In Chapter 3, the *in vivo* exposure to the same Ag materials showed they (as total Ag and form unknown) were able to transverse the gut epithelium and distribute to other organs around the body. The liver was the main organ of accumulation; following the 4 week exposure, the total Ag concentrations were 122 ± 10, 129 ± 17 and 11 ± 1 µg/g in the $AgNO_3$, Ag NPs and Ag_2S NPs treatments, respectively. These represented a percent body burden of 38 ± 3, 38 ± 4 and 44 ± 5% in the liver for the $AgNO_3$, Ag NPs and Ag_2S NPs, respectively. This pattern of accumulation revealed the Ag_2S NPs as being less bioavailable compared to both the $AgNO_3$ and Ag NP treatment; an observation that was also repeated in all other tissues. From the *in vivo* exposure, the order of magnitude of bioaccumulation potential was $AgNO_3$ = Ag NPs > Ag_2S NPs.

The difference in ranking between the *ex vivo* and *in vivo* studies is mainly concerning the positioning of the Ag NP treatment in the ranking of accumulation (i.e., joint first *in vivo* versus second *ex vivo*). One explanation for this difference in ranking is the appreciable dissolution of the Ag NPs under *in vivo* acidic conditions found in the stomach; this idea is supported by the release of dissolved Ag from the Ag NP diet under similar conditions using the *in chemico* digestibility assay. Equally, the same assay showed no detectable release of dissolved Ag from the Ag_2S NP diet. Therefore, it is reasonable to assume, based on the total Ag data alone, that the $AgNO_3$ and Ag NP tissue concentration were from dissolved Ag, whereas the Ag_2S NP treatment concentrations were from particulate Ag. Therefore, by combining in physico-chemical characterisation (*in chemico* digestibility) and the *ex vivo* gut sac experiment, it may be possible to predict these patterns of *in vivo* bioaccumulation. This would be greatly advantageous for ENM testing as the latter approach would be reasonably high throughput, it would reduce the number of

animals used and the cost associated with running long term tests. Clearly, more data is required on other ENMs to verify this.

To the author's knowledge, this is the first instance where the same materials have been used to demonstrate such a tiered approach using appropriate controls. Indeed, TiO_2 experiments have been conducted both *ex vivo* (Al-Jubory and Handy 2013) and *in vivo* (Ramsden et al. 2009), but the latter study did not include the bulk material control (outside of the aim of the study). Therefore, ranking treatments based on accumulation is not possible. It seems that for TiO_2, the bioavailability to the intestine was higher in *ex vivo* preparations for 4 h (2000 ng/g or less, Al-Jubory and Handy 2013) rather than when fed to the fish over 8 weeks (500 ng/g or less, Ramsden et al. 2009), which may reflect the complicated effects of the chyme which are largely absent in the former.

The work in Chapters 2 and 3 indicate the gut sac technique could be used prior to *in vivo* tests (e.g. TG305). For the gut sac to become a regulatory test, there is a need for standardisation. Certainly, at least one attempt has been made to assess the inter-laboratory effect of TiO_2 on rodent pulmonary responses. Not all assays between laboratories responded in a similar manner, and unfortunately Ti accumulation was not assessed (Bonner et al. 2013). To ensure the experimenter is measuring just biological variability, definitive guidelines are needed for inter-lab testing. Standardisation would be required at two stages: the conductance of the experiment itself, and the subsequent analysis of the samples. Currently, there are two ways for conducting the dosing of the gut sacs, by filling as much as possible (Chapter 2), or adding a fixed volume (e.g. 1 mL; Bury et al. 2001). The former has the benefits of optimising the chance of getting a signal in the tissue, which is particularly important for small gastrointestinal tract regions like the oesophagus. The latter has the benefit of being able to discriminate between different bioavailabilites of materials. As such, the preferred method should be chosen based on the question asked

(e.g., comparing a variety of difference chemical accumulation or determining where accumulation takes place).

The analysis (and preparation) of tissue samples would also need standardising. Sample preparation involves drying the tissues, acid digestion and determination of the concentration of the test substance in the media and tissue by an appropriate analytical method. Typically, oven drying a piece of tissue to a constant weight is used; yet this can leave/adhere parts of tissue to the vessel/tube. Such small discrepancies have knock on effects for the accuracy of results where tissues are already small (e.g. a few mg for the gut mucosa) and a known weight into the tube for acid digestion. This will be particularly important for experiments where materials with background concentrations in tissues are used (e.g. copper, zinc and iron), where detection of newly accumulated material is required (e.g. detecting accumulation from µmol/L exposure against mmol/g background concentration). Alternatively, a freeze drier can be used which reduces or abolishes this problem. Once dried the tissue is digested, diluted and analysed by ICP-MS (or ICP-OES). Indeed, how the user operates the analytical equipment, in this case ICP-MS, also varies. There is a tendency to not report analytical controls such as limits of detection, procedural blanks, reference materials and the use of internal standards in scientific reports. While each is important for analytical confidence and instrument diagnostics (e.g. to determine contamination from materials or instrument blockages), internal standards are especially important for quantifying drift when a large number of samples. Over prolonged period, the ICP-MS can drift, causing deviations in signals, such that the signal can reduce to as little as 40% (personal observation). Additionally, as spICP-MS becomes increasingly used, there will be a need to standardise this. One study found a large degree of variability, even between users within the same laboratory (Bustos et al. 2015). Clearly, a detailed guidance document would be beneficial to help make inter-lab testing possible.

The gut environment of fish is dynamic, which could be problematic when standardising ENM safety assessments based on one species being tested. As such, there are three main areas where standardisation is difficult. Firstly, the inorganic composition of the gut lumen changes within the same gastrointestinal tract, notably pH and cation concentration. For example, a 6-fold increase in the stomach fluid phase Ca^{2+} concentration can be seen up to 72 h post feed (Bucking and Wood 2007). The lumen concentrations can be explained through time-dependent tissue fluxes in Ca^{2+} (Bucking and Wood 2007); such alterations in Ca^{2+} concentrations could have implications for ENM stability in the gut lumen, and is likely to change with the environment (e.g., marine versus freshwater). Secondly, the gut physiology of fish are known to differ based on life history strategy. Here, rainbow trout were used (Chapter 2), which are carnivorous fish and contain a distinct stomach with low pH of 2. However, herbivorous fish lack a distinct stomach and do not have pH below 7 (Nalbant et al. 1999), making extrapolation difficult. Thirdly, microbiomes have been related to gut functions in fish such as nutrient absorption efficiency (Givens et al. 2015). The microbiome of fish is different within the same species (Givens et al. 2015), with trophic level, salinity (Wong and Rawls 2012) and throughout ontogeny (de la Morinière et al. 2003). Indeed, this raises potential concern over the effect of commercial feed on laboratory reared fish compared to those in natural habitats. The above highlights the problems of standardising and extrapolating from one experimental system.

Two experimental factors used in Chapter 3 differ from other literature of ENM exposures: diet preparation and the use of chemically aged ENMs. Several methods exist for exposing fish to dietary contaminants; top dressing commercial diets (Chapter 3), contaminating the raw ingredients of the diet and synthesising the food pellets in house (e.g. Ramsden et al. 2009), or exposing animals and incorporating them into diets (Galvez

et al. 2001). Top dressing has been considered a less environmentally relevant method as well as forcing an exposure to the gut when a large proportion of material is kept in solid phase of the digestion process (e.g., Nadella et al. 2006). Galvez et al. (2001) incorporated 3.1 mg/kg Ag into a diet fed to trout, which is around 30-fold lower compared to the concentration used here. The resultant tissue concentration of the intestine are similar to those reported here (Chapter 3), demonstrating the potential of the defence mechanisms in the gut to regulate uptake of metals and ENMs, and that only a small fraction of the exposure is internalised. For non-essential metals, this can become bound to non-specific metal chelators such as metallothionein and become lost by sloughing. The data in Chapters 3 and 5 highlight the importance of testing the effects of the transformed Ag_2S NP material chemistry. Some work has been conducted on TiO_2 in marine mussels, where laboratory ageing occurred (simulated sunlight for 7 days), whereby there was no difference in accumulation or toxicity (as metallothionein gene expression and histological analysis) when compared to "fresh" stock exposures (D'Agata et al. 2014). Additionally, the effect of aged (1 year) soils that were doped with Cu NPs were also compared to freshly spiked material, with transient changes in biochemical responses depending on material coatings (Tatsi et al. 2018). In such experiments, the effect of dissolution over time cannot be excluded given only total Cu measurements in soil were made. The same materials used in the present work were also exposed to earthworms and found that the Ag_2S NPs were less bioavailable compared to both the $AgNO_3$ and Ag NP treatments, with equal accumulation in the latter two treatments (Baccaro et al. 2018). This is the first report of the use of environmentally aged materials in fish and demonstrates how environmental chemistry is an important factor to consider for ENM testing.

7.2 ICP-MS versus single particle ICP-MS

One of the limiting factors to interpreting hazard data is the ability to determine if particulate material is within the tissues following ENM exposure. The results of Chapter 4 demonstrate the method development leading to the determination of particle number concentrations in the organs of fish. Most ENM extraction protocols have given no consideration to the equivalent dissolved metal or bulk material, which is clearly important for hazard assessment (i.e. is the hazard of the nano form more or less than that of the equivalent dissolved form). It is also important to ensure the reagents used in any extraction procedure do not alter the dissolved forms within tissues. A range of published methods for extracting ENMs from tissues were tried. However, it seemed that these were all inapplicable to Ag-based materials in fish tissue, and hence modifications were made to ensure quality control was achieved (e.g., no false positives, good analytical recovery etc.). Indeed, the effects here for Ag may be metal-specific, so when the method is applied to other materials, the process of validation will need to be repeated.

Ultimately, the question that needs addressing is the form of Ag in the tissue following an *in vivo* exposure (Chapter 5). When the appropriate extraction method was applied to spICP-MS, particles were found in the tissues of all treatments, including the $AgNO_3$. The profiles of particulate Ag in the $AgNO_3$ and Ag NP treatments were very similar, indicating they underwent the same processes. Initially (Chapter 3), it was thought the $AgNO_3$ and Ag NPs treatments would release equal magnitudes of dissolved Ag in the acidic conditions of the stomach. However, other factors will influence dissolution; the dissolution of CuO NPs in gut physiological saline at pH 7.8 are influenced by the presence of amino acids. Without amino acids, the dissolution of CuO NPs was around 1% after 4 h, but in the presence of 5 mm cysteine or histidine this increased to around 25 and 50 %, respectively (Boyle et al. unpublished data.). This has also been demonstrated with dissolved zinc (Glover and Hogstrand 2002). When the Ag NPs and Ag_2S NPs were used

(Chapter 2), the profile of amino acids may not have been right to elucidate the same increase in dissolution. Therefore, it is likely the Ag from the $AgNO_3$ and Ag NP diets would be ionic in the stomach. For nano-sized Ag to form from dissolved silver following the stomach, the dissolved Ag would need to precipitate under the relatively higher pH conditions of the intestine (Bucking and Wood 2009) as Ag_2O or AgOH, or be synthesised in the gut tissue as AgCl before being taken up into the blood as particulates and then transported to the kidney and liver.

There was consistently more particles in the organs from $AgNO_3$ and Ag NP treatments compared to the Ag_2S NP treatment. For example, at week 4 the liver contained 83 ± 20, 73 ± 17 and 5 ± 2 $x10^9$/g dw for the $AgNO_3$, Ag NP and Ag_2S NP treatments, respectively (Chapter 5). There was no evidence of dissolution of Ag_2S NPs in any of the simulated stomach conditions (Chapters 2 and 3). Additionally, the size distribution of the material in ultrapure water shows the minimal size was around 35-40 nm, similar to those found in the hind intestine and kidney. Equally, the behaviour of the Ag_2S NP treatment has some subtle differences to the other Ag treatments. For example, at the percent body burden of the kidney at week 4 was 3.9 ± 0.6, 4.2 ± 0.7 and 3.1 ± 2.2% in the $AgNO_3$, Ag NP and Ag_2S NP treatments, respectively. Following the 2 week depuration period, these values became 9.0 ± 1.6, 9.3 ± 0.9 and 0.5 ± 0.1% in the $AgNO_3$, Ag NP and Ag_2S NP treatments, respectively. This suggests the GIT may have had minimal influence on the uptake of Ag_2S NP but could also be an effect of the fish handling different internal concentrations of Ag.

Future work may benefit from collection of food material at different anatomical regions of the GIT and characterising the form of Ag the gut epithelium will be exposed too. This could also act as an intermediate where the exposure lasts only a few hours/days, and sit between the gut sac and a full dietary bioaccumulation experiments in the testing

strategy. Additionally, it would reduce the number of animals used; theoretical sample sizes could be n = 8/treatment.

Few reports show total Ag measurements and particle mass concentration in the same tissue via spICP-MS *in vivo*. One report (Baccaro et al. 2018) found earthworms exposed to $AgNO_3$, Ag NPs and Ag_2S NP for 28 days had between 3 and 45% of the total Ag in the particulate form. This was based on a mass balance of total Ag and particulate Ag, the former using acid extraction and the latter using TMAH alone to extract particles. The data from Chapter 3 and Chapter 5 show that the mass balance might not be appropriate for materials as the particle mass concentration was above the total Ag measurements in some organs. For example, the livers from Ag NP exposed fish at week 4 showed 129 ± 17 and 315 ± 70 µg/g of Ag by acid digestion and alkali digestion, respectively. As Baccaro et al. (2018) used TMAH alone to extract Ag particles, it is possible that some of the Ag was precipitated during digestion in their method (see Chapter 4 on TMAH extraction alone). Clearly, more work on validating the method for mass concentrations of particle from *in vivo* experiments is required for different species of organisms and tissue types.

For the rat gut sac, a different approach was used because the tissues were too small to separate and analyse total and particulate Ag separately. Instead, the particle number concentration and total Ag concentration were expressed as a percent in the mucosa (Table 6-2 and 6-5). Therefore, the particle number concentration was presented as a percent in the mucosa compared to the whole tissue (mucosa and muscularis), as was the total Ag. This latter approach to data processing gave good congruency between Ag methods; 41 ± 4, 61 ± 4 and 57 ± 4% for total Ag, and 35 ± 20, 51 ± 6 and 49 ± 4% for particulate Ag in the $AgNO_3$, Ag NP and Ag_2S NP treatments, respectively. This suggests the possibility of using total Ag analysis to inform on particulate Ag within a tissue.

Critically, with the determination of the presence of nano-sized Ag in tissues, it is possible to determine if the presence and number of particles can be correlated with any biological effects observed in the tissue, such as the incidence of any specific pathologies. Although not a main aim of the thesis, it was importance to relate *in vivo* data on any Ag accumulation to any potential pathology. The current data on bioaccumulation potential was collected at sub-lethal concentration in order to understand the uptake. There was no overt toxicity, as expected, but also no nano-specific effects were observed (e.g., on tissue electrolyte composition, biochemistry or histology; Chapter 3). Indeed, in the present study, if pathology was demonstrated, it would be through the presence of nano-sized silver, and not any dissolved metal.

Early reviews hypothesising the internal handling of ENMs (Handy et al. 2008a) highlighted many unknowns. For instance, there was a discussion whether ENMs could be metabolised by an organ once internalised. The data here suggest the liver may play a role in this; the particle size distributions included larger particles in the liver compared to both the hind intestine and kidney (Chapter 5). Although some aggregation of particles in the spICP-MS samples cannot be entirely excluded. The most likely explanation for this observation is that the primary particle size increased inside the liver. In this instance the term metabolism may be misleading, whereas biotransformation may be more appropriate for ENMs. Another unknown was if ENMs can be excreted (Handy et al. 2008a). Presence of total Ag in the gallbladder suggest this may occur via secretion of particles into the bile, which raises a concern for entero-hepatic re-circulation, where the gut and then the liver can be exposed to the same modified material twice. Also, the redistribution of Ag towards the kidney (4 and 10% at weeks 4 and 6, respectively) suggests this organ as a possible route of excretion. However, the macrophage activity in the kidney could also act as a scavenger of ENMs (e.g. Al-Jubory et al. 2013), where they are not excreted. Certainly, the

particles in the kidney do not change between week 4 and 6 (Chapter 5), suggesting they are not altered whilst associated with the tissue.

7.3 General considerations for spICP-MS

Within the spICP-MS literature, there is no clear consensus for setting the LOD for particle measurements. For the present study, the mass LOD was determined through signal discrimination from particle versus dissolved frequency plots, or visually to determine the dissolved signal. Mitrano et al. (2011) advocate an iterative method where the standard deviation of the time scan is multiplied by 5, and any signal above this is a particle, and the process repeated until no signals are removed. However, this may not be useful for ENMs that undergo aggregation during the sample which do not seem to be reversible by conventional methods of sonication (Gray et al. 2013). For example, when multiple particles are measured in the same dwell time, there is a potential for the ion cloud to be longer than the 3 ms whereby small intensities are observed in neighbouring dwells. These have been observed by Loeschner et al. (2014) and ignored as they were incomplete events. This is a likely reason for the abrupt cut-off that can be seen in the gut sac samples as some of the mass of the particles is being included as the dissolved fraction. Similar observations have been made when endogenously made SiO_2 NPs were extracted from yeast (Jiménez-Lamana et al. 2018), Ag NPs in earthworms (Makama et al. 2016) and when assessing Ag NP accumulation into plants (Bao et al. 2016). Additionally, agglomerative behaviour will invalidate the assumption that the particles are spherical; but may exist in multiples of the average size.

Also, for the particle size LOD, there is no clear consensus in the literature to what the minimum signal constitutes as a particle. Theoretically, this is 333 CPS (1 count in 3 msec dwell time = 333 counts per second), and can occur when the LOD is set. This gives

a theoretical size LOD as 17 nm when processed as above. However, clearly 1 ion arrival (e.g. 333 cps) is not a "true" particle event but will be processed as such in the spreadsheet. Indeed, it is also possible that if Ag NPs are being extracted, other nano-sized particulate material can as well. For example, in the liver of fish exposed to dietary $CuSO_4$, nano-sized granules have been observed (Lanno et al. 1987). As such, there is a potential for ions to adhere to such particles; if the particle size is sufficiently large for the ion cloud to be produced in one dwell time (3 ms here) after ablation, it would be registered as a particle event. A similar problem has been described with multiple ENM attachment to soil particles (Navratilova et al. 2015). Therefore, characterisation of smaller ENMs is problematic in complex matrices. This effect may be more profound in samples where dissolution can or is known to occur.

TMAH-based extractions have been provided fruitful analysis of Ag ENMs (Gray et al. 2013; Baccaro et al. 2018). For inert ENMs, such as TiO_2, acid extractions are possible (Deng et al. 2017), but will not be suitable for metal oxide ENMs that will dissolved under low pH conditions. In contrast, enzymatic digestion is preferred for plant based tissues (Dan et al. 2015; 2016). The use of TMAH to extract ENMs from plants is yet to be assessed; however, the method should be sufficient to break down the plant wall, and in the instance of application to tissues, provides a superior recovery compared to enzymatic methods (Loeschner et al. 2013). Several data gaps in reported extraction methods mean it is difficult to ascertain exactly the cause of differences in measurements between protocols, so that a 'best method' can be derived for the purposed of standardisation of protocols for regulatory bioaccumulation tests. For example, the methods detailed by Dan et al. (2015) and in Dan et al. (2016) does not compare the size distribution of the ENMs in ultrapure water compared to the extraction matrix. As a buffer is used, containing salts, it is prudent for this information to be included so that potential aggregative behaviour is monitored and not

miss-reported as a biotransformative process. Indeed, extraction at pH 5 increased the presence of a dissolve profile, but the authors concluded this was because of biotransformation (Dan et al. 2016).

The elemental composition is important because it is used to determine the particles size (e.g., the median particle size and particle size distribution). Indeed, ICP-MS will only be able to measure the total Ag in each particle. Unfortunately the EDS on the TEM is not useful for routine determining the particle composition due to the scarcity and dispersion of the particle in the tissue. Some elements show high binding affinity for Ag ions, notably chloride and sulphur, which make the particle size bigger (with densities of 5.56, 7.23 g/cm^3, respectively, compared to 10.50 g/cm^3 for silver [see equation 4.4]). Equally, silver oxide formation is also possible (7.14 g/cm^3). If the density of the particle is changed through the binding of anions or oxidation, the mean size would increase.

It is clear that there are many challenges to overcome in the field of spICP-MS. The method works well for characterising samples in matrices, but there are many challenges for applying this method to *in vivo* tissue samples. Currently, the method may be used to screen for more advanced analysis such as the use of a synchrotron or hyphenated spICP-MS (e.g., HPLC-spICP-MS); for example, do particles exist in the sample.

7.4 Comparison of gastrointestinal accumulation of ENMs

The aim of Chapter 6 was to assess the gastrointestinal accumulation of the ENMs in rats, using the same methodology in Chapter 2 for rainbow trout, to provide a species comparison. For accuracy, the same method, of course, needs to be conducted in both species. In theory this may provide evidence of replacing rodents gut accumulation tests with fish instead, similarly to the postulated immunological and oxidative stress response (Johnston et al. 2018). Currently, the reduction, replacement and refinement of vertebrates

used in toxicology is required to be considered under the REACH legislation for new substances, including ENMs. The scientific community has developed a number of *in vitro* methods. For example, cell culture-based *in vitro* animal alternatives are being developed (Baron et al. 2017; Langan et al. 2017). In general, both the fish (Chapter 2) and rat (Chapter 6) tests showed that the Ag ENMs accumulated less compared to the $AgNO_3$ treatment. Equally, both species showed preferential accumulation towards the intestinal regions for all Ag materials. However, some species differences were noted. In the rodent gut sac experiment, there was evidence of transepithelial accumulation, which was no observed in the fish. This is not surprising given that fish intestine is thicker, and the temperature is lower in fish experiments which will inherently affect the uptake kinetics. Interestingly, temperature seems to have had a potential effect on the form of Ag in the intestine from the $AgNO_3$ treatment. Particles were observed in the mucosa of the duodenum in the rat, which were not observed in the mid intestine of fish. These potential temperature-linked effect in Ag should be explored as it is likely to affect the bioavailability in rodent compared to fish. The Q_{10} values for the hind intestine are 1.49, 1.65 and 1.38 for the $AgNO_3$, Ag NP and Ag_2S NP treatments, respectively, showing some thermal independence (Reyes et al. 2008). This also highlights the importance for trying to replace the use of certain animal models; an appropriate way to deal with this in the testing strategy may be to characterise materials under different physiological conditions (e.g. temperature) to indicate species testing. As such, an *in vivo* experiment using a rodent model should be conducted to corroborate this influence. Due to these differences, fish may not be suitable replacements of rodent dietary accumulation tests.

The tiered testing strategy advocated here for fish (Chapter 2 and 3) would also be appropriate for mammalian models. Indeed, the use of tiered testing approaches have been suggested, whereby testing starts with *in vivo* assessments of pathology following exposure

(tier 1), with subsequent testing for fate in the body, reproductive effects and mechanistic studies (tier 2, Oberdörster et al. 2005). Such approaches may lead to unnecessary testing of ENMs that dissolve easily in biological fluids (e.g. ZnO) but still cause pathology due to high concentrations used in the tests. Such testing strategies to not actually reduce the number of animals used. Here, for dietary bioaccumulation, the proposed testing strategy will reduce the number of animals used, in accordance with the 3 R's. Indeed, the use of fish as surrogates may be possible, with the addition of temperature appropriate characterisation of metals and ENMs.

There has been concern over the environmental safety of nanomaterials. And the testing strategy should provide data that enables the protection of populations of organisms and the services from ecosystems as well as biodiversity. The proposed bioaccumulation testing strategy for ENMs involved a dietary bioaccumulation method (Handy et al. 2018). The current data (Chapter 3) show there is minimal concern from dietary exposure to fish through no biochemical, electrolyte or histological disturbances. However, snails seem to be particularly sensitive to dietary exposures. For example, snails fed ZnO particles resulted in damage to the digestive tract causing a reduction in appetite; and of the food consumed, it was processed less efficiently (Croteau et al. 2011a). Similar observations were also made when snails were exposed to Ag NPs (Croteau et al. 2011b). Also, snails exposed to aged TiO_2 particles showed decreased growth and reproduction, potentially through altered gastrointestinal physiology (Fouqueray et al. 2012). Therefore, current regulatory testing may not be protective of all organisms where testing strategies are designed for dissolved chemicals.

7.5 Conclusions and future work

In conclusion, the data here provides evidence for the utility of a tiered approach for bioaccumulation testing using chemical characterisation to *ex vivo* and finally *in vivo* testing. In order to advocate for its use, more materials should be tested (e.g. cadmium quantum dots and gold NPs). If this works for ENMs, it may be possible to transfer to other classes of emerging contaminants (e.g. microplastics).

The chemistry steps required to demonstrate the suitability of an extraction matrix has been presented. The data here are specific to the chemistry of silver, but the step-wise process should be able to be applied to other elements. There is still a need to adequately define the particle metrics from *in vivo* tissue samples for the limit of detection to ensure particle measurements (e.g., primary particle size) are made, and not artefacts of data handling. Additionally, particle size measurements that are endogenously made come with uncertainly in size due to the lack of knowledge of speciation of particulate Ag. It may be beneficial to incorporate the use of hyphenated ICP-MS techniques (e.g., HPLC). Equally, the potential speciation could be analysed as reported here; for example, look for elevated sulphur particles in treatments, which would indicate particulate Ag_2S formation.

These Ag materials exist as particles *in vivo* when exposed to the gut in a carnivorous fish. There is uncertainty over where particle are being made in the fish, either the gut lumen or in the tissue. A future experiment could consider collecting the gut contents of trout fed the Ag-containing diets, extract the Ag and determine its form using spICP-MS. This would allow quantification of dissolution in the stomach and potential precipitation in the intestine, and determine which form of Ag the gut is exposed to. Alternatively, it may be possible to use molecular techniques (e.g., proteomics) to help understand the mechanisms of uptake into the gut and internal organs.

It would be interesting to see the same experimental design used in the dietary bioaccumulation study but in a zebrafish. Zebrafish do not possess an acidic stomach, with

the pH of the gut lumen remaining 7 or higher. By feeding the same diets to zebrafish, it would allow a side-by-side comparison as to the role of the acidic stomach in Ag NP transformation. The use of zebrafish as a model organism would allow an assessment of the effects of trophic transfer (e.g., Daphnia to zebrafish); would Ag NPs remain particulate when incorporated into an invertebrate diet.

References

Al-Bairuty, G. A., Boyle, D., Henry, T. B. and Handy, R. D. (2016). Sublethal effects of copper sulphate compared to copper nanoparticles in rainbow trout (*Oncorhynchus mykiss*) at low pH: physiology and metal accumulation. *Aquatic Toxicology*. 174, 188-198.

Al-Jubory, A. R. and Handy, R. D. (2013). Uptake of titanium from TiO_2 nanoparticle exposure in the isolated perfused intestine of rainbow trout: nystatin, vanadate and novel Co_2-sensitive components. *Nanotoxicology*. 7, 1282-1301.

Andersen, O., Nielsen, J. B., Sorensen, J. A. and Scherrebeck, L. (1994). Experimental localization of intestinal uptake sites for metals (Cd, Hg, Zn, Se) *in vivo* in mice. *Environmental Health Perspectives*. 102, 199-206.

Ates, M., Arslan, Z., Demir, V., Daniels, J. And Farah, I. O. (2015). Accumulation and toxicity of CuO and ZnO nanoparticles through waterborne and dietary exposure of goldfish (*Carassius auratus*). *Environmental Toxicology*. 30, 119-128.

Auffan, M., Rose, J., Bottero, J.-Y., Lowry, G. V., Jolivet, J.-P. And Wiesner, M. R. (2009). Towards a definition of inorganic nanoparticles from an environmental, health and safety perspective. *Nature Nanotechnology*. 4, 534-641.

Baccaro, M., Undas, A. K., de Vriendt, J., van den Berg, J. H. J., Peters, R. J. B. and van den Brink, N. W. (2018). Ageing, dissolution and biogenic formation of nanoparticles: how do these factors affect the uptake kinetics of silver nanoparticles in earthworms? *Environmental Science: Nano*. 5, 1107-1116.

Baker, T. J., Tyler, C. R. and Galloway, T. S. (2014). Impacts of metal and metal oxide nanoparticles on marine organisms. *Environmental Pollution*. 186, 257-271.

Bakke, A. M., Glover, C. and Krogdahl, Å. (2011). Feeding, digestion and absorption of nutrients. In: The Multifunctional Gut of Fish. *Elsevier*. 57-110.

Bao, D., Oh, Z. G. and Chen, Z. (2016). Characterization of silver nanoparticles internalized by *Arabidopsis* plants using single Particle ICP-MS analysis. *Frontiers in Plant Science*. DOI: 10.3389/fpls.2016.00032.

Baron, M. G., Mintram, K. S., Owen, S. F., Hetheridge, M. J., Moody, J., Purcell, W. M., Jackson, S. K. and Jha, A. N. (2017). Pharmaceutical metabolism in fish: using a 3-D hepatic *in vitro* model to assess clearance. *PLOS ONE*. DOI: 10.1371/journal.pone.0168837.

Barron, M. G., Stehly, G. R. and Hayton, W. L. (1990). Pharmacokinetic modelling in aquatic animals I. Models and concepts. *Aquatic Toxicology*. 18, 61-86.

Besinis, A., Peralta, T. D. and Handy, R. D. (2014). The antibacterial effects of silver, titanium dioxide and silica dioxide nanoparticles compared to the dental disinfectant chlorhexidine on *Steptococcus mutans* using a suite of bioassays. *Nanotoxicology*. 8, 1-16.

Bisesi, J. H., Merten, J., Liu, K., Parks, A. N., Afrooz, A. R. M. N., Glenn, J. B., Klaine, S. J., Kane, A. S., Saleh, N. B., Ferguson, P. L. and Sabo-Attwood. (2014). Tracking and quantification of single-walled carbon nanotubes in fish using near infrared fluorescence. *Environmental Science and Technology*. 48, 1973-1983.

Bleeker, E. A. J., de Jong, W, H., Geertsma, R. E., Groenewold, M., Heugens, E. H. W., Koers-Jacquemijns, M., van de Meent, D., Popma, J. R., Rietveld, A. G., Wijnhoven, S. W. P., Cassee, F. R. and Oomen, A. G. (2013). Considerations on the EU definition of a nanomaterial: Science to support policy making. *Regulatory Toxicology and Pharmacology*. 65, 119-125

Bobo, D., Robinson, K. J., Islam, J., Thurecht, K. J. and Corrie, S. R. (2016). Nanoparticle-based medicines: A review of FDA-approved materials and clinical trials to date. *Pharmaceutical Research*. 33, 2373-2387.

Bondarenko, O., Juganson, K., Ivask, A., Kasemets, K., Mortimer, M. and Kahru, A. (2013). Toxicity of Ag, CuO and ZnO nanoparticles to selected environmentally relevant test

organisms and mammalian cells in vitro: a critical review. *Archives of Toxicology*. 87, 1181-1200.

Borgå, K., Fisk, A. T., Hoekstra, P. F. and Muir, D. C. G. (2004). Biological and chemical factors of importance in the bioaccumulation and trophic transfer of persistent organochlorine contaminants in Arctic marine food webs. *Environmental Toxicology and Chemistry*. 23, 2367-2385.

Bouwmeester, H., Brandhoff, P., Marvin, H. J., Wiegel, S. and Peters, R. J. (2014). State of the safety assessment and current use of nanomaterials in food and food production. *Trends in food science and technology*. 40, 200-210.

Boyle, D., Al-Bairuty, G., Henry, T. B. and Handy, R. D. (2013). Critical comparison of intravenous injection of TiO_2 nanoparticles with waterborne and dietary exposures concludes minimal environmentally-relevant toxicity in juvenile rainbow trout *Oncorhynchus mykiss*. *Environmental Pollution*. 182, 70-79.

Boyle, D., Clark, N. J., Botha, T. L. and Handy, R. D. (in preparation). Gut environment is a determinant of dietary bioavailability of copper oxide nanomaterials in rainbow trout (*Oncorhynchus mykiss*).

Boyle, D., Sutton, P. A., Handy, R. D. and Henry, T. B. (2018). Intravenous injection of uncfunctionaized carbon-based nanomaterials confirms the minimal toxicity observed in aqueous and dietary exposures in juvenile rainbow trout (*Oncorhynchus mykiss*). *Environmental Pollution*. 232, 191-199.

Bron, P. A., Kleerebezem, M., Brummer, R.-J., Cani, P. D., Mercenier, A., MacDonald, T. T., Garcia-Ródenas, C. L. and Wells, J. M. (2017). Can probiotics modulate human disease by impacting intestinal barrier function? *British Journal of Nutrition*. 117, 93-107.

Bucking, C. and Wood, C. M. (2006). Gastrointestinal processing of Na^+, Cl^-, and K^+ during digestion: implications for homeostatic balance in freshwater rainbow trout. *American*

Journal of Physiology – Regulatory, Integrative and Comparative Physiology. 291, R1764-R1772.

Bucking, C. and Wood, C. M. (2007). Gastrointestinal transport of Ca^{2+} and Mg^{2+} during the digestion of a single meal in the freshwater rainbow trout. *Journal of Comparative Physiology B*. 177, 349-360.

Bucking, C. and Wood, C. M. (2009). The effect of postprandial changes in pH along the gastrointestinal tract on the distribution of ions between the solid and fluid phases of chyme in rainbow trout. *Aquaculture Nutrition*. 15, 282-296.

Burke, J and Handy, R. D. (2005). Sodium-sensitive and –insensitive copper accumulation by isolated intestinal cells of rainbow trout *Oncorhynchus mykiss*. *The Journal of Experimental Biology*. 208, 391-407.

Bury, N. R. and Wood, C. M. (1999). Mechanism of branchial apical silver uptake by rainbow trout is via the proton-coupled Na^{+} channel. *American Journal of Physiology – Regulatory, Integrative and Comparative Physiology*. 277, R1385-R1391.

Bury, N. R., Galvez, F. and Wood, C. M. (1999). Effects of chloride, calcium and dissolved organic carbon on silver toxicity: comparison between rainbow trout and fathead minnows. *Environmental Toxicology and Chemistry*. 18, 56-62.

Bury, N. R., Grosell, M., Wood, C. M., Hogstrand, C., Wilson, R. W., Rankin, J. C., Busk, M., Lecklin, T. and Jensen, F. B. (2001). Intestinal iron uptake in the European flounder (*Platichthys flesus*). *The Journal of Experimental Biology*. 204, 3779-3787.

Bustos, A. R. M., Petersen, E. J., Possolo, A. and Winchester, M. R. (2015). Post hoc interlaboratory comparison of single particle ICP-MS size measurements of NIST gold nanoparticle reference materials. *Analytical Chemistry*. 87, 8809-8817.

Campbell, H. A., Handy, R. D. and Nimmo, M. (1999). Copper uptake kinetics across the gills of rainbow trout (*Oncorhynchus mykiss*) measured using an improved isolated perfused head technique. *Aquatic Toxicology*. 46, 177-190.

Chaudhry, Q., Aitken, R., Scotter, R., Blackburn, J., Ross, B., Boxall, A., Castle, L. and Watkins, R. (2008). Applications and implications of nanotechnologies for the food sector. *Food Additives and Contaminants*. 25, 241-258.

Choi, H. S., Liu, W., Misra, P., Tanaka, E., Zimmer, J. P., Ipe, B. I., Bawendi, M. G. and Frangioni, J. V. (2007). Renal clearance of quantum dots. *Nature Biotechnology*. 25, 1165-1170.

Chowdhury, M. J., Baldisserotto, B. and Wood, C. M. (2005). Tissue-specific cadmium and metallothionein levels in rainbow trout chronically acclimated to waterborne or dietary cadmium. *Archives of Environmental Contamination and Toxicology*. 48, 381-390.

Christian, P., Von der Kammer, F., Baalousha, M. And Hofmann, Th. (2008). Nanoparticles: structure, properties, preparation and behaviour in environmental media. *Ecotoxicology*. 17, 326-343.

Clark, N. J., Shaw, B. J. and Handy, R. D. (2018). Low hazard of silver nanoparticles and silver nitrate to the haematopoietic system of rainbow trout. *Ecotoxicology and Environmental Safety*. 152, 121-131.

Clearwater, S. J., Baskin, S. J., Wood, C. M. and McDonald, D. G. (2000). Gastrointestinal uptake and distribution of copper in rainbow trout. *The Journal of Experimental Biology*. 203, 2455-2466.

Clearwater, S. J., Farag, A. M. and Meyer, J. S. (2002). Bioavailability and toxicity of dietborne copper and zinc to fish. *Comparative Biochemistry and Physiology Part C*. 132, 269-313.

Comber, M. H. I., Walker, J. D., Watts, C. and Hermens, J. (2003). Quantitative structure-activity relationships for predicting potential ecological hazard of organic chemicals for use in regulatory risk assessments. *Environmental Toxicology and Chemistry*. 22, 1822-1828.

Conner, S. D. and Schmid, S. L. (2003). Regulated portals of entry into the cell. *Nature*. 422, 37-44.

Connolly, M., Fernándsez, M., Conde, E., Torrent, F., Navas, J. M. and Fernández-Cruz, M. L. (2016). Tissue distribution of zinc and subtle oxidative stress effects after dietary administration of ZnO nanoparticles to rainbow trout. *Science of the Total Environment*. 551-552, 334-343.

Cooper, C. A., Bury, N. R. and Grosell, M. (2006). The effects of pH and the iron redox state on iron uptake in the intestine of a marine teleost fish, gulf toadfish (*Opsanus beta*). *Comparative Biochemistry and Physiology, Part A*. 143, 292-298.

Croteau, M.-N., Dybowska, A. D., Luoma, S. N. and Valsami-Jones, E. (2011a). A novel approach reveals that zinc oxide nanoparticles are bioavailable and toxic after dietary exposures. *Nanotoxicology*. 5, 79-90.

Croteau, M.-N., Misra, S. K., Luoma, S. N. and Valsami-Jones, E. (2011b). Silver bioaccumulation dynamics in a freshwater invertebrate after aqueous and dietary Exposures to nanosized and ionic Ag. *Environmental Science and Technology*. 45, 6600-6607.

D'Agata, A., Fasulo, S., Dallas, L. J., Fisher, A. S., Maisano, M., Readman, J. W. and Jha, A. N. (2014). Enhanced toxicity of 'bulk' titanium dioxide compared to 'fresh' and 'aged' nano-TiO_2 in marine mussels (*Mytilus galloprovincialis*). *Nanotoxicology*. 8, 549-558.

da Silva, C. F., Severine, P., Martins, F., Chaud, M. V. and Santana, M. H. A. (2009). The intestinal permeation of didanosine from granules containing microspheres using the everted gut sac model. *Journal of microencapsulation*. 26, 523-528.

Dan, Y., Ma, X., Zhang, W., Liu, K., Stephan, C. and Shi, H. (2016). Single particle ICP-MS method development for the determination of plant uptake and accumulation of CeO_2 nanoaprticles. *Analytical and Bioanalytical Chemistry*. 408, 5157-5167.

Dan, Y., Zhang, W., Xue, R., Ma, X., Stephan, C. and Shi, H. (2015). Characterization of gold nanoparticle uptake by tomato plants using enzymatic extraction followed by single-particle inductively coupled plasma-mass spectrometry. *Environmental Science and Technology*. 49, 3007-3014.

Degueldre, C. and Favarger, P.-Y. (2003). Colloid analysis by single particle inductively coupled plasma-mass spectrometry: a feasibility study. *Colloids and Surfaces A: Physicochemical and Engineering Aspects*. 217, 137-142.

de la Morinière, E. C., Pollux, B. J. A., Nagelkerken, I., Hemminga, M. A., Huiskes, A. H. L. and van der Velde, G. (2003). Ontogenetic dietary changes of coral reef fishes in the mangrove-seagrass continuum: stable isotope and gut-content analysis. *Marine Ecology Progress Series*. 246, 279-289.

Deng, Y., Petersen, E. J., Challis, K. E., Rabb, S. A., Holbrook, R. D., Ranville, J. F., Nelson, B. C. and Xing, B. (2017). Multiple method analysis of TiO_2 nanoparticle uptake in rice (*Oryza sativa* L.) plants. *Environmental Science and Technology*. 51, 10615-10623.

Deniz, V., Boström, M., Bratko, D., Tavares, F. W. and Ninham, B. W. (2009). Specific ion effects: Interaction between nanoparticles in electrolyte solutions. *Colloids and Surfaces A: Physicochemical Engineering Aspects*. 319, 98-102.

Dhanakumar, S., Solaraj, G. and Mohanraj, R. (2015). Heavy metal partitioning in sediments and bioaccumulation in commercial fish species of three major reservoirs of river Cauvery delta region, India. *Ecotoxicology and Environmental Safety*. 113, 145-151.

Dixon, C. and Mizen, L. W. (1977). Absorption of amino penicillins from everted rat intestine. *The Journal of Physiology*. 269, 549-559.

Dowdle, E. B., Schachter, D. and Schenker, H. (1960). Active transport of Fe^{59} by everted segments of rat duodenum. *American Journal of Physiology*. 3, 609-613.

Dumont, E., Johnson, A. C., Keller, V. D. J. and Williams, R. J. (2015). Nano silver and nano zinc-oxide in surface waters – Exposure estimation for Europe at high spatial and temporal resolution. *Environmental Pollution*. 196, 341-349.

El Basuini, M. F., El-Hais, A. M., Dawood, M. A. O., Abou-Zeid, A. E.-S., El-Damrawy, S. Z., Khalafalla, M. M. E.-S., Koshio, S., Ishikawa, M. and Dossou, S. (2016). Effect of different levels of dietary copper nanoparticles and copper sulphate on growth performance, blood biochemical profile, antioxidant status and immune response of red sea bream (*Pagrus major*). *Aquaculture*. 455, 32-40.

Elle, R. E., Gaillet, S., Vidé, J., Romain, C., Lauret, C., Rugani, N., Cristol, J. P. and Rouanet, J. M. (2013). Dietary exposure to silver nanoparticles in Sprague-Dawley rats: Effects on oxidative stress and inflammation. *Food and Chemical Toxicology*. 60, 297-301.

El-Sayed, R., Bhattacharya, K., Gu, Z., Yang, Z., Weber, J. K., Li, H., Leifer, K., Zhao, Y., Toprak, M. S., Zhou, R. and Fadeel, B. (2016). Single-walled carbon nanotubes inhibit the cytochrome P450 enzyme, CYP3A4. *Scientific Reports*. 6. DOI: 10.1038/srep21316.

Escher, B. I. and Sigg, L. (2004). Chemical speciation of organics and of metals at biological interphases. In: Physicochemical Kinetics and Transport at Biointerfaces.John Wiley and Sons Ltd, UK. 205-269.

Fabrega, J., Luoma, S. N., Tyler, C. R., Galloway, T. S. and Lead, J. R. (2011). Silver nanoparticles: Behaviour and effects in the aquatic environment. *Environmental International*. 37, 517-531.

Farag, A., Boese, C. J., Woodward, D. F. and Bergman, H. L. (1994). Physiological changes and tissue metal accumulation in rainbow trout exposed to foodborne and waterborne metals. *Environmental Toxicology and Chemistry*. 13, 2021-2029.

Ferguson, E. A. and Hogstrand, C. (1998). Acute silver toxicity to seawater-acclimated rainbow trout: influence of salinity on toxicity and silver speciation. *Environmental Toxicology and Chemistry*. 17, 589-593.

Fjällborg, B. and Dave, G. (2004). Toxicity of Sb and Cu in sewage sludge to terrestrial plants (lettuce, oat, radish), and sludge elutriate to aquatic organisms (Daphnia and Lemna) and its interaction. *Water, Air, and Soil Pollution*. 155, 3-20.

Flemming, C. A. and Trevors, J. T. (1989) Copper toxicity and chemistry in the environment: a review. *Water, Air, and Soil Pollution*. 44, 143-158.

Folkmann, J. K., Risom, L., Jacobsen, N. R., Wallin, H., Loft, S. and Møller, P. (2009). Oxidatively damaged DNA in rats exposed by oral gavage to C_{60} fullerenes and single-walled carbon nanotubes. *Environmental Health Persepctives*. 117, 703-708.

Fouqueray, M., Dufils, B., Vollat, B., Chaurand, P., Botta, C., Abacci, K., Labille, J., Rose, J. and Garric, J. (2012). Effect of aged TiO_2 nanomaterial from sunscreen on *Daphnia magna* exposed by dietary route. *Environmental Pollution*. 163, 55-61.

Fraser, T. W. K., Reinardy, H. C., Shaw, B. J., Henry, T. B. and Handy, R. D. (2011). Dietary toxicity of single-walled carbon nanotubes and fullerenes (C_{60}) in rainbow trout (*Oncorhynchus mykiss*). *Nanotoxicology*. 5, 98-108.

Gaiser, B. K., Fernandes, T. F., Jepson, M. A., Lead, J. R., Tyler, C. R., Baalousha, M., Biswas, A., Britton, G. J., Cole, P. A., Johnston, B. D., Ju-Nam, Y., Rosenkranz, P., Scown, T. M. and Stone, V. (2012). Interspecies comparisons on the uptake and toxicity of silver and cerium dioxide nanoparticles. *Environmental Toxicology and Chemistry*. 31, 144-154.

Gajewicz, A., Cronin, M. T. D., Rasulev, B., Leszczynski, J. and Puzyn, T. (2015). Novel approach for efficient predictions properties of large pool of nanomaterials based on limited set of species: nano-read-across. *Nanotechnology*. 26, 015701.

Galvez, F. and Wood, C. (1999). Physiological effects of dietary silver sulphide exposure in rainbow trout. *Environmental Toxicology and Chemistry*. 18, 84-88.

Galvez, F., Hogstrand, C., McGeer, J. C. and Wood, C. M. (2001). The physiological effects of a biologically incorporated silver diet on rainbow trout (*Oncorhynchus mykiss*). *Aquatic Toxicology*. 55, 95-112.

García-Alonso, J., Khan, F. R., Misra, S. K., Turmaine, M., Smith, B. D., Rainbow, P. S., Luoma, S. N. and Valsami-Jones, E. (2011). Cellular Internalisation of silver nanoparticles in gut epithelial of the estuarine polychaete *Nereis diversicolor*. *Environmental Science and Technology*. 45, 4630-4636.

Gargiulo, A. M., Ceccarelli, P., Aglio, C.D. and Pedini, V. (1998). Histology and ultrastructure of the gut of the tilapia (*Tilapia* spp), a hybrid teleost. *Anatomia, Histologia, Embryologia*.27, 89-94.

Ge, C., Du, J., Zhao, L., Wang, L., Liu, Y., Li, D., Yang, Y., Zhou, R., Zhao, Y., Chai, Z. and Chen, C. (2011). Binding of blood proteins to carbon nanotubes reduced cytotoxicity. *Proceedings of the National Academy of Sciences of the United States of America*. 108, 16968-16973.

Geraets, L., Oomen, A. G., Krystek, P., Jacobsen, N. R., Wallin, H., Laurentie, M., Verharen, H. W., Brandon, E. F. A. and de Jong, W. H. (2014). Tissue distribution and elimination after oral and intravenous administration of different titanium dioxide nanoparticles in rats. *Particle and Fibre Toxicology*. DOI: 10.1186/1743-8977-11-30.

Gitrowski, C., Al-Jubory, A. and Handy, R. D. (2014). Uptake of different crystal structures of TiO_2 nanoparticles by Caco-2 intestinal cells. *Toxicology Letters*. 226, 264-276.

Givens, C. E., Ransom, B., Bano, N. and Hollibaugh, J. T. (2015). Comparison of the gut microbiome of 12 bony fish and 3 shark species. *Marine Ecology Progress Series*. 518, 20-233.

Glover, C. N. and Hogstrand, C. (2002). Amino acid modulation of *in vivo* intestinal zinc absorption in freshwater rainbow trout. *The Journal of Experimental Biology*. 205, 151-158.

Gottschalk, F., Sun, T. Y. and Nowack, B. (2013). Environmental concentrations of engineered nanomaterials: Review of modelling and analytical studies. *Environmental Pollution*. 181, 287-300.

Gray, E. P., Coleman, J. G., Bednar, A. J., Kennedy, A. J., Ranville, J. F. and Higgins, C. P. (2013). Extraction and analysis of silver and gold nanoparticles from biological tissues using single particle inductively coupled plasma mass spectrometry. *Environmental Science and Technology*. 47, 14315-14323.

Grombe, R., Allmaier, G., Charoud-Got, J., Dudkiewicz, A., Emteborg, H., Hofmann, T., Larsen, E. H., Lehner, A., Llinàs, M., Loeschner, K., Mølhave, K., Peters, R. J., Seghers, J., Solans, C., von der Kammer, F., Wagner, S., Weigel, S. and Linsinger, T. P. J. (2015). Feasibility of the development of reference materials for the detection of Ag nanoparticles in food: meat dispersions and spiked chicken meat. *Accreditation and Quality Assurance*. 20, 3-16.

Grosell, M. (2012). Copper. In: Homeostasis and Toxicology of Essential Metals. Elsevier. 54-133.

Grosell, M. H., Hogstrand, C. and Wood, C. M. (1998). Renal Cu and Na excretion and hepatic Cu metabolism in both Cu acclimated and non acclimated rainbow trout (*Oncorhynchus mykiss*). *Aquatic Toxicology*. 40, 275-291.

Hadrup, N. and Lam, H. R. (2014). Oral toxicity of silver ions, silver nanoparticles and colloidal silver – A review. *Regulatory Toxicology and Pharmacology*. 68, 1-7.

Handy, R. D. and Eddy, B. F. (2004). Transport of solutes across biological membranes in Eukaryotes: an environmental perspective. In: Physicochemical Kinetics and Transport at Biointerfaces.John Wiley and Sons Ltd, UK. 337-356.

Handy, R. D. and Eddy, F. B. (1991). Effects of inorganic cations on Na^+ adsorption to the gill and body surface of rainbow trout, *Oncorhnychus mykiss*, in dilute solutions. *Canadian Journal of Fisheries and Aquatic Sciences*. 48, 1829-1837.

Handy, R. D. and Eddy, F. B. (2004) Transport of solutes across biological membranes in eukaryotes: An environmental perspective. In Physicochemical Kinetics and Transport at Chemical-Biological Interphases (editors H. P. van Leeuwen and W. Köster), IUPAC series, pp. 337-356, John Wiley, Chichester.

Handy, R. D. and Eddy, F.B. (1989). Surface absorption of aluminium by gill tissue and body mucus of rainbow trout, *Salmo gairdneri*, at the onset of episodic exposure. 34, 865-874.

Handy, R. D. and Maunder, R. J. (2009). The biological roles of mucus: importance for osmoregulation and osmoregulatory disorders of fish health. In: Osmoregulation and ion transport: integrating physiological, molecular and environmental aspects. *Essential Reviews in Experimental Biology.* London: Society for Experimental Biology Press.

Handy, R. D., Ahtiainen, J., Navas, J. M., Goss, G., Bleeker, E. A. J. and von der Kammer, F. (2018) Proposal for a tiered dietary bioaccumulation testing strategy for engineered nanomaterials using fish. *Environmental Science: Nano*. 5, 2030-2046.

Handy, R. D., Al-Bairuty, G., Al-Jubory, A., Ramsden, C. S., Boyle, D., Shaw, B. J. and Henry, T. B. (2011). Effects of manufactured nanomaterials on fishes: a target organ and body systems physiology approach. *Journal of Fish Biology*. 79, 821-853.

Handy, R. D., Cornelis, G., Fernandes, T., Tsyusko, O., Decho, A., Sabo-Attwood, Metcalfe, C., Steevens, J. A., Klaine, S. J., Koelmans, A. A. and Horne, N. (2012). Ecotoxicity test methods for engineered nanomaterials: practical experiences and recommendations from the bench. *Environmental Toxicology and Chemistry*. 31, 15-31.

Handy, R. D., Henry, T. B., Scown, T. M., Johnston, B. D. and Tyler, C. R. (2008a). Manufactured nanoparticles: their uptake and effects on fish-a mechanistic analysis. *Ecotoxicology*. 17, 396-409.

Handy, R. D., McGeer, J. C., Allen, H. E., Drevnick, P. E., Gorsuch, J. W., Green, A. S., Lundebye, A.-K., Hook, S. E., Mount, D. R. and Stubblefield, W. A. (2005). Toxic effects of dietborne metals: laboratory studies. In *Toxicity of Dietborne Metals to Aquatic Organisms* (Meyer, J. S., Adams, W. J., Brix, K. V., Luoma, S. N., Mount, D. R., Stubblefield, W. A. and Wood, C. M., eds). 59-112. Pensacola, FL: SETAC Press.

Handy, R. D., Musonda, M. M., Phillips, C. and Falla, S. J. (2000). Mechanisms of gastrointestinal copper absorption in the African Walking Catfish: copper dose-effects and a novel anion-dependent pathway in the intestine. *The Journal of Experimental Biology*. 203, 2365-2377.

Handy, R. D. and Poxton, M. G. (1993). Nitrogen pollution in mariculture: toxicity and excretion of nitrogenous compounds by marine fish. *Reviews in Fish Biology and Fisheries*. 3, 205-241.

Handy, R. D., von der Kammer, F., Lead, J. R., Hassellöv, M., Owen, R. and Crane, M. (2008b). The ecotoxicology and chemistry of manufactured nanoparticles. *Ecotoxicology*. 17, 287-314.

Hermenean, A., Damache, G., Albu, P., Ardelean, A., Ardelean, G., Ardelean, D. P., Horge, M., Nagy, T., Braun, M., Zsuga, M., Kéki, S., Costache, M. and Dinischiotu, A. (2015). Histopathological alterations and oxidative stress in liver and kidney of *Leuciscus cephalus* following exposure to heavy metals in the Tur River, North Western Romania. *Ecotoxicology and Environmnetal Safety*. 119, 198-205.

Hickman, C. P. (1968). Ingestion, intestinal adsorption, and elimination of seawater and salts in the southern flounder, *paralichthys lethostigma*. *Canadian Journal of Zoology*. 46, 457-466.

Hoadley, J. E. and Johnson, D. R. (1987). Effects of calcium on cadmium uptake and binding in the rat intestine. *Fundamental and Applied Toxicology*. 9, 1-9.

Hogstrand, C. (2012). Zinc. In: Homeostasis and Toxicology of Essential Metals. Elsevier. 136-200.

Hogstrand, C. and Wood, C. M. (1998). Toward a better understanding of the bioavailability, physiology, and toxicity of silver in fish: implications for water quality criteria. *Environmental Toxicology and Chemistry*. 17, 547-561.

Hogstrand, C., Grosell, M., Wood, C. M. and Hansen, H. (2003). Internal redistribution of radiolabelled silver among tissues of rainbow trout (*Oncorhynchus mykiss*) and European eel (*Anguila Anguilla*): the influence of silver speciation. *Aquatic Toxicology*. 63, 139-157.

Hou, W.-C., Westerhoff, P. And Posner, J. D. (2013). Biological accumulation of engineered nanomaterials: a review of current knowledge. *Environmental Science: Processes and Impacts*. 15, 103-122.

Hoyle, I. and Handy, R. D. (2005). Dose-dependent inorganic mercury absorption by isolated perfused intestine of rainbow trout, *Oncorhynchus mykiss*, involves both amiloride-sensitive and energy-dependent pathways. *Aquatic Toxicology*. 72, 147-159.

Hoyle, I., Shaw, B. J. and Handy, R. D. (2007). Dietary copper exposure in the African walking catfish, *Clarias gariepinus*: Transient osmoregulatory disturbances and oxidative stress. *Aquatic Toxicology*. 83, 62-72.

Jafvert, C. T. and Kulkarni, P. P. (2008). Buckminsterfullerene's (C_{60}) octanol-water partition coefficient (K_{OW}) and aqueous solubility. *Environmental Science and Technology*. 42, 5945-5950.

Javurek, A., Suresh, D., Spollen, W. G., Hart, M. L., Hanesen, S. A., Ellersieck, M. R., Bivens, N. J., Givan, S. A., Upendran, A., Kannan, R. and Rosenfeld, C. S. (2017). Gut dysbiosis and neurobehavioural alterations in rats exposed to silver nanoparticles. *Scientific Reports*. DOI: 10.1038/s41598-017-02880-0.

Jiménez-Lamana, J., Abad-Álvaro, I., Bierla, K., Laborda, F., Szpunar, J. and Lobinski, R. (2018). Detection and characterization of biogenic selenium nanoparticles in selenium-rich yeast by single particle ICP-MS. *Journal of Analytical Atomic Spectrometry*. 33, 452-460.

Johari, S. A., Kalbassi, M. R., Yu, I. J. and Lee, J. H. (2014). Chroinc effect of waterborne silver nanoparticles on rainbow trout (*Oncorhnuchus mykiss*): histopathology and bioaccumulation. *Comparative Clinical Pathology*. 24, 995-1007.

Johnston, B. D., Scown, T. M., Moger, J., Cumberland, S. A., Baalousha, M., Linge, K., van Aerle, R., Jarvis, K., Lead, J. R. and Tyler, C. R. (2010). Bioavailability of nanoscale metal oxides TiO_2, CeO_2, and ZnO to fish. *Environmental Science and Technology*. 44, 1144-1151.

Johnston, H. J., Verdon, R., Gillies, S., Brown, D. M., Fernandes, T. F., Henry, T. B., Rossi, A. G., Tran, L., Tucker, C., Tyler, C. R. and Stone, V. (2018). Adoption of *in vitro* systems and zebrafish embryos as alternative models for reducing rodent use in assessments of immunological and oxidative stress responses to nanomaterials. *Critical Reviews in Toxicology*. 48, 252-271.

Kaegi, R., Voegelin, A., Ort, C., Sinnet, B., Thalmann, B., Krismer, J., Hagenorfer, H., Elumelu, M. and Mueller, E. (2013). Fate and transformation of silver nanoparticles in urban wastewater systems. *Water Research*. 47, 3866-3877.

Kahru, A. and Dubourguier, H.-C. (2010). From ecotoxicology to nanoecotoxicology. *Toxicology*. 269, 105-119.

Kamunde, C. and Wood, C. M. (2003). The influence of ration size on copper homeostasis during sublethal dietary copper exposure in juvenile rainbow trout, *Oncorhynchus mykiss*. *Aquatic Toxicology*. 62, 235-254.

Karickhoff, S. W. (1984). Organic pollutant sorption in aquatic systems. *Journal of Hydraulic Engineering*. 111, 707-735.

Karthikeyeni, S., Vijayakumar, T. S., Vasanth, S., Ganesh, A., Manimegalai, M. and Subramanian, P. (2013). Biosynthesis of iron oxide nanoparticles and its haematological effects on fresh water fish *Oreochromis mossambicus*. *Journal of Academia and Industrial Research*. 1, 645-649.

Katouzian, I. and Jafari, S. M. (2014) Nano-encapsulation as a promising approach for targeted delivery and controlled release of vitamins. *Trends in Food Science and Technology*. 53, 34-48.

Khan, F. R., Misra, S. K., García-Alonso, J., Smith, B. D., Strekopytov, S., Rainbow, P. S., Luoma, S. N. and Valsami-Jones, E. (2012). Bioaccumulation dynamics and modeling in an estuarine invertebrate following aqueous exposure to nanosized and dissolved Silver. *Environmental Science and Technology*.

Khan, M. S., Jabeen, F., Qureshi, N. A., Asghar, M. S., Shakeel, M. and Noureen, A. (2015). Toxicity of silver nanoparticles in fish: a critical review. *Journal of Biodiversity and Environmental Sciences*. 6, 211-227.

Kiser, M. A., Westerhoff, P., Benn, T., Wang, Y., Pérez-Rivera, J. And Hristovski, K. (2009). Titanium nanomaterial removal and release from wastewater treatment plants. *Environmental Science and Technology*. 43, 6757-6763.

Klaine, S. J., Koelmans, A. A., Horne, N., Carley, S., Handy, R. D., Kapustka, L., Nowack, B. and von der Kammer, F. (2012). Paradigms to assess the environmental impact of manufactured nanomaterials. *Environmental Toxicology and Chemistry*. 31, 3-14.

Kleiven, M., Rosseland, B. O., Teien, H.-C., Joner, E. J. and Oughton, D. H. (2018). Route of exposure has a major impact on uptake of silver nanoparticles in Atlantic salmon (*Salmo salar*). *Environmental Toxicology and Chemistry*. 37, 2895-2903.

Koelmans, A. A., Diepends, N. J., Velzeboer, I., Besseling, E., Quik, J. T. K. And van de Meent, D. (2015). Guidance for the prognostic risk assessment of nanomaterial in aquatic ecosystems. *Science of the Total Environment*. 141-149.

Köster, W. and van Leeuwen, H. P. (2004). Physicochemical kinetics and transport at the biointerface: Setting the stage. In: Physicochemical Kinetics and Transport at Biointerfaces.John Wiley and Sons Ltd, UK. 1-14.

Kreyling, W. G., Holzawarth, U., Haberl, N., Kozempel, J., Him, S., Wenk, A., Schleh, C., Schäffler, M., Lipka, J., Semmler-Behnke, M. and Gibson, N. (2017). Quantitative biokinetics of titanium dioxide nanoparticles after intravenous injection in rats: Part 1. *Nanotoxicology*. 11, 434-442.

Kwong, R. W. M. and Niyogi, S. (2009). The interactions of iron with other divalent metals in the intestinal tract of a freshwater teleost, rainbow trout (*Oncorhynchus mykiss*). *Comparative Biochemistry and Physiology, Part C*. 150, 442-449.

Labille, J., Harns, C., Bottero, J.-Y. And Brant, J. (2015). Heteroaggregation of titanium dioxide nanoparticles with natural clay colloids. *Environmental Science and Technology*. 49, 6608-6616.

Laborda, F., Jiménez-Lamana, J., Bolea, E. and Castillo, J. R. (2011). Selective identification, characterization and determination of dissolved silver (I) and silver nanoparticles based on single particle detection by inductively coupled plasma mass spectrometry. *Journal of Analytical Atomic Spectrometry.* 26, 1362-1371.

Ladhar, C., Geffroy, B., Cambier, S., Treguer-Delapierre, M., Durand, E., Brèthes, D. and Bourdineaud, J.-P. (2014). Impact of dietary cadmium sulphide nanoparticles on *Danio rerio* zebrafish at very low contamination pressure. *Nanotoxicology*. 8, 676-685.

Langan, L. M., Harper, G. M., Owen, S. F., Purcell, W. M., Jackson, S. K. and Jha, A. N. (2017). Application of the rainbow trout derived intestinal cell line (RTgutGC) for ecotoxicological studies: molecular and cellular responses following exposure to copper. *Ecotoxicology*. 26, 1117-1133.

Lanno, R. P., Hicks, B. and Hilton, J. W. (1987). Histological observations on intrahepatocytic copper-containing granules in rainbow trout reared on diets containing elevated levels of copper. *Aquatic Toxicology*. 10, 251-263.

Lead, J. R., Batley, G. E., Alvarez, P. J. J., Croteau, M.-N., Handy, R. D., McLaughlin, M. J., Judy, J. D. and Schirmer, K. (2018). Nanomaterials in the environment: behaviour, fate, bioavailability, and effects–An updated review. *Environmental Toxicology and Chemistry*. DOI: 10.1002/etc.4147.

Lemes, M. and Wang, F. (2009). Methylmercury speciation in fish muscle by HPLC-ICP-MS following enzymatic hydrolysis. *Journal of Analytical Atomic Spectrometry*. 24, 663-668.

Lesniak, A., Fenaroli, F., Monopoli, M. P., Aberg, C., Dawson, K. A. And Salvati, A. (2012). Effects of the presence or absence of a protein corona on silica nanoparticle uptake and impact on cells. *ACS Nano*. 6, 5845-5857.

Leung, H. M., Leung, A. O. W., Wang, H. S., Ma, K. K., Liang, Y., Ho, K. C., Cheung, K. C., Tohidi, F. and Yung, K. K. L. (2014). Assessment of heavy metals/metalloid (As, Pb, Cd, Ni, Zn, Cr, Cu, Mn) concentrations in edible fish species tissue in the Pearl River Delta (PRD), China. *Marine Pollution Bulletin*. 78, 235-245.

Levard, C., Hotze, E. M., Lowry, G. V. and Brown, Jr., G. E. (2012). Environmental transformations of silver nanoparticles: Impact on stability and toxicity. *Environmental Science and Technology*. 46, 6900-6914.

Li, S., Wallis, L., K., Ma, H. and Diamond, S. A. (2014). Phototoxicity of TiO_2 nanoparticles to a freshwater benthic amphipod: Are benthic systems at risk? *Science of the Total Environment*. 466-467, 800-808.

Lillicrap, A., Springer, T and Tyler, C. R. (2016). A tiered assessment strategy for more effective evaluation of bioaccumulation of chemicals in fish. *Regulatory Toxicology and Pharmacology*. 75, 20-26.

Linder, M. C. (2002). Biochemistry and molecular biology of copper in mammals. In Massoro EJ (ed.). *Handbook of Copper Pharmacology and Toxicology* (Tootwa NJ: Human Press, 3-12).

Liu, J., Chao, J., Liu, R., Tan, Z., Yin, Y., Wu, Y. and Jiang, G. (2009). Cloud point extraction as an advantageous preconcentration approach for analysis of trace silver nanoparticle in environmental waters. *Analytical Chemistry*. 81, 6496-6502.

Loeschner, K., Brabrand, M. S. J., Sloth, J. J. and Larsen, E. H. (2014). Use of alkaline or enzymatic sample pretreatment prior to characterization of gold nanoparticles in animal tissue by single-particle ICP-MS. *Analytical and Bioanalytical Chemistry*. 406, 3845-3851.

Loeschner, K., Navratilova, J., Købler, C., Mølhave, K., Wagner, S., von der Kammer, F. and Larsen, E. H. (2013). Detection and characterization of silver nanoparticles in chicken meat by asymmetric flow field fractionation with detection by conventional or single particle ICP-MS. *Analytical and Bioanalytical Chemistry*. 405, 8185-8195.

Loretz, C. A. (1995). Electrophysiology of ion transport in teleost intestinal cells. In: Wood, C. M. and Shuttleworth, T. J. (Eds), Cellular and Molecular Approaches to Fish Ionic Regulation. Academic Press, San Diego, CA, pp 25-56.

Lowry, G. V., Gregory, K. B. Apte, S. C. and Lead, J. R. (2012). Transformations of nanomaterials in the environment. *Environmental Science and Technology*. 46, 6893-6899.

Lundqvist, M., Stigler, J., Elia, G., Lynch, I., Cedervall, T. And Dawson, K. A. (2008). Nanoparticle size and surface properties determine the protein corona with possible implications for biological impacts. *Proceedings of the National Academy of Sciences of the United States of America*. 105, 14265-14270.

Luoma, S. N., Ho, Y. B. and Bryan, G. W. (1995). Fate, bioavailability and toxicity of silver in estuarine environments. *Marine Pollution Bulletin*. 31, 44-54.

Ma, H., Williams, P. L. and Diamond, S.A. (2013). Ecotoxicity of manufactured ZnO nanoparticles – A review. *Environmental Pollution*. 172, 76-85.

MacCormack, T. J., Clark, R. J., Dang, M. K. M., Ma, G., Kelly, J. A., Veinot, J. G. C. and Goss, G. G. (2012). Inhibition of enzyme activity by nanomaterials: Potential mechanisms and implications for nanotoxicity testing. *Nanotoxicology*. 6, 514-525.

Makama, S., Piella, J., Undas, A., Dimmers, W. J., Peters, R., Putnes, V. F. and van den Brink, N. W. (2016). Properties of silver nanoparticles influencing their uptake in and toxicity to the earthworm *Lumbricus rubellus* following exposure in soil. *Environmental Pollution*. 218, 870-878.

Manabe, M., Tatarazako, N. and Kinoshita, M. (2011). Uptake, excretion and toxicity of nano-sized latex particles on medaka (*Oryzias latipes*) embryos and larvae. *Aquatic Toxicology*. 105, 576-581.

Mandal, S., Gole, A., Lala, N., Gonnade, R., Ganvir, V. and Sastry, M., 2001. Studies on the reversible aggregation of cysteine-capped colloidal silver particles interconnected via hydrogen bonds. Langmuir, 17(20), 6262-6268.

Martirosyan, A. and Schneider, Y.J. (2014). Engineered nanomaterials in food: Implications for food safety and consumer health. *International Journal of Environmental Research and Public Health*. 11, 5720-5750.

Martirosyan, A. and Schneider, Y.-J. (214). Engineered nanomaterials in food: Implications for food safety and consumer health. *International Journal of Environmental Research and Public Health*. 11, 5720-5750.

McGeer, J. C., Niyogi, S. and Smith, D. S. (2012). Cadmium. In: Homeostasis and Toxicology of Non-Essential Metals. Elsevier. 126-184.

McKim, J., Schmieder, P. and Veith, G. (1985). Absorption dynamics of organic chemical transport across trout gills as related to octanol-water partition coefficient. *Toxicology and Applied Pharmacology*. 77, 1-10.

Meermann, B. and Nischwitz, V. (2018). ICP-MS for the analysis at the nanoscale – a tutorial review. *Journal of Analytical Atomic Spectrometry*. 33, 1432-1468.

Menard, A., Drobne, D. and Jemec, A. (2011). Ecotoxicity of nanosized TiO_2. Review of in vivo data. *Environmental Pollution*. 159, 677-684.

Mendoza-Carranza, M., Sepúlveda-Lozada, A., Dias-Ferreira, C. And Geissen, V. (2016). Distribution and bioconcentration of heavy metals in a tropical aquatic food web: A case study of a tropical estuarine lagoon in SE Mexico. *Environmental Pollution*. 155-165.

Merrifield, D. L., Shaw, B. J., Harper, G. M., Saoud, I. P., Davies, S. J., Handy, R. D. and Henry, T. B. (2013). Ingestion of metal-nanoparticle contaminated food disrupts endogenous microbiota in zebrafish (*Danio rerio*). *Environmental Pollution*. 174, 157-163.

Meyer, J. S. (2002). The utility of the terms “bioavailability” and “bioavailable fraction” for metals. *Marine Environmental Research*. 53, 417-423.

Minghetti, M. and Schirmer, K. (2016). Effect of media composition on bioavailability and toxicity of silver and silver nanoparticles in fish intestinal cells (RTgutGC). *Nanotoxicology*. 10, 1526-1534.

Mitrano, D. M., Lesher, E. K., Bednar, A., Monserud, J., Higgins, C. P. and Ranville, J. F. (2011). Detecting nanoparticulate silver using single-particle inductively coupled plasma-mass spectrometry. *Nanomaterials in the Environment*. 31, 115-121.

Montaño, M. D., Olesik, J. W., Barber, A. G., Challis, K. and Ranville, J. F. (2016). Single Particle ICP-MS: Advances toward routine analysis of nanomaterials. *Analytical and Bioanalytical Chemistry*. 408, 5053-5074.

Morgan, I. J., Henry, R. P. and Wood, C. M. (1997). The mechanism of acute silver nitrate toxicity in freshwater rainbow trout (*Oncorhynchus mykiss*) is inhibition of gill Na^+ and Cl^- transport. *Aquatic Toxicology*. 38, 145-163.

Mueller, N. C. and Nowack, B. (2008). Exposure modeling of engineered nanoparticles in the environment. *Environmental Science and Technology*. 42, 4447-4453.

Nadella, S. R., Bucking, C., Grosell, M. and Wood, C. M. (2006). Gastrointestinal assimilation of Cu during digestion of a single meal in the freshwater rainbow trout (*Oncorhynchus mykiss*). *Comparative Biochemistry and Physiology, Part C*. 143, 394-401.

Nalbant, P., Boehmer, C., Dehmelt, L., Wehner, F. and Werner, A. (1999). Functional characterization of a Na^+-phosphate cotransporter (NaP_i-II) from zebrafish and identification of related transcripts. *Journal of Physiology*. 520, 79-89.

Navratilova, J., Praetorius, A., Gondikas, A., Fabienke, W., von der Kammer, F. and Hofmann, T. (2015). Detection of engineered copper nanoparticles in soil using single particle ICP-MS. *International Journal of Environmental Research and public Health*. 12, 15756-15768.

Nocchetti, M., Donnadio, A., Ambrogi, V., Andreani, P., Bastianini, M., Pietrella, D. and Latterini, L. (2013). Ag/AgCl nanoparticle decorated layered double hydroxides: synthesis, characterization and antimicrobial properties. *Journal of Materials Chemistry B.* 1, 2383-2393.

O'Donnell, J. M. and Smith, M. W. (1972). Uptake of calcium and magnesium by rat duodenal mucosa analysed by means of competing metals. *The Journal of Physiology*. 229, 733-749.

Oberdörster, G., Maynard, A., Donaldson, K., Castranova, V., Fitzpatrick, J., Ausman, K., Carter, J., Karn, B., Kreyling, W., Lai, D., Olin, S., Monteiro-Riviere, N., Warheit, D. and Yang, H. (2005). Principles for characterising the potential human health effects from exposure to nanomaterials: elements of a screening strategy. *Particle and Fibre Toxicology*. DOI: 10.1186/1743-8977-2-8.

Oberleas, D., Muhrer, M. E. and O'Dell, B. L. (1966). Dietary Metal-complexing Agents and Zinc Availability in the Rat. *The Journal of Nutrition*. 90, 56-62.

OECD (1995). Partition coefficient (n-octanol/water): Shake Flask Method.

OECD (2012). Bioaccumulation in fish: Aqueous and Dietary Exposure.

Ojo, A. A. and Wood, C. M. (2007). *In vitro* analysis of the bioavailability of six metals via the gastro-intestinal tract of the rainbow trout (*Oncorhynchus mykiss*). *Aquatic Toxicology*. 83, 10-23.

Osborne, O. J., Johnston, B. D., Moger, J., Balousha, M., Lead, J. R., Kudoh, T. and Tyler, C. R. (2013). Effects of particle size and coating on nanoscale Ag and TiO_2 exposure in zebrafish (*Danio rerio*) embryos. *Nanotoxicology*. 7, 1315-1324.

Pace, H. E., Rogers, N. J., Jarolimek, C., Coleman, V. A., Higgins, C. P. and Ranville, J. F. (2011). Determining transport efficiency for the purpose of counting and sizing nanoparticles via single particle inductively coupled plasma-mass spectrometry. Analytical Chemistry. 83, 9361-9369.

Park, J. D., Cherrington, N. J. and Klaassen, C. D. (2002). Intestinal absorption of cadmium is associated with divalent metal Transporter 1 in rats. *Toxicological Sciences*. 68, 288-294.

Pele, L. C, Thoree, V., Bruggraber, S. F. A., Koller, D., Thompson, R. P. H., Lomer, M. C. and Powell, J. J. (2015). Pharmaceutical/food grade titanium dioxide particles are absorbed into the bloodstream of human volunteers. *Particle and Fibre Toxicology*. DOI 10.1186/s12989-015-0101-9.

Pereira, J. L., Antunes, S. C., Castro, B. B., Marques, C. R., Gonçalves, A. M. M., Gonçalves, F. And Pereira, R. (2009). Toxicity evaluation of three pesticides on non-target aquatic and soil organisms: commercial formulation versus active ingredient. *Ecotoxicology*. 18, 455-463.

Perera, S. A. D. S. and Pathiratne, A. (2012). Haemato-immunological and histological responses in Nile tilapia, *Oreochromis niloticus* exposed to titanium dioxide nanoparticles. *Sri Lanka Journal of Aquatic Sciences*. 17, 1-18.

Pérez, S. and Bertoft, E. (2010). The molecular structures of starch components and their contribution to the architecture of starch granules: A comprehensive review. *Starch*. 62, 389-420.

Peters, R. J. B., Rivera, Z. H., van Bemmel, G., Marvin, H. J. P., Weigel, S. and Bouwmeester, H. (2014b). Development and validation of single particle ICP-MS for sizing and quantitative determination of nano-silver in chicken meat. Analytical and Bioanalytical Chemistry. 406, 3875-3885.

Peters, R. J. B., van Bemmel, G., Herrera-Rivera, Z., Helsper, H. P. F. G., Marvin, H. J. P., Weigel, S., Tromp, P. C., Oomen, A. G., Rietveld, A. G. and Bouwmeester, H. (2014a). Characterization of titanium dioxide nanoparticle in food products: analytical methods to define nanoparticles. *Journal of Agricultural and Food Chemistry*. 62, 6285-6293.

Peters, R., Herrera-Rivera, Z., Undas, A., van der Lee, M., Marvin, H., Bouwmeester, H. and Weigel, S. (2015). Single particle ICP-MS combined with a data evaluation tool as a routine technique for the analysis of nanoparticles in complex matrices. *Journal of Analytical Atomic Spectrometry*. 30, 1274-1285.

Powell, J. J., Faria, N., Thomas-McKay, E., Pele, L. C. (2010). Origin and fate of dietary nanoparticles and microparticles in the gastrointestinal tract. *Journal of Autoimmunity*. 34, J226-J233.

Powell, J. J., Jugdaohsingh, R. and Thompson, R. P. H. (1999a). The regulation of mineral absorption in the gastrointestinal tract. *Proceedings of the Nutrition Society*. 58, 147-153.

Powell, J. J., Whitehead, M. W., Ainley, C. C., Kendall, M. D., Nicholson, J. K. and Thompson, R. P. H. (1999b). Dietary minerals in the gastrointestinal tract: hydroxypolymerisation of aluminium is regulated by luminal mucins. *Journal of Inorganic Biochemistry*. 75, 167-180.

Praetorius, A., Labille, J., Scheringer, M., Thil, A., Hungerbühler, K. And Bottero, J.Y. (2014a). Heteroaggregation of titanium dioxide nanoparticles with model natural colloids under environmentally relevant conditions. *Environmental Science and Technology*. 48, 10690-10698.

Praetorius, A., Tufenkji, N., Goss, K.U., Scheringer, M., von der Kammer, F. And Elimelech, M. (2014b). The road to nowhere: equilibrium partition coefficients for nanoparticles. *Environmental Science: Nano*. 1, 317-323.

Ramsden, C., Smith, T. J., Shaw, B. J. and Handy, R. D. (2009). Dietary exposure to titanium dioxide nanoparticle in rainbow trout, (*Oncorhynchus mykiss*): no effect on growth, but subtle biochemical disturbances in the brain. *Ecotoxicology*. 18, 939-951.

Rana, S., and Kalaichelvan, P. T. (2013). Ecotoxicty of Nanoparticles. *ISRN Toxicology*. 2013 DOI: org/10.1155/2013/574648.

Ratte, H. T. (1999). Bioaccumulation and toxicity of silver compounds: A review. *Environmental Toxicology and Chemistry*. 18, 89-108.

Reed, R. B., Faust, J. J., Yang, Y., Doudrick, K., Capco, D. G., Hristovski, K. and Westerhoff, P. (2014). Characterization of nanomaterials in metal colloid-containing dietary supplement drinks and assessment of their potential interactions after ingestion. *ACS Sustainable Chemistry & Engineering*. 2, 1616-1624.

Reyes, B. A., Pendergast, J. S. and Yamazaki, S. (2008). Mammalian peripheral circadian oscillators are temperature compensated. *Journal of Biological Rhythms*. 23, 95-98.

Ringø, E., Løvmo, L., Kristiansen, M., Bakken, Y., Salinas, I., Myklebust, R., Olsen, R. E. And Mayhew, T. M. (2010). Lactic acid bacteria vs. pathogens in the gastrointestinal tract of fish: a review. *Aquaculture*. 41, 451-467.

Rombout, J. H. W. M., Lamers, C. H. J., Helfrich, M. H., Dekker, A. and Taverne-Thiele, J. J. (1985). Uptake and transport of intact macromolecules in the intestinal epithelium of carp (*Cyprinus carpio* L.) and the possible immunological implications. *Cell and Tissue Research*. 239, 519-530.

Schenone, N. F., Avigliano, E., Goessler, W. and Cirelli, A. F. (2014). Toxic metals, trace and major elements determined by ICPMS in tissues of *Parapimelodus valenciennis* and *Prochilodus lineatus* from Chascomus Lake, Argentina. *Microchemical Journal*. 112, 127-131.

Scown, T. M., Santos, E. M., Johnston, B. D., Gaiser, B., Baalousha, M., Mitov, S., Lead, J. R., Stone, V., Fernandes, T. F., Jepson, M., van Aerle, R. and Tyler, C. R. (2010). Effects of aqueous exposure to silver nanoparticles of different sizes in rainbow trout. *Toxicological Sciences*. 115, 521-534.

Scown, T. M., van Aerle, R., Johnston, B. D., Cumberland, S., Lead, J. R., Owen, R. and Tyler. C. R. (2009). High dose of intravenously administered titanium dioxide nanoparticles

accumulate in the kidneys of rainbow trout but no observable impairment of renal function. *Toxicological Sciences*. 109, 372-380.

Selck, H., Handy R. D., Fernandes, T. F., Klaine, S. J. and Petersen, E. J. (2016). Nanomaterials in the aquatic environment: A European Union-United States perspective on the status of ecotoxicity testing, research priorities, and challenges ahead. *Environmental Toxicology and Chemistry*. 5, 1055-1067.

Setyawati, M. I., Tay, C. Y., China, S. L., Goh, S. L., Fang, W., Neo, M. J., Chong, H. C., Tan, S. M., Loo, S. C., Ng, K. W., Xie, J. P., Ong, C. N., Tan, N. S. and Leong, D. T. (2013). Titanium dioxide nanomaterials cause endothelial cell leakiness by disrupting the homophilic interaction of VE-cadherin. *Nature Communications*. 4 DOI: 10.1038/ncomms2655.

Shaw, B. J. and Handy, R. D. (2006). Dietary copper exposure and recovery in Nile tilapia, *Oreochromis niloticus*. *Aquatic Toxicology*. 76, 111-121.

Shaw, B. J. and Handy, R. D. (2011). Physiological effects of nanoparticles on fish: A comparison of nanometals versus metal ions. *Environment International*. 37, 1083-1097.

Shaw, B. J., Al-Bairuty, G. and Handy, R. D. (2012). Effects of waterborne copper nanoparticles and copper sulphate on rainbow trout, (*Oncorhynchus mykiss*): Physiology and accumulation. *Aquatic Toxicology*. 116-117, 90-101.

Shaw, B. J., Liddle, C. C., Windeatt, K. M. and Handy, R. D. (2016). A critical evaluation of the fish early-life stage toxicity test for engineered nanomaterials: experimental modifications and recommendations. *Archives of Toxicology*. 90, 2077-2107.

Shaw, B. J., Ramsden, C. S., Turner, A. and Handy, R. D. (2013). S simplified method for determining titanium from TiO_2 nanoparticles in fish tissue with a concomitant multi-element analysis. *Chemosphere*. 92, 1136-1144.

Shehadeh, Z. H. and Gordon, M. S. (1969). The role of the intestine in salinity adaptation of the rainbow trout, *Salmo gairdneri. Comparative Biochemistry and Physiology*. 30, 397-418.

Shephard, K. L. (1984). The influence of mucus on the diffusion of chloride ions across the oesophagus of the minnow (*Phoxinus phoxinus*). *The Journal of Physiology*. 346, 449-460.

Smith, C. J., Shaw, B. J. and Handy, R. D. (2007). Toxicity of single walled carbon nanotubes to rainbow trout, (*Oncorhynchus mykiss*): Respiratory toxicity, organ pathologies, and other physiological effects. *Aquatic Toxicology*. 82, 94-104.

Smith, D.S., Bell, R.A. and Kramer, J.R., 2002. Metal speciation in natural waters with emphasis on reduced sulfur groups as strong metal binding sites. Comparative Biochemistry and Physiology Part C: Toxicology & Pharmacology, 133(1-2), pp.65-74.

Sohrabi, N., Rasouli, N. and Torkzadeh, M. (2014). Enhanced stability and catalytic activity of immobilized a-amylase on modified Fe_3O_4 nanoparticles. *Chemical Engineering Journal*. 240, 426-433.

Soltani, M., Ghodratnema, M., Ahari, H., Mousavi, E. H. A., Atee, M., Dastmalchi, F. and Rahmanya, J. (2009). The inhibitory effect of silver nanoparticles on the bacterial fish pathogens, *Steptococcus iniae*, *Lactococcus garvieae*, *Yersinia ruckeri* and *Aeromonas hydrophilia*. *International Journal of Veterinary Science and Medicine*. 3, 137-142.

Sørmo, E. G., Salmer, M. P., Jenssen, B. M., Hop, H., Baek, K., Kovacs, K. M., Lydersen, C., Falk-Petersen, S., Gabrielsen, G. W., Lie, E. and Skaare, J. U. (2006). Biomagnification of polybrominated diphenyl ether and hexabromocyclododecane flame retardants in the polar bear food chain in Svalbard, Norway. *Environmental Toxicology and Chemistry*. 25, 2502-2511.

Souris, J. S., Lee, C.-H., Cheng, S.-H., Chen, C.T., Yang, C.-S., Hoe, J. A., Mou, C.-Y. and Lo, L.-W. (2010). Surface charge-mediated rapid hepatobiliary excretion of mesoporous silica nanoparticles. *Biomaterials*. 31, 5564-5574.

Sovová, T., Boyle, D., Sloman, K. A., Pérez, C.V. and Handy, R. D. (2014). Impaired behavioural response to alarm substance in rainbow trout exposed to copper nanoparticles. *Aquatic Toxicology*. 152, 195-204.

Spry, D. J. and Wiener, J. G. (1991). Metal bioavailability and toxicity to fish in low-alkalinity lakes: A critical review. *Environmental Pollution*. 71, 243-304.

Stone, V., Nowack, B., Baun, A., van den Brink, N., von der Kammer, F., Dusinska, M., Handy, R., Hankin, S., Hassellöv, M., Joner, E. and Fernandes, T. F. (2010). Nanomaterials for environmental studies: Classification, reference material issues, and strategies for physico-chemical characterisation. *Science of the Total Environment*. 408, 1745-1754.

Suganthi, P., Murali, M., Bukhari, A. S., Mohamed, S., S. E., Basu, H. and Singhal, R. K. (2013). Haematological studies on freshwater Tilapia treated with ZnO nanoparticles. *Journal of Advanced Applied Scientific Research.* 1, 41-67.

Sun, T. Y., Gottschalk, F., Hungerbühler, K. and Nowack, B. (2014). Comprehensive probabilistic modelling of environmental emissions of engineered nanomaterials. *Environmental Pollution*. 185, 69-76.

Szebedinszky, C., McGeer, J. C., McDonald, G. and Wood, C. M. (2001). Effects of chronic Cd exposure via the diet or water on internal organ-specific distribution and subsequent gill Cd uptake kinetics in juvenile rainbow trout (*Oncorhynchus mykiss*). *Environmental Toxicology and Chemistry*. 20, 597-607.

Tangaa, S. R., Selck, H., Winther-Nielsen, M. and Khan, F. R. (2016). Trophic transfer of metal-based nanoparticles in aquatic environments: a review and recommendations for future research focus. Environmental Science: Nano. 3, 966-981.

Tatsi, K., Shaw, B. J., Hutchinson, T. H. and Handy, R. D. (2018). Copper accumulation and toxicity in earthworms exposed to CuO nanomaterials: Effects of particle coating and soil ageing. *Ecotoxicology and Environmental Safety*. 166, 462-473.

Taylor, M. G. and Simkiss, K. (2004). Transport of colloids and particles across biological membranes. In: Physicochemical Kinetics and Transport at Biointerfaces.John Wiley and Sons Ltd, UK. 357-400.

Tervonen, K., Waissi, G., Petersen, E. J., Akkanen, J. and Kukkonen, J. V. (2010). Analysis of fullerene-C_{60} and kinetic measurements for its accumulation and depuration in Daphnia magna. *Environmental Toxicology and Chemistry*. 29, 1072-1078.

Tiede, K., Boxall, A. B., Tear, S. P., Lewis, J., David, H. and Hassellöv, M (2008). Detection and characterization of engineered nanoparticles in food and the environment. *Food Additives and Contaminants*. 25, 795-821.

Treuel, L., Jiang, X. and Nienhaus, G. U. (2013). New views on cellular uptake and trafficking of manufactured nanoparticles. *Journal of The Royal Society Interface*. DOI: 10.1098/rsif.2012.0939.

Van der Zande, M., Vandebriel, R. J., Doren, E. V., Kramer, E., Rivera, Z., Serrano-Rojero, C. S., Gremmer, E. R., Mast, J., Peters, R. J. B., Hollman, P. C. H., Hendriksen, P. J. M., Marvin, H. J. P., Peijnenburg, A. A. C. M. and Bouwmeester, H. (2012). Distribution, elimination and toxicity of silver nanoparticles and silver ions in rats after 28-day oral exposure. *ACS Nano*. 6, 7427-7442.

Vassello, J., Tatsi, K., Boden, R. and Handy, R. D. (2019). Determination of the bioaccessible fraction of cupric oxide nanoparticles in soils using an *in vitro* human digestibility simulation. *Environmental Science: Nano*. DOI: 10.1039/C8N00687C

Veith, G. D., DeFoe, D. L. and Bergstedt, B. V. (1979). Measuring and estimating the bioconcentration factor of chemicals in fish. *Journal of the Fisheries Research Board and Canada*. 36, 1040-1048.

Verwey, E. J. W. and Overbeek, J. Th. G. (1948). Theory of the stability of lycophobic colloids. Elsevier, New York. 1-65.

Visscher, M. B. and Johnston, J. A. (1953). The Fick principle: analysis of potential errors in its conventional application. *Journal of Applied Physiology*. 5, 635-638.

Voelker, D., Schlich, K., Hohndorf, L., Koch, W., Kuehnen, U., Polleichtner, C., Kussatz, C. and Hund-Rinke, K. (2015). Approach on environmental risk assessment of nanosilver released from textiles. *Environmental Research*. 140, 661-672.

Von der Kammer, F., Ferguson, P. L., Holden, P. A., Maison, A., Rogers, K. R., Klaine, S. J., Koelmans, A. A., Horne, N. and Unrine, J. M. (2012). Analysis of engineered nanomaterials in complex matrices (environment and biota): general considerations and conceptual case studies. *Environmental Toxicology and Chemistry*. 31, 32-49.

Walczak, A. P., Fokkink, R., Peters, R., Tromp, P., Herrera Rivera, Z. E., Rietjens, I. M. C. M., Hendriksen, P. J. M. and Bouwmeester, H. (2013). Behaviour of silver nanoparticles and silver ions in an *in vitro* human gastrointestinal digestion model. *Nanotoxicology*. 7, 1198-1210.

Walkey, C. D. and Chan, W. C. W. (2012). Understanding and controlling the interaction of nanomaterials with proteins in a physiological environment. *Chemical Society Reviews*. 41, 2780-2799.

Wang, J. and Wang, W.X. (2014). Low Bioavailability of silver Nanoparticles Presents Trophic Toxicity to Marine Medaka (*Oryzias melastigma*). *Environmental Science and Technology*. 48, 8152-8161.

Wapnir, R. A. and Stiel, L. (1987). Intestinal adsorption of copper: Effect of sodium. *Experimental Biology and Medicine*. 185, 277-282.

Ward, J. E. and Kach, D. J. (2009). Marine aggregates facilitate ingestion of nanoparticles by suspension-feeding bivalves. *Marine Environmental Research*. 68, 137-142.

Weigel, S., Peters, R., Loeschner, K., Grombe, R. and Linsinger, T. P. J. (2017). Results of an interlaboratory method performance study for the size determination and quantification of

silver nanoparticles in chicken meat by single-particle inductively coupled plasma mass spectrometry. *Analytical and Bioanalytical Chemistry*. 409, 4839-4848.

Wei, H. and Wang, E. (2013). Nanomaterials with enzyme-like characteristics (nanozymes): next-generation artificial enzymes. *Chemical Society Reviews*. 42, 6060-6093.

Weir, A., Westerhoff, P., Fabricius, L. and von Goetz, N. (2012). Titanium dioxide nanoparticles in food and personal care products. *Environmental Science and Technology*. 46, 2242-2250.

Williams, R. J. P. (1981). Physico-chemical aspects of inorganic element transfer through membranes. *Philosophical Transactions of The Royal Society B.* 294, 57-74.

Wong, S. W. Y., Leung, P. T. Y., Djurišić, A. B. and Leung, K. M. Y. (2010). Toxicities of nano zinc oxide to five marine organisms: influences of aggregate size and ion solubility. *Analytical and Bioanalytical Chemistry*. 396, 609-618.

Wood, C. M. (2012). Silver. In: Homeostasis and Toxicology of Non-Essential Metals. Elsevier. 2-65.

Wood, C. M., Grosell, M., Hogstrand, C. and Hansen, H. (2002). Kinetics of radiolabelled silver uptake and depuration in the gills of rainbow trout (*Oncorhynchus mykiss*) and European eel (*Anguilla Anguilla*): the influence of silver speciation. *Aquatic Toxicology*. 56, 197-213.

Wu, J.-P., Guan, Y.-T., Zhang, Y., Luo, X.-J., Zhi, H., Chen, S.-J., Mai, B.-X. (2011). Several current-use, non-PBDE brominated flame retardants are highly bioaccumulative: Evidence from field determined bioaccumulation factors. 37, 210-215.

Wu, J.-P., Luo, X.-J., Zhang, Y., Luo, Y., Chen, S.-J., Mai, B.-X. And Yang, Z.-Y. (2008). Bioaccumulation of polybrominated diphenyl ethers (PBDEs) and polybrominated biphenyls (PCBs) in wild aquatic species from an electronic waste (e-waste) recycling sire in South China. *Environment International*. 34, 1109-1113.

Wu, L.-G., Wang, T. and Jiang, Z. (2013). Formation of AgCl nanoparticle in reverse microemulsion using polymerizable surfactant and the resulting copolymer hybrid membranes. *Journal of Membrane Science*. 429, 95-102.

Wulff, J. L. (1997). Parrotfish predation on cryptic sponges of Caribbean coral reefs. *Marine Biology*. 129, 41-52.

Xiao, Y. and Wiesner, M. R. (2012). Characterisation of surface hydrophobicity of engineered nanoparticles. *Journal of Hazardous Materials*. 215-216, 146-151.

Xu, Y. and Wang, W.-X. (2002). Exposure and potential food chain transfer factor of Cd, Se and Zn in marine fish *Lutjanus argentimaculatus*. *Marine Ecology Progress Series*. 238, 173-186.

Yang, Y., Luo, L., Li, H.-P., Wang, Q., Yang, Z.G. and Long, C.-L. (2016). Separation and determination of silver nanoparticle in environmental water and the UV-induced photochemical transformations study of Ag NPs by cloud point extraction combined ICP-MS. *Talanta*. 161, 342-349.

Yoo-iam, M., Chaichana, R. and Satapanajaru, T. (2014). Toxicity, bioaccumulation and biomagnification of silver nanoparticles in green algae (*Chlorella sp*.), water flea (*Moina macrocopa*), blood worm (*Chironomus spp*.) and silver barb (*Barbonymus gonionotus*). *Chemical Speciation and Bioavailability*. 26, 257-265.

Yoshida, T., Yoshioka, Y., Takahashi, H., Misato, K., Mori, T., Hirai, T., Nagano, K., Abe, Y., Mukai, Y., Kamada, H., Tsunoda, S., Nabeshi, H., Yoshikawa, T., Higashisaka, K. and Tsutsumi, Y. (2014). Intestinal absorption and biological effects of orally administered amorphous silica particles. *Nanoscale Research Letters*. DOI: 10.1186/1556-276X-9-532.

Zhang, H., Chen, B. and Banfield, J. F. (2010b). Particle Size and pH Effects on Nanoparticle Dissolution. The *Journal of Physical Chemistry C.* 114, 14876-14884.

Zhang, Z., Bu, H., Gao, Z., Huang, Y., Gao, F. and Li, Y. (2010a). The characteristics and mechanism of simvastatin loaded lipid nanoparticles to increase oral bioavailability in rats. *International Journal of Pharmaceuticals*. 394, 147-153.

Zhao, B., Sun, L., Zhang, W., Wang, Y., Zhu, J., Zhu, X., Yang, L., Li, C., Zhang, Z. and Zhang, Y. (2014). Secretion of intestinal goblet cells: A novel excretion pathway of nanoparticles. *Nanomedicine: Nanotechnology, Biology and Medicine*. 10, 839-849.

Zhou, X., Wang, Y., Gu, Q. and Li, W. (2009). Effects of different dietary selenium sources (selenium nanoparticle and selenomethionine) on growth performance, muscle composition and glutathione peroxidase enzyme activity of crucian carp (*Carassius auratus gibelio*). *Aquaculture*. 291, 78-81.

Zhu, Z.-J., Carboni, R., Quercio Jr, M. J., Yan, B., Miranda, O. R., Anderton, D. L. And Arcaro, K. F. (2010). Surface properties dictate uptake, distribution, excretion, and toxicity of nanoparticles in fish. *Small*. 6, 2261-2265.

Zirino, A. and Yamamoto, S. (1972). A pH-dependent model for the chemical speciation of copper, zinc, cadmium, and lead in seawater. *Limnology and Oceanography*. 17, 661-671.